How are human gait and energetics modified when walking over substrates of varying compliance?

Thesis submitted in accordance with the requirements of
the University of Liverpool for the degree of
Doctor in Philosophy by

Barbara Frances Grant

February 2023

Acknowledgements

It would not have been possible to write this thesis without the help, guidance and support from many people around me.

Firstly, I would like to thank my supervisors who provided lots of time, support and guidance over the past few years, it is greatly appreciated. In particular, I would like to thank my primary supervisor Karl Bates for his support, direction and detailed and timely feedback. Thanks to my secondary supervisors, Kristiaan D'Août and Peter Falkingham for their advice and support. I would also like to thank Jamie Gardiner for his assistance with matlab. A special thanks goes to James Charles, who at times was basically another supervisor when he wasn't being my assistant during data collection!

Secondly, I would like to thank my fellow EMB friends and colleagues who have made my PhD studies more enjoyable. A special thanks goes to Alice Maher who I don't think I could have gotten through the past couple years without. Thank "youse" for all your support! Thanks to Nick Thomas and Rory Curtis for providing great banter. Thank you to Roger Kissane for your baking treats. Thank you to Marcela Cárdenas Serna, Mie Kronberg Olesen and all the demonstrators on the Life 107 module.

Thirdly, I would like to thank all the participants who took up a lot of time and effort to participate in these studies, these studies wouldn't have been possible without you.

I would also like to thank my friends at the Blackburn and Darwen brass band for their support and questions at the pub, especially Thomas Helm (even if you do "think" I work at Clarks shoe shop measuring feet).

Thank you to all my family for their support. To my older sisters and brother, thank you for putting up with the "little" one. To my niece and nephews- thank you for thinking I'm a cool auntie (you'll probably change your mind when you get older). To my parents, thank you for always supporting me to pursue my interests.

The biggest thanks has to go to the person who has had to put up with me the most, especially during lockdown. Thank you Jamie for your love and support, I couldn’t have done this without you. And of course to our cats, Midori and Picasso, Meow.

Abstract

Locomotion in the real-world requires humans to negotiate a variety of surfaces that have different material and mechanical properties and thus, require gait adjustments to maintain stability and efficiency. However, our current understanding of human gait and energetics is dominated by studies on hard, level surfaces in a laboratory environment. Previous research has shown that when walking on more irregular terrains such as loose rock surfaces, uneven surfaces and compliant substrates such as snow, grass and sand, there is an increase in energy expenditure. However, the primary mechanistic causes of this increase in energy costs is unclear. Previous studies suggest various biomechanical mechanisms including disruption to pendular energy recovery, increased muscle work, decreased muscle-tendon efficiency and increased gait variability. Yet, comparisons between studies is hindered by the measurement of different variables across studies and variation in substrates used. In this thesis, I focus on human walking over compliant substrates. This thesis aims to improve our understanding of the relationship between energetic costs, substrate properties, gait biomechanics and muscle activities. This is done by presenting a large experimental data set of human walking on both artificial (foam) and natural (sand) compliant substrates. The studies showed that compliant substrates had a considerable effect on gait biomechanics, muscle activation and energetics. On foam, there was greater energetic expenditure on more compliant substrates. On all compliant substrates, participants displayed greater ankle dorsiflexion during stance and greater knee and hip flexion during swing, increased muscle activation and changes to spatiotemporal parameters such as increased cycle time, stance time and swing time and decreased walking speed. The findings of this thesis suggests that overall gross adaptations like sagittal kinematics, spatiotemporal parameters and muscle activation are adopted in response to the depth of depression into a compliant substrate. However, there are specific gait changes due to substrate properties. Further research is required to explore gait adaptations on substrates with different material and mechanical properties. Furthermore, some of our results suggest there is large participant variability even in a relatively homogeneous study population. Therefore, future work should not only look at other demographic groups but also

explore individual participant differences such as gender effects and variations in anatomical parameters.

Table of Contents

List of Tables

List of Figures

List of abbreviations

BFL	Biceps femoris (long head)
CO	Congruity (the time when potential and kinetic energy are moving in the same direction)
CoL	Cost of locomotion
CoM	Centre of mass
CoT	Cost of transport
EMG	Surface electromyography
EO_L	Left internal abdominal oblique
EO_R	Right internal abdominal oblique
GMax	Gluteus maximus
iEMG	Integrated EMG (surface electromyography)
IO_L	Left external abdominal oblique
IO_R	Right external abdominal oblique
LES_L	Left longissimus erector spinae
LES_R	Right longissimus erector spinae
LG	Lateral gastrocnemius
LMM	Linear mixed-effect model
MG	Medial gastrocnemius
nEMG	Normalised EMG (surface electromyography)
R	Recovery of mechanical energy
RA	Relative amplitude (of potential and kinetic energy)
RF	Rectus femoris
SOL	Soleus
TA	Tibialis anterior
VL	Vastus lateralis
VM	Vastus medialis

Chapter one: Introduction

1.1 Purpose of research

In everyday life, animals navigate a wide range of terrains which have different material and mechanical properties that impact how they choose to walk across a surface. Certain surfaces are more challenging to walk on and require adjustments to maintain stability and efficiency. However, our current understanding of human gait and energetics is dominated by studies on hard, level surfaces in a laboratory environment, which do not reflect most naturally occurring terrains. Previous studies on locomotion on compliant substrates have usually only involved one substrate type and have only tested a few specific variables. Furthermore, substrate properties are rarely reported which makes comparisons across studies difficult. Therefore, our understanding of how different substrate properties affects human gait and energetics remains unclear. The goal of this thesis was to investigate how human gait is actively altered or moderated by the level of compliance with a deformable substrate, on both artificial and natural compliant substrates. To understand how human gait changes during locomotion on compliant substrates, it is necessary to understand normal human locomotion on level non-deforming substrates first. Chapter one of this thesis introduces human gait during locomotion on hard, level surfaces. It will then review the extent and limitations of the current literature on human gait during locomotion on compliant substrates. Then, the overall goals of this thesis are summarised and the thesis structure is outlined.

1.2 Background

1.2.1 Human gait on hard, level surfaces

Humans have evolved an upright striding bipedal locomotion that distinguishes modern humans from all other extant animals (Schmitt 2003). This has led to a number of musculoskeletal adaptations including a mobile lower back, a short pelvis, elongation of the lower limbs, adducted femora and a stable rigid foot to support the weight of the body and to ensure an effective ground reaction force in the stance phase (O'Neill et al. 2022). Human locomotion is a very complex behaviour which requires co-ordination of the central nervous system, muscles and limbs (Nielsen 2003). Walking is the most common form of locomotion used by humans and can be described as a cyclic pattern of body movements which advances the individual forwards. The gait cycle begins when one foot makes contact with the ground and ends when the same foot contacts the ground again and is usually expressed as percentages with 0% and 100% indicating heel-strike of the same foot (Perry & Burnfield 2010). Figure 1.1 depicts the gait cycle for a normal healthy adult during walking, illustrating the different stages of the cycle (Tunca et al. 2017). Within one gait cycle, each foot has a period where it is in contact with the ground, known as the stance phase and a period when the foot is lifted off the ground, known as the swing phase. In normal walking, the stance phase accounts for about 60-62% of the entire gait cycle and the swing phase accounts for 38-40% (Fig. 1.1) (Perry & Burnfield 2010). In human running, both feet never touch the ground at the same time whereas in human walking, there are two periods when both feet are in contact with the ground, known as double-support (Fig. 1.1) (Silva & Stergiou 2020). However, the normal gait cycle can be affected by other variables. For example, percentages of single and double-support time within a gait cycle can be altered by walking speed; if walking speed is higher, single-leg support time will increase and double-leg support time will decrease and vice-versa (Silva & Stergiou 2020). There are a number of spatiotemporal characteristics of human walking that are used to identify changes to normal gait, including step length, step width, step time, cadence and gait speed. Spatiotemporal parameters are often used to investigate gait impairments or

the influence of ageing as individuals will alter spatiotemporal variables to improve stability (Fukuchi, Fukuchi & Duarte 2019; Niederer et al. 2021).

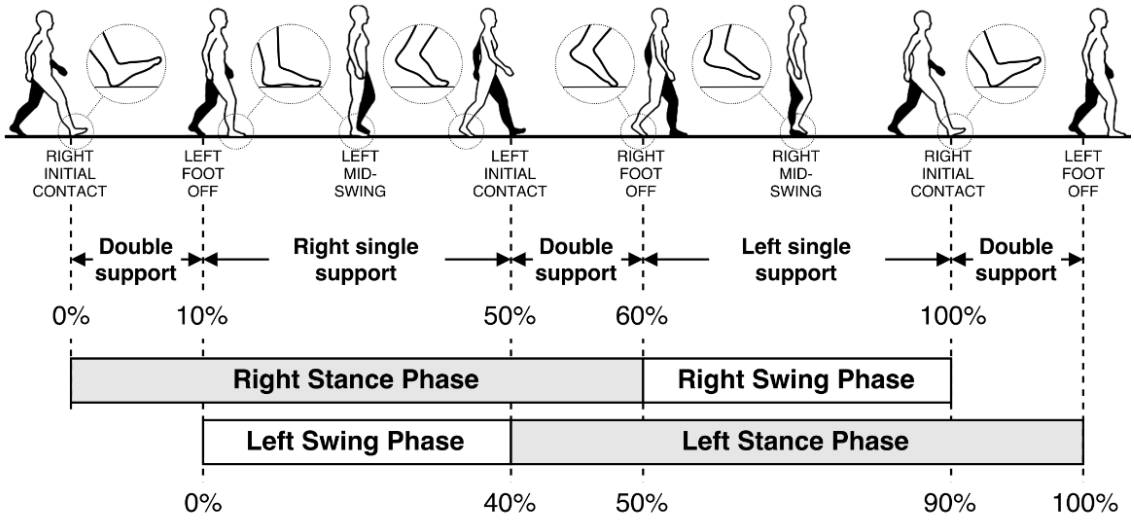

Figure 1.1: Illustration of a human gait cycle during normal adult walking indicating stance and swing phases and single- and double-support periods. From Tunca et al. (2017, p. 4).

Human walking is a highly efficient form of locomotion and is often modelled as the stance leg behaving as an inverted pendulum (Alexander 1976). During level walking, the centre of mass (CoM) of the human body rises and falls with equal magnitude (Cavagna, Heglund & Taylor 1977). Figure 1.2 depicts the mechanics of the inverted pendulum model and energy recycling during human walking (Collins & Kuo 2010). At heel-strike, CoM is at its lowest point and at mid-stance, CoM is at its highest (Fig. 1.2a). During the first half of the single support period, the kinetic energy (E_{kin}) of the CoM decreases and is converted into gravitational potential energy (E_{pot}). During the second half of the single support period, E_{pot} decreases and is converted into E_{kin} (Cavagna, Heglund & Taylor 1977). For optimum mechanical energy exchange to take place, the magnitudes of E_{kin} and E_{pot} need to be the same and occur at opposite times with maximum E_{pot} occuring when E_{kin} is at its minimum and vice versa (Cavagna, Heglund & Taylor 1977). This exchange of energies can reduce the work required by the muscles and potentially lower the metabolic costs of locomotion. Theoretically, this pendular mechanism could result in maximum 100%

recovery of energy (R) with no additional work from the muscles required. However, during normal walking, R reaches a maximum of ~65% at a speed of 1.39ms^{-1} due to costs associated with the redirection of the CoM (Dewolf et al. 2017). To maximise energy recycling, positive work is performed by the trailing leg during push-off and timed just before the heel-strike of the opposite leg, reducing both dissipation and the amount of positive work needed to offset the loss (Fig. 1.2b-1.2c) (Kuo, Donelan & Ruina 2005). %R can be affected by variables such as walking speeds with %R decreasing with slow or high walking speeds. The self-selected speed of human walking as well as step length and cadence, are close to those allowing the minimal total energy expenditure and external work and maximisation of %R (Dewolf et al. 2017; Tesio & Rota 2019).

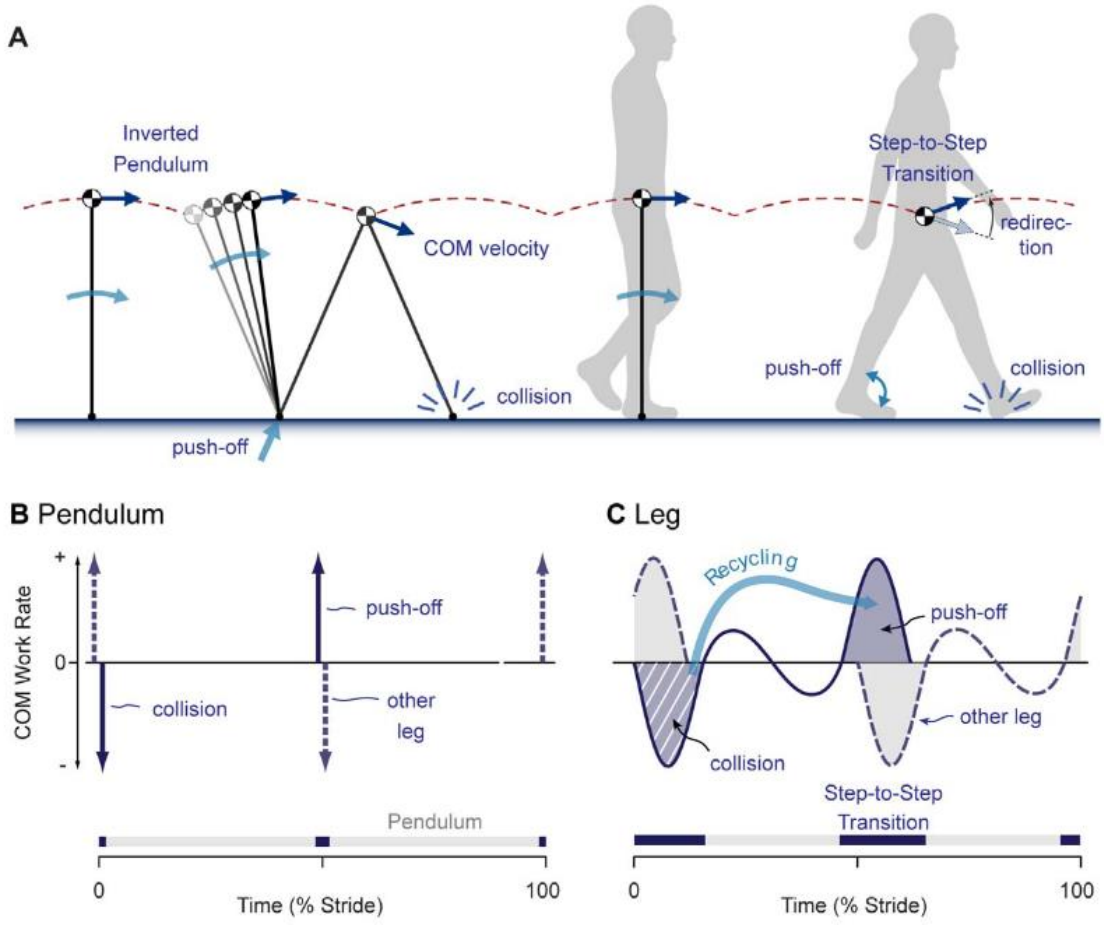

Figure 1.2: The inverted pendulum model of human walking ***(a)*** the inverted pendulum motion of the centre of mass of the body while pivoted about the stance foot. The CoM velocity is redirected between steps ***(b)*** The rate of work performed on the CoM by optimum pendulum mechanism. Work is minimised when push-off occurs just before collision of the opposite leg ***(c)*** Conceptual plot of CoM work with potential recycling if energy is stored during collision and later released for push-off. Adapted from Collins and Kuo (2010, p. 2).

During a normal gait cycle, the hip, knee and ankle joints experience a range of motion. The hip and knee joints are characterised by extension during the stance phase followed by flexion during the swing phase. During the stance phase, the hip is responsible for stabilising the trunk and the knee is responsible for limb stability and during the swing phase, hip and knee flexion ensures toe clearance from the ground (Brunner & Rutz 2013). The ankle joint is characterised by dorsiflexion during stance followed by plantarflexion during the push-off to early-swing phase (Brockett & Chapman 2016). During the stance phase, the ankle is responsible for progression and shock absorption (Brunner & Rutz 2013). At the start of the gait cycle the foot contacts the ground and according to Newton's third law, force is exerted by the ground onto the foot (Horsak et al. 2020). This force is commonly referred to as the ground reaction force (GRF) and has vertical, anteroposterior and mediolateral components. The GRF passes upwards from the foot and produces movement at each lower extremity joint (Winter 1984). However, ground reaction forces are not the only force that influences the joints. A large magnitude of force is transmitted by the muscles through the tendons across the joint (Wilson & Lichtwark 2011). There are a number of different muscles acting on each joint and the various actions of the leg muscles are delicately timed by the central nervous system to lift and accelerate the body whilst maintaining balance about a relatively small base of support (Brunner & Rutz 2013). There is considerable flexibility in the activity of individual muscles; there can be different combinations and scaling of muscle activities that result in the correct movement trajectory of a joint (Hansen et al. 2001; Wilson & Lichtwark 2011; Winter 1984). The muscles that contribute most considerably to the accelerations of the CoM during human walking are the gluteus maximus, gluteus medius, vasti, soleus and gastrocnemius (Pandy & Andriacchi 2010). The vasti decelerates the CoM in early stance, the gluteus medius actively controls balance by accelerating the CoM medially and the soleus and gastrocnemius accelerate the CoM forwards in late stance (Pandy & Andriacchi 2010).

Locomotion is dependent on the dynamic interaction of the muscle and tendon forming the muscle-tendon complex. Many terrestrial animals exploit the elastic properties of tendons in their legs and feet to reduce muscular energy (Alexander 2002). The inverted pendulum model assumes a stiff stance leg during walking

whereas humans have been shown to modify leg stiffness during hopping and running (Ferris & Farley 1997; Ferris, Louie & Farley 1998). This led researchers to question the suitability of the inverted pendulum model during human walking. By using a simple spring-loaded inverted pendulum model, with appropriate leg stiffness, the CoM trajectory and GRFs during walking are more closely reproduced than a rigid inverted pendulum model (Geyer, Seyfarth & Blickhan 2006). This suggests that walking efficiency relies to some extent on how much energy can be stored elastically when redirecting CoM in the double-support phase of stride.

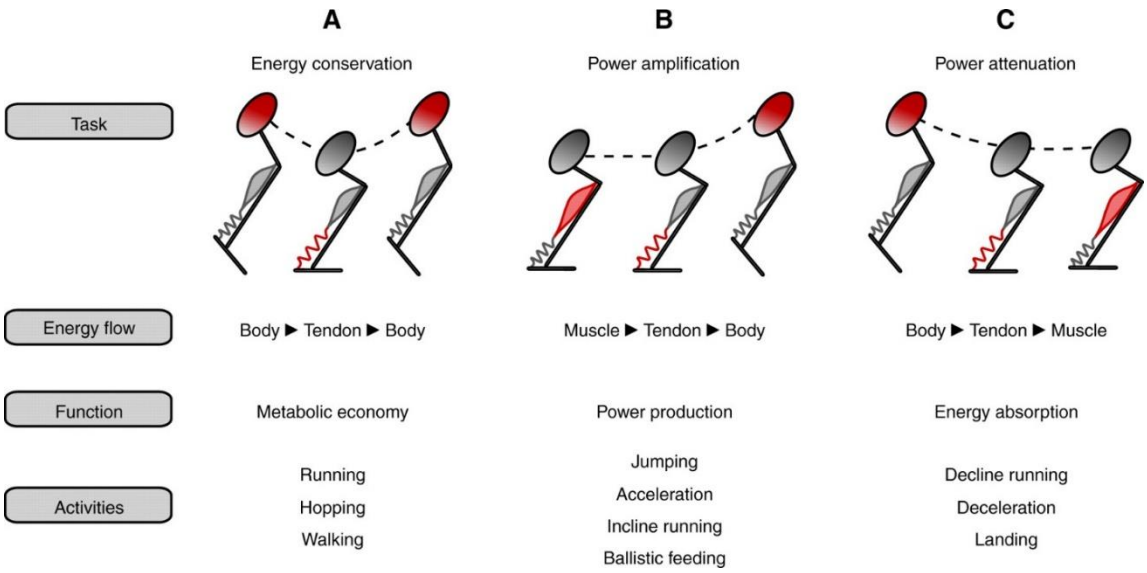

Figure 1.3: A schematic illustrating how the directional flow of energy in muscle-tendon systems determine mechanical function ***(a)*** energy conservation: elastic structures storing and recovering energy ***(b)*** power amplification: tendons loaded directly by the work of muscle contraction can release energy rapidly to the body ***(c)*** power attenuation: energy can be temporarily stored as elastic strain energy then released later to do work on active muscles. Red indicates the flow of energy. From Roberts and Azizi (2011, p. 354).

During the foot's impact with the ground, E_{kin} and E_{pot} are stored as strain energy in tendons and muscles and as the foot leaves the ground, most of the stored energy is reverted back to E_{kin} and E_{pot} through elastic recoil (Alexander 1983). In large animals, metabolic energy savings can be as high as 50% during fast locomotion (Alexander 1984; Cavagna, Heglund & Taylor 1977). Roberts and Azizi (2011) proposed three main functions of the mechanism of elastic strain energy in biological springs in locomotion: metabolic energy conservation (fig. 1.3a), amplification of muscle power output (fig. 1.3b) and attenuation of muscle power input (Fig. 1.3c). In

this framework, the direction and timing of the flow of energy between the contracting muscle, the elastic element and the body determine the function served by the elastic mechanism (Roberts & Azizi 2011).

Locomotion represents one of the most important and largest components of energy expenditure in animals and minimising energy cost is considered one of the selective pressures on locomotor behaviour (Biewener & Patek 2018). However, despite its importance, reducing energy costs may not always take priority. Certain environments and scenarios may prevent an animal from prioritising energy minimisation (e.g. pursuing prey), and consequently, there will be an energy economy trade-off (Halsey 2016). One of the selective pressures on locomotor behaviour is environment and terrain. In everyday life, animals navigate complex environments with heterogeneous terrain where variations in substrate such as ground compliance impact how they choose to walk across the surface to maintain manoeuvrability, grip and stability (Peyré-Tartaruga & Coertjens 2018). For locomotion, stability is necessary. Stability in human locomotion is the ability to return to a steady-state, periodic gait to maintain the forward progression of the CoM in spite of perturbations (Full et al. 2002). Some surfaces require necessary adjustments to maintain stability, creating the possibility for conflict between adjustments necessary to reduce energetic costs and adjustments necessary to maintain stability.

1.2.2 Current literature on human gait and energetics on compliant substrates

The energetic costs and gait biomechanics of human locomotion on hard, level surfaces have been studied extensively (Cappellini et al. 2006; Cavagna & Kaneko 1977; Cavagna, Thys & Zamboni 1976). However, humans regularly move on a variety of non-firm surfaces. In particular, outdoor locomotion occurs over various complex surfaces including artificial substrates such as pavements and sports tracks,

and natural substrates such as rocks, grass and sand. Some studies have looked at the energetic costs of moving on more complex substrates like loose rock surfaces (Gates et al. 2012), ballast (Wade et al. 2010), uneven surfaces (Voloshina et al. 2013) and compliant substrates such as snow (Pandolf, Haisman & Goldman 1976; Ramaswamy et al. 1966), grass (Davies & Mackinnon 2006; Pinnington & Dawson 2001) and sand (Davies & Mackinnon 2006; Lejeune, Willems & Heglund 1998; Pinnington & Dawson 2001; Zamparo et al. 1992) and found that there is typically an increase in energy expenditure on complex substrates relative to uniform, non-deforming substrates. A study by Davies and Mackinnon (2006) investigated energetic costs during walking on sand and grass by individuals who regularly transverse such terrain and found increases of 1.34 times greater energetic costs at 3 $km \cdot h^{-1}$ on sand and up to 1.63 times greater at 5 $km \cdot h^{-1}$ on sand compared to grass. Therefore, the type of terrain influences energy expenditure. However, the reported increases in energy expenditure not only vary between different substrate types but also between different studies during locomotion on the same substrate type. For example, Lejeune et al. (1998) found that energy expenditure was up to 2.7 times greater when walking on sand at speeds between 0.5-2.5ms^{-1} compared to hard floor (Fig. 1.4c) and running was 1.6 times greater (Fig. 1.4d). Whereas, Zamparo et al. (1992) who also investigated energy expenditure during locomotion on sand found an increase in energetic costs of 1.8 times greater when walking on sand at a speed of 0.8-2.0 ms^{-1} and 1.2 times greater when running on sand compared to a hard surface. It is unclear why there is considerable variance in the reported increase in energy costs on sand compared to a hard surface between these two studies, but it is likely due to variations in sand properties (e.g. different moisture content) and/or methodology. Pinnington and Dawson (2001) suggested that the sand used by Zamparo et al. (1992) may have been relatively firmer than the sand used by Lejeune et al. (1998). Unfortunately, there were insufficient details on the substrate properties to compare the sand used in both studies. However, a study by Pandolf et al. (1976) found a positive linear relationship between increasing footprint depth in snow and an increase in energetic costs during walking at 0.6ms^{-1} and 1.1ms^{-1}, suggesting there may be some causative link between depth of depression into a compliant substrate and energy expenditure.

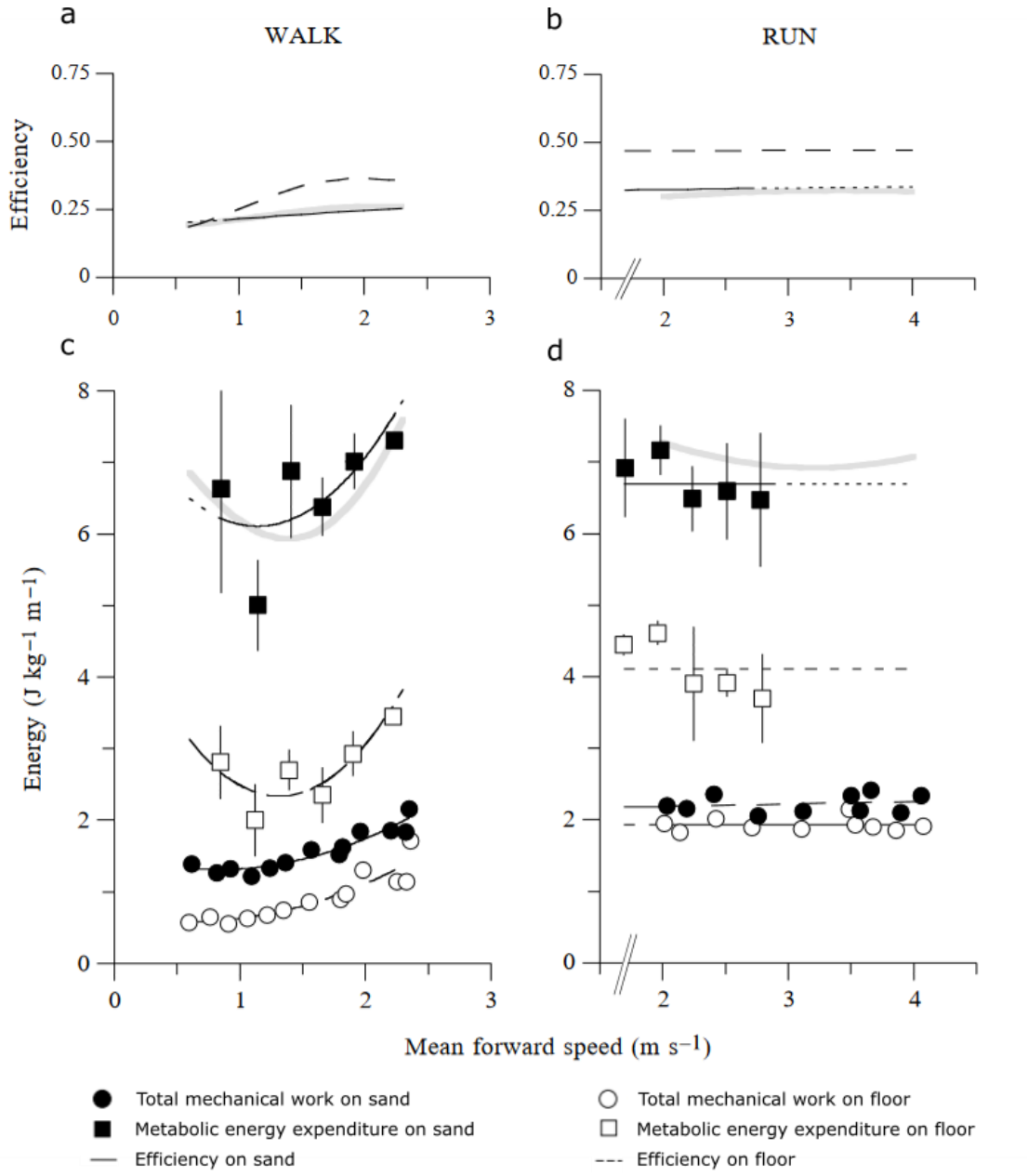

Figure 1.4: The metabolic cost, mechanical work and muscle-tendon efficiency during walking and running on hard floor and sand surfaces. Muscle tendon efficiency calculated as the ratio between the total mechanical work done and the energy expended (assuming an energetic equivalent of 20.1 $J \cdot ml^{-1}{}_{O_2}$) during ***(a)*** walking and ***(b)*** running. Total mechanical work (squares) and metabolic cost (circles) as a function of speed during ***(c)*** walking and ***(d)*** running. Filled symbols and continuous lines refer to locomotion on sand and open symbols and broken lines refer to locomotion on floor. Adapted from Lejeune et al. (1998, p. 2077).

The different authors propose slightly different, yet possibly associated, reasons for the increased energetic costs. Zamparo et al. (1992) attributed the increased energetic costs on sand to a reduced recovery of potential and kinetic energy at each stride whereas Lejeune et al. (1998) suggest that when walking on sand, humans retain a

relatively high pendular energy exchange mechanism, whilst running maintains a bouncing mechanism. Instead, Lejeune et al. (1998) attributed the increased energetic costs to increased mechanical work done on the sand and a decrease in the efficiency of positive work done by the muscles and tendons (Fig. 1.4). Efficiency is defined as the ratio of mechanical work done to metabolic energy expended (Lejeune, Willems & Heglund 1998). During each ground contact, the individual performs work on the surface, resulting in deformation energy being input into the surface (Fig. 1.5a) and as the foot leaves the surface, some of this energy can be transferred back to the person (Fig. 1.5b). The amount of energy storage is dependent on surface properties such as surface stiffness and surface deformation (Nigg 2007). Substrates that exhibit elastic deformation can return most of the energy with minimal energy loss (Fig. 1.5c). Resilient compliant substrates can effectively store and recycle energy from step to step, as shown by research into optimising sports tracks and footwear (Baroud, Nigg & Stefanyshyn 1999; Hoogkamer et al. 2018; McMahon & Greene 1979).

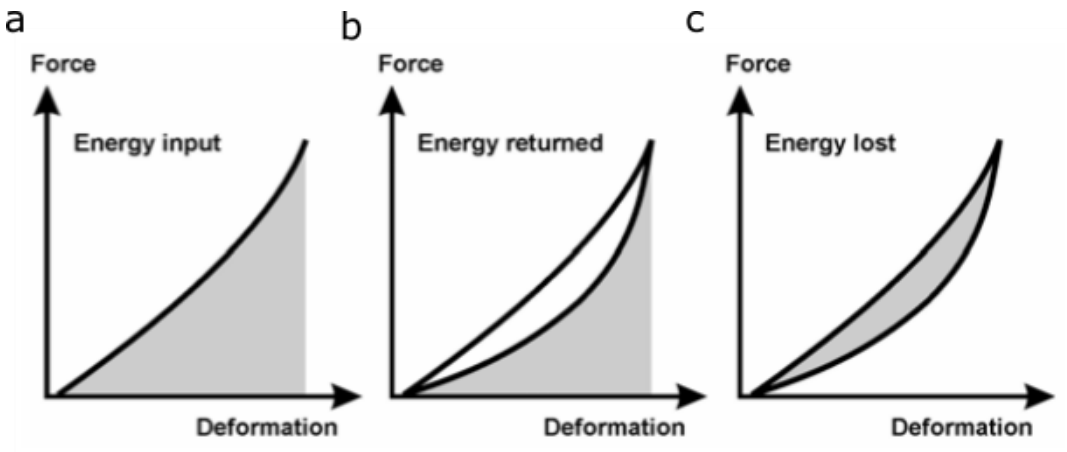

Figure 1.5: Energy ***(a)*** input, ***(b)*** return and ***(c)*** lost in substrates with elastic deformation. The shaded region depicts the magnitude of the energy. From Stefanyshyn and Nigg (2003, p. 34).

On the other hand, natural compliant substrates such as sand act like a damper, which absorbs and dissipates energy. During locomotion on sand, the substrate is subjected to both elastic and plastic deformation. Initially, the substrate is subjected to a period of elastic deformation as the sediment resists deformation but as loading increases, the yield stress is reached, leading to plastic deformation and the

formation of a footprint and thus, greater energy loss to the substrate (Allen 1997). On sand, the foot sinks and often slip backwards as the sand is displaced. Zamparo et al. (1992) and Pinnington and Dawson (2001) suggested that foot slippage during push-off contribute to increased energetic costs when walking on sand. Reduced elastic energy absorption and greater energy loss due to slipping has been shown in studies on running and jumping on sand (Giatsis et al. 2004; Impellizzeri et al. 2008). Reduced elastic energy return means greater mechanical work is required by the muscles to ensure acceleration and forward movement of the centre of mass (CoM) during the propulsive phase into push-off (Tesio & Rota 2019).

During locomotion on sand, the sand is displaced under the foot. The unpredictable nature of the sand require muscles in the leg to constantly work to ensure stability, resulting in additional external work (Lejeune, Willems & Heglund 1998; Zamparo et al. 1992). Pinnington and Dawson (2001) found greater co-activation of the knee and ankle muscles during walking and running on sand and Bates et al. (2013b) speculated that increased activation of ankle extensors, specifically, may be a major contributor to increased energetic costs on sand. Voloshina et al. (2013) found increased variability in ankle angle, an increase in mean muscle activity and increased mechanical work at the hip and knee joint on uneven substrates and suggested there may be a potential increase in muscle co-activation. There was also greater co-activation at the ankle joint observed on slippery surfaces (Cappellini et al. 2010; Marigold & Patla 2002). Giatsis et al. (2004) observed an increased range of motion at the ankle joint prior to push-off during jumping on sand, which may be have been caused by foot slippage. Pinnington and Dawson (2001) suggested that when running on sand, compared to a non-compliant surface, the foot is in contact with the ground for longer as a mechanism to improve stability and reduce foot slippage.

Several studies have shown that individuals will adapt their spatiotemporal parameters according to the substrate. Humans will self-select slower speeds when moving on snow (Ramaswamy et al. 1966), rough terrain (Gast, Kram & Riemer 2019) and slippery surfaces (Cappellini et al. 2010). On uneven surfaces, Voloshina

et al. (2013) found greater step width and length variability. During walking on loose rock surfaces, humans subjects lowered their CoM and enlarged their base of support to increase stability (Gates et al. 2012). On slippery surfaces, as well as slower walking speeds, participants displayed shorter stride lengths, flatter foot-floor angles at heel-strike and increased muscle activation (Cappellini et al. 2010; Marigold & Patla 2002). These changes seem to reflect a gait strategy to keep the CoM centred over the supporting limb and increase limb stiffness. It has been shown that during running and hopping on compliant substrates, humans adjust leg stiffness to accommodate reductions in surface stiffness and preserve gait mechanics such as CoM vertical displacement and ground contact time to increase stability (Ferris, Liang & Farley 1999; Ferris, Louie & Farley 1998).

Therefore, while it is generally well accepted that energy expenditure increases on complex, uneven and compliant substrates, there is no clear consensus as to which mechanisms are responsible for this increase. It is possible that different strategies can be applied for different substrates. Furthermore, on compliant substrates, there may be different mechanisms according to the level of substrate compliance. This uncertainty on gait mechanisms on compliant substrates indicate that further research is required to determine the changes in walking biomechanics on compliant substrates and how they might relate to increased metabolic cost.

1.3 Aims and thesis structure

1.3.1 Aims and objectives

Whilst a substantial body of literature has sought to understand the elevated energetic costs on complex, uneven and compliant substrates, the primary mechanistic causes behind this increase is unclear. Possible reasons for this uncertainty include the measurement of different variables across studies and

variation in substrates used. This thesis aims to address these issues by presenting a large experimental data set of human walking on both artificial (foam) and natural (sand) compliant substrates. The overall aim of this thesis is to improve our understanding of the relationship between substrate properties, gait biomechanics and muscle activities. This aim will be pursued through the following objectives:

- To determine energetics costs, muscle activity of the lower limb and trunk and lower limb motion on foam versus hard floor (chapter 2)
- To determine muscle activity of the lower limb and trunk and lower limb motion on sand versus hard floor (chapter 3)
- To determine the similarities and differences between gait changes and muscle activities between walking on foam and sand (chapter 4)

In conducting studies to address these aims, we can further our understanding of how substrate properties affects human gait. The overall hypothesis of this thesis is that gross gait adaptations like sagittal kinematics, mechanical energy exchange and spatiotemporal parameters are adopted in response to the depth of depression into a compliant substrate rather than the complex properties of the substrate itself.

1.3.2 Thesis structure

1.3.2.1 Chapter 2 overview

This chapter formed the basis of a manuscript that has been published. While I carried out the majority of the experimental research, the work benefited from the contribution of a number of co-authors as follows:

Dr Karl Bates (KB), Dr Kristiaan D'Août (KD) and Dr Peter Falkingham (PF) conceived the study.

KB, KD, PF, Dr James Charles (JC) and Barbara Grant (BFG) designed the study.

JC and BFG collected the experimental data.

Dr Brendan Geraghty (BG) performed the material testing of substrates.

JC performed the multi-body dynamics analysis.

BFG processed and analysed the experimental data and conducted the statistical analyses with some coding assistance from Dr Jamie Gardiner (JG) and guidance from KB, KD and PF.

BFG, JC, BG contributed to writing the manuscript.

All authors contributed to editing the manuscript.

1.3.2.2 Chapter 3 overview

This chapter formed the basis of a manuscript that is currently being developed for publication. While I carried out the majority of the research, the work benefited from the contribution of a number of co-authors as follows:

KB, KD and PF conceived the study.

KB, KD, PF, and BFG designed the study.

JC and BFG collected the experimental data.

BFG processed and analysed the experimental data and conducted the statistical analyses with guidance from all co-authors.

The present thesis version was drafted by BFG and benefited from editorial suggestions from KB.

1.3.2.3 Chapter 4 overview

This chapter includes a comparison between experimental data collected from the two studies discussed in chapters 2-3. This chapter is currently being developed for publication. While I carried out the majority of the research, the work benefited from the contribution of co-authors as follows:

BFG processed and analysed the experimental data and conducted the statistical analyses with guidance from all co-authors.

The present thesis version was drafted by BFG and benefited from editorial suggestions from KB.

1.3.2.4 Chapter 5 overview

This chapter provides a general discussion of the findings presented in this thesis, limitations of the research conducted and how the methods, results and implications of these studies can be used to direct future research.

1.4 References

Alexander, R.M. (1976) 'Mechanics of bipedal locomotion', *Perspectives in experimental biology*, vol. 1, pp. 493-504.

Alexander, R.M. (1983) *Animal mechanics*, Blackwell.

Alexander, R.M. (1984) 'Elastic energy stores in running vertebrates', *American Zoologist*, vol. 24, no. 1, pp. 85-94.

Alexander, R.M. (2002) 'Tendon elasticity and muscle function', *Comp Biochem Physiol A Mol Integr Physiol*, vol. 133, no. 4, pp. 1001-1011.

Allen, J.R.L. (1997) 'Subfossil mammalian tracks (Flandrian) in the Severn Estuary, S. W. Britain: mechanics of formation, preservation and distribution', *Philosophical Transactions of the Royal Society of London. Series B: Biological Sciences*, vol. 352, no. 1352, pp. 481-518.

Baroud, G., Nigg, B. & Stefanyshyn, D. (1999) 'Energy storage and return in sport surfaces', *Sports Engineering*, vol. 2, no. 3, pp. 173-180.

Bates, K.T., Savage, R., Pataky, T.C., Morse, S.A., Webster, E., Falkingham, P.L., Ren, L., Qian, Z., Collins, D., Bennett, M.R., McClymont, J. & Crompton, R.H. (2013) 'Does footprint depth correlate with foot motion and pressure?', *J R Soc Interface*, vol. 10, no. 83, p. 20130009.

Biewener, A. & Patek, S. (2018) Energetics of Locomotion, in A.A. Biewener & S.N. Patek (eds), *Animal Locomotion*, Oxford University Press, p. 0.

Brockett, C.L. & Chapman, G.J. (2016) 'Biomechanics of the ankle', *Orthop Trauma*, vol. 30, no. 3, pp. 232-238.

Brunner, R. & Rutz, E. (2013) 'Biomechanics and muscle function during gait', *J Child Orthop*, vol. 7, no. 5, pp. 367-371.

Cappellini, G., Ivanenko, Y.P., Dominici, N., Richard, E. & Lacquaniti, F. (2010) 'Motor Patterns During Walking on a Slippery Walkway', *Journal of Neurophysiology*, vol. 103, no. 2, pp. 746-760.

Cappellini, G., Ivanenko, Y.P., Poppele, R.E. & Lacquaniti, F. (2006) 'Motor patterns in human walking and running', *J Neurophysiol*, vol. 95, no. 6, pp. 3426-3437.

Cavagna, G.A., Heglund, N.C. & Taylor, C.R. (1977) 'Mechanical work in terrestrial locomotion: two basic mechanisms for minimizing energy expenditure', *American Journal of Physiology-Regulatory, Integrative and Comparative Physiology*, vol. 233, no. 5, pp. R243-R261.

Cavagna, G.A. & Kaneko, M. (1977) 'Mechanical work and efficiency in level walking and running', *J Physiol*, vol. 268, no. 2, pp. 467--481.

Cavagna, G.A., Thys, H. & Zamboni, A. (1976) 'The sources of external work in level walking and running', *J Physiol*, vol. 262, no. 3, pp. 639-657.

Collins, S.H. & Kuo, A.D. (2010) 'Recycling energy to restore impaired ankle function during human walking', *PLoS One*, vol. 5, no. 2, p. e9307.

Davies, S.E.H. & Mackinnon, S.N. (2006) 'The energetics of walking on sand and grass at various speeds', *Ergonomics*, vol. 49, no. 7, pp. 651-660.

Dewolf, A.H., Ivanenko, Y.P., Lacquaniti, F. & Willems, P.A. (2017) 'Pendular energy transduction within the step during human walking on slopes at different speeds', *PLOS ONE*, vol. 12, no. 10, p. e0186963.

Ferris, D.P. & Farley, C.T. (1997) 'Interaction of leg stiffness and surface stiffness during human hopping', *Journal of Applied Physiology*, vol. 82, no. 1, pp. 15-22.

Ferris, D.P., Liang, K. & Farley, C.T. (1999) 'Runners adjust leg stiffness for their first step on a new running surface', *Journal of Biomechanics*, vol. 32, no. 8, pp. 787-794.
Ferris, D.P., Louie, M. & Farley, C.T. (1998) 'Running in the real world: adjusting leg stiffness for different surfaces', *Proc Biol Sci*, vol. 265, no. 1400, pp. 989-994.
Fukuchi, C.A., Fukuchi, R.K. & Duarte, M. (2019) 'Effects of walking speed on gait biomechanics in healthy participants: a systematic review and meta-analysis', *Systematic Reviews*, vol. 8, no. 1, p. 153.
Full, R.J., Kubow, T., Schmitt, J., Holmes, P. & Koditschek, D. (2002) 'Quantifying Dynamic Stability and Maneuverability in Legged Locomotion1', *Integrative and Comparative Biology*, vol. 42, no. 1, pp. 149-157.
Gast, K., Kram, R. & Riemer, R. (2019) 'Preferred walking speed on rough terrain: is it all about energetics?', *Journal of Experimental Biology*, vol. 222, no. 9.
Gates, D.H., Wilken, J.M., Scott, S.J., Sinitski, E.H. & Dingwell, J.B. (2012) 'Kinematic strategies for walking across a destabilizing rock surface', *Gait & Posture*, vol. 35, no. 1, pp. 36-42.
Geyer, H., Seyfarth, A. & Blickhan, R. (2006) 'Compliant leg behaviour explains basic dynamics of walking and running', *Proc Biol Sci*, vol. 273, no. 1603, pp. 2861-2867.
Giatsis, G., Kollias, I., Panoutsakopoulos, V. & Papaiakovou, G. (2004) 'Biomechanical differences in elite beach-volleyball players in vertical squat jump on rigid and sand surface', *Sports Biomech*, vol. 3, no. 1, pp. 145-158.
Halsey, L.G. (2016) 'Terrestrial movement energetics: current knowledge and its application to the optimising animal', *Journal of Experimental Biology*, vol. 219, no. 10, pp. 1424-1431.
Hansen, N.L., Hansen, S., Christensen, L.O., Petersen, N.T. & Nielsen, J.B. (2001) 'Synchronization of lower limb motor unit activity during walking in human subjects', *J Neurophysiol*, vol. 86, no. 3, pp. 1266-1276.
Hoogkamer, W., Kipp, S., Frank, J.H., Farina, E.M., Luo, G. & Kram, R. (2018) 'A Comparison of the Energetic Cost of Running in Marathon Racing Shoes', *Sports Medicine*, vol. 48, no. 4, pp. 1009-1019.
Horsak, B., Slijepcevic, D., Raberger, A.-M., Schwab, C., Worisch, M. & Zeppelzauer, M. (2020) 'GaitRec, a large-scale ground reaction force dataset of healthy and impaired gait', *Scientific Data*, vol. 7, no. 1, p. 143.
Impellizzeri, F.M., Rampinini, E., Castagna, C., Martino, F., Fiorini, S. & Wisloff, U. (2008) 'Effect of plyometric training on sand versus grass on muscle soreness and jumping and sprinting ability in soccer players', *British Journal of Sports Medicine*, vol. 42, no. 1, pp. 42-46.
Kuo, A.D., Donelan, J.M. & Ruina, A. (2005) 'Energetic Consequences of Walking Like an Inverted Pendulum: Step-to-Step Transitions', *Exercise and Sport Sciences Reviews*, vol. 33, no. 2, pp. 88-97.
Lejeune, T.M., Willems, P.A. & Heglund, N.C. (1998) 'Mechanics and energetics of human locomotion on sand', *Journal of Experimental Biology*, vol. 201, no. 13, pp. 2071-2080.
Marigold, D.S. & Patla, A.E. (2002) 'Strategies for Dynamic Stability During Locomotion on a Slippery Surface: Effects of Prior Experience and Knowledge', *Journal of Neurophysiology*, vol. 88, no. 1, pp. 339-353.
McMahon, T.A. & Greene, P.R. (1979) 'The influence of track compliance on running', *J Biomech*, vol. 12, no. 12, pp. 893-904.

Niederer, D., Engeroff, T., Fleckenstein, J., Vogel, O. & Vogt, L. (2021) 'The age-related decline in spatiotemporal gait characteristics is moderated by concerns of falling, history of falls & diseases, and sociodemographic-anthropometric characteristics in 60–94 years old adults', *European Review of Aging and Physical Activity*, vol. 18, no. 1, p. 19.

Nielsen, J.B. (2003) 'How we Walk: Central Control of Muscle Activity during Human Walking', *The Neuroscientist*, vol. 9, no. 3, pp. 195-204.

Nigg, B.M. (2007) *Biomechanics of the musculo-skeletal system*, John Wiley & Sons Incorporated.

O'Neill, M.C., Demes, B., Thompson, N.E., Larson, S.G., Stern, J.T. & Umberger, B.R. (2022) 'Adaptations for bipedal walking: Musculoskeletal structure and three-dimensional joint mechanics of humans and bipedal chimpanzees (Pan troglodytes)', *Journal of Human Evolution*, vol. 168, p. 103195.

Pandolf, K.B., Haisman, M.F. & Goldman, R.F. (1976) 'Metabolic energy expenditure and terrain coefficients for walking on snow', *Ergonomics*, vol. 19, no. 6, pp. 683-690.

Pandy, M.G. & Andriacchi, T.P. (2010) 'Muscle and joint function in human locomotion', *Annu Rev Biomed Eng*, vol. 12, pp. 401-433.

Perry, J. & Burnfield, J.M. (2010) 'Gait analysis. Normal and pathological function 2nd ed', *California: Slack*.

Peyré-Tartaruga, L.A. & Coertjens, M. (2018) 'Locomotion as a Powerful Model to Study Integrative Physiology: Efficiency, Economy, and Power Relationship', *Front Physiol*, vol. 9, p. 1789.

Pinnington, H.C. & Dawson, B. (2001) 'The energy cost of running on grass compared to soft dry beach sand', *Journal of Science and Medicine in Sport*, vol. 4, no. 4, pp. 416-430.

Ramaswamy, S.S., Dua, G.L., Raizada, V.K., Dimri, G.P., Viswanathan, K.R., Madhaviah, J. & Srivastava, T.N. (1966) 'Effect of looseness of snow on energy expenditure in marching on snow-covered ground', *Journal of Applied Physiology*, vol. 21, no. 6, pp. 1747-1749.

Roberts, T.J. & Azizi, E. (2011) 'Flexible mechanisms: the diverse roles of biological springs in vertebrate movement', *Journal of Experimental Biology*, vol. 214, no. 3, pp. 353-361.

Schmitt, D. (2003) 'Insights into the evolution of human bipedalism from experimental studies of humans and other primates', *Journal of Experimental Biology*, vol. 206, no. 9, pp. 1437-1448.

Silva, L.M. & Stergiou, N. (2020) Chapter 7 - The basics of gait analysis, in N. Stergiou (ed.), *Biomechanics and Gait Analysis*, Academic Press, pp. 225-250.

Stefanyshyn, D.J. & Nigg, B.M. (2003) 'Energy and performance aspects in sports surfaces', *Sports Biomech*, pp. 31-46.

Tesio, L. & Rota, V. (2019) 'The Motion of Body Center of Mass During Walking: A Review Oriented to Clinical Applications', *Frontiers in Neurology*, vol. 10.

Tunca, C., Pehlivan, N., Ak, N., Arnrich, B., Salur, G. & Ersoy, C. (2017) 'Inertial Sensor-Based Robust Gait Analysis in Non-Hospital Settings for Neurological Disorders', *Sensors*, vol. 17, no. 4, p. 825.

Voloshina, A.S., Kuo, A.D., Daley, M.A. & Ferris, D.P. (2013) 'Biomechanics and energetics of walking on uneven terrain', *Journal of Experimental Biology*, vol. 216, no. 21, pp. 3963-3970.

Wade, C., Redfern, M.S., Andres, R.O. & Breloff, S.P. (2010) 'Joint kinetics and muscle activity while walking on ballast', *Human Factors*, vol. 52, no. 5, pp. 560-573.

Wilson, A. & Lichtwark, G. (2011) 'The anatomical arrangement of muscle and tendon enhances limb versatility and locomotor performance', *Philos Trans R Soc Lond B Biol Sci*, vol. 366, no. 1570, pp. 1540-1553.

Winter, D.A. (1984) 'Kinematic and kinetic patterns in human gait: Variability and compensating effects', *Human Movement Science*, vol. 3, no. 1, pp. 51-76.

Zamparo, P., Perini, R., Orizio, C., Sacher, M. & Ferretti, G. (1992) 'The energy cost of walking or running on sand', *European Journal of Applied Physiology and Occupational Physiology*, vol. 65, no. 2, pp. 183-187.

Chapter two: Why does the metabolic cost of walking increase on compliant substrates?

This chapter formed the basis of a manuscript that has been published:

Grant, B., Charles, J., Geraghty, B., Gardiner, J., D'Août, K., Falkingham, P.L. and Bates, K.T. (2022). Why does the metabolic cost of walking increase on compliant substrates? *Journal of the Royal Society Interface*, **19**(196): 20220483. doi:10.1098/rsif.2022.0483

Author contributions. Dr Karl Bates (KB), Dr Kristiaan D'Août (KD) and Dr Peter Falkingham (PF) conceived the study. KB, KD, PF, Dr James Charles (JC) and Barbara Grant (BFG) designed the study. JC and BFG collected the experimental data. Dr Brendan Geraghty (BG) performed the material testing of substrates. JC performed the multi-body dynamics analysis. BFG processed and analysed the experimental data and conducted the statistical analyses with some coding assistance from Dr Jamie Gardiner (JG) and guidance from KB, KD and PF. BFG, JC, BG contributed to writing the manuscript. All authors contributed to editing the manuscript.

This chapter incorporates additional text and figures in the methods section that are not included in the manuscript. All other figures included in this chapter are available in the main text or supplementary material for publication.

The energy expenditure values calculated from this study are included in a published paper:

Charles, J. P., Grant, B., D'Août, K., and Bates, K.T. (2021). "Foot anatomy, walking energetics, and the evolution of human bipedalism." *Journal of human evolution* 156: 103014.

2.1 Abstract

Walking on compliant substrates requires more energy than walking on hard substrates but the biomechanical factors that contribute to this increase are debated. Previous studies suggest various causative mechanical factors, including disruption to pendular energy recovery, increased muscle work, decreased muscle efficiency and increased gait variability. We test each of these hypotheses simultaneously by collecting a large kinematic and kinetic data set of human walking on foams of differing thickness. This allowed us to systematically characterise changes in gait with substrate compliance, and, by combining data with mechanical substrate testing, drive the very first subject-specific computer simulations of human locomotion on compliant substrates to estimate the internal kinetic demands on the musculoskeletal system. Negative changes to pendular energy exchange or ankle mechanics are not supported by our analyses. Instead we find that the mechanistic causes of increased energetic costs on compliant substrates are more complex than captured by any single previous hypothesis. We present a model in which elevated activity and mechanical work by muscles crossing the hip and knee are required to support the changes in joint (greater excursion and maximum flexion) and spatiotemporal kinematics (longer stride lengths, stride times and stance times, and duty factors) on compliant substrates.

2.2 Introduction

The evolution of animal locomotion has mostly occurred on substrates with complex heterogeneous topography and material properties. However, our current understanding of animal gait and energetics is dominated by studies on hard, level surfaces in laboratories, which do not reflect most naturally occurring terrains. Recent work on humans has shown that locomotion on complex substrates like loose rock surfaces (Gates et al. 2012), ballast (Wade et al. 2010), uneven (Holowka et al.

2022; Voloshina et al. 2013) and compliant (Davies & Mackinnon 2006; Kerdok et al. 2002; Lejeune, Willems & Heglund 1998; Pinnington & Dawson 2001; Soule & Goldman 1972; Zamparo et al. 1992) terrains is typically associated with an increase in energy expenditure relative to uniform, non-deforming substrates. The term 'compliant' has been used broadly within the field (Davies & Mackinnon 2006; Kerdok et al. 2002; Lejeune, Willems & Heglund 1998; Pinnington & Dawson 2001; Soule & Goldman 1972; Zamparo et al. 1992) to refer to any substrate that has non-neglible deformation under loads typically generated during human locomotion. A substantial body of literature has sought to understand elevated energetic costs on compliant substrates like sand, mud and snow (Lejeune, Willems & Heglund 1998; Pandolf, Haisman & Goldman 1976; Soule & Goldman 1972; Zamparo et al. 1992) but at present there remains little consensus about the primary mechanistic causes.

Lejeune et al. (1998) and Zamparo et al. (1992) compared the change in the energetic cost of transport (CoT) on sand across a range of speeds. These studies discovered different magnitudes and nature of change in CoT with speed on compliant sands and invoked different biomechanical mechanisms to explain these increases. Lejeune et al. (1998) attributed the higher energetic costs to an increase in muscle-tendon work and a decrease in muscle-tendon efficiency whereas Zamparo et al. (1992) proposed that it was due to a lower energy recovery through a reduction in the efficiency of pendular energy exchange in walking and in the reduced recovery of elastic energy storage in running. Pinnington and Dawson (2001) suggested a potential increase in muscle co-activation and an increase in foot contact time on compliant substrates may lead to increased oxygen consumption due to a reduction in elastic energy storage and recovery, and ultimately a decrease in muscle-tendon efficiency. These authors noted that foot slippage may also play a role, as postulated by Zamparo et al. (1992). Voloshina et al. (2013) found an increase in mean muscle activity and increased mechanical work on uneven substrates and suggested there may be a potential increase in muscle co-activation. Bates et al. (2013b) speculated that increased activation of ankle extensors, specifically, may be a major contributor to increased CoT on sand. Pandolf et al. (1976) proposed that increasing work to

raise the CoM, a stooping posture and difficulties maintaining stability are the primary causes of increased CoT when walking on snow.

Therefore, while it is widely accepted that compliant substrates incur an increase in CoT, there remains considerable uncertainty about the relative contribution of different biomechanical factors underpinning this increase. Possible reasons include the measurement of different variables across studies (Davies & Mackinnon 2006), variation in footwear (e.g. barefoot, different types of shoes; but see Pinnington & Dawson (2001)), substrates used, and the gaits and speeds tested. Unfortunately, the absence of quantification of the mechanical properties of the compliant substrates used across past studies impedes comparison. In this study, we attempt to address these issues and provide an exhaustive evaluation of why the energetic cost of walking increases as substrate compliance increases. To achieve this, we present a large experimental kinematic and kinetic data set of human walking on foams of differing thickness, with detailed characterisation of substrate mechanical properties by uniaxial compression testing. Quantification of substrate properties not only facilitates repeatability and systematic comparison to other substrates but also allows us to carry out subject-specific computer simulations of locomotion across compliant substrates. This validated individualised computational framework (Charles et al. 2020) allows for the prediction of aspects of internal kinetics and muscle performance that cannot be measured non-invasively, so could give further insights into the mechanisms behind locomotor cost beyond those allowed by experimental methods alone. Through this integrated experimental-computational workflow we test the previously proposed hypotheses that increased CoT on compliant substrates is primarily the result of (HYP1) negative disruption to pendular energetic exchange (Zamparo et al. 1992), (HYP2a) increased muscle activation throughout the support limb (Voloshina et al. 2013) or (HYP2b) within specific muscle groups (Bates et al. 2013b), (HYP3) increased musculotendon unit (MTU) work and decreased efficiency (Lejeune, Willems & Heglund 1998) and/or (HYP4) correcting greater instabilities indicated by increased variability in gait (Pandolf, Haisman & Goldman 1976).

2.3 Methods

2.3.1 Substrates

To examine how variance in substrate compliance impacts gait, the compliant substrates used in this study are the same foam but with different levels of thickness. In total, there were three different substrates included in this study: 1) hard, level floor, 2) compliant polyether polyurethane foam with a thickness of 6 cm ("Thin foam") and 3) the same foam of 13 cm thickness ("Thick foam") (eFoam.co.uk. Medium Foam. Density Range: 31-34 kgm-3, Hardness strength: 100-130Nm) seen in figure 2.1. The foam walkways were made up of several foam sections, totalling 13.2m in length and a width of 0.6m.

Figure 2.1: Example of the compliant substrates: 13cm "thick" compliant foam (back) and 6cm "thin" compliant foam (front).

2.3.2 Participant set-up

Thirty young, healthy individuals were recruited to take part in this study involving walking experiments on foam. This study was conducted at the University of Liverpool Gait Lab at the Institute of Life Course and Medical Sciences and all participants signed informed consent before participating in the study in accordance with ethical approval from the University of Liverpool's Central University Research Ethics Committee for Physical Interventions (#3757). The participants had their key biometrics recorded, including height and weight (15 males, 15 females; age = 27.4 ± 3.8 years; height= 1.76 ± 0.1 m; body mass = 71.1 ± 9.0 kg; body mass index = 23.0 ± 2.1 kgm^{-2}; see Table 3.1). Participants were then prepared for the walking trials by attaching reflective markers for 3D kinematics and surface-electromyography (sEMG) for muscle activity data. A total of 69 reflective markers were attached at key anatomical landmarks on the participant following an adapted version of the University of Liverpool Evolutionary Morphology and Biomechanics (EMB) whole-body standard marker set and Oxford Foot Model (Carson et al. 2001; Dixon, Böhm & Döderlein 2012) (Table 2.2). For sEMG, standard skin preparation methods were utilised: 1) locate sensor site 2) shave any excess body hair 3) wipe with alcohol 4) attach sensor (Hermens et al. 2000). Sensors were placed on the muscle belly in-line with the approximate expected direction of the muscle fibres in humans. The signal of each sensor was tested by asking the participant to perform certain actions (e.g. flexing and extending knee) and checked for baseline noise and impedance. If the signal was poor, the sensors were re-attached following the previous steps. Electrodes were positioned to record the activity of 8 left lower extremity muscles: biceps femoris (BFL), rectus femoris (RF), vastus lateralis (VL), vastus medialis (VM), tibialis anterior (TA), lateral gastrocnemius (LG), medial gastrocnemius (MG) and soleus (SOL) on the left side only (Figure 2.2; for muscle function and attachments see Table 6.1). All markers and sensors were attached by the same examiner for all participants, with the exception of one (Subject 27).

Table 2.1. Anthropometric measurements from each subject: subject number, age (years), gender (male/female), height (m), body mass (kg) and BMI (kgm^{-2}) with mean and standard deviation of all 30 participants.

Subject	Age	Gender	Height (m)	Body mass (kg)	BMI (kgm^{-2})
1	35	m	1.76	68	21.95
2	25	m	1.75	71.1	23.22
3	32	m	1.82	74.7	22.55
4	26	f	1.76	72.6	23.44
5	21	f	1.77	76	24.26
6	21	f	1.7	57.5	19.90
7	24	m	1.75	68	22.20
8	27	m	1.93	90	24.16
9	23	m	1.8	77.4	23.89
10	29	m	1.8	80.6	24.88
11	33	f	1.65	60.6	22.26
12	26	m	1.81	68	20.76
13	29	m	1.77	68.9	21.99
14	29	f	1.67	62.5	22.41
15	32	f	1.68	53.7	19.03
16	28	m	1.86	83.3	24.08
17	39	f	1.78	80	25.25
18	25	m	1.72	71.2	24.07
19	27	f	1.7	68	23.53
20	26	f	1.635	53.5	20.01
21	29	f	1.8	66	20.37
22	26	f	1.71	57.6	19.70
23	27	f	1.72	81	27.38
24	27	f	1.75	65.1	21.26
25	25	m	1.78	78	24.62
26	26	f	1.69	77	26.96
27	27	m	1.74	78	25.76
28	26	m	1.78	77.2	24.37
29	27	f	1.72	65.5	22.14
30	25	m	1.91	81.2	22.26
Mean	27.40	15m 15f	1.76	71.07	22.95
SD	3.76		0.07	8.99	2.06

Table 2.2: Reflective marker set-up based on the full body EMB standard marker set and the Oxford foot model.

Trunk: 5 markers	
LACR RACR	Acromion (left and right)
JUG	Jugular notch
XYPH	Xyphisternal joint
C7	Spine of the 7th cervical vertebra

Head: 4 markers	
HEADF HEADB HEADL HEADR	Band with four markers (1 front, 1 back, 2 side)

Pelvis: 6 markers	
LASIS RASIS	Anterior superior iliac spine
LPSI RPSI	Posterior superior iliac spine
LICR RICR	Iliac crest tubercle

Upper leg: 7 markers (x2)	
LGTR RGTR	Greater trochanter
LLEPI RLEPI	Lateral epicondyle
LMEPI RMEPI	Medial epicondyle
LTHPA LTHPP LTHDA LTDP RTHPA RTHPP RTHDA RTDP	Left and Right THIGH plates: proximal/distal and anterior/posterior

Lower leg: 8 markers (x2)	
LFIB RFIB	Fibular head
LLMAL RLMAL	Lateral malleolus
LMMAL RMMAL	Medial malleolus
LSHPA LSHPP LSHDA LSHP RSHPA RSHPP RSHDA RSHDP	Left and Right SHANK plates: proximal/distal and anterior/posterior
LTUB RTUB	Tibial tuberosity

Foot: 10 markers (x2)	
LLCA RLCA	Lateral calcaneus
LCAL RCAL	Back of Heel
LSTL RSTL	Sustentaculum tail
LNAV RNAV	Navicular
LP1M RP1M	Metatarsal I base
LP5M RP5M	Metatarsal V base
LD1M RD1M	Metatarsal I head
LD5M RD5M	Metatarsal V head
LTOE RTOE	Between metatarsal I and II heads
LHALL RHALL	Hallux (tip)

Arms: 2 markers (x2)	
LHUM RHUM	Lateral humeral epicondyle
LULNA RULNA	Ulnar head (distal epiphysis)

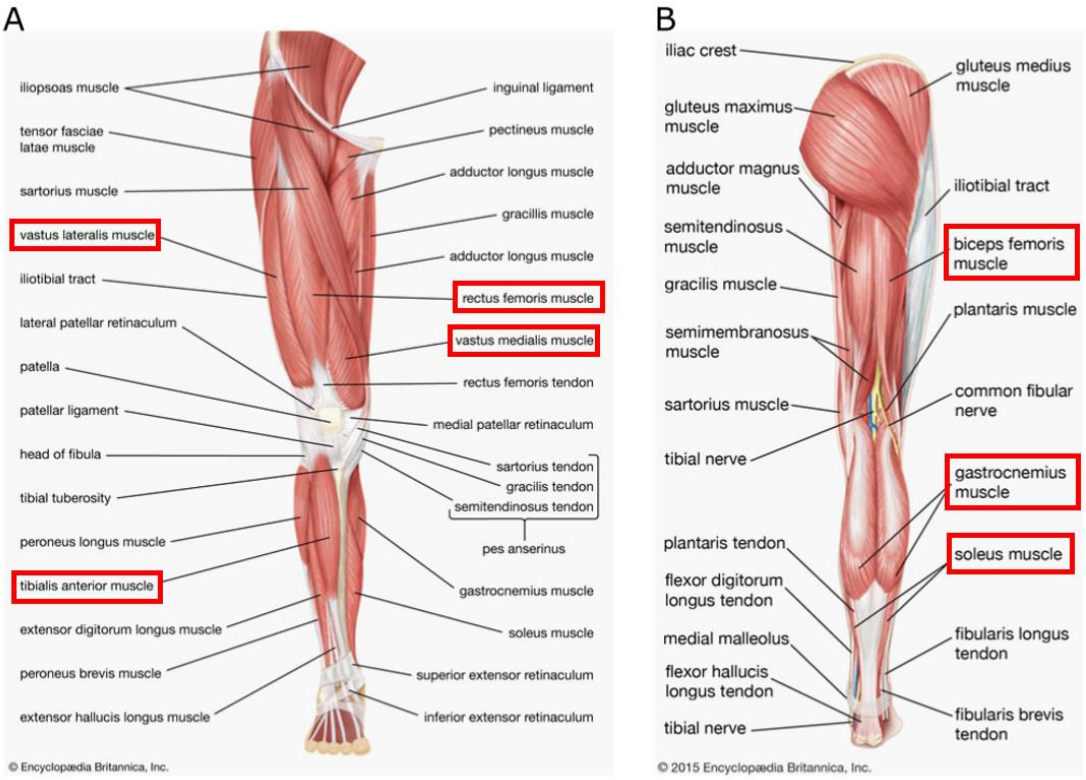

Figure 2.2: sEMG sensor set-up on the lower limbs: ***a)*** Anterior view (rectus femoris, vastus lateralis, vastus medialis and tibialis anterior) and ***b)*** posterior view (biceps femoris long head, lateral gastrocnemius, medial gastrocnemius and soleus muscle). Muscles measured in this study are highlighted with a red box. All lower limb muscles were measured on the left side only. From Britannica (2022).

2.3.3 Data collection

Before participant set-up, the participants spent 15 minutes of lying in a supine position in order to record resting metabolic rates. A K5 wearable metabolic unit (COSMED, Rome) was used to measure oxygen uptake ($\dot{V}O_{2,}$ ml s^{-1}) and carbon dioxide produced ($\dot{V}CO_{2,}$ ml s^{-1}) in a breath-by-breath analysis. Then after participant set-up, participants performed two sets of walking trials: continuous walking trials (walking back and forth in both directions by turning at the end of each walkway) and single trials (walking from one end of the walkway to the other end in one direction). First, participants stood still with their arms outstretched and the person was photographed from different angles for the creation of the simulation models using photogrammetry. Then, a static trial in the anatomical position was recorded.

Participants performed 7 minutes of continuous walking at a self-selected speed on each substrate, with the foams placed over 3 in-series force plates (Kistler 9281E) in the centre of their length, with respirometry measured throughout and 3D kinematics, ground reaction forces (GRFs) and EMG recorded for 30 s at every minute from 3 min onwards (Fig. 2.3). Participants had a 5 minute resting period before and after each recording.

Figure 2.3: Example of walking on thin foam substrate placed over 3 in-series force plates with kinematic markers, sEMG sensors and a K5 wearable metabolic unit measuring oxygen uptake ($\dot{V}_{O_2}$, ml s^{-1}) and carbon dioxide produced ($\dot{V}_{CO_2}$, ml s^{-1}).

An additional 15 single trials were collected where a participant completed a single continuous passage across the substrates (with substrate order randomised) while only 3D kinematics and EMG were measured. Marker tracking and EMG registration were all synchronized. For all trials, whole-body kinematics were

recorded at 200Hz using 69 reflective markers and a 12-camera Qualisys Oqus 7 motion capture system (Qualisys Inc., Götenborg, Sweden). EMGs were recorded using the wireless Trigno EMG (Delsys, MA, USA) system at a sampling rate of 1110 Hz.

2.3.4 Data processing

To measure and quantify the energy efficiency of walking of each subject on different types of terrain, data from only the final 4 minutes of the total 7 minutes of walking were analysed to account for the delay in the stabilisation of physiological parameters. For the resting metabolic rates, only data from the final 10 minutes of the total 15 minutes were analysed to allow for stabilisation of values. The net oxygen consumption values ($\dot{V}_{O_2}$, ml s^{-1}) were calculated by deducting the total ($\dot{V}_{O_2}$, ml s^{-1}) measured during resting from the total ($\dot{V}_{O_2}$, ml s^{-1}) measured during walking. Mass-specific cost of locomotion (CoL) ($\dot{V}_{O_2}$, ml kg^{-1} s^{-1}) was calculated by dividing the net rate of oxygen consumption by body mass. Then mass-specific cost of transport (CoT) ($\dot{V}_{O_2}$, ml m^{-1}) was calculated by dividing CoL by forward speed. Average walking speeds were derived from the speed of a spherical infra-red marker placed on the xyphoid process. For each participant, CoT for each trial was combined per substrate and then all participants were combined together. Due to a data collection error, data from one participant was excluded.

Motion capture data was processed using Qualisys Track Manager (QTM) 2.15 (2017). In QTM, the markers were labelled according to their respective anatomical references specified in Table 2.2. For some trials, it was necessary to use the automatic gap-fill when the marker was not visible to the cameras at all times. During the single trials, the first two and last two steps were removed to ensure the participant was walking at a steady speed in the steps included in the analyses. The continuous trials were cropped to single trials, usually with 2 trials included from

each 30-second recording, with the first two and last two steps that occurred at the ends of the walkways removed. The files were then exported as C3D files to be analysed in Visual 3D (C-Motion Inc., Germantown, MD, USA).

In Visual 3D, each labelled marker was assigned to a body segment with a kinematic model comprised of 13 segments: bilateral feet, shanks, thighs, upper arms, forearms, and head, trunk and pelvis. In some cases, it was necessary to create artificial markers, which were positioned using anatomical knowledge of the landmark position. Each participant had their own workspace created containing the static trial and the walking trials for all substrates and the static trial was used to create the multi-segment kinematic model and applied to all trials. The marker positions were filtered with a low-pass, zero phase-shift 2nd order 10Hz Butterworth filter. Kinematic gait events were calculated automatically using a co-ordinate based algorithm that used foot positions relative to the pelvis (Zeni Jr, Richards & Higginson 2008) but these were checked manually for every trial. Accuracy was checked by comparing gait events calculated using Visual 3D with the force plate data, which showed good similarity. The gait events that were defined were heel-strike and toe-off for both left and right feet; heel-strike was taken as the first weight-bearing contact between the substrate and the foot and toe-off was taken as the last weight-bearing contact between the substrate and the hallux. Several pipelines were then applied to all files which calculated joint angles, centre of mass position and spatiotemporal variables. Joint angles are defined as the orientation of one segment relative to another segment. The cardan sequence (the ordered sequence of rotations x, y and z) specified was X = flexion/extension, Y = abduction/adduction and Z = longitudinal rotation (Kadaba, Ramakrishnan & Wootten 1990). Hip, knee and ankle angles were calculated for all trials as well as maximum, minimum and mean metrics for every gait cycle. In Visual 3D, the spatiotemporal variables calculated were speed, stride length, stride width, cycle time, stance time, swing time and double-support time. Visual 3D calculates the mass, moments of inertia (IXX, IYY, IZZ) and centre of gravity location for each segment. Centre of mass (CoM) of the whole body was calculated using the position of the kinematic model in relation to the lab based on mechanical principle patterns (Hanavan Jr 1964). All the calculated data were exported from Visual 3D as text files for further analyses

performed in MATLAB v.2019a (Mathworks, Natick, USA) and R (Team). In MATLAB, duty factor (the ratio between stance phase and gait cycle) was also calculated.

All EMG processing was performed in MATLAB v.2019b (Mathworks, Natick, USA). As the marker tracking and EMG were synchronised, the EMG files could be cropped according to the start and end times of the QTM files to ensure only the relevant steps were analysed. The raw EMG signals were high pass filtered at 12Hz with a second-order Butterworth filter to remove any artifacts and noise and then full-wave rectified (Fig. 2.4a). Using the exported gait events from Visual 3D, the trials were cropped to stride and the EMG values at gait events were extracted (Fig. 2.4b). These data were then normalised (nEMG) to maximum amplitude within each muscle during all walking trials for that participant to allow for between-participant comparison, and then the integrated values were calculated (iEMG). Then, data were grouped together according to the substrate type and the mean and standard deviations was calculated for each muscle. All data processing and analyses were performed on each participant individually as well as all participants combined together. Due to synchronization issues, EMG data for participants 1-6 were not included.

Mechanical energy data was processed in MATLAB and yielded gravitational potential energy (E_{pot}), kinetic energy (E_{kin}) and total mechanical energy (E_{tot}) of the mass-normalised 3D Centre of Mass (CoM). The recovery of mechanical energy (expressed as a percentage; R), relative amplitude (RA) and congruity (the time when potential energy and kinetic energy are moving in the same direction; CO) were calculated (Cavagna, Thys & Zamboni 1976).

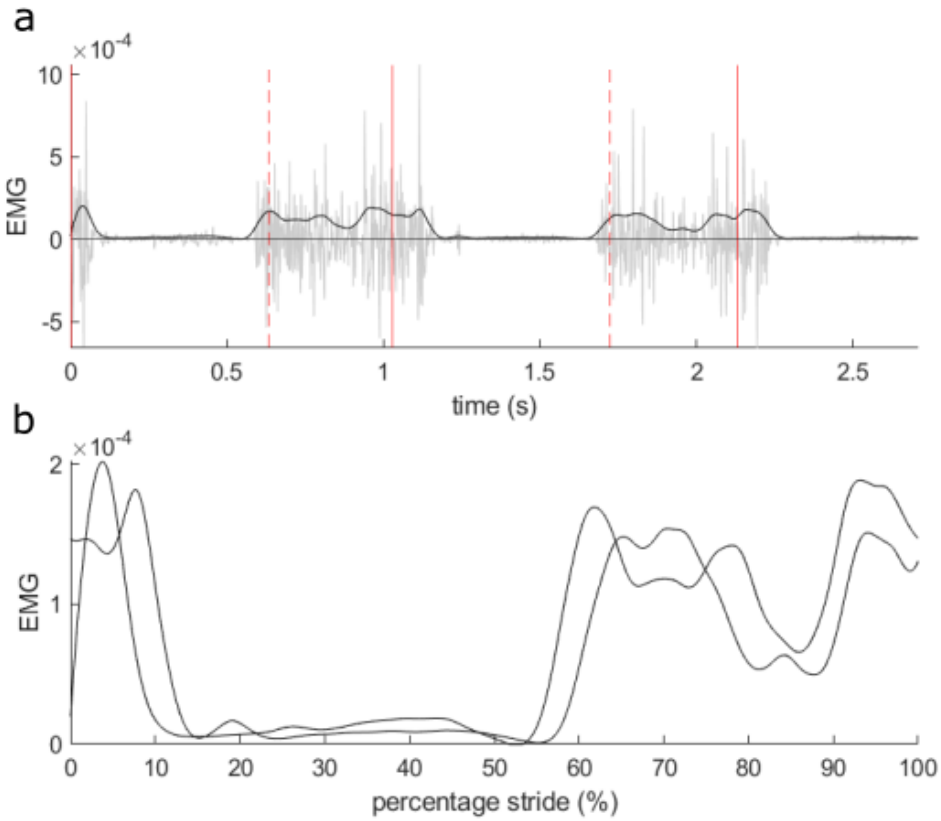

Figure 2.4: Example of electromyography signal processing: ***(a)*** raw EMG signal in grey with filtered EMG signal in black. Solid red lines indicate left heel-strike and dashed red lines indicate left toe-off ***(b)*** Filtered EMG signal after trial was cropped to stride (0-100%).

2.3.5 Statistical analysis of experimental data

Joint kinematics were analysed using two statistical approaches: One dimensional statistical parametric mapping (1D-SPM) (Pataky, Robinson & Vanrenterghem 2013), and Linear mixed-effect models (LMMs). 1D-SPM has the benefit of allowing continuous statistical analysis without treating time points as independent, but does not allow incorporation of additional factors (e.g. random or fixed effects) as LMMs do. 1D-SPM analyses were performed using MATLAB to compare hip, knee and ankle joint angles across substrates, with null hypothesis of no difference and alpha of 0.05. The mean and standard deviation of the joint angles were plotted for the duration of a gait cycle (0-100%). Vertical dotted lines were plotted to indicate the toe-off timings for each substrate. Differences between the different

substrate types were detected by 1D-SPM, utilising paired t-tests with Bonferroni corrections to reduce the probability of a type-II error occurring as a result of applying t-tests to three groups. The Bonferroni corrections led to an alpha value of 0.0170. Joint angles at gait events (heel-strike and toe-off), spatiotemporal data, iEMG data and mass-normalised mechanical energy exchange variables were analysed using LMMs, where restricted maximum likelihood was used to assess the significance of the fixed effects, substrate and trial type (continuous walking and single trials) in explaining variation. As gait speed (Fukuchi, Fukuchi & Duarte 2019) and gender (Chumanov, Wall-Scheffler & Heiderscheit 2008) can have an effect on gait biomechanics, LMMs were repeated with the inclusion of speed and gender set as fixed effects. Subjects were set as random effects, which allowed different intercepts for each subject. All LMM's were performed in R (Team) using the lmer function in the R package lme4 (Bates et al. 2014) and lmerTest (Kunzetsova, Brockhoff & Christensen 2017). The coefficient of variation (CV) (the ratio of the standard deviation to the mean) was calculated for all spatiotemporal data as a measure of relative gait variability ($CV = (SD/\bar{x}) * 100$).

2.3.6 Material testing of substrates

Mechanical behaviour of the thin and thick foam substrates was characterised by uniaxial compression using an Instron 3366 universal testing machine (UTS) with a 2350 series 5kN load cell (Instron, Norwood, MA) attached. A 203mm diameter flat indenter foot was connected to the load cell by means of a swivel joint and the UTS was fitted with a bespoke horizontal base plate to support the samples during testing. The base plate was perforated with 6.5mm diameter holes at 20mm centres to allow for rapid escape of air from the sample during the test (ASTM 2001). Initial trials were carried out to assess the effect of cyclic loading and strain rate on the samples. Ultimately, one 380mm x 380mm sample of each thickness was subjected to a single loading cycle at a rate of 500mm/min up to a compressive strain of 90%.

The indenter load and displacement were recorded and used to calculate the corresponding compressive strain, stress and modulus of the foam substrates. Compressive strain was calculated as the change in thickness divided by the original thickness and compressive stress was quantified by dividing the indenter load by the area of the foam substrate under direct compression which corresponded to the area of the flat indenter foot. Hertz theory of non-adhesive elastic contact was applied to the resulting force and deformation data to calculate the compressive modulus of the foams. For a cylindrical indenter, the load-displacement relationship relevant to the free surface beneath the indenter is:

$$P = 2Eau \qquad \text{Eq. 1}$$

where P is the indenter load, E is modulus of the substrate, a is the contact radius of the indenter foot and u is the resulting displacement relative to the free surface beneath the indenter (Fischer-Cripps 2007). Rearranging Eq. 1 in terms of E allowed compressive modulus of the substrates to be determined where:

$$E = \frac{P}{2au} \qquad \text{Eq. 2}$$

2.3.7 Multi-body dynamics (MDA) analysis

To investigate potential internal kinetic mechanisms behind differences in CoT between the hard floor and foam surfaces, one walking cycle was simulated over each substrate with one subject-specific, 12 joint degree of freedom, 92 musculotendon unit (MTU) actuated lower limb musculoskeletal model in OpenSim

4.2 (Seth et al. 2018) (age= 23, height= 180 cm, body mass= 77.4 kg; BMI= 23.8 kgm^{-2}) seen in figure 2.5.

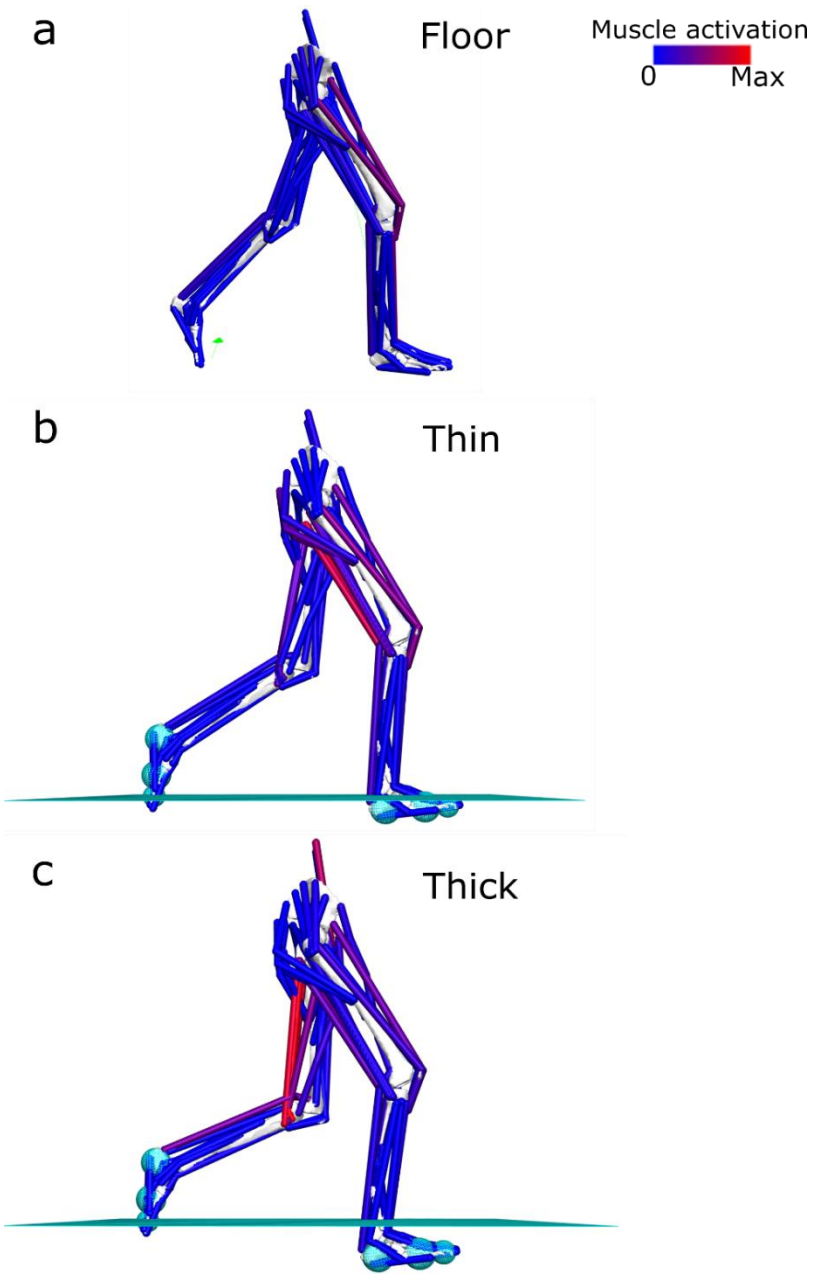

Figure 2.5: Lateral views of the subject-specific models and simulations of walking on the ***(a)*** floor, ***(b)*** thin foam and ***(c)*** thick foam, with predicted muscle activations shown. The cyan planes in (a) and (b) represent the top surface of the foams.

This model is part of a previously published set of subject-specific models (Charles et al. 2020), and freely available at the following link (10.17638/datacat.liverpool.ac.uk/1536) as Subject 4, while the same individual is referred in the larger dataset presented here as Subject 9 (Table 2.1). This model included muscle-force generating properties from the subject's MRI that was matched to the subject's own kinematics collected in this study. This subject was selected as their lower limb kinematics during walking on all substrates fell entirely within one standard deviation of the means for all subjects throughout each gait cycle (Fig 2.6).

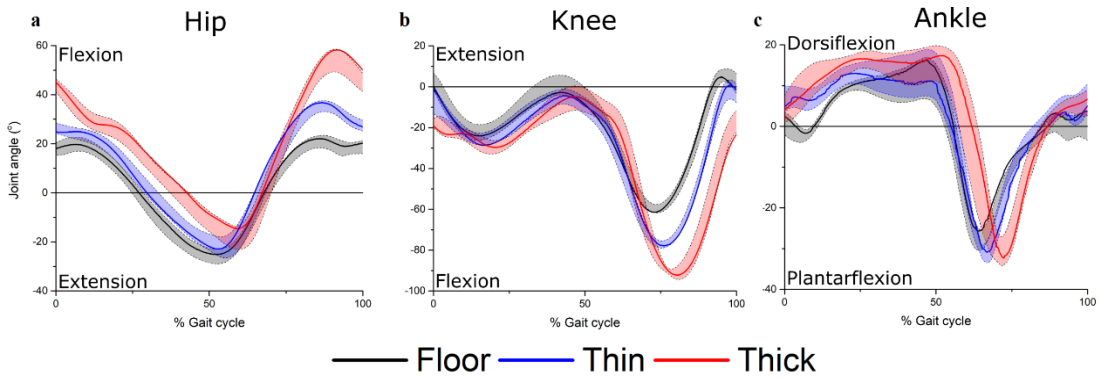

Figure 2.6: The ***(a)*** hip, ***(b)*** knee and ***(c)*** ankle kinematics of experimental subject 9 (solid lines) used to simulate single gait cycles of walking on the hard floor as well as the thin and thick foam substrates using subject-specific musculoskeletal modelling, relative to +/- 1 standard deviation of the all-subjects mean (shaded zones between dashed lines). Subject 9's joint kinematics remain within the +/- 1 standard deviation zone demonstrating that their limb motions are strongly representative of the data set as a whole.

Inverse kinematics was used to generate the generalised coordinates of each unlocked degree of freedom from the motion capture marker positions, and computed muscle control (CMC) was used to predict muscle activations and powers during walking over each surface. Experimentally measured GRFs recorded during the floor walking trials were applied to the model to simulate walking on the hard floor. Contact geometries were used to simulate contact between the foot and the foam surfaces during the thin and thick foam walking simulations. Here, contact spheres were placed at the centre of mass of the calcaneus, forefoot and toes bodies

of each lower limb to represent the soft tissue of each foot segment, while a contact half-space was placed at different heights to represent each foam surface (thin foam = 6cm; thick foam = 13cm). In OpenSim, the contact forces between each sphere and the foam surfaces were defined as Hunt Crossley forces (Sherman, Seth & Delp 2011), where the stiffness parameters were set at 0.047 MPa (47005 Nm^{-2}) for the thin foam and 0.029 MPa (28763 Nm^{-2}) for the thick foam. These stiffness values were derived from the uniaxial behaviour of the foams using the Hertz contact equation for a cyclindrical indenter and based on the subjects body mass of 77.4kg. Since OpenSim is restricted to modelling linear behaviour and the polyether polyurethane foam exhibits nonlinear behaviour, an average stiffness value was determined for each foam based on the results of the compression testing. The other contact parameters were set at the following values in each model: dissipation = 0.5 (ms^{-1}), static friction = 0.8, dynamic friction = 0.4, viscous friction = 0.4.

In each simulation, the activations of the BFL, RF, VL, VM, TA, LG, MG and SOL MTUs were constrained to match the muscle activities measured experimentally using EMG as much as possible. Residual and reserve actuators were applied to each unlocked degree of freedom in all simulations to provide forces to the model if the MTU actuators were not strong enough to satisfy the externally applied forces. As recommended by Hicks et al. (2015), we ensured that these reserve actuators provided no more than 5% of the total net moments at each degree of freedom to produce valid simulations of muscle dynamics. The mechanical work generated from each MTU was calculated by integrating the simulated power curves over the entire gait cycle.

2.4 Results

2.4.1 Energetic costs

Walking CoT significantly increased with foam thickness ($p \leq 0.05$; Fig. 2.7), with CoT highest on the Thick foam (14.25 ± 3.17 ($\dot{V}_{O_2}$, ml m^{-1}) (mean ± s.d.)), and

lowest on the floor (8.02 ± 1.84 ($\dot{V}_{O_2}$, ml m^{-1})) (Fig. 2.7) (previously published by Charles et al. (2021)). Although females tend to exhibit larger variability in CoT values, t-tests suggested there was no significant ($p>0.05$) difference between genders (Fig. 2.8).

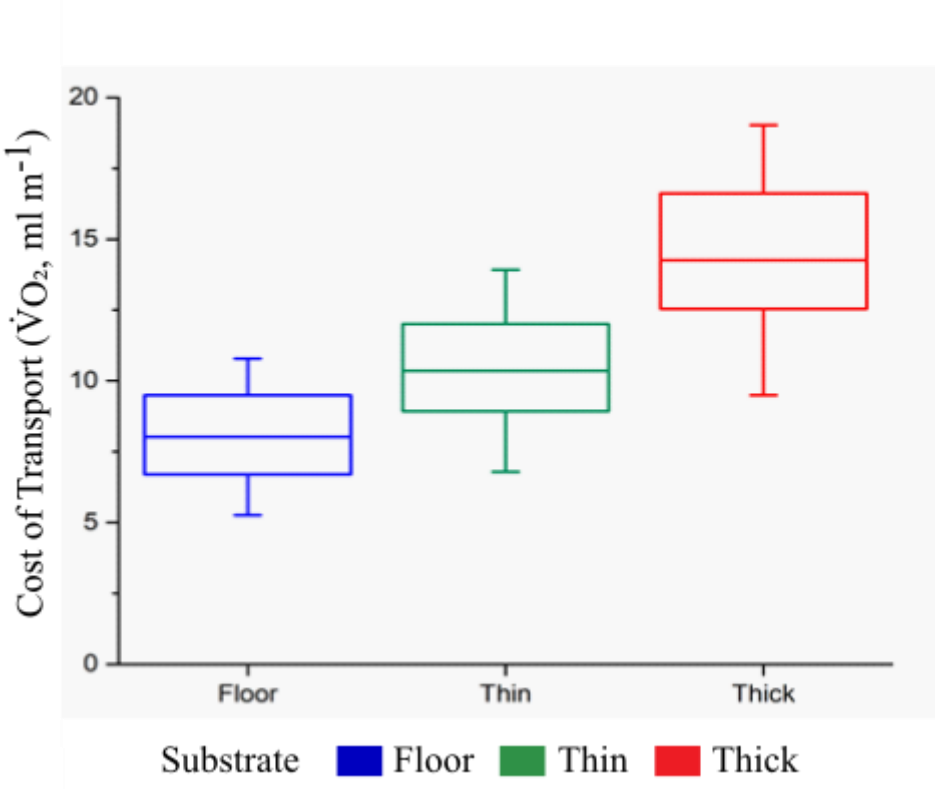

Figure 2.7: The metabolic cost of transport (CoT) ($\dot{V}_{O_2}$, ml m^{-1}) during walking for all subjects (n=29) while walking on the three different substrates: floor (blue), thin foam (green) and thick foam (red). The centre line denotes the median value (50th percentile) while the boxes contain the 25th to 75th percentiles of dataset. The boundaries of the whiskers mark the 1.5 IQR. Adapted from Charles et al. (2021).

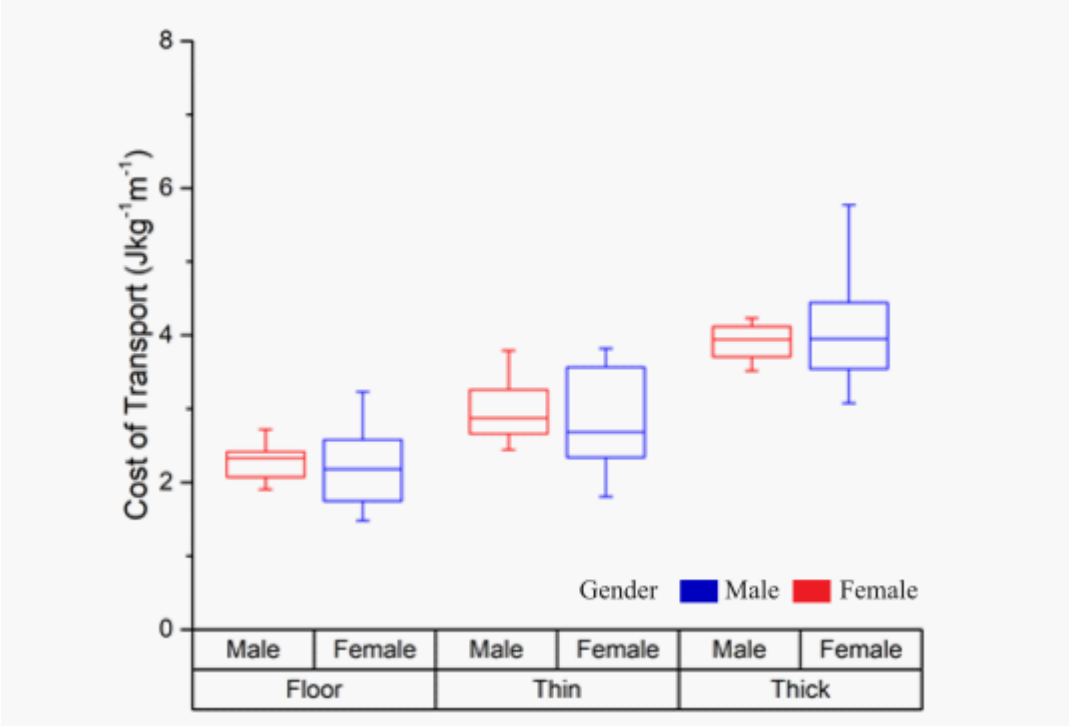

Figure 2.8: Comparison of cost of transport between males (red) and females (blue) on each substrate (floor, thin and thick). The centre line denotes the median value (50th percentile) while the boxes contain the 25th to 75th percentiles of dataset. The boundaries of the whiskers mark the minimum and maximum values. T-tests suggest there are no statistically significant difference between genders, though females are recovered with slightly lower mean and median values, but higher inter-subject variability, on each substrate.

2.4.2 Experimental data

LMMs found a significant ($p<0.001$) effect of trial type (continuous walking and single trials) for all spatiotemporal variables (Tables 6.2- 6.3), hip, knee and ankle joint angles at heel-strike (Table 6.4) and toe-off (Table 6.5) and all iEMG values (Tables 6.6-6.7). There were significant ($p<0.05$) interaction effects between substrate and trial type for most spatiotemporal variables (Tables 6.2- 6.3), joint angles (Tables 6.4-6.5) and iEMG (Tables 6.6-6.7). However, for both trial types, substrate effects were similar; therefore, when only individual trial data results are presented visually (Figs. 2.7- 2.13), similar differences between substrates also occurred on the continuous trials.

2.4.2.1 Spatiotemporal variables

As substrate compliance increased, walking speed (Fig. 2.9a) and stride width (Fig. 2.9c) decreased and stride length (Fig. 2.9b), cycle time (Fig. 2.9d), stance time (Fig. 2.9e), swing time (Fig. 2.9f), double-support time (Fig. 2.9g) and duty factor (Fig. 2.9h) all increased significantly ($p<0.001$) (Tables 2.3-2.4). The coefficient of variation (CV) was similar for speed but decreased by 8% and 12% for stride length between floor and thin and thick foam, respectively. CV increased by 16% and 43% for stride width, 14% and 12% cycle time, 24% and 18% stance time and 28% and 24% swing time between floor and thin and thick foam, respectively (Table 2.5). LMMs found a significant ($p<0.001$) effect of speed for all spatiotemporal variables and significant ($p<0.001$) interaction effects between speed and substrate for most spatiotemporal variables (Tables 2.3-2.4). LMMs found a significant ($p<0.001$) effect of gender for stride length and stance time and cycle time, swing time and duty factor ($p<0.05$). There were significant ($p<0.05$) interaction effects between gender, speed and substrate for most spatiotemporal variables (Tables 2.3-2.4).

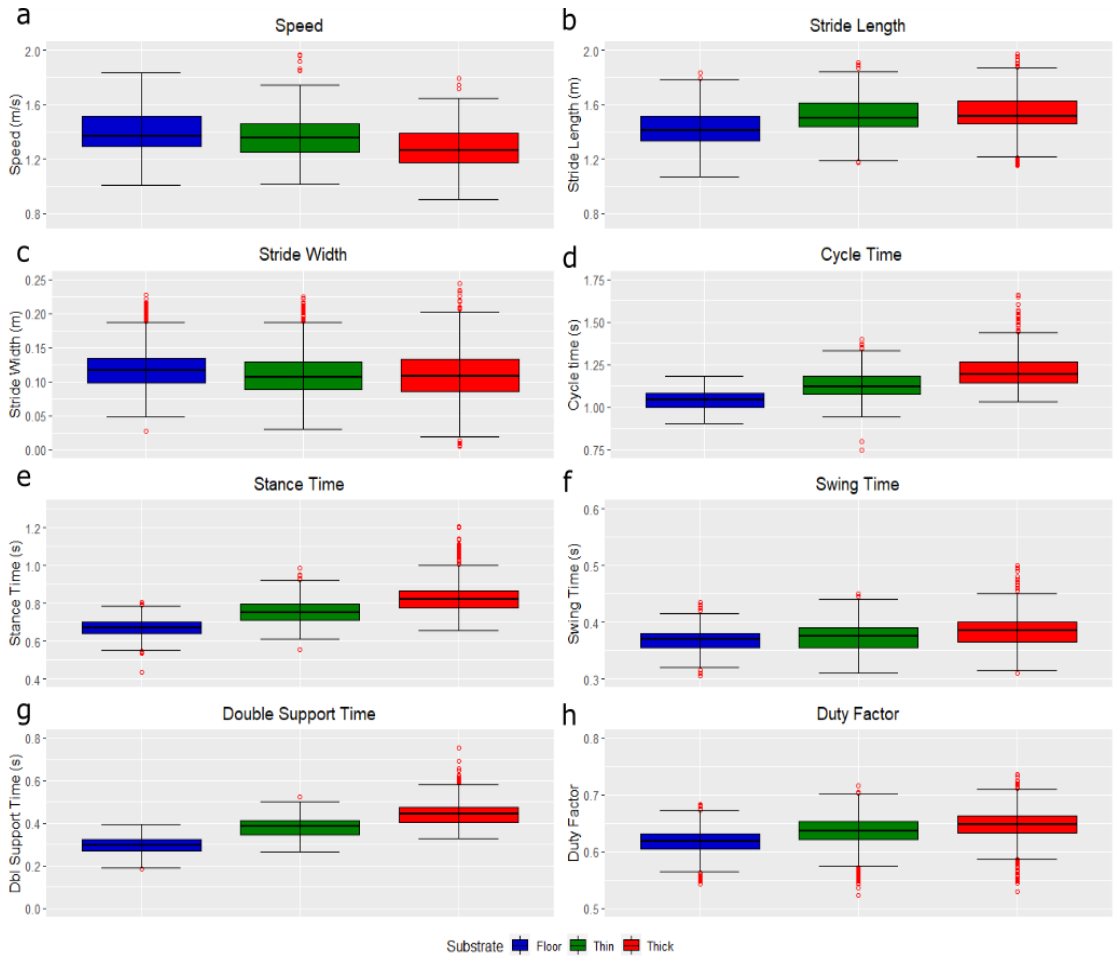

Figure 2.9: The distribution of spatiotemporal parameters for all participants combined (n=30) while walking on the three different substrates: floor (blue), thin foam (green) and thick foam (red). ***(a)*** speed, ***(b)*** stride length, ***(c)*** stride width, ***(d)*** cycle time, ***(e)*** stance time, ***(f)*** swing time, ***(g)*** double support time and ***(h)*** duty factor. Data includes all strides for individual trials (n = 5023). The centre line denotes the median value (50th percentile) while the boxes contain the 25th to 75th percentiles of dataset. The boundaries of the whiskers mark the 1.5 IQR with red circles denoting an individual stride from any subject that represents a statistical outlier.

Table 2.3: The results of the linear mixed-effect models on the spatiotemporal parameters: speed (ms^{-1}), stride length (m), stride width (m) and cycle time (s); fixed effects = speed, gender and substrate and random effects = subjects. Statistical significance is set as $p<0.05$ with significant p-values shown in bold. σ^2 = random effect variance, τ_{00} = subject variance, intraclass correlation coefficient (ICC) = proportion of random variance to total variance, N = number of subjects, observations = number of data points (strides), marginal R^2 = proportion of variance explained by the fixed factors, conditional R^2 = proportion of variance explained by both the fixed and random factors.

	Speed			**Stride_Length**			**Stride_Width**			**Cycle_Time**		
Predictors	*Estimates*	*CI*	*p*	*Estimates*	*CI*	*p*	*Estimates*	*CI*	*p*	*Estimates*	*CI*	*p*
(Intercept)	1.39	1.32 – 1.47	**<0.001**	0.67	0.59 – 0.74	**<0.001**	0.03	-0.00 – 0.07	0.088	1.42	1.37 – 1.48	**<0.001**
Substrate [Thick]	-0.14	-0.16 – -0.13	**<0.001**	0.13	0.05 – 0.20	**0.001**	0.06	0.02 – 0.10	**0.004**	0.41	0.36 – 0.47	**<0.001**
Substrate [Thin]	-0.03	-0.05 – -0.02	**<0.001**	0.29	0.22 – 0.36	**<0.001**	0.00	-0.03 – 0.04	0.806	0.18	0.13 – 0.23	**<0.001**
Gender [M]	0.02	-0.08 – 0.13	0.669	-0.27	-0.39 – -0.15	**<0.001**	0.05	-0.01 – 0.11	0.096	-0.14	-0.23 – -0.05	**0.002**
Substrate [Thick] * Gender [M]	0.04	0.02 – 0.05	**<0.001**	0.17	0.06 – 0.27	**0.001**	-0.07	-0.13 – -0.02	**0.008**	0.07	-0.01 – 0.14	0.078
Substrate [Thin] * Gender [M]	0.00	-0.01 – 0.02	0.605	-0.01	-0.11 – 0.08	0.776	-0.03	-0.09 – 0.02	0.204	0.15	0.08 – 0.22	**<0.001**
Speed				0.54	0.49 – 0.59	**<0.001**	0.06	0.03 – 0.09	**<0.001**	-0.29	-0.32 – -0.25	**<0.001**
Substrate [Thick] * Speed				0.01	-0.04 – 0.07	0.691	-0.04	-0.07 – -0.01	**0.009**	-0.22	-0.26 – -0.18	**<0.001**
Substrate [Thin] * Speed				-0.14	-0.19 – -0.09	**<0.001**	-0.01	-0.03 – 0.02	0.650	-0.07	-0.11 – -0.04	**<0.001**
Gender [M] * Speed				0.23	0.15 – 0.31	**<0.001**	-0.04	-0.08 – 0.00	0.080	0.12	0.07 – 0.18	**<0.001**
(Substrate [Thick] * Gender [M]) * Speed				-0.09	-0.16 – -0.01	**0.027**	0.05	0.01 – 0.09	**0.012**	-0.02	-0.07 – 0.04	0.507
(Substrate [Thin] * Gender [M]) * Speed				0.01	-0.06 – 0.08	0.693	0.03	-0.01 – 0.06	0.181	-0.10	-0.16 – -0.05	**<0.001**
Random Effects												
σ^2	0.00			0.00			0.00			0.00		
τ_{00}	0.02_{Subject}			0.00_{Subject}			0.00_{Subject}			0.00_{Subject}		
ICC	0.82			0.72			0.46			0.74		
N	30_{Subject}			30_{Subject}			30_{Subject}			30_{Subject}		
Observations	1325			1324			1325			1322		
Marginal R^2 / Conditional R^2	0.110 / 0.836			0.662 / 0.906			0.049 / 0.489			0.703 / 0.923		

Table 2.4: The results of the linear mixed-effect models on the spatiotemporal parameters: stance time (s), swing time (s), double support time (s) and duty factor; fixed effects = speed, gender and substrate and random effects = subjects. Statistical significance is set as $p<0.05$ with significant p-values shown in bold. σ^2 = random effect variance, τ_{00} = subject variance, intraclass correlation coefficient (ICC) = proportion of random variance to total variance, N = number of subjects, observations = number of data points (strides), marginal R^2 = proportion of variance explained by the fixed factors, conditional R^2 = proportion of variance explained by both the fixed and random factors.

	Stance_Time			**Swing_Time**			**Double_Limb_Support_Time**			**Duty_Factor**		
Predictors	*Estimates*	*CI*	*p*	*Estimates*	*CI*	*p*	*Estimates*	*CI*	*p*	*Estimates*	*CI*	*p*
(Intercept)	1.01	0.96 – 1.05	**<0.001**	0.44	0.41 – 0.46	**<0.001**	0.53	0.49 – 0.56	**<0.001**	0.68	0.65 – 0.71	**<0.001**
Substrate [Thick]	0.36	0.32 – 0.40	**<0.001**	0.07	0.05 – 0.10	**<0.001**	0.31	0.27 – 0.35	**<0.001**	-0.02	-0.06 – 0.02	0.261
Substrate [Thin]	0.12	0.08 – 0.16	**<0.001**	0.05	0.02 – 0.07	**<0.001**	0.05	0.02 – 0.09	**0.002**	-0.03	-0.07 – 0.00	0.057
Gender [M]	-0.13	-0.20 – -0.06	**<0.001**	-0.05	-0.09 – -0.01	**0.010**	-0.03	-0.09 – 0.03	0.322	-0.06	-0.11 – -0.01	**0.015**
Speed	-0.25	-0.28 – -0.22	**<0.001**	-0.05	-0.07 – -0.04	**<0.001**	-0.16	-0.19 – -0.14	**<0.001**	-0.04	-0.07 – -0.02	**<0.001**
Substrate [Thick] * Gender [M]	0.08	0.02 – 0.14	**0.014**	-0.00	-0.04 – 0.03	0.796	0.05	0.00 – 0.11	**0.042**	0.12	0.07 – 0.18	**<0.001**
Substrate [Thin] * Gender [M]	0.14	0.08 – 0.20	**<0.001**	0.00	-0.03 – 0.04	0.924	0.15	0.10 – 0.20	**<0.001**	0.09	0.04 – 0.14	**<0.001**
Substrate [Thick] * Speed	-0.19	-0.22 – -0.15	**<0.001**	-0.05	-0.07 – -0.03	**<0.001**	-0.15	-0.18 – -0.12	**<0.001**	0.04	0.01 – 0.06	**0.010**
Substrate [Thin] * Speed	-0.03	-0.06 – 0.00	0.060	-0.04	-0.05 – -0.02	**<0.001**	0.02	-0.00 – 0.05	0.092	0.04	0.02 – 0.06	**0.001**
Gender [M] * Speed	0.11	0.06 – 0.15	**<0.001**	0.05	0.02 – 0.07	**<0.001**	0.03	-0.01 – 0.06	0.211	0.04	0.01 – 0.08	**0.014**
(Substrate [Thick] * Gender [M]) * Speed	-0.03	-0.07 – 0.02	0.233	0.01	-0.02 – 0.04	0.509	-0.03	-0.06 – 0.01	0.215	-0.10	-0.13 – -0.06	**<0.001**
(Substrate [Thin] * Gender [M]) * Speed	-0.10	-0.14 – -0.06	**<0.001**	0.00	-0.02 – 0.03	0.730	-0.11	-0.15 – -0.08	**<0.001**	-0.07	-0.11 – -0.04	**<0.001**
Random Effects												
σ^2	0.00			0.00			0.00			0.00		
τ_{00}	0.00_{Subject}			0.00_{Subject}			0.00_{Subject}			0.00_{Subject}		
ICC	0.71			0.53			0.66			0.15		
N	30_{Subject}			30_{Subject}			30_{Subject}			30_{Subject}		
Observations	1323			1325			1325			1321		
Marginal R^2 / Conditional R^2	0.758 / 0.930			0.311 / 0.679			0.777 / 0.924			0.263 / 0.377		

Table 2.5. The mean, s.d. and coefficient of variation (CV) for each spatiotemporal parameters: Speed (ms^{-1}), stride length (m), stride width (m), cycle time (s), stance time (s), swing time (s), double support time (s) and duty factor while walking on the three different substrates "floor", "thin" and "thick" during continuous walking trials (continuous) and during additional individual trials (single). The CV is a measure of relative variability expressed as a percentage (CV = (SD/$\bar{x}$) * 100).

Substrate	Trial Type		Speed (ms^{-1})	Stride Length (m)	Stride Width (m)	Cycle Time (s)	Stance Time (s)	Swing Time (s)	Dbl Support Time (s)	Duty Factor
Floor	Continuous	Mean	1.25	1.33	0.11	1.10	0.71	0.39	0.32	0.63
		SD	0.19	0.17	0.03	0.07	0.06	0.02	0.05	0.02
		CV	15.17	12.45	24.30	6.24	7.90	5.49	14.63	3.63
	Single	Mean	1.40	1.42	0.12	1.04	0.67	0.37	0.30	0.62
		SD	0.16	0.15	0.03	0.07	0.05	0.02	0.04	0.03
		CV	11.54	10.71	23.66	6.89	7.82	5.48	13.78	4.77
Thin	Continuous	Mean	1.20	1.42	0.11	1.21	0.81	0.40	0.41	0.65
		SD	0.16	0.15	0.03	0.09	0.07	0.03	0.05	0.02
		CV	13.72	10.68	28.36	7.71	8.64	8.35	12.76	3.44
	Single	Mean	1.37	1.51	0.11	1.12	0.75	0.37	0.38	0.63
		SD	0.16	0.15	0.03	0.09	0.07	0.03	0.05	0.04
		CV	11.89	9.83	27.52	7.84	9.68	7.03	12.07	7.04
Thick	Continuous	Mean	1.08	1.44	0.11	1.31	0.90	0.41	0.49	0.65
		SD	0.24	0.17	0.04	0.15	0.11	0.04	0.09	0.04
		CV	22.69	11.90	38.35	11.28	12.10	9.90	17.76	6.37
	Single	Mean	1.28	1.53	0.11	1.21	0.83	0.39	0.45	0.65
		SD	0.15	0.14	0.04	0.09	0.08	0.03	0.07	0.03
		CV	11.58	9.39	33.80	7.72	9.26	6.78	14.51	4.02

2.4.2.2 Mechanical energy exchange

When averaged across each subject, E_{tot} (Fig. 2.10a) and E_{kin} (Fig. 2.10b) decreased over most of the stride as substrate compliance increased. There were much bigger decreases observed on the thick foam, with E_{tot} being lower on thick foam than floor and thin foam over most of the stride (Fig. 2.10a) and E_{kin} (Fig. 2.10b) being lower over the whole stride (Fig. 2.10b). During most of the stride, E_{pot} increased on the foams, except during early- to mid-stance (Fig. 2.10c). Differences in E_{pot} around toe-off are due to different toe-off timings (Fig. 2.10c).

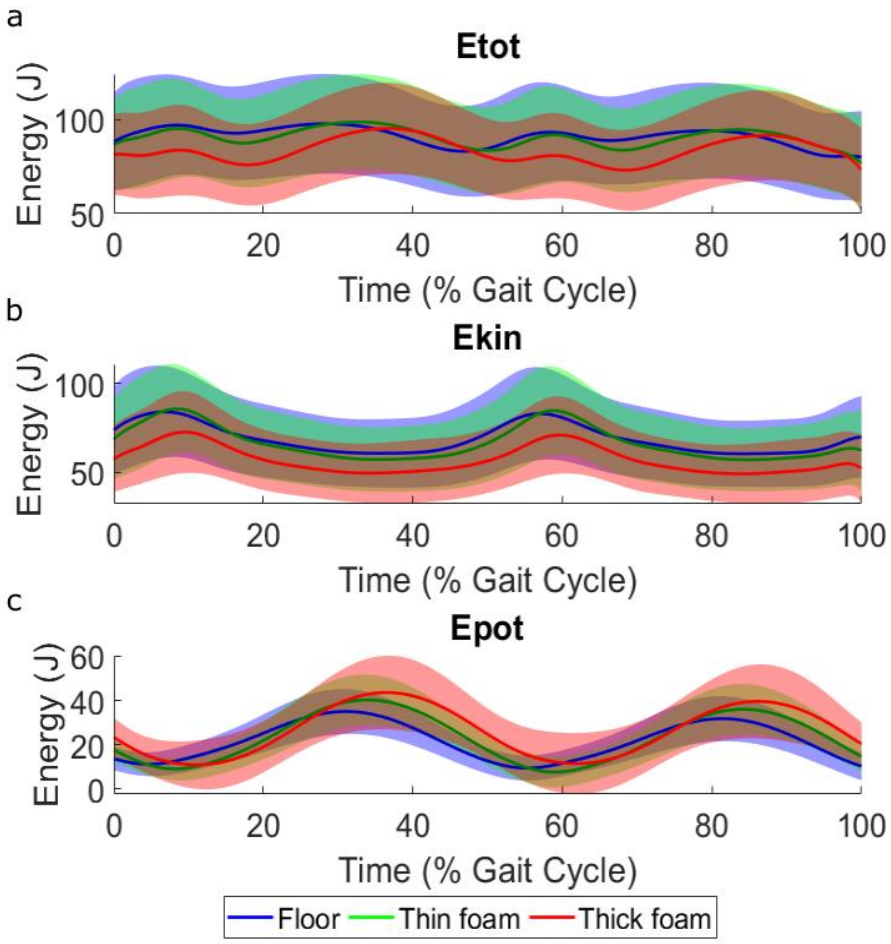

Figure 2.10: ***(a)*** Mass-normalised total (E_{tot}) mechanical energy, ***(b)*** kinetic (E_{kin}) energy and ***(c)*** the gravitational potential (E_{pot}) energy of the COM, normalised to walking stride for all participants combined (n=30) while walking on the three different substrates: floor (blue), thin foam (green) and thick foam (red). Bold lines indicate the mean value and shaded regions show the standard deviation.

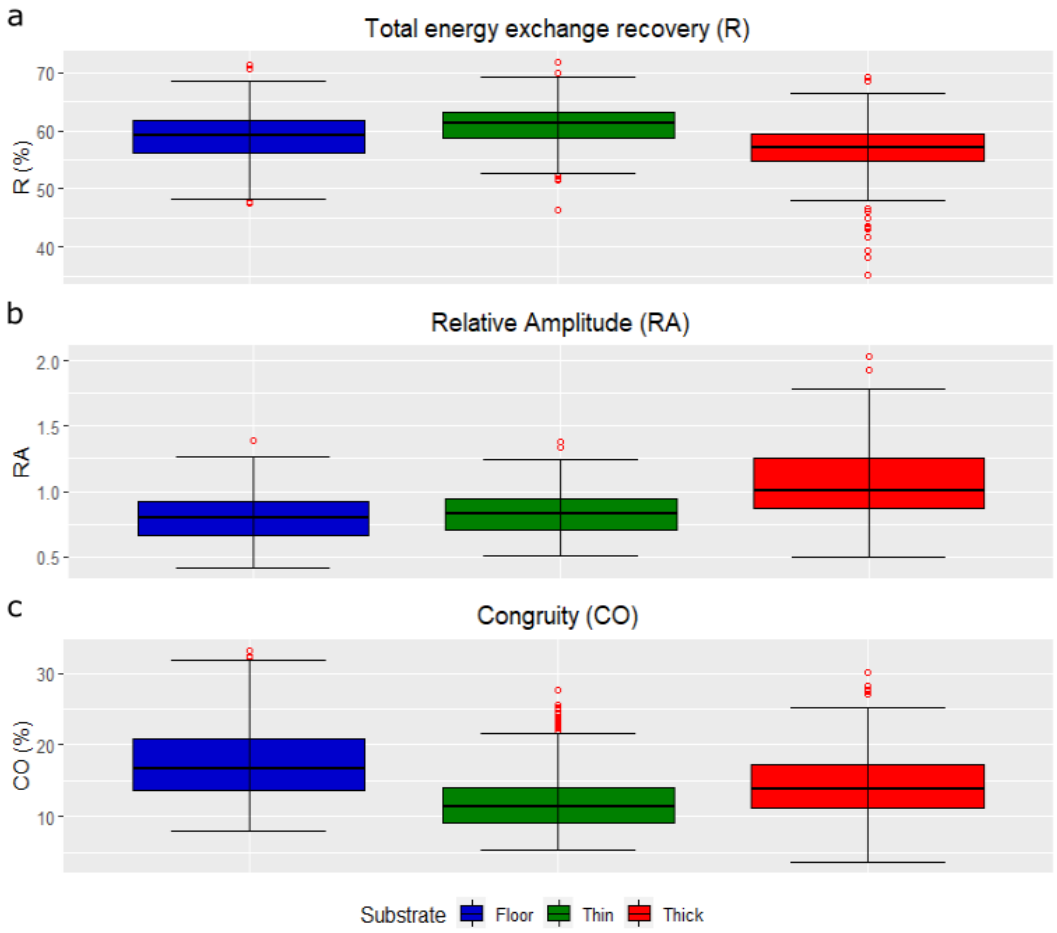

Figure 2.11: The distribution of pendulum-like determining variables: ***(a)*** The recovery of total energy exchange as a percentage (R), ***(b)*** Relative Amplitude (RA), and ***(c)*** Congruity percentage (CO) for all participants combined (n=30) while walking on the three different substrates: floor (blue), thin foam (green) and thick foam (red). The centre line denotes the median value (50th percentile) while the boxes contain the 25th to 75th percentiles of dataset. The boundaries of the whiskers mark the 1.5 IQR with red circles denoting an individual stride from any subject that represents a statistical outlier.

As substrate compliance increased, relative amplitude (RA) increased by ~4.6% and ~33.4% and congruity percentage (CO) decreased by ~30% and ~18% between floor and thin/thick foams respectively (Fig. 2.11). The recovery of total energy exchange (R) increased by ~3.2% between floor and thin foam but decreased by ~3.7% between floor and thick foam (Fig. 2.11). LMMs showed that the effect of substrate is significant for all variables between floor and thick foam ($p<0.001$), and between floor and thin foam for RA ($p<0.05$) and CO ($P<0.001$) (Table 2.6). There were significant ($p<0.05$) effects of gender for all variables and significant interaction effects between gender and substrate for R and RA ($p<0.01$). LMMs found a significant ($p<0.001$) effect of speed for all variables and significant interaction

effects between speed and substrate for all variables between floor and thick foam ($p \leq 0.001$) and between floor and thin foam for R ($p < 0.05$) and CO ($p < 0.001$). There were also some significant ($p < 0.05$) interaction effects between speed, gender and substrate and significant ($p < 0.001$) intercepts for all variables (Table 2.6).

Table 2.6: The results of the linear mixed-effect models on the mass normalised mechanical energy exchange variables: the recovery of mechanical energy (expressed as a percentage; R), relative amplitude (RA) and congruity (the time when potential energy and kinetic energy are moving in the same direction; CO). Fixed effects = substrate, gender and speed and random effects = subjects. Statistical significance is set as $p < 0.05$ with significant p-values shown in bold. σ^2 = random effect variance, τ_{00} = subject variance, intraclass correlation coefficient (ICC) = proportion of variance explained by random effects, N = number of subjects, observations = number of data points (strides), marginal R^2 = proportion of variance explained by the fixed factors, conditional R^2 = proportion of variance explained by both the fixed and random factors.

	R			**RA**			**CO**		
Predictors	*Estimates*	*CI*	*p*	*Estimates*	*CI*	*p*	*Estimates*	*CI*	*p*
(Intercept)	76.85	72.04 – 81.66	**<0.001**	1.62	1.40 – 1.83	**<0.001**	45.06	39.59 – 50.53	**<0.001**
Substrate [Thick]	-16.82	-21.96 – -11.68	**<0.001**	0.50	0.27 – 0.72	**<0.001**	-34.58	-40.28 – -28.89	**<0.001**
Substrate [Thin]	-4.02	-8.68 – 0.64	0.091	-0.21	-0.42 – -0.01	**0.045**	-24.61	-29.78 – -19.44	**<0.001**
Gender [M]	-11.97	-19.53 – -4.41	**0.002**	-0.59	-0.92 – -0.25	**0.001**	-10.69	-19.27 – -2.10	**0.015**
Speed	-13.40	-16.74 – -10.05	**<0.001**	-0.57	-0.72 – -0.42	**<0.001**	-19.27	-23.03 – -15.52	**<0.001**
Substrate [Thick] * Gender [M]	7.91	0.61 – 15.21	**0.034**	0.50	0.18 – 0.82	**0.002**	2.21	-5.89 – 10.30	0.593
Substrate [Thin] * Gender [M]	11.41	4.42 – 18.39	**0.001**	0.46	0.15 – 0.77	**0.003**	3.24	-4.50 – 10.98	0.412
Substrate [Thick] * Speed	10.70	6.76 – 14.64	**<0.001**	-0.29	-0.47 – -0.12	**0.001**	22.94	18.56 – 27.31	**<0.001**
Substrate [Thin] * Speed	4.39	1.02 – 7.75	**0.011**	0.15	-0.00 – 0.29	0.054	13.72	9.99 – 17.44	**<0.001**
Gender [M] * Speed	9.90	4.67 – 15.13	**<0.001**	0.40	0.17 – 0.63	**0.001**	6.73	0.84 – 12.62	**0.025**
(Substrate [Thick] * Gender [M]) * Speed	-6.28	-11.75 – -0.82	**0.024**	-0.26	-0.50 – -0.01	**0.038**	-1.71	-7.76 – 4.35	0.581
(Substrate [Thin] * Gender [M]) * Speed	-8.68	-13.67 – -3.69	**0.001**	-0.28	-0.50 – -0.06	**0.012**	-2.41	-7.94 – 3.12	0.393
Random Effects									
σ^2	8.94			0.02			10.98		
τ_{00}	5.48_{Subject}			0.01_{Subject}			9.79_{Subject}		
ICC	0.38			0.42			0.47		
N	30_{Subject}			30_{Subject}			30_{Subject}		
Observations	1287			1287			1287		
Marginal R^2 / Conditional R^2	0.248 / 0.534			0.414 / 0.658			0.290 / 0.625		

2.4.2.3 Joint kinematics

1D-SPM analyses of sagittal plane joint angles found significant differences between all substrates at different stages of the stride (Fig. 2.12; Tables 6.6-6.10 in appendix). During heel-strike, as substrate compliance increased, there was a significant ($p<0.005$) increase in hip flexion (Fig. 2.12a), knee flexion (Fig. 2.12b) and ankle plantarflexion (Fig. 2.12c) between all the substrates. LMMs at heel-strike showed that the effect of substrate is significant ($p<0.001$) for hip angle and knee angle on all substrates and between floor and thin foam for ankle angle (Table 2.7). Also, there was a significant ($p<0.001$) effect of speed for hip, knee and significant ($p<0.05$) interaction effects between speed and substrate for hip and knee angle. There was also a significant ($p<0.001$) effect of gender and significant ($p<0.01$) interaction effects between gender and substrate for hip, knee and ankle angle (Table 2.7). During early-stance, there was significantly less plantarflexion at the ankle joint ($p<0.001$) on the foams and during late-stance, there was less dorsiflexion at the ankle joint ($p<0.05$) on the foams (Fig. 2.12a). Throughout much of stance phase, hip (Fig. 2.12c) and knee (Fig. 2.12b) joint angles were similar on all substrates. During toe-off, all joint angles were similar but the foot is in contact with the foams for longer. LMMs at toe-off found a significant ($p\leq0.001$) effect of substrate for hip and knee angles between all substrates and between floor and thin foam for ankle angle (Table 2.8). There was also a significant ($p<0.001$) effect of gender and interaction effects between gender and substrate, and significant ($p<0.001$) effect of speed and interaction effects between speed and substrate for hip and knee angle ($p<0.05$) (Table 2.8). During swing, there were significant increases in plantarflexion at the ankle joint ($p<0.01$) (Fig. 2.12a) and in flexion at the knee ($p<0.001$) (Fig. 2.12b) and hip joint ($p<0.001$) (Fig. 2.12c) as substrate compliance increased. There were also some significant ($p<0.05$) interaction effects between speed, gender and substrate at both heel-strike and toe-off (Tables 2.7-2.8).

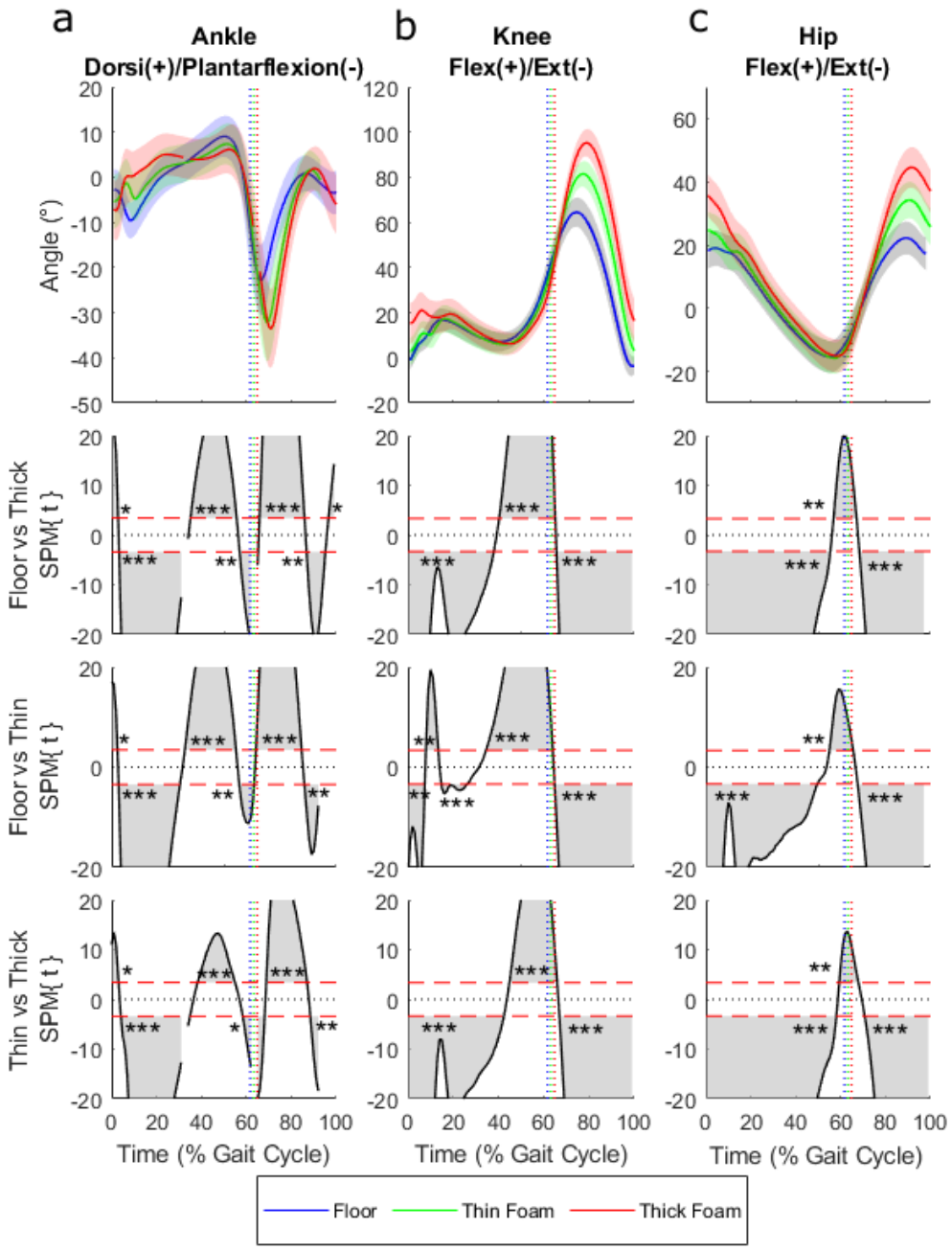

Figure 2.12: ***(a)*** Ankle, ***(b)*** knee and ***(c)*** hip joint angles in the sagittal plane for all participants combined (n=30) while walking on the three different substrates: floor (blue), thin foam (green) and thick foam (red). Bold lines indicate the mean value and shaded regions show the standard deviation. The vertical dotted lines indicate toe-off. 1D-SPM (utilising paired t-tests with Bonferroni corrections) indicate regions of statistically significant differences between walking conditions, when 1D-SPM lines exceed the critical threshold values denoted by the horizontal red dotted lines. Shaded regions (within the SPM graphs) correspond to the period within the gait cycle where walking conditions are statistically significantly different from one another. "*, **, ***" represent p-values of less than 0.05, 0.01 and 0.001 respectively.

Table 2.7. The results of the linear mixed-effect models on the ankle, knee and hip joint angles in the sagittal plane for all subjects combined (n=30) at heel-strike. Fixed effects = substrate, gender and speed and random effects = subjects. Statistical significance is set as $p<0.05$ with significant p-values shown in bold. σ^2 = random effect variance, τ_{00} = subject variance, intraclass correlation coefficient (ICC) = proportion of variance explained by random effects, N = number of subjects, observations = number of data points (strides), marginal R^2 = proportion of variance explained by the fixed factors, conditional R^2 = proportion of variance explained by both the fixed and random factors.

	Ankle_Angle			**Knee_Angle**			**Hip_Angle**		
Predictors	*Estimates*	*CI*	*p*	*Estimates*	*CI*	*p*	*Estimates*	*CI*	*p*
(Intercept)	2.28	-0.84 – 5.40	0.153	-7.90	-11.33 – -4.46	**<0.001**	6.13	3.05 – 9.21	**<0.001**
Substrate [Thick]	-1.94	-4.36 – 0.49	0.118	35.82	32.59 – 39.06	**<0.001**	33.84	31.58 – 36.10	**<0.001**
Substrate [Thin]	-3.53	-5.63 – -1.42	**0.001**	9.01	6.21 – 11.81	**<0.001**	14.41	12.53 – 16.29	**<0.001**
Speed	-3.71	-5.05 – -2.37	**<0.001**	4.60	2.81 – 6.39	**<0.001**	7.98	6.71 – 9.25	**<0.001**
Gender [M]	9.55	5.03 – 14.07	**<0.001**	16.29	11.26 – 21.31	**<0.001**	10.03	5.56 – 14.49	**<0.001**
Substrate [Thick] * Speed	-1.09	-2.97 – 0.78	0.253	-12.54	-15.05 – -10.04	**<0.001**	-11.68	-13.43 – -9.93	**<0.001**
Substrate [Thin] * Speed	1.48	-0.06 – 3.01	0.060	-2.42	-4.47 – -0.37	**0.021**	-5.12	-6.50 – -3.74	**<0.001**
Substrate [Thick] * Gender [M]	-23.48	-26.90 – -20.06	**<0.001**	-25.50	-30.06 – -20.93	**<0.001**	-6.93	-10.08 – -3.78	**<0.001**
Substrate [Thin] * Gender [M]	-19.33	-22.57 – -16.08	**<0.001**	-11.72	-16.05 – -7.39	**<0.001**	-3.90	-6.85 – -0.96	**0.009**
Speed * Gender [M]	-6.11	-8.12 – -4.10	**<0.001**	-10.90	-13.58 – -8.23	**<0.001**	-6.40	-8.32 – -4.48	**<0.001**
(Substrate [Thick] * Speed) * Gender [M]	15.00	12.44 – 17.55	**<0.001**	13.95	10.54 – 17.36	**<0.001**	3.67	1.30 – 6.03	**0.002**
(Substrate [Thin] * Speed) * Gender [M]	12.05	9.71 – 14.39	**<0.001**	5.44	2.32 – 8.56	**0.001**	1.60	-0.53 – 3.73	0.141
Random Effects									
σ^2	13.76			24.55			10.37		
τ_{00}	24.36 $_{\text{Subject}}$			21.56 $_{\text{Subject}}$			24.78 $_{\text{Subject}}$		
ICC	0.64			0.47			0.71		
N	30 $_{\text{Subject}}$			30 $_{\text{Subject}}$			30 $_{\text{Subject}}$		
Observations	10835			10866			9817		
Marginal R^2 / Conditional R^2	0.113 / 0.680			0.514 / 0.741			0.585 / 0.878		

Table 2.8. The results of the linear mixed-effect models on the ankle, knee and hip joint angles in the sagittal plane for all subjects combined (n=30) at toe-off. Fixed effects = substrate, gender and speed and random effects = subjects. Statistical significance is set as $p<0.05$ with significant p-values shown in bold. σ^2 = random effect variance, τ_{00} = subject variance, intraclass correlation coefficient (ICC) = proportion of variance explained by random effects, N = number of subjects, observations = number of data points (strides), marginal R^2 = proportion of variance explained by the fixed factors, conditional R^2 = proportion of variance explained by both the fixed and random factors.

	Ankle_Angle			**Knee_Angle**			**Hip_Angle**		
Predictors	*Estimates*	*CI*	*p*	*Estimates*	*CI*	*p*	*Estimates*	*CI*	*p*
(Intercept)	2.28	-0.84 – 5.40	0.153	-7.90	-11.33 – -4.46	**<0.001**	6.13	3.05 – 9.21	**<0.001**
Substrate [Thick]	-1.94	-4.36 – 0.49	0.118	35.82	32.59 – 39.06	**<0.001**	33.84	31.58 – 36.10	**<0.001**
Substrate [Thin]	-3.53	-5.63 – -1.42	**0.001**	9.01	6.21 – 11.81	**<0.001**	14.41	12.53 – 16.29	**<0.001**
Speed	-3.71	-5.05 – -2.37	**<0.001**	4.60	2.81 – 6.39	**<0.001**	7.98	6.71 – 9.25	**<0.001**
Gender [M]	9.55	5.03 – 14.07	**<0.001**	16.29	11.26 – 21.31	**<0.001**	10.03	5.56 – 14.49	**<0.001**
Substrate [Thick] * Speed	-1.09	-2.97 – 0.78	0.253	-12.54	-15.05 – -10.04	**<0.001**	-11.68	-13.43 – -9.93	**<0.001**
Substrate [Thin] * Speed	1.48	-0.06 – 3.01	0.060	-2.42	-4.47 – -0.37	**0.021**	-5.12	-6.50 – -3.74	**<0.001**
Substrate [Thick] * Gender [M]	-23.48	-26.90 – -20.06	**<0.001**	-25.50	-30.06 – -20.93	**<0.001**	-6.93	-10.08 – -3.78	**<0.001**
Substrate [Thin] * Gender [M]	-19.33	-22.57 – -16.08	**<0.001**	-11.72	-16.05 – -7.39	**<0.001**	-3.90	-6.85 – -0.96	**0.009**
Speed * Gender [M]	-6.11	-8.12 – -4.10	**<0.001**	-10.90	-13.58 – -8.23	**<0.001**	-6.40	-8.32 – -4.48	**<0.001**
(Substrate [Thick] * Speed) * Gender [M]	15.00	12.44 – 17.55	**<0.001**	13.95	10.54 – 17.36	**<0.001**	3.67	1.30 – 6.03	**0.002**
(Substrate [Thin] * Speed) * Gender [M]	12.05	9.71 – 14.39	**<0.001**	5.44	2.32 – 8.56	**0.001**	1.60	-0.53 – 3.73	0.141
Random Effects									
σ^2	13.76			24.55			10.37		
τ_{00}	24.36 $_{\text{Subject}}$			21.56 $_{\text{Subject}}$			24.78 $_{\text{Subject}}$		
ICC	0.64			0.47			0.71		
N	30 $_{\text{Subject}}$			30 $_{\text{Subject}}$			30 $_{\text{Subject}}$		
Observations	10835			10866			9817		
Marginal R^2 / Conditional R^2	0.113 / 0.680			0.514 / 0.741			0.585 / 0.878		

2.4.2.4 Muscle activity

Overall there was a small increase in muscle activity for all measured muscles as substrate compliance increased (Fig. 2.13).

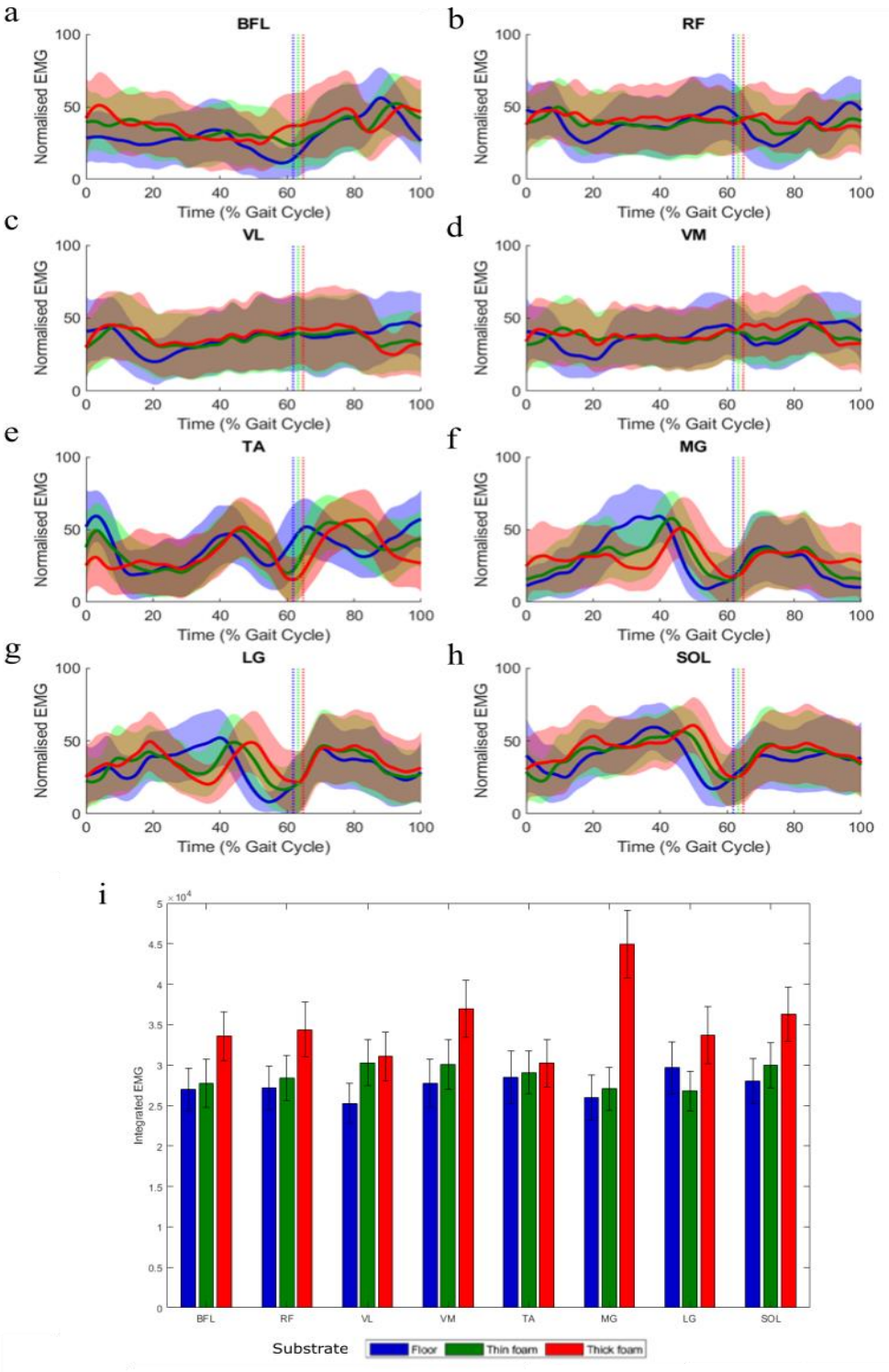

Figure 2.13. nEMG values for 8 left lower extremity muscles for participants combined (n=24) while walking on the three different substrates: floor (blue), thin foam (green) and thick foam (red) ***(a)*** biceps femoris (BFL), ***(b)*** rectus femoris (RF), ***(c)*** vastus lateralis (VL), ***(d)*** vastus medialis (VM), ***(e)*** tibialis anterior (TA), ***(f)*** lateral gastrocnemius (LG), ***(g)*** medial gastrocnemius (MG) and ***(h)*** soleus (SOL). Bold lines indicate the mean value, shaded regions show the standard deviation and the vertical dotted lines indicate toe-off. ***(i)*** iEMG values (mean ± s.d.).

However, nEMG for the TA (Fig. 2.13e) during heel-strike and toe-off and for RF (Fig. 2.13b), VL (Fig. 2.13c), VM (Fig. 2.13d) during heel-strike were higher on the hard floor than on the compliant surfaces. During mid-stance, on the hard floor, nEMG for the MG (Fig. 2.13f) and LG (Fig. 2.13g) were also higher than on the foam substrates. This pattern is generally consistent with iEMG values, which show increases for all muscles as substrate compliance increased, except LG on the thin foam (Fig. 2.13i). LMMs for the iEMG values shows the effect of substrate is significant ($p<0.05$) for VL, VM, and TA for all substrates, between floor and thin foam for BFL ($p\leq0.001$) and between floor and thick foam for MG ($p<0.001$) (Tables 2.9- 2.10). There were no significant ($p>0.05$) effect of substrate for RF, LG and SOL. LMMs found a significant ($p<0.01$) effect of speed for BFL, RF, VL, VM, TA, MG, LG and SOL and gender for VM, TA and SOL (Tables 2.9- 2.10). There were also some significant ($p<0.05$) interaction effects between speed, gender and substrate (Tables 2.9 – 2.10).

Table 2.9: The results of the linear mixed-effect models on the integrated EMG data for the muscles BFL, RF, VL and VM; fixed effects = substrate, gender and speed and random effects = subjects. Statistical significance is set as $p<0.05$ with significant p-values shown in bold. σ^2 = random effect variance, τ_{00} = subject variance, intraclass correlation coefficient (ICC) = proportion of variance explained by random effects, N = number of subjects, observations = number of data points (strides), marginal R^2 = proportion of variance explained by the fixed factors, conditional R^2 = proportion of variance explained by both the fixed and random factors.

	TA			**MG**			**LG**			**SOL**		
Predictors	*Estimates*	*CI*	*p*	*Estimates*	*CI*	*p*	*Estimates*	*CI*	*p*	*Estimates*	*CI*	*p*
(Intercept)	30272.92	22600.96 – 37944.88	**<0.001**	19177.31	11525.95 – 26828.67	**<0.001**	16115.51	8900.59 – 23330.42	**<0.001**	25196.83	16943.87 – 33449.79	**<0.001**
Substrate [Thick]	-15445.22	-22358.35 – -8532.10	**<0.001**	-31061.57	-37456.63 – -24666.51	**<0.001**	-2675.40	-8233.47 – 2882.67	0.345	-1031.47	-7254.55 – 5191.61	0.745
Substrate [Thin]	-7514.24	-13186.93 – -1841.54	**0.009**	-2893.32	-8139.72 – 2353.07	0.280	3554.87	-1004.27 – 8114.01	0.126	4131.96	-972.55 – 9236.46	0.113
Gender [M]	-21470.07	-33259.86 – -9680.29	**<0.001**	-5289.94	-16928.25 – 6348.36	0.373	-9207.69	-20072.72 – 1657.34	0.097	-18146.41	-30544.49 – -5748.33	**0.004**
Speed	6107.87	1503.34 – 10712.40	**0.009**	8538.71	4264.61 – 12812.80	**<0.001**	12618.58	8896.49 – 16340.67	**<0.001**	11797.66	7628.70 – 15966.62	**<0.001**
Substrate [Thick] * Gender [M]	13826.52	3985.57 – 23667.46	**0.006**	32252.90	23150.24 – 41355.56	**<0.001**	9422.48	1511.59 – 17333.37	**0.020**	24527.35	15670.02 – 33384.68	**<0.001**
Substrate [Thin] * Gender [M]	3473.71	-5516.74 – 12464.15	0.449	-2727.07	-11041.93 – 5587.80	0.520	-4578.20	-11803.88 – 2647.48	0.214	17872.29	9782.26 – 25962.31	**<0.001**
Substrate [Thick] * Speed	10511.67	5156.73 – 15866.62	**<0.001**	26177.18	21222.67 – 31131.70	**<0.001**	6573.20	2266.70 – 10879.71	**0.003**	5796.45	974.58 – 10618.31	**0.018**
Substrate [Thin] * Speed	5888.44	1790.57 – 9986.31	**0.005**	3290.59	-499.36 – 7080.54	0.089	-500.78	-3794.28 – 2792.72	0.766	-222.44	-3909.92 – 3465.03	0.906
Gender [M] * Speed	11642.81	4433.52 – 18852.10	**0.002**	296.88	-6395.98 – 6989.75	0.931	2633.93	-3195.03 – 8462.90	0.376	6090.47	-438.42 – 12619.36	0.067
(Substrate [Thick] * Gender [M]) * Speed	-9079.58	-16459.23 – -1699.94	**0.016**	-24718.79	-31545.34 – -17892.24	**<0.001**	-7996.90	-13929.95 – -2063.85	**0.008**	-17058.32	-23701.24 – -10415.40	**<0.001**
(Substrate [Thin] * Gender [M]) * Speed	-3399.48	-9789.76 – 2990.79	0.297	1610.06	-4300.02 – 7520.15	0.593	2587.24	-2548.67 – 7723.14	0.323	-12688.80	-18439.07 – -6938.53	**<0.001**
Random Effects												
σ^2	32452205.49			27756861.25			20960624.99			26275090.83		
τ_{00}	53145098.13 $_{Subject}$			70244939.06 $_{Subject}$			77190492.15 $_{Subject}$			105605139.62 $_{Subject}$		
ICC	0.62			0.72			0.79			0.80		
N	24 $_{Subject}$			24 $_{Subject}$			24 $_{Subject}$			24 $_{Subject}$		
Observations	2662			2662			2662			2662		
Marginal R^2 / Conditional R^2	0.126 / 0.669			0.102 / 0.746			0.140 / 0.816			0.179 / 0.836		

Table 2.10: The results of the linear mixed-effect models on the integrated EMG data for the muscles TA, MG, LG and SOL; fixed effects = substrate, gender and speed and random effects = subjects. Statistical significance is set as $p<0.05$ with significant p-values shown in bold. σ^2 = random effect variance, τ_{00} = subject variance, intraclass correlation coefficient (ICC) = proportion of variance explained by random effects, N = number of subjects, observations = number of data points (strides), marginal R^2 = proportion of variance explained by the fixed factors, conditional R^2 = proportion of variance explained by both the fixed and random factors.

	TA			**MG**			**LG**			**SOL**		
Predictors	*Estimates*	*CI*	*p*	*Estimates*	*CI*	*p*	*Estimates*	*CI*	*p*	*Estimates*	*CI*	*p*
(Intercept)	30272.92	22600.96 – 37944.88	**<0.001**	19177.31	11525.95 – 26828.67	**<0.001**	16115.51	8900.59 – 23330.42	**<0.001**	25196.83	16943.87 – 33449.79	**<0.001**
Substrate [Thick]	-15445.22	-22358.35 – -8532.10	**<0.001**	-31061.57	-37456.63 – -24666.51	**<0.001**	-2675.40	-8233.47 – 2882.67	0.345	-1031.47	-7254.55 – 5191.61	0.745
Substrate [Thin]	-7514.24	-13186.93 – -1841.54	**0.009**	-2893.32	-8139.72 – 2353.07	0.280	3554.87	-1004.27 – 8114.01	0.126	4131.96	-972.55 – 9236.46	0.113
Gender [M]	-21470.07	-33259.86 – -9680.29	**<0.001**	-5289.94	-16928.25 – 6348.36	0.373	-9207.69	-20072.72 – 1657.34	0.097	-18146.41	-30544.49 – -5748.33	**0.004**
Speed	6107.87	1503.34 – 10712.40	**0.009**	8538.71	4264.61 – 12812.80	**<0.001**	12618.58	8896.49 – 16340.67	**<0.001**	11797.66	7628.70 – 15966.62	**<0.001**
Substrate [Thick] * Gender [M]	13826.52	3985.57 – 23667.46	**0.006**	32252.90	23150.24 – 41355.56	**<0.001**	9422.48	1511.59 – 17333.37	**0.020**	24527.35	15670.02 – 33384.68	**<0.001**
Substrate [Thin] * Gender [M]	3473.71	-5516.74 – 12464.15	0.449	-2727.07	-11041.93 – 5587.80	0.520	-4578.20	-11803.88 – 2647.48	0.214	17872.29	9782.26 – 25962.31	**<0.001**
Substrate [Thick] * Speed	10511.67	5156.73 – 15866.62	**<0.001**	26177.18	21222.67 – 31131.70	**<0.001**	6573.20	2266.70 – 10879.71	**0.003**	5796.45	974.58 – 10618.31	**0.018**
Substrate [Thin] * Speed	5888.44	1790.57 – 9986.31	**0.005**	3290.59	-499.36 – 7080.54	0.089	-500.78	-3794.28 – 2792.72	0.766	-222.44	-3909.92 – 3465.03	0.906
Gender [M] * Speed	11642.81	4433.52 – 18852.10	**0.002**	296.88	-6395.98 – 6989.75	0.931	2633.93	-3195.03 – 8462.90	0.376	6090.47	-438.42 – 12619.36	0.067
(Substrate [Thick] * Gender [M]) * Speed	-9079.58	-16459.23 – -1699.94	**0.016**	-24718.79	-31545.34 – -17892.24	**<0.001**	-7996.90	-13929.95 – -2063.85	**0.008**	-17058.32	-23701.24 – -10415.40	**<0.001**
(Substrate [Thin] * Gender [M]) * Speed	-3399.48	-9789.76 – 2990.79	0.297	1610.06	-4300.02 – 7520.15	0.593	2587.24	-2548.67 – 7723.14	0.323	-12688.80	-18439.07 – -6938.53	**<0.001**
Random Effects												
σ^2	32452205.49			27756861.25			20960624.99			26275090.83		
τ_{00}	53145098.13 $_{Subject}$			70244939.06 $_{Subject}$			77190492.15 $_{Subject}$			105605139.62 $_{Subject}$		
ICC	0.62			0.72			0.79			0.80		
N	24 $_{Subject}$			24 $_{Subject}$			24 $_{Subject}$			24 $_{Subject}$		
Observations	2662			2662			2662			2662		
Marginal R^2 / Conditional R^2	0.126 / 0.669			0.102 / 0.746			0.140 / 0.816			0.179 / 0.836		

2.4.3 Material testing

Both thick and thin foams exhibited highly nonlinear force-deformation behaviour when subjected to compressive loading (Fig. 2.14a) with marked hysteresis between the loading and unloading stress-strain curves (Fig. 2.14b). The stress-strain behaviour was characterised by three distinct regions namely, an initial linear elastic region at low stress followed by a long “plateau” region of gradually increasing stress and a final region of rapid stress increase due to densification of the foam (Fischer-Cripps 2007). Plotting stiffness against strain illustrates the high variation in stiffness as the foam was compressed (Fig. 2.14c). The average foam stiffness was calculated as a function of applied subject mass (Fig. 2.14d), with little variation in average stiffness over the range of deformation resulting from the application of masses between 40 and 100kg, which matched the range of subject masses used in this study.

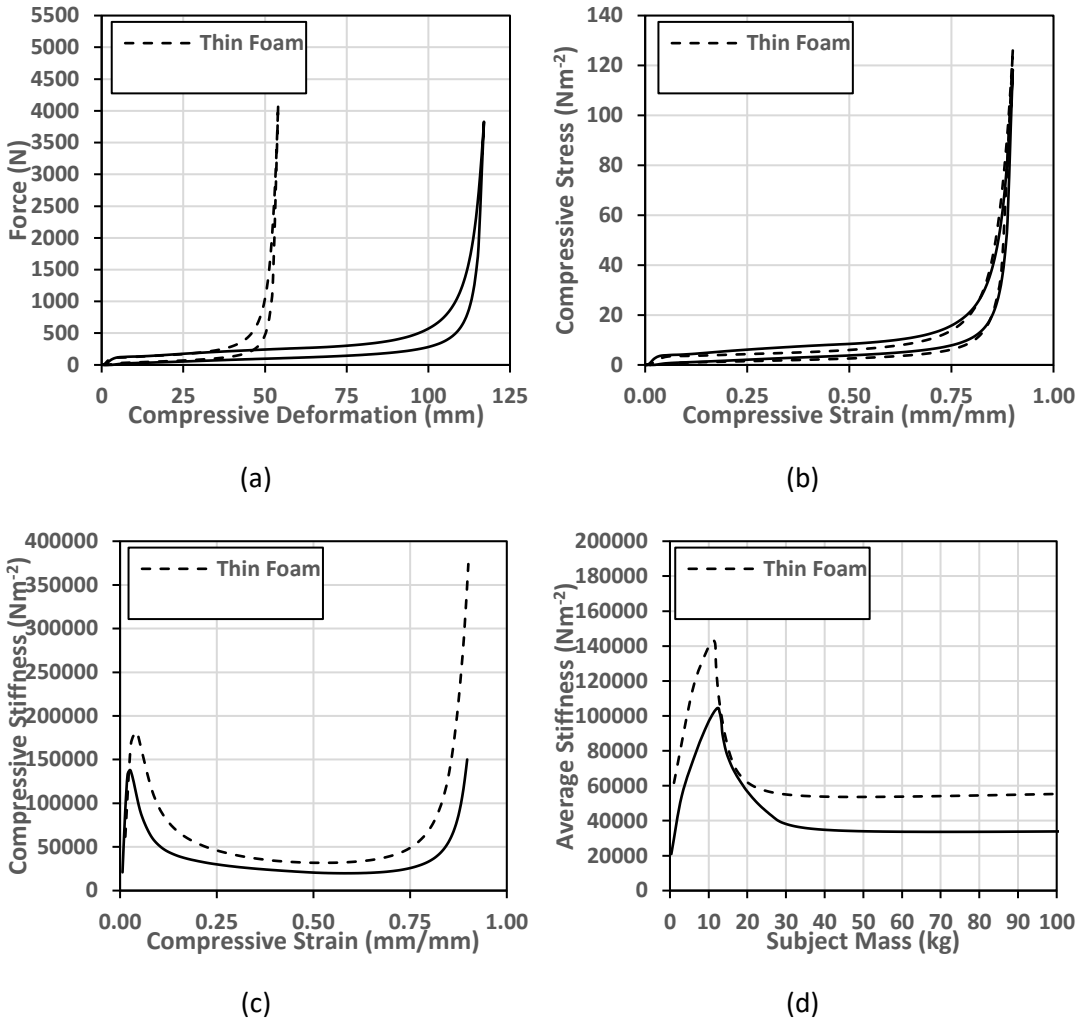

Figure 2.14: Material behaviour of thick and thin foam substrates under compressive loading showing ***(a)*** force-deformation, ***(b)*** stress-strain, ***(c)*** modulus-strain and ***(d)*** average modulus as a function of applied subject mass. Average stiffness values were taken for a subject mass of 81kg (as per subject 9) as 0.047 MPa (47005 Nm^{-2}) for thin foam and 0.029 MPa (28763 Nm^{-2}) for the thick foam for input into the simulation model.

2.4.4 Musculoskeletal modelling

The CMC simulations produced valid representations of walking over the hard floor and the foam surfaces. The outputs accurately replicated the kinetics and energetics of the experimental subject, with estimated CoT values of 2.77 $Jkg^{-1}m^{-1}$, 3.01 $Jkg^{-1}m^{-}$

^{1} and 3.40 $Jkg^{-1}m^{-1}$ on the floor, thin and thick foams respectively (compared to experimental values of 2.70 $Jkg^{-1}m^{-1}$, 3.11 $Jkg^{-1}m^{-1}$ and 3.99 $Jkg^{-1}m^{-1}$) and a good match between predicted activations and experimental EMG data in the majority of muscles on all substrates (Fig. 2.15). Simulations predicted that positive and negative MTU power and work increased with surface compliance in the muscles crossing the hip and knee joints (GMax, BFL, RF, VL, VM; Fig. 2.16a-e), but decreased in the more distal muscles crossing the ankle (TA, MG, LG, SOL; Fig. 2.16f-i). Specifically, the peak negative power produced by proximal muscles such as GMax increased from -0.62 Wkg^{-1} on the floor to -1.63 Wkg^{-1} on the thick foam, while the peak positive power produced by VL increased from 0.89 Wkg^{-1} to 2.51 Wkg^{-1} (Fig. 2.16d). This translated to changes in positive and negative work from 0.03 Jkg^{-1} and -0.10 Jkg^{-1} to 0.26 Jkg^{-1} and -0.36 Jkg^{-1} on the thick foam in GMax and from 0.20 Jkg^{-1} and -0.55 Jkg^{-1} to 0.61 Jkg^{-1} and -0.97 Jkg^{-1} in VL (Fig. 2.16j). These patterns of power and work were different in the distal muscles such as LG, where peak positive power decreased from 0.45 Wkg^{-1} on the floor to 0.33 Wkg^{-1} on the thick foam (Fig. 2.16h), which translated to decreases in positive and negative work from 0.04 Jkg^{-1} to -0.07 Jkg^{-1} to 0.03 Jkg^{-1} and -0.04 Jkg^{-1} (Fig. 2.16j).

These patterns of power and work in individual muscles were also seen at the functional muscle group level (Fig. 2.16k). For instance, the hip and knee extensors produced more positive and negative work on the thick foam (hip extensors = 0.57 Jkg^{-1}/ -0.90 Jkg^{-1}; knee extensors = 1.18 Jkg^{-1}/ -2.01 Jkg^{-1}) relative to the hard floor (hip extensors = 0.12 Jkg-1/ -0.30 Jkg^{-1}; hip extensors = 0.46 Jkg^{-1}/ -1.13 Jkg^{-1}), while this pattern was reversed in the ankle plantarflexors (thick foam = 0.11 Jkg^{-1}/ -0.13 Jkg^{-1}; floor = 0.12 Jkg^{-1}/ -0.25 Jkg^{-1}).

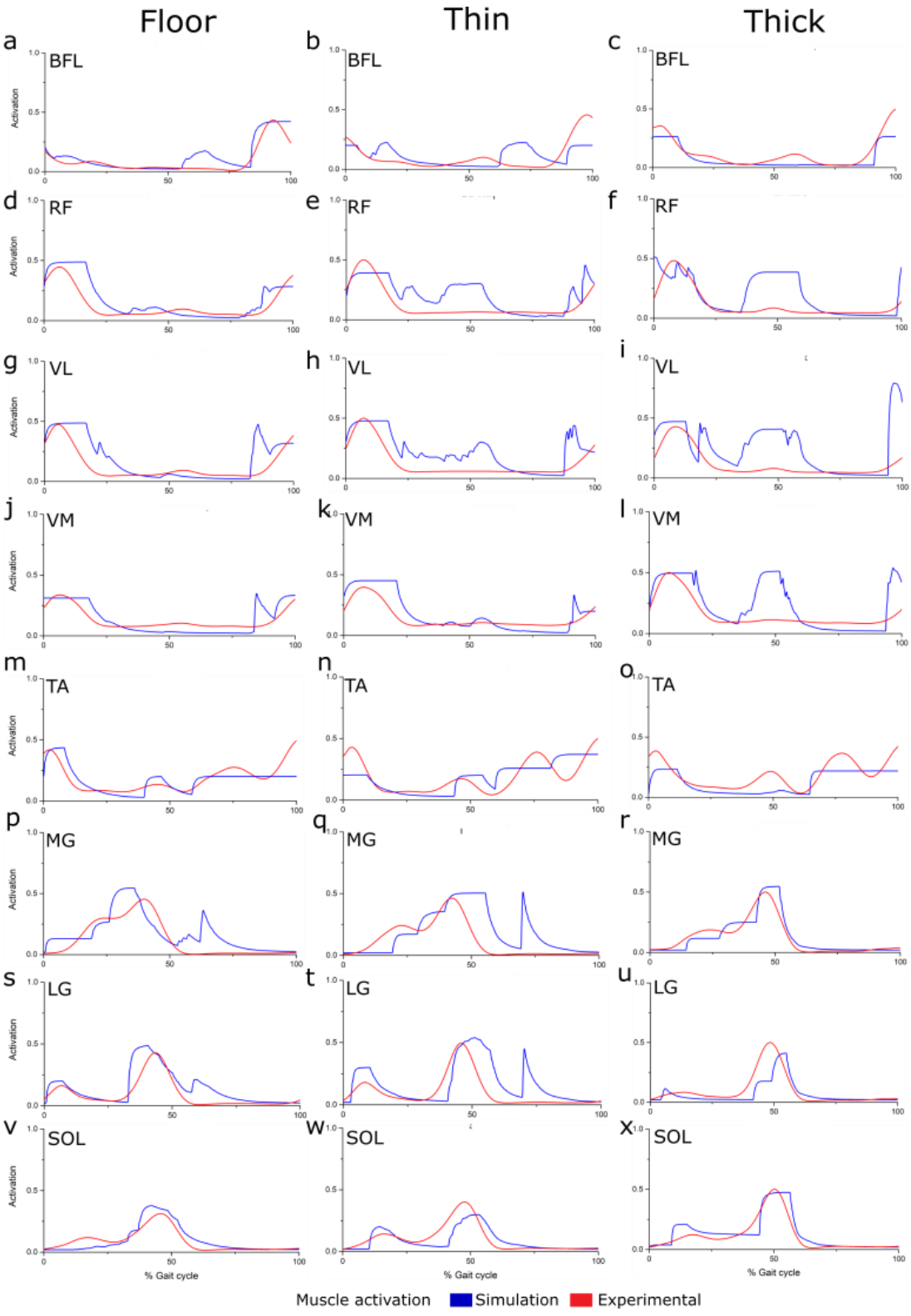

Figure 2.15: Comparison between predicted activations of select muscles from the model of Subject 9 (blue) and those measured experimentally through electromyography (EMG; red) from the same individual during single gait cycles of walking over the floor as well as the thin and thick foam surfaces. ***(a-c)*** BFL, ***(d-f)*** RF, ***(g-i)*** VL, ***(j-l)*** VM, ***(m-o)*** TA, ***(p-r)*** MG, ***(s-u)*** LG and ***(v-x)*** SOL.

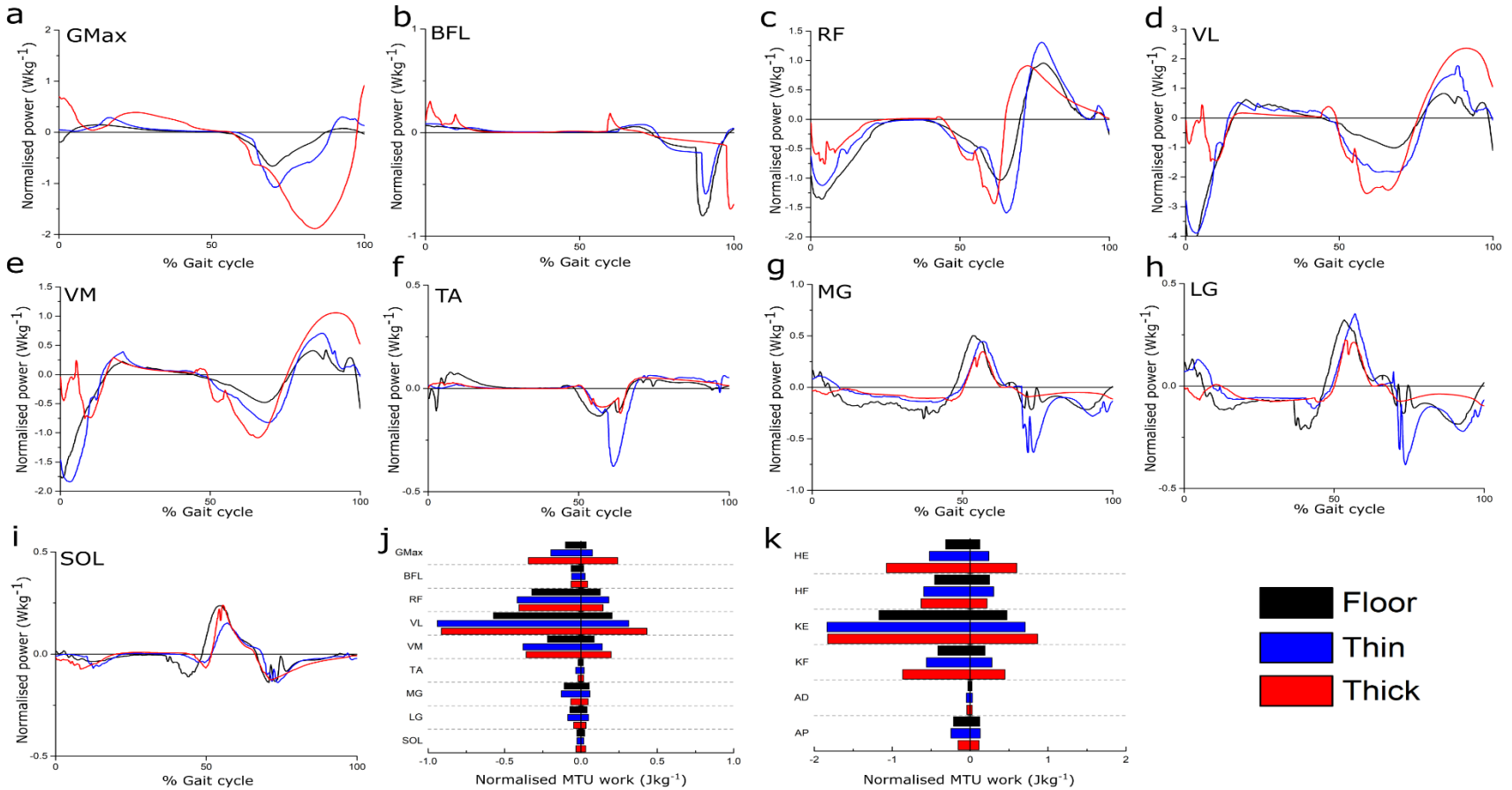

Figure 2.16: Normalised power (Wkg^{-1}; a-i) and mechanical work (Jkg^{-1}; j) outputs from select lower limb musculotendon units (MTU), as well as functional group totals (k), as predicted by subject-specific simulations of walking on the floor (black), thin foam (blue) and thick foam (red) substrates. HE- Hip extensors (GMax, BFL, semimembranosus, semitendinosus), HF- Hip flexors (iliacus, psaos, RF), KE- Knee extensors (RF, VL, VM, vastus intermedius), KF- Knee flexors (BFL, biceps femoris short head, semimembranosus, semitendinosus), AD- Ankle dorsiflexors (TA, extensor digitorum longus, extensor hallucis longus), AP- Ankle plantarflexors (MG, LG, SOL, flexor digitorum longus, flexor hallucis longus, tibialis posterior).

2.5 Discussion

It has long been recognised that animals incur a higher energetic cost when moving on compliant substrates like sand, snow and foam (Davies & Mackinnon 2006; Lejeune, Willems & Heglund 1998; Pandolf, Haisman & Goldman 1976; Pinnington & Dawson 2001; Zamparo et al. 1992). However, as noted by Davies and Mackinnon (2006), the methods and data used to elucidate the underlying mechanical causes of this increase have varied considerably in the literature, while substrate properties are rarely quantified. By collecting a comprehensive and relatively large experimental motion data set we were able to systematically characterise changes in walking gait with substrate compliance, and, by combining data with mechanical substrate testing, drive the first subject-specific computer simulations of human locomotion on compliant substrates to estimate the altered internal kinetic demands on the musculoskeletal system. These analyses lead us to reject a number of previous hypotheses related to increased locomotor costs, and instead lead us to modify other previous mechanisms to propose a more intricate explanatory model for increased energetic costs of walking on compliant terrains.

Our results found walking cost of transport (CoT) significantly increased with foam thickness ($p \leq 0.05$; Fig. 2.7), with CoT highest on the Thick foam (14.25 ± 3.17 ($\dot{V}_{O_2}$, ml m^{-1})), and lowest on the floor (8.02 ± 1.84 ($\dot{V}_{O_2}$, ml m^{-1})) (Fig. 2.7). Our LMMs show that gender and walking speed have significant interaction effects in our statistical models of spatiotemporal parameters, energy exchange variables, joint angles at gait events and muscle activation (Tables 2.3-2.4, 2.6-2.10). However, we find no significant difference in CoT between males and females on any substrate (Fig. 2.8), which is consistent with previous findings on hard substrates (Weyand et al. 2010). Although we do find increased variability in CoT in females (Fig. 2.8). However, in a previous study we found no statistically significant relationships between CoT and various morphological variables that are likely to have gender biases such as lower limb length, body stature and maximum isometric ankle plantarflexion torques (Charles et al. 2021). Given these results, and more importantly that the qualitative differences in kinematics between substrates are the

same for males and females, we conclude that gender does not influence this examination of the causative mechanisms underpinning CoT increases on the foams generally and universally across the cohort. Walking speed has an intrinsic mechanistic link with most gait parameters and as such it is not surprising that significant interaction effects are recovered in the LMMs. Average walking speeds were 1.36ms^{-1}, 1.32ms^{-1} and 1.23ms^{-1} on the floor, thin and thick foams respectively, and these differences are recovered as statistically significant. However, studies of changes in CoT with walking speeds on hard substrates recover small increases in CoT as speed increases across the range observed here e.g. (Abe, Yanagawa & Niihata 2004), in contrast to our negative relationship between CoT and speed. Given this different polarity of change in CoT, and the small magnitude of speed change, we suggest that as an isolated variable, speed is not an important causative contributor to the observed increase in CoT across the substrates.

Walking is most efficient when the whole-body CoM moves in an inverted pendulum motion, allowing for an optimal exchange of kinetic and potential energy between gait cycles (Cavagna, Thys & Zamboni 1976). It has been proposed (HYP1) that disruptions to the inverted pendulum mechanics of walking contribute to the observed increase in energetic costs on compliant substrates such as sand (Zamparo et al. 1992). However, in this study we observed little differences in the recovery of total energy exchange (R) with a 3.2% increase in R between floor and thin foam and a 3.7% decrease in R between floor and thick foam (Fig. 2.11). However, on both foams, E_{kin} and E_{pot} curves were more equal in amplitude and opposite in phase (Fig. 2.10). There was a decrease of 30% and 18% in CO between floor and the thin/thick foams respectively (Fig. 2.11). A potential explanation for the greater efficiency of the pendular energy exchange on the thin foam may be there is some elastic rebound of the substrate (Kerdok et al. 2002) and there is reduced collisional losses, as seen in compliant running shoes (Hoogkamer et al. 2018). However, Lejeune et al. (1998) also found a relatively efficient pendular mechanism when walking on sand with as much as 60% mechanical energy recovery despite sand having low resilience. Although there was a slight decrease on thick foam, we found up to 57% mechanical energy recovery (Fig. 2.11). Therefore, while energy recover may vary slightly

across different compliant substrates, the beneficial or detrimental effects on foam was probably negligible. We therefore reject HYP1.

The mechanical work needed to move CoM is directly related to the cost of walking, particularly at step-to-step transitions (Donelan, Kram & Kuo 2002; Kuo, Donelan & Ruina 2005). Stance phase is important as it requires active braking with the absorption of external power, followed by active propulsion to allow the CoM to be directed towards the opposite side. Pontzer et al. (2009) found a strong correlation between CoT and estimated volume of muscle activated per metre travelled. Based on previous work, we hypothesised (HYP2a) that increased muscle activation either throughout the limb (Voloshina et al. 2013) or (HYP2b) within specific muscle groups (Bates et al. 2013b) was responsible for increased energetic costs on compliant terrains. Overall we saw increased activation in all measured muscles (Fig. 2.13), partially supporting HYP2a. Bates et al. (2013b) previously suggested that walking on compliant substrates will increase energetic costs as greater muscle-tendon forces are required by the ankle extensors to generate the propulsion needed from mid-stance to reaccelerate into the swing phase. In partial support of this, we found slightly increased ankle extensor values during terminal stance- or push-off on the foams. However, our computer simulations suggest there is no increase in the mechanical work done by the TA (Fig. 2.16f), MG (Fig. 2.16g), LG (Fig. 2.16h) and SOL (Fig. 2.16i) during mid-stance to push-off on these compliant substrates compared to the hard floor. These findings (and others; see below) indicate, that while muscle activations do increase on compliant terrains, these increases do not uniformly or simplistically translate into increased locomotor costs, suggesting HYP2 is too simplistic as a standalone explanation.

In similar vein, we find partial support for (HYP3) increased MTU work and decreased efficiency, but our results (Fig. 2.16) emphasise a much more complex pattern across MTUs on compliant substrates (Lejeune, Willems & Heglund 1998; Pinnington & Dawson 2001). While our simulations predicted that positive and negative MTU power and work increased with substrate compliance in muscles crossing the hip and knee joints (GMax, BFL, RF, VL, VM; Fig. 2.16a-e), a decrease

(contra HYP3) was predicted in the more distal muscles crossing the ankle (Fig. 2.16). These patterns of muscle activation (Fig. 2.13) and power production (Fig. 2.16) are related to the significant kinematic differences on the three substrates, most notably at heel-strike and during swing (Figs. 2.12). When the joints are more flexed and less aligned with the resultant ground reaction force, a greater volume of active muscle is required (Pontzer, Raichlen & Sockol 2009). In particular, increased hip and knee flexion is clearly mechanistically related to greater mechanical work done by the muscles crossing the knee and hip joints (Gmax, BFL, RF, VL, VM) (Fig. 2.16). Previous studies have suggested that walking on uneven or irregular terrain (Gates et al. 2012; Voloshina et al. 2013) also incurs increased mechanical work at the knee and hip due to greater knee and hip flexion, and thus the patterns of muscle activation and force production recovered here may apply to other terrain types with elevated energetic costs.

The nature and magnitude of changes in ankle joint kinematics are consistent with the little or no increase in mechanical work seen in distal limb muscles in our simulations (Fig. 2.16). Here, a larger total joint excursion (i.e. the range of motion through both greater maximum dorsiflexion and plantarflexion angles) is observed on the hard floor during stance rather than foams, where ankle angle remains relatively constant during mid-stance (Fig. 2.12a) compared to the continuous dorsiflexion observed on the hard floor. nEMG data (Fig. 2.13) suggests greater activation of LG, MG and to a lesser extent SOL during mid-stance on the hard floor, with active dorsiflexion of the ankle suggesting that activation of these muscles is eccentric versus near-isometric on the foams (Fig. 2.12a). As a result, these muscles are predicted to incur greater negative mechanical power and work during stance on the hard floor compared to the foams (Fig. 2.16). Therefore we propose that previous hypotheses that changes in muscle kinetics and energetics (HYPs 2 and 3; (Lejeune, Willems & Heglund 1998; Voloshina et al. 2013)) should be refined, and that increased mechanical work at the knee and hip due to greater flexion and overall joint excursion, is primarily responsible for increased energetics costs on compliant substrates, with negligible contribution from distal muscles.

These changes to joint kinematics and associated muscle kinetics are mechanistically related to the changes observed in spatiotemporal gait parameters (Fig. 2.9). We found that more compliant substrates resulted in significant increases in stride length, stride time, cycle time, stance time, swing time and duty factor, but decreases in speed and stride width (Fig. 2.9). Cotes and Meade (1960) found an increase in step length resulting in greater vertical displacements of the CoM. Previous simulation (Faraji, Wu & Ijspeert 2018) and experimental (Donelan, Kram & Kuo 2002) studies also concluded that larger steps increased energetic costs due to CoM redirection. Slower stride frequencies, rather than reduced stride length, account for the observed slower speeds. The increase in stride time, cycle time, stance time, swing time and duty factor are partly due to the reduction in speed, however, the increase in duty factor on compliant substrates suggests there is a proportionally longer stance time. As peak ground reaction forces will be lower on compliant substrates, an increase in stance time ensures there is enough time to exert force on the ground to redirect the CoM. This reduction in efficiency for the redirection of the CoM would produce an increase in mechanical work and thus, consume more metabolic energy. Similar mechanisms are observed in smaller animals (Usherwood 2013), in young children (Hubel & Usherwood 2015) and adults walking on uneven terrain (Voloshina et al. 2013) who adopt a more crouched gait, coupled with an increase in stance time, to ameliorate the power costs. These changes are ultimately inter-linked with the postural or kinematic changes (Fig. 2.12), and their muscular mechanisms (Fig. 2.16) observed here (see below).

It was also hypothesised that (HYP4) correcting greater instabilities indicated by increased variability in gait (Pandolf, Haisman & Goldman 1976) increase energetic costs. While, there was no change in CV for speed and a decrease in CV for stride length, we found large increases in CV for stride width, cycle time, stance time and swing time on the compliant foams compared to the hard floor (Table 2.5). However, while previous studies that have correlated increased step-to-step variability with increased CoT, they have noted that even relatively high levels of variability yield modest increases in metabolic costs (Donelan et al. 2004; O'Connor, Xu & Kuo 2012). For example, O'connor (2012) found that a 65% increase in step width

variability was correlated with a 5.9% increase in energetic costs. Here we find lesser increases in CV for stride width on the foam but greater increases in CoT. Therefore, while we find support for HYP4, we infer that changes in hip and knee joint kinematics and kinetics represent the major contributor to increased CoT on compliant substrates.

Here, we chose foams as the focus substrate and through material testing of mechanical properties we were able to simulate locomotion on compliant terrain using a highly detailed musculoskeletal model for the first time. This leads us a present an explanatory model of CoT increase in which elevated activity and mechanical work by muscles crossing the hip and knee are required to support the changes in joint (greater excursion and maximum flexion) and spatiotemporal kinematics (longer stride lengths, stride times and stance times, and duty factors) on compliant substrates. Other compliant substrates, such as sand (and indeed even other types of foams) likely exhibit different mechanical properties to our foams, and therefore the extent to which our explanatory factors apply universally to compliant terrains remains to be tested. However, we hypothesise that the modified joint kinematics and spatiotemporal kinematics, and associated increase in muscle work at the hip and knee, are likely to occur (albeit to varying degrees) on most compliant substrates, and therefore the model of CoT increase we present here will be widely applicable for similar human populations, and potentially mammals more widely where relatively upright limb postures are utilised. Of course, our relatively homogenous study population presented here may limit the wider applicability of these results, however applying these methods to other demographics such as elderly individuals or elite athletes will deepen our insights into the mechanisms behind CoT variability. It would also be interesting for future work to explore changes in musculoskeletal mechanics on compliant substrates in animals that utilise more crouched postures. For example, birds typically use considerably less hip motion than humans and power the stride predominantly from the knee and ankle joints (Gatesy & Biewener 1991). It is therefore possible that greater responses to changes in substrate compliance may be observed in distal, rather than proximal, joints in birds and other animals with crouched postures.

2.6 Conclusion

Our analyses lead us to reject a number of previous hypotheses related to increased locomotor costs, such as disruptions to the inverted pendulum mechanics and increased mechanical work at distal limb muscles. Instead we find that the mechanistic causes of increased energetic costs on compliant substrates lie predominantly in the proximal limb and are more complex than captured by any single previous hypothesis. Specifically, elevated activity and greater mechanical work by muscles crossing hip and knee are required to support the changes in joint (greater excursion and maximum flexion) and spatiotemporal kinematics (longer stride lengths, stride times, stance times, duty factors and increased variability) on our compliant substrates. The validation of a computer simulation of locomotion on compliant substrates herein demonstrates the potential of this approach to explore morphological and mechanical adaptations to different substrates in other animal groups.

2.7 References

Abe, D., Yanagawa, K. & Niihata, S. (2004) 'Effects of load carriage, load position, and walking speed on energy cost of walking', *Applied Ergonomics*, vol. 35, no. 4, pp. 329-335.

ASTM, D. (2001) '3574—Standard test methods for flexible cellular materials—slab', *Bonded, and Molded Urethane Foams*, vol. 164.

Bates, D., Mächler, M., Bolker, B. & Walker, S. (2014) 'Fitting linear mixed-effects models using lme4', *arXiv preprint arXiv:1406.5823*.

Bates, K.T., Savage, R., Pataky, T.C., Morse, S.A., Webster, E., Falkingham, P.L., Ren, L., Qian, Z., Collins, D., Bennett, M.R., McClymont, J. & Crompton, R.H. (2013) 'Does footprint depth correlate with foot motion and pressure?', *J R Soc Interface*, vol. 10, no. 83, p. 20130009.

Britannica, E. (2022) *The muscle groups and their actions* [Online], Available from: https://www.britannica.com/science/human-muscle-system#ref322749 (Accessed: 16/08/2022).

Carson, M.C., Harrington, M.E., Thompson, N., O'Connor, J.J. & Theologis, T.N. (2001) 'Kinematic analysis of a multi-segment foot model for research and clinical applications: a repeatability analysis', *J Biomech*, vol. 34, no. 10, pp. 1299-1307.

Cavagna, G.A., Thys, H. & Zamboni, A. (1976) 'The sources of external work in level walking and running', *J Physiol*, vol. 262, no. 3, pp. 639-657.

Charles, J.P., Grant, B., D'Août, K. & Bates, K.T. (2020) 'Subject-specific muscle properties from diffusion tensor imaging significantly improve the accuracy of musculoskeletal models', *Journal of Anatomy*, vol. 237, no. 5, pp. 941-959.

Charles, J.P., Grant, B., D'Août, K. & Bates, K.T. (2021) 'Foot anatomy, walking energetics, and the evolution of human bipedalism', *Journal of Human Evolution*, vol. 156, p. 103014.

Chumanov, E.S., Wall-Scheffler, C. & Heiderscheit, B.C. (2008) 'Gender differences in walking and running on level and inclined surfaces', *Clinical Biomechanics*, vol. 23, no. 10, pp. 1260-1268.

Cotes, J.E. & Meade, F. (1960) 'The energy expenditure and mechanical energy demand in walking', *Ergonomics*, vol. 3, pp. 97-120.

Davies, S.E.H. & Mackinnon, S.N. (2006) 'The energetics of walking on sand and grass at various speeds', *Ergonomics*, vol. 49, no. 7, pp. 651-660.

Dixon, P.C., Böhm, H. & Döderlein, L. (2012) 'Ankle and midfoot kinetics during normal gait: A multi-segment approach', *Journal of Biomechanics*, vol. 45, no. 6, pp. 1011-1016.

Donelan, J.M., Kram, R. & Kuo, A.D. (2002) 'Mechanical work for step-to-step transitions is a major determinant of the metabolic cost of human walking', *Journal of Experimental Biology*, vol. 205, no. 23, pp. 3717-3727.

Donelan, J.M., Shipman, D.W., Kram, R. & Kuo, A.D. (2004) 'Mechanical and metabolic requirements for active lateral stabilization in human walking', *Journal of Biomechanics*, vol. 37, no. 6, pp. 827-835.

Faraji, S., Wu, A.R. & Ijspeert, A.J. (2018) 'A simple model of mechanical effects to estimate metabolic cost of human walking', *Scientific Reports*, vol. 8, no. 1, p. 10998.

Fischer-Cripps, A.C. (2007) *Introduction to contact mechanics*, vol. 101, Springer.

Fukuchi, C.A., Fukuchi, R.K. & Duarte, M. (2019) 'Effects of walking speed on gait biomechanics in healthy participants: a systematic review and meta-analysis', *Systematic Reviews*, vol. 8, no. 1, p. 153.

Gates, D.H., Wilken, J.M., Scott, S.J., Sinitski, E.H. & Dingwell, J.B. (2012) 'Kinematic strategies for walking across a destabilizing rock surface', *Gait & Posture*, vol. 35, no. 1, pp. 36-42.

Gatesy, S.M. & Biewener, A.A. (1991) 'Bipedal locomotion: effects of speed, size and limb posture in birds and humans', *Journal of Zoology*, vol. 224, no. 1, pp. 127-147.

Hanavan Jr, E.P. (1964) *A mathematical model of the human body*, Air Force Aerospace Medical Research Lab Wright-patterson AFB OH,

Hermens, H.J., Freriks, B., Disselhorst-Klug, C. & Rau, G. (2000) 'Development of recommendations for SEMG sensors and sensor placement procedures', *Journal of Electromyography and Kinesiology*, vol. 10, no. 5, pp. 361-374.

Hicks, J.L., Uchida, T.K., Seth, A., Rajagopal, A. & Delp, S.L. (2015) 'Is my model good enough? Best practices for verification and validation of musculoskeletal models and simulations of movement', *Journal of Biomechanical Engineering*, vol. 137, no. 2.

Holowka, N.B., Kraft, T.S., Wallace, I.J., Gurven, M. & Venkataraman, V.V. (2022) 'Forest terrains influence walking kinematics among indigenous Tsimane of the Bolivian Amazon', *Evolutionary Human Sciences*, vol. 4, p. e19.

Hoogkamer, W., Kipp, S., Frank, J.H., Farina, E.M., Luo, G. & Kram, R. (2018) 'A Comparison of the Energetic Cost of Running in Marathon Racing Shoes', *Sports Medicine*, vol. 48, no. 4, pp. 1009-1019.

Hubel, T.Y. & Usherwood, J.R. (2015) 'Children and adults minimise activated muscle volume by selecting gait parameters that balance gross mechanical power and work demands', *Journal of Experimental Biology*, vol. 218, no. 18, pp. 2830-2839.

Kadaba, M.P., Ramakrishnan, H. & Wootten, M. (1990) 'Measurement of lower extremity kinematics during level walking', *Journal of orthopaedic research*, vol. 8, no. 3, pp. 383-392.

Kerdok, A.E., Biewener, A.A., McMahon, T.A., Weyand, P.G. & Herr, H.M. (2002) 'Energetics and mechanics of human running on surfaces of different stiffnesses', *Journal of Applied Physiology*, vol. 92, no. 2, pp. 469-478.

Kunzetsova, A., Brockhoff, P. & Christensen, R. (2017) 'lmerTest package: Tests in linear mixed effect models', *J Stat Softw*, vol. 82, pp. 1-26.

Kuo, A.D., Donelan, J.M. & Ruina, A. (2005) 'Energetic Consequences of Walking Like an Inverted Pendulum: Step-to-Step Transitions', *Exercise and Sport Sciences Reviews*, vol. 33, no. 2, pp. 88-97.

Lejeune, T.M., Willems, P.A. & Heglund, N.C. (1998) 'Mechanics and energetics of human locomotion on sand', *Journal of Experimental Biology*, vol. 201, no. 13, pp. 2071-2080.

O'Connor, S.M., Xu, H.Z. & Kuo, A.D. (2012) 'Energetic cost of walking with increased step variability', *Gait & Posture*, vol. 36, no. 1, pp. 102-107.

Pandolf, K.B., Haisman, M.F. & Goldman, R.F. (1976) 'Metabolic energy expenditure and terrain coefficients for walking on snow', *Ergonomics*, vol. 19, no. 6, pp. 683-690.

Pataky, T.C., Robinson, M.A. & Vanrenterghem, J. (2013) 'Vector field statistical analysis of kinematic and force trajectories', *Journal of Biomechanics*, vol. 46, no. 14, pp. 2394-2401.

Pinnington, H.C. & Dawson, B. (2001) 'The energy cost of running on grass compared to soft dry beach sand', *Journal of Science and Medicine in Sport*, vol. 4, no. 4, pp. 416-430.
Pontzer, H., Raichlen, D.A. & Sockol, M.D. (2009) 'The metabolic cost of walking in humans, chimpanzees, and early hominins', *Journal of Human Evolution*, vol. 56, no. 1, pp. 43-54.
Seth, A., Hicks, J.L., Uchida, T.K., Habib, A., Dembia, C.L., Dunne, J.J., Ong, C.F., DeMers, M.S., Rajagopal, A., Millard, M., Hamner, S.R., Arnold, E.M., Yong, J.R., Lakshmikanth, S.K., Sherman, M.A., Ku, J.P. & Delp, S.L. (2018) 'OpenSim: Simulating musculoskeletal dynamics and neuromuscular control to study human and animal movement', *PLOS Computational Biology*, vol. 14, no. 7, p. e1006223.
Sherman, M.A., Seth, A. & Delp, S.L. (2011) 'Simbody: multibody dynamics for biomedical research', *Procedia IUTAM*, vol. 2, pp. 241-261.
Soule, R.G. & Goldman, R.F. (1972) 'Terrain coefficients for energy cost prediction', *Journal of Applied Physiology*, vol. 32, no. 5, pp. 706-708.
Team, R.C. 'R: A language and environment for statistical computing'.
Usherwood, J.R. (2013) 'Constraints on muscle performance provide a novel explanation for the scaling of posture in terrestrial animals', *Biology Letters*, vol. 9, no. 4, p. 20130414.
Voloshina, A.S., Kuo, A.D., Daley, M.A. & Ferris, D.P. (2013) 'Biomechanics and energetics of walking on uneven terrain', *Journal of Experimental Biology*, vol. 216, no. 21, pp. 3963-3970.
Wade, C., Redfern, M.S., Andres, R.O. & Breloff, S.P. (2010) 'Joint kinetics and muscle activity while walking on ballast', *Human Factors*, vol. 52, no. 5, pp. 560-573.
Weyand, P.G., Smith, B.R., Puyau, M.R. & Butte, N.F. (2010) 'The mass-specific energy cost of human walking is set by stature', *Journal of Experimental Biology*, vol. 213, no. 23, pp. 3972-3979.
Zamparo, P., Perini, R., Orizio, C., Sacher, M. & Ferretti, G. (1992) 'The energy cost of walking or running on sand', *European Journal of Applied Physiology and Occupational Physiology*, vol. 65, no. 2, pp. 183-187.
Zeni Jr, J., Richards, J. & Higginson, J. (2008) 'Two simple methods for determining gait events during treadmill and overground walking using kinematic data', *Gait & posture*, vol. 27, no. 4, pp. 710-714.

Chapter three: Human walking biomechanics and muscle activities over natural compliant substrates

This chapter is currently being developed for publication.

Author contributions: KB, KD and PF conceived the study. KB, KD, PF, and BFG designed the study. JC and BFG collected the experimental data. BFG processed and analysed the experimental data and conducted the statistical analyses with guidance from all co-authors. The present thesis version was drafted by BFG and benefited from editorial suggestions from KB.

3.1 Abstract

To understand how, when and why upright bipedalism evolved we have long relied on the shape of fossil footprints to infer locomotor behaviour used by our ancestors. Fossilised tracks are the combined result of foot anatomy, gait kinematics, and substrate properties. Our current understanding of human gait and energetics is mostly based on studies on hard, level surfaces in a laboratory environment. However, locomotion recorded in footprints (and often more generally in the real-world) by definition represents the interaction of moving limbs across a challenging, compliant surface, with different demands in terms of stability and efficiency. Previous studies have shown that walking on natural compliant substrates such as sand, there is an increase in energy expenditure and muscle activity. Yet, the extent to which gait is actively altered or moderated by the level of compliance with a deformable substrate is still poorly understood. The main aim of this study is to provide a mechanistic understanding of how human walking is altered by a natural compliant substrate. A total of 21 young, healthy individuals were recruited for this study. Participants walked at a self-selected speed on four surfaces: 1) hard, level floor 2) wet building sand 3) dry building sand and 4) play sand while 3D kinematics and EMG were measured synchronously. Footprint depth was also measured.

Analysis suggests that in softer, more deformable substrates in which the foot sinks more deeply, participants display greater hip and knee flexion, a slower walking speed and an increase in cycle time, stance time and swing time. Contrary to previous hypotheses, pendular energy exchange is not less efficient during locomotion on the sand. Increased energetic costs on natural compliant substrates are primarily due to increased mechanical work due to greater flexion and greater work lost to the substrate.

3.2 Introduction

The transition to terrestrial bipedalism is considered one of the most significant adaptations to occur within the hominin lineage (Crompton, Sellers & Thorpe 2010; Crompton, Vereecke & Thorpe 2008). Deciphering when, why and how this transition occurred requires an understanding of the anatomy and biomechanics in living apes, in conjunction with interpretations of the locomotor capabilities of fossil hominins. In the latter respect, the most direct evidence we have of the locomotor dynamics of our ancestors comes from fossilised footprint trails, which represent a primary record of the actual gaits they employed. However, we are currently lacking the depth understanding of limb-substrate interactions in compliant sediments required to robustly reverse-engineer limb motions from the preserved shape of fossil footprints (Bates et al. 2013b; D'Aout et al. 2010; Hatala et al. 2013). As a result, interpretations about the evolution of bipedal locomotion based on fossil hominin footprints vary widely (Bennett et al. 2009; Crompton et al. 2012; Hatala, Demes & Richmond 2016; Raichlen et al. 2010). One of the primary assumptions that underpins biomechanical inferences from footprints is that footprint topology is directly indicative of dynamic foot pressure and therefore, overall limb motion (Bates et al. 2013b; Bennett et al. 2009; Crompton et al. 2012). However, recent biomechanical research has suggested that the link between footprint morphology and locomotion may not be so straightforward (Bates et al. 2013a; D'Aout et al. 2010). Furthermore, the shape of footprints may vary according to the mechanical properties of the substrate, as often demonstrated by drastically different

morphologies within long or continuous footprint trails (Morse et al. 2013). However, the nature of this variation is not well understood.

During the footprint process, the substrate is subjected to a combination of elastic and plastic deformation by the foot. Natural compliant substrates such as sand, initially deform elastically as the sediment resists deformation but once its yield stress has been reached, plastic deformation occurs and the foot will go through the superficial layer of the substrate (Allen 1997). While some terrain types such as snow can be highly compressible, others such as dry sand are not and a volume of material under the foot needs to be moved transversely. The amount of compression and lateral displacement of the substrate are parameterised by the material's Young modulus and Poisson ratio (Allen 1997). The resistance to vertical loads provided by sand can vary across different regions of the foot and thus, affect how closely a footprint shape matches the distribution of vertical forces (Hatala et al. 2013). When moving on compliant substrates, the deformation of the material under the foot will impact the walking gait. The extent to which gait is actively altered or moderated by the level of compliance with a deformable substrate therefore represents a fundamentally important, but currently poorly understood, variable in the interpretation of fossil footprints.

Previous studies have found that humans incur a much greater metabolic energetic cost of locomotion when walking or running on natural compliant substrates such as grass (Davies & Mackinnon 2006; Pinnington & Dawson 2001), snow (Pandolf, Haisman & Goldman 1976) and sand (Davies & Mackinnon 2006; Lejeune, Willems & Heglund 1998; Zamparo et al. 1992). Lejeune et al. (1998) found that energy expenditure on sand compared to a hard surface was up to 2.7 times greater when walking at a speed of 0.5-2.5ms^{-1} and 1.6 times greater when running. Whereas Zamparo et al. (1992) found an increase of 1.8 times greater when walking on sand at a speed of 0.8-2.0 ms^{-1} and 1.2 times greater when running on sand compared to a hard surface. Pandolf et al. (1976) investigated energy costs and footprint depression in a variety of snow depths at walking speeds of 0.6ms^{-1} and 1.1ms^{-1} and found that energy expenditure increased linearly with increasing footprint depth. Although a

systematic mechanism for increased metabolic costs has not been proposed, different authors have highlighted how specific kinematic and kinetic aspects of gait are altered as substrate compliance changes.

During level walking, kinetic (E_k) and gravitational potential (E_p) energies of the centre of mass of the body (CoM) are largely out of phase, resulting in an efficient exchange of energy so that muscles are not required to perform much work (Cavagna, Heglund & Taylor 1977). Lejeune et al. (1998) suggested that when walking on sand, humans retain an efficient pendular energy exchange, whilst running maintains a bouncing mechanism. In contrast, Zamparo (1992) proposed that the increase in energetic costs on sand could be attributed to a reduced recovery of potential and kinetic energy during walking and a reduced recovery of elastic energy when running. Lejeune et al. (1998) attributed the higher energetic costs to an increase in muscle-tendon work and a decrease in muscle-tendon efficiency. When walking on a hard surface, minimal amount of work is done on the environment and so positive work done by the muscles and tendons can be reabsorbed from one phase of a step to the next. However, when walking on compliant substrates such as sand, there is a greater amount of work done on the environment and thus, energy is lost and has to be replaced by the muscles. Zamparo et al. (1992) propose that foot slippage during push-off contributes to the increase in energetic costs. Natural substrates such as sand contain air gaps and as the foot strikes the surface, the pressure of the foot will compress and displace the surface and causes the foot to slip and sink. Thus, lower limb muscles are required to carry out additional work to stabilise the point of reaction force on the surface and to control joint excursion (Lejeune, Willems & Heglund 1998; Zamparo et al. 1992).

Pinnington and Dawson (2001) suggested a potential increase in muscle co-activation and an increase in foot contact time on compliant substrates may lead to increased oxygen consumption due to a reduction in elastic energy storage and recovery, and ultimately a decrease in muscle-tendon efficiency as postulated by Zamparo et al. (1992). When walking on uneven or slippery surfaces, humans increase muscle co-activation about the ankle joint to maintain stabilisation

(Marigold & Patla 2002; Wade et al. 2010). Bates et al. (2013b) propose that increased activation of ankle extensors are required from mid-stance through to the swing phase of gait due to the deceleration of the foot and the greater muscle-tendon forces required to generate propulsion through increased forefoot motion. While Bates et al. (2013b) did not directly measure energy expenditure, they did investigate the relationship between footprint depth, foot pressure and lower limb motion. As footprint depth increased, there was a change in footprint shape suggesting potential differences in lower limb kinematics.

Previous studies have shown that when traversing more complex or compliant substrates, subjects will adopt a gait with greater hip and knee flexion compared to that on a hard surface (Gates et al. 2012; Pinnington et al. 2005; Voloshina et al. 2013). Greater joint flexion is accompanied by greater mechanical work, particularly at the hip and knee joint (Voloshina et al. 2013). Pandolf et al. (1976) found that when walking on snow, locomotion was affected by increasing lift work, a stooping posture and reduced stability. Adjusting step parameters and increased gait variability are likely to affect the metabolic energy costs during locomotion on compliant substrates (Donelan, Kram & Kuo 2002; O'Connor, Xu & Kuo 2012). On soft or uneven substrates, stride width increases and stride lengths tend to become shorter and more variable (Pinnington et al. 2005; Voloshina et al. 2013). Humans tend to adopt a shorter step length and increased step frequency and step width as a strategy to maintain medio-lateral balance during walking and reduce the risk of falls (Hak et al. 2012).

The purpose of this study was to determine the changes in walking biomechanics on sand, how they might vary as compliance increases, and how they might relate to increased metabolic cost. This study aims to investigate the influence of specific properties of sand on gait kinematics as well as footprint depth which will be done by comparing human locomotion on different types of sand and moisture content. More specifically this study will aim to address the following questions:

1. How does substrate compliance affect gait kinematics and muscle activity?
2. Do the different sand types affect gait in the same way?

3. Can we predict relative aspects of gait from footprint depth?

In order to tackle the questions presented, we hypothesised the following:

1. As substrate compliance increases, the pendular energy exchange mechanism will have reduced efficiency
2. As substrate compliance increases, stance time will increase and walking speed, stride width and stride length will decrease
3. As substrate compliance increases, there will be greater joint excursions at the hip, knee, and ankle joints due primarily to an increase in peak joint flexion
4. As substrate compliance increases, there will be greater muscle activation for lower limb muscles, and particularly the ankle extensors
5. The changes in gait kinematics and kinetics will be similar on both the dry, soft sand types compared to the hard floor
6. The wet, compact sand will produce intermediate gait changes between the hard floor and the more compliant softer sand types

3.3 Materials and methods

3.3.1 Substrates

There were two different sands used in this study: playing sand and building sand. To examine how variance in compliance due to moisture content impacts gait we generated two experimental substrates from the building sand with differing moisture contents (see below) thereby yielding three compliant substrates in total to compare to locomotion on a hard, level floor. As the substrates were not intended to imitate an existing terrain, we decided the appropriate moisture content through trial and error by adding water gradually until we got shallower footprint depths to the drier sand by several test subjects. The sand used is readily available as standard sandbags and

was purchased from Wickes. To ensure the sand substrates were comparable for each participant, several measurements were taken prior to the participant's arrival in the gait lab. This included taking measurements from different points of each walkway using a shear vane tester, force gauge and measuring the depth of footprints made by the lead investigator on each walkway (Fig. 3.1).

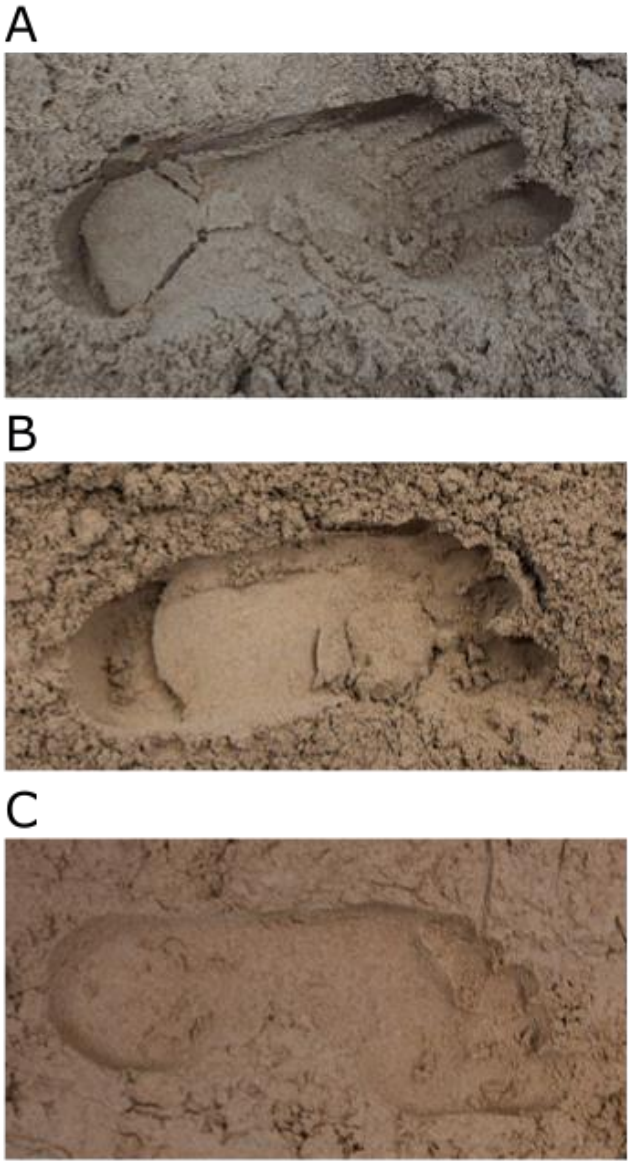

Figure 3.1: Example of the control footprints created in the three sand walkways: ***a)*** play sand, ***b)*** build dry and ***c)*** build wet.

First, the sand was loosened thoroughly using handheld rakes and if there had been some loss of sand then the sand was topped up to ensure the height of the sand was the full 10cm of the walkway and then raked over to create a level surface. For the play sand and dry building sand, the surface of the sand was left as it was after raking but for the wet building sand, it was pressed down lightly to create a smooth surface. Following this, the lead investigator would walk across each substrate to create a control set of footprints, as seen in figure 3.1. From each walkway, the depth of the middle 6 footprints was recorded using a ruler at the hallux, mid-foot and heel. These were compared to the previous 'expected' values (previously recorded values from when the walkways were first set-up as desired). For the shear vane and force gauge, five values was taken from different points of each walkway (around half-way between each recorded footprint). A shear vane test is a method of measuring shear strength of a cohesive soil using equipment consisting of a rod with four vanes on the end which is inserted into the sand to a depth of 500mm and rotated at rate of between 6-12 degrees per minute. On the top of the rod, a gauge measures the torque required to cause failure of the soil and converts the value into shear strength (kN/m^2) (Bell 2013). A digital force gauge (RS PRO Force Gauge RS232) was used to measure compression and tension of the sand. The device was inserted into the sand to a depth of 300mm and then the device converted the voltage of the load into a force value (kg) (Holtz, Kovacs & Sheahan 1981). As the walkways were inside the gait lab, some moisture may evaporate between data-collection days. If the values recorded using the different methods (lead investigators footprint depths, shear vane and/or force gauge) were not deemed comparable to previous studies, then additional water would be added to ensure the moisture content was similar. The steps outlined above would be repeated until acceptable values were recorded.

3.3.2 Participant set-up

Twenty-one young, healthy individuals were recruited to take part in this study involving walking experiments on sand. This study was conducted at the University of Liverpool Gait Lab at the Institute of Life Course and Medical Sciences and all

participants signed informed consent before participating in the study in accordance with ethical approval from the University of Liverpool's Central University Research Ethics Committee for Physical Interventions (#3757). The participants had their key biometrics recorded, including height and weight (9 males, 12 females; age = 26.7 ± 5.3 years; height= 1.73 ± 0.1 m; body mass = 68.45 ± 9.25 kg; body mass index = 22.75 ± 2.37 kgm-2; see Table 3.1). Participant set-up for this study is nearly identical to those described in chapter 2. Participants had reflective markers for 3D and surface-electromyography (sEMG) sensors for muscle activities attached at the relevant locations. This included a total of 69 markers at key anatomical landmarks over the whole body (see Table 2.2 for the full list of location sites). For sEMG, standard skin preparation methods were utilised and sensors were placed on the muscle belly in-line with the approximate expected direction of the muscle fibres. The signal of each sensor was tested for baselines noise and impedance by getting the participant to perform certain actions (e.g. flexing and extending knee) and sensors were re-attached if the signal was poor. Electrodes were positioned to record the activity of 8 left lower extremity muscles: biceps femoris (BFL), rectus femoris (RF), vastus lateralis (VL), vastus medialis (VM), tibialis anterior (TA), lateral gastrocnemius (LG), medial gastrocnemius (MG) and soleus (SOL) (seen in Figure 2.2) and 6 torso muscles: longissimus erector spinae (LES_L and LES_R), external abdominal oblique (EO_L EO_R) and internal abdominal oblique (IO_L and IO_R) (Figure 3.2) (Muscle functions and attachment details are in appendix Table 6.1). Sensors were attached to the left side only for the lower limb muscles but were attached to both the left and right side for the torso muscles. The number of muscles instrumented was limited by the number of available sensors. All markers and sensors were attached by the same examiner for all participants, with the exception of one (Subject 11).

Table 3.1: Anthropometric measurements from each subject: subject number, age (years), gender (male/female), height (m), body mass (kg) and BMI (kgm^{-2}) with mean and standard deviation of all 30 participants.

Subject	Age	Gender	Height (m)	Body mass (kg)	BMI (kgm^{-2})
1	37	m	1.76	68	21.95
2	27	m	1.75	65.4	21.36
3	27	f	1.76	72.6	23.44
4	26	m	1.75	68	22.2
5	25	m	1.8	81.8	25.25
6	31	m	1.8	80.6	24.88
7	33	f	1.68	56.45	20
8	29	m	1.86	83.3	24.08
9	29	f	1.7	68	23.53
10	28	f	1.72	81	27.38
11	27	f	1.69	77	26.96
12	28	m	1.74	78	25.76
13	38	m	1.79	75.9	23.69
14	29	f	1.64	58.7	21.82
15	22	f	1.65	64.95	23.86
16	20	f	1.67	58	20.8
17	19	f	1.73	55.8	18.64
18	20	f	1.76	67.85	21.9
19	20	f	1.78	62.6	19.76
20	19	f	1.64	53.8	20
21	27	m	1.71	59.8	20.45
Mean	26.71	9m 12f	1.73	68.45	22.75
SD	5.30		0.06	9.25	2.37

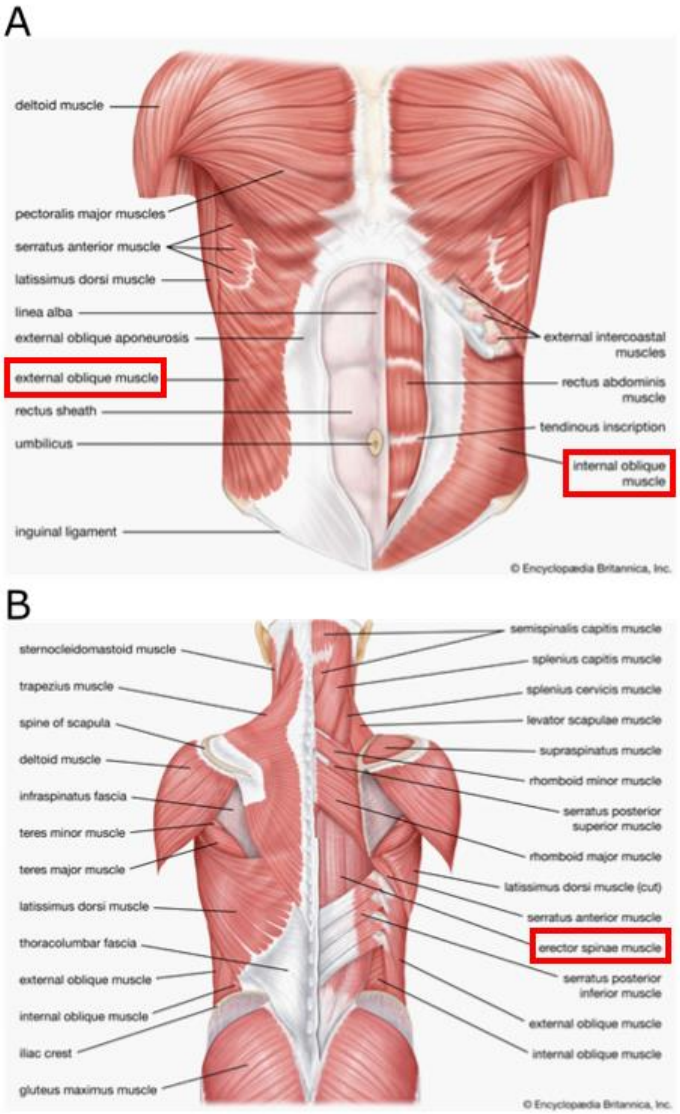

Figure 3.2: sEMG sensor set-up on the torso: ***a)*** Anterior view (external oblique and internal oblique muscle) and ***b)*** posterior view (erector spinae muscle). Muscles measured in this study are highlighted with a red box. All torso muscles were measured on both the left and right side. From Britannica (2022).

3.3.3 Data Collection

First, a static trial in the anatomical position was recorded. Then, participants walked at a self-selected speed on four surfaces: 1) hard, level floor 2) wet building sand 3) dry building sand and 4) play sand (Figure 3.3). All three sand walkways were identical in size: 9.6m (length) x 0.6m (width) x 0.1m (height). This included a 2.4m

long wooden walkway at the start and end of the walkway with a 4.8m long middle section filled with sand. On the floor, the participant walked a length of 10m. Participants performed a total of three trials on the hard lab floor and five trials on each sand walkway with substrate order randomised while 3D kinematics and EMG were measured synchronously. A single trial involved walking from one end of the walkway to the other end in one direction (the same direction for all trials). For all trials, whole-body kinematics were recorded using a 12-camera Qualisys Oqus 7 infrared cameras (12MP) operating at 200 Hz, controlled by Qualisys Track Manager (QTM) software (Qualisys Inc., Götenborg, Sweden). EMGs were recorded using the wireless Trigno EMG (Delsys, MA, USA) system at a sampling rate of 1110 Hz.

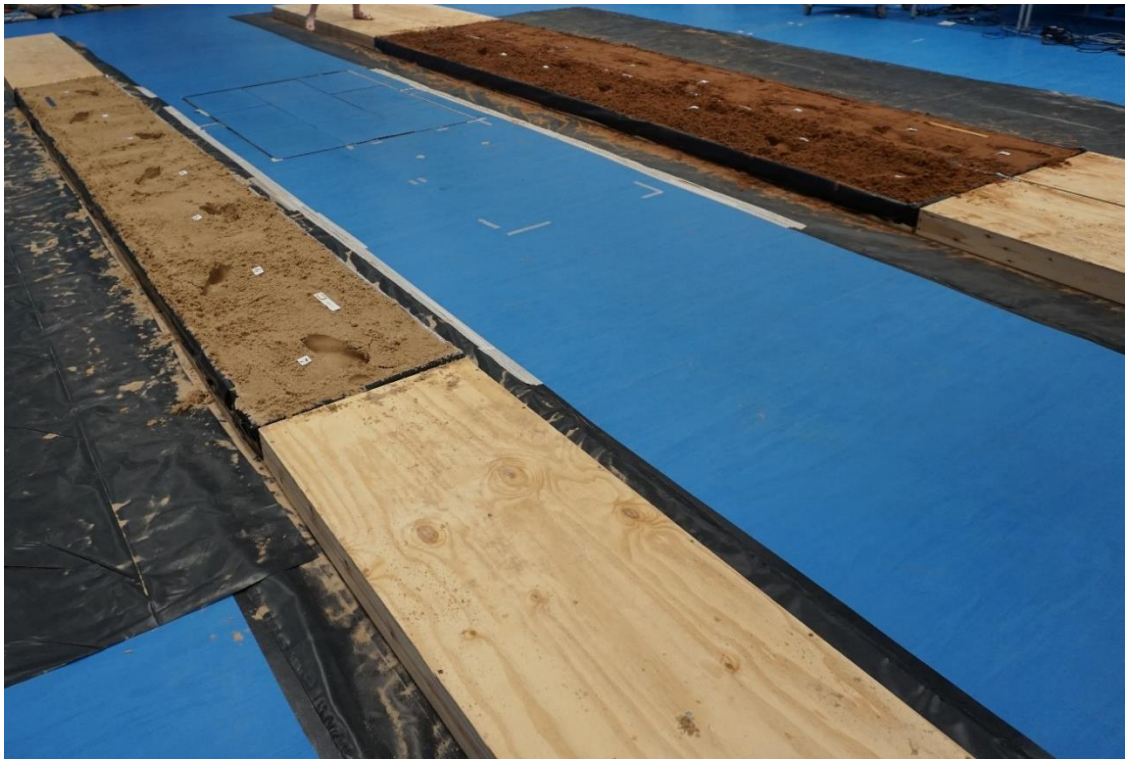

Figure 3.3: Example of the set-up of the wooden walkways and the four different substrates: play sand (far left), hard lab floor (centre left), dry building sand (centre right) and wet building sand (far right).

3.3.4 Data Processing

Motion capture data was processed using Qualisys Track Manager (QTM) 2.15 (2017). In QTM, the markers were labelled according to their respective anatomical references. Some trials required automatic gap-fill for small ranges of frames when the marker was not registered by the cameras at all times. The files were then cropped; the steps at the beginning and end of the trial that took place on the wooden walkways were removed as well as the first step on the sand to ensure that all steps included in the analyses comprised of the steady walking on the compliant substrate only. On the floor, the first two and last two steps were also removed to ensure the participant was walking at a steady speed in the steps included in the analyses. The files were cropped to full strides. For most participants, after cropping, the files included 5-6 steps on the sand trials and 6-7 steps on the floor. For some trials, there was only 4 steps included to ensure that all required markers were visible throughout. In rare cases, the markers had very poor recognition by the cameras, which created large gaps and therefore some trials had to be discarded e.g. all build wet files for participant 21. The files were then exported as C3D files to be analysed in Visual 3D (C-Motion Inc., Germantown, MD, USA).

In Visual 3D, each labelled marker was assigned to a body segment with a kinematic model comprised of 13 segments: bilateral feet, shanks, thighs, upper arms, forearms, and head, trunk and pelvis. In some cases, it was necessary to create artificial markers, which were positioned using anatomical knowledge of the landmark position. The static trial was used to create the multi-segment model which was applied to all walking trials. The marker positions were filtered with a low-pass, zero phase-shift 2nd order 10Hz Butterworth filter. Kinematic gait events were calculated automatically using a co-ordinate based algorithm that used foot positions relative to the pelvis (Zeni Jr, Richards & Higginson 2008). Automatically calculated gait events were checked manually for every trial. The gait events that were defined were heel-strike and toe-off for both left and right feet. The first weight-bearing contact between the substrate and the foot was taken as heel-strike and the last weight-bearing contact between the substrate and the hallux was taken as toe-off.

Numerous pipelines were applied to all files which calculated joint angles, centre of mass position and spatiotemporal variables. The cardan sequence specified was X = flexion/extension, Y = abduction/adduction and Z = longitudinal rotation (Kadaba, Ramakrishnan & Wootten 1990). Joint angles are defined as the orientation of one segment relative to another segment. In Visual 3D, speed, stride length, stride width, cycle time, stance time, swing time and double-support time were calculated automatically. The 3D centre of gravity locations of each segment was also calculated. These were used to calculate centre of mass (CoM) of the whole body using the position of the kinematic model in relation to the lab based on mechanical principle patterns (Hanavan Jr 1964). All the calculated data were exported from Visual 3D as text files for further analyses performed in MATLAB v.2019a (Mathworks, Natick, USA) and R (Team). In MATLAB, duty factor (the ratio between stance phase and gait cycle) was also calculated.

All EMG processing was performed in MATLAB (Mathworks, Natick, USA). As the marker tracking and EMG were synchronised, the EMG files were cropped according to QTM start and end times. The raw EMG signals were high pass filtered at 12Hz with a second-order Butterworth filter to remove any artifacts and noise and full-wave rectified (see Fig. 2.4a). The exported gait events from Visual 3D were used to crop the trials to stride (see Fig. 2.4b). For each muscle, the data was normalised (nEMG) to maximum amplitude during all walking trials for that participant to allow for between-participant comparison. The integrated values (iEMG) were calculated in MATLAB. For each participant, data was grouped according to substrate and the mean and standard deviations were calculated for each muscle. Then, participants were combined together according to substrate type. Due to problems in muscle data acquisition for some participants, there is only a total of 19 participant's EMG data included in the analysis.

The mass-normalised 3D CoM exported from Visual 3D were used to calculate the gravitational potential energy (E_{pot}), kinetic energy (E_{kin}) and total mechanical energy (E_{tot}) in MATLAB. Then, the recovery of mechanical energy (expressed as a

percentage; R), relative amplitude (RA) and congruity (the time when potential energy and kinetic energy are moving in the same direction; CO) were calculated (Cavagna, Thys & Zamboni 1976).

3.3.5 Statistical analysis of experimental data

Joint kinematics were analysed using two statistical approaches: One dimensional statistical parametric mapping (1D-SPM) (Pataky, Robinson & Vanrenterghem 2013), and Linear mixed-effect models (LMMs) (Faraway 2016). 1D-SPM is a topological method used to compare complete time series data but does not allow the incorporation of additional factors (e.g. random or fixed effects) as LMMs do. 1D-SPM analyses were performed using MATLAB to compare hip, knee and ankle joint angles across substrates, with null hypothesis of no difference and alpha of 0.05. The mean and standard deviation of the joint angles were plotted for the duration of a gait cycle (0-100%). Vertical dotted lines were plotted to indicate the toe-off timings for each substrate. Differences between the different substrate types were detected by 1D-SPM, utilising paired t-tests with Bonferroni corrections to reduce the probability of a type-II error occurring as a result of applying t-tests to four groups. The Bonferroni corrections led to an alpha value of 0.0170. Joint angles at gait events (heel-strike and toe-off), spatiotemporal data, iEMG data and mass-normalised mechanical energy exchange variables were analysed using LMMs, where restricted maximum likelihood was used to assess the significance of the fixed effects, substrate type, gender and speed in explaining variation. Participants were set as random effects, which allowed different intercepts for each subject. All LMM's were performed in R (Team) using the lmer function in the R package lme4 (Bates et al. 2014) and lmerTest (Kunzetsova, Brockhoff & Christensen 2017). Spatiotemporal variables and mechanical energy exchange variables are also presented as box-and-whisker plots to visualise the distribution of data. The coefficient of variation (CV) (the ratio of the standard deviation to the mean) was calculated for all spatiotemporal data as a measure of relative gait variability ($CV = (SD/\bar{x}) * 100$).

3.3.6 Footprint depth calculations

Footprint depth was estimated using the z-positions of the kinematic markers positioned at the left hallux (LHALL) and left calcaneus (LCAL). Before every data collection session, the lab is calibrated with Z = 0 as the height of the lab floor and markers on each end of the sand walkways were used to calculate the Z-value of the sand substrates. After data processing, the lowest z-values for LCAL and LHALL for every stride was exported from Visual 3D. These values were deducted from the Z-value of the substrate to estimate the lowest sinking point of the foot in each substrate as a proxy for footprint depth.

3.4 Results

3.4.1 Footprint depth

Figure 3.4 shows the footprints depths recorded at the left calcaneus (Fig. 3.4a) and left hallux (Fig. 3.4b) for all participants. The values for LCAL (mean ± s.d.) was 1.12 ± 0.82cm, 2.17 ± 0.99cm, 2.62 ± 0.99 cm and 4.46 ± 1.36cm, on the floor, wet building sand, dry building sand and play sand substrate, respectively (Fig. 3.4a). The values for LHALL (mean ± s.d.) was 0.74 ± 0.75cm, 3.73 ± 0.94cm, 4.13 ± 1.32 cm and 5.54 ± 1.44cm, on the floor, wet building sand, dry building sand and play sand substrate, respectively (Fig. 3.4b).

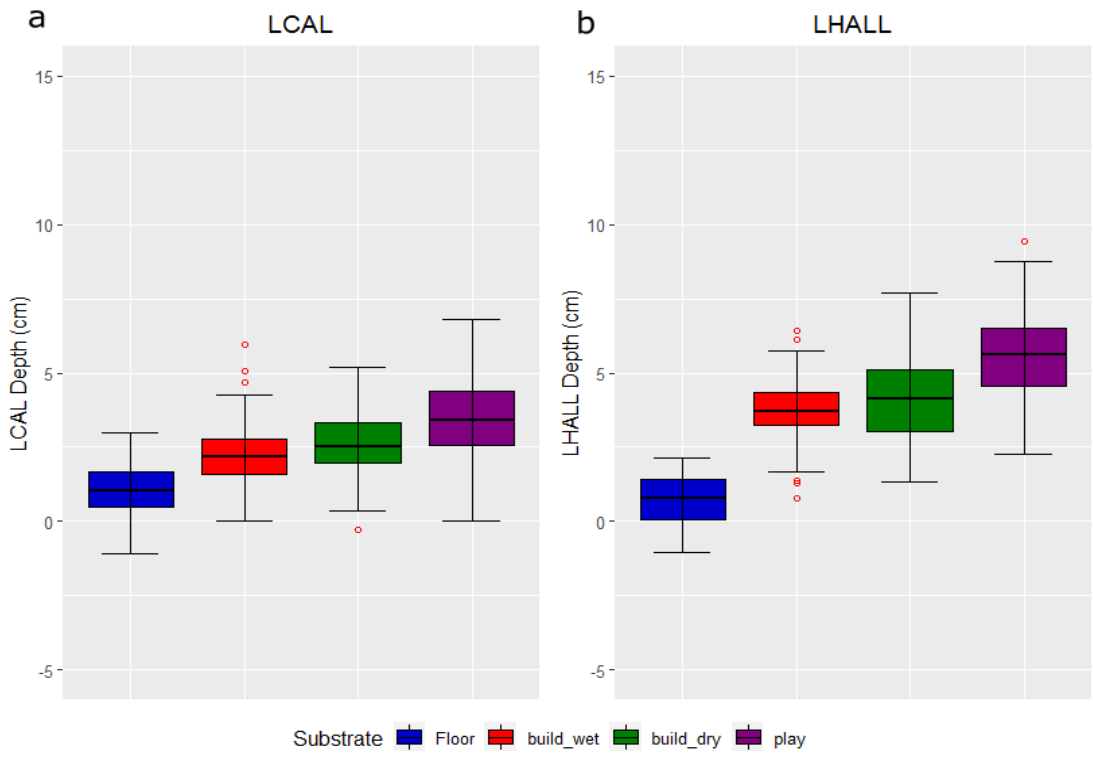

Figure 3.4: Sinking depth measurements calculated using lowest z-value positions for every stride for all participants combined (n=21) while walking on the four different substrates: floor (blue), build wet sand (green), build dry sand (red) and play sand (purple): ***(a)*** Left calcaneus (n=574), ***(b)*** Left hallux (n=574). The centre line denotes the median value (50th percentile) while the boxes contain the 25th to 75th percentiles of dataset. The boundaries of the whiskers mark the 1.5 IQR with outliers shown as red circles. Values used as a proxy for footprint depth.

3.4.1 Spatiotemporal variables

For some spatiotemporal variables, the magnitudes of differences between substrates were small. In general, on all sand substrates, cycle time, stance time, swing time and double-limb-support-time increased in comparison to the hard floor (Fig. 3.5). LMMs show that there was significant ($p<0.001$) differences between all substrates for speed (Table 3.2), and between all substrates except the two most compliant sands, build dry and play sand, for cycle time, stance time and double limb support time ($p<0.05$) (Table 3.3). There was no significant ($p>0.05$) difference between any substrates for stride width (Table 3.2). There were significant ($p<0.05$) differences between some substrates for stride length, swing time and duty factor. Gender had a

significant ($p<0.05$) effect on stride length, cycle time, stance time and duty factor, which is also reflected in the significant ($p<0.05$) interaction effects between substrate and gender for these variables. Speed had a significant ($p<0.001$) effect on stride length, cycle time, stance time, swing time and double-limb-support-time and ($p<0.05$) duty factor. This is also shown by the significant ($p<0.05$) interaction effects between substrate and speed, particularly between the less compliant substrates (floor and build wet sand) and the more compliant substrates (build dry and play sand) (Tables 3.2-3.3). There was also some significant ($p<0.05$) interaction effects between substrate, speed and gender for most spatiotemporal variables. There is a significant ($p<0.001$) different intercept for participants for all spatiotemporal variables (Tables 3.2- 3.3).

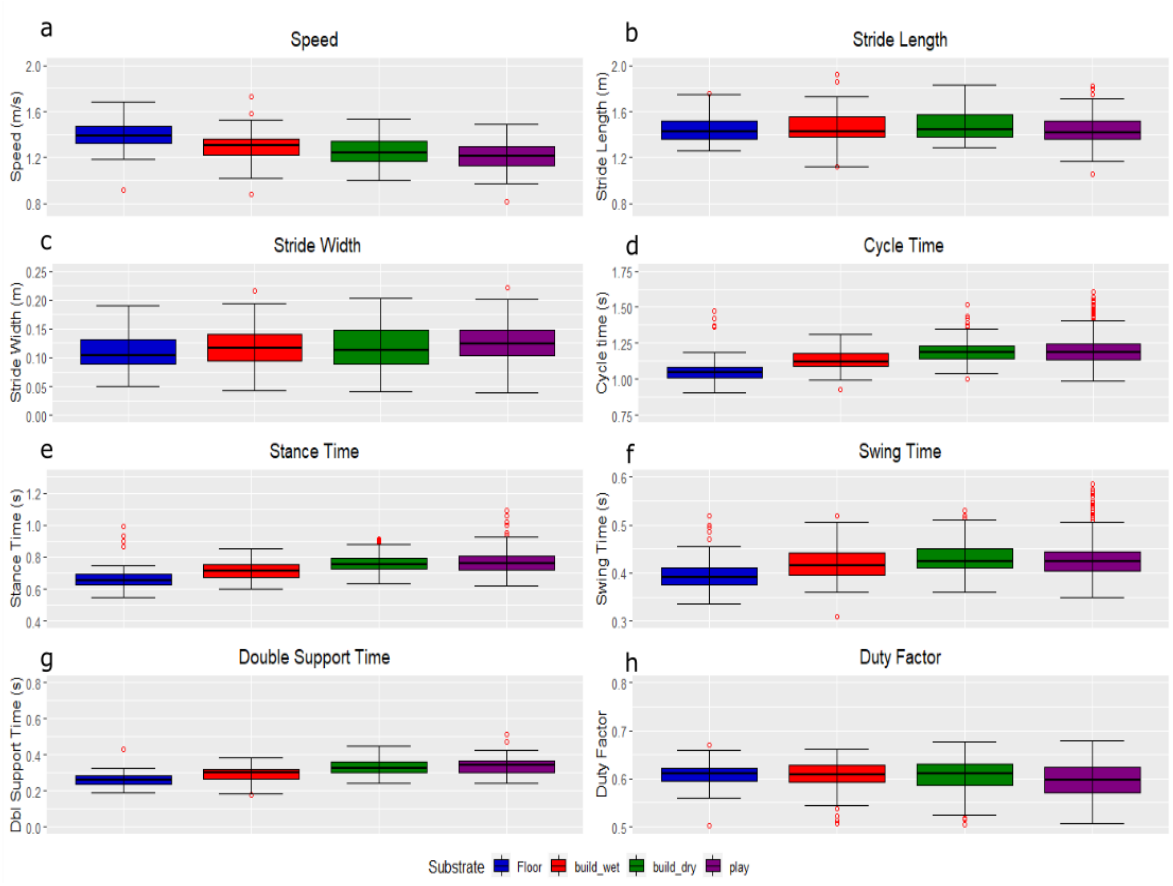

Figure 3.5: The distribution of spatiotemporal parameters for all participants combined (n=21) while walking on the four different substrates: floor (blue), build wet (green), build dry (red) and play sand (purple). ***(a)*** speed, ***(b)*** stride length, ***(c)*** stride width, ***(d)*** cycle time, ***(e)*** stance time, ***(f)*** swing time, ***(g)*** double support time and ***(h)*** duty factor. Data includes all strides for individual trials (n = 301). The centre line denotes the median value (50^{th} percentile) while the boxes contain the 25^{th} to 75^{th} percentiles of dataset. The boundaries of the whiskers mark the 1.5 IQR with red circles denoting an individual stride from any subject that represents a statistical outlier.

Table 3.2: The results of the linear mixed-effect models on the spatiotemporal parameters: speed (ms^{-1}), stride length (m), stride width (m) and cycle time (s); fixed effects = substrate, speed and gender and random effects = subjects. Statistical significance is set as $p<0.05$ with significant p-values shown in bold. σ^2 = random effect variance, τ_{00} = subject variance, intraclass correlation coefficient (ICC) = proportion of variance explained by random effects, N = number of subjects, observations = number of data points (strides), marginal R^2 = proportion of variance explained by the fixed factors, conditional R^2 = proportion of variance explained by both the fixed and random factors.

	Speed			**Stride_Length**			**Stride_Width**			**Cycle_Time**		
Predictors	*Estimates*	*CI*	*p*	*Estimates*	*CI*	*p*	*Estimates*	*CI*	*p*	*Estimates*	*CI*	*p*
(Intercept)	1.22	1.16 – 1.27	**<0.001**	0.83	0.69 – 0.97	**<0.001**	0.17	0.10 – 0.23	**<0.001**	1.87	1.76 – 1.98	**<0.001**
Substrate [build_wet]	0.06	0.04 – 0.08	**<0.001**	-0.35	-0.52 – -0.17	**<0.001**	-0.01	-0.10 – 0.08	0.833	-0.34	-0.48 – -0.20	**<0.001**
Substrate [Floor]	0.14	0.13 – 0.16	**<0.001**	-0.04	-0.21 – 0.13	0.630	-0.07	-0.15 – 0.02	0.111	-0.25	-0.39 – -0.12	**<0.001**
Substrate [play]	-0.03	-0.04 – -0.02	**<0.001**	0.05	-0.11 – 0.20	0.553	-0.05	-0.13 – 0.03	0.191	0.08	-0.04 – 0.20	0.208
Gender [M]	0.08	-0.00 – 0.16	0.065	-0.30	-0.51 – -0.09	**0.005**	-0.04	-0.14 – 0.06	0.483	-0.20	-0.36 – -0.03	**0.019**
Substrate [build_wet] * Gender [M]	0.01	-0.01 – 0.04	0.359	0.34	0.07 – 0.61	**0.015**	-0.12	-0.25 – 0.02	0.082	0.21	-0.01 – 0.42	0.058
Substrate [Floor] * Gender [M]	-0.01	-0.03 – 0.02	0.524	-0.06	-0.30 – 0.17	0.599	0.00	-0.11 – 0.12	0.989	0.08	-0.11 – 0.26	0.407
Substrate [play] * Gender [M]	-0.03	-0.05 – -0.01	**0.005**	-0.05	-0.27 – 0.17	0.663	0.06	-0.05 – 0.17	0.262	0.05	-0.12 – 0.23	0.550
Speed				0.48	0.37 – 0.60	**<0.001**	-0.04	-0.09 – 0.02	0.206	-0.58	-0.67 – -0.49	**<0.001**
Substrate [build_wet] * Speed				0.25	0.11 – 0.40	**0.001**	0.01	-0.06 – 0.08	0.817	0.25	0.14 – 0.37	**<0.001**
Substrate [Floor] * Speed				-0.03	-0.16 – 0.11	0.685	0.04	-0.02 – 0.11	0.217	0.15	0.04 – 0.26	**0.006**
Substrate [play] * Speed				-0.04	-0.17 – 0.08	0.500	0.04	-0.02 – 0.11	0.172	-0.07	-0.17 – 0.03	0.172
Speed * Gender [M]				0.31	0.15 – 0.47	**<0.001**	0.02	-0.06 – 0.10	0.586	0.22	0.09 – 0.34	**0.001**
(Substrate [build_wet] * Speed) * Gender [M]				-0.28	-0.50 – -0.07	**0.008**	0.08	-0.02 – 0.19	0.122	-0.18	-0.35 – -0.01	**0.033**
(Substrate [Floor] * Speed) * Gender [M]				-0.00	-0.18 – 0.18	0.965	0.00	-0.08 – 0.09	0.918	-0.09	-0.23 – 0.05	0.201
(Substrate [play] * Speed) * Gender [M]				0.05	-0.13 – 0.23	0.596	-0.05	-0.14 – 0.04	0.261	-0.04	-0.18 – 0.11	0.630
Random Effects												
σ^2	0.01			0.00			0.00			0.00		
τ_{00}	0.01 $_{Subject}$			0.00 $_{Subject}$			0.00 $_{Subject}$			0.00 $_{Subject}$		
ICC	0.60			0.64			0.46			0.66		
N	21 $_{Subject}$			21 $_{Subject}$			21 $_{Subject}$			21 $_{Subject}$		
Observations	1537			922			922			935		
Marginal R^2 / Conditional R^2	0.311 / 0.724			0.610 / 0.861			0.060 / 0.493			0.617 / 0.868		

Table 3.3: The results of the linear mixed-effect models on the spatiotemporal parameters: stance time (s), swing time (s), double support time (s) and duty factor; fixed effects = substrate, speed and gender and random effects = subjects. Statistical significance is set as $p<0.05$ with significant p-values shown in bold. σ^2 = random effect variance, τ_{00} = subject variance, intraclass correlation coefficient (ICC) = proportion of variance explained by random effects, N = number of subjects, observations = number of data points (strides), marginal R^2 = proportion of variance explained by the fixed factors, conditional R^2 = proportion of variance explained by both the fixed and random factors.

	Stance_Time			**Swing_Time**			**Double_Limb_Support_Time**			**Duty_Factor**		
Predictors	*Estimates*	*CI*	*p*	*Estimates*	*CI*	*p*	*Estimates*	*CI*	*p*	*Estimates*	*CI*	*p*
(Intercept)	1.36	1.28 – 1.43	**<0.001**	0.54	0.49 – 0.59	**<0.001**	0.79	0.70 – 0.88	**<0.001**	0.72	0.64 – 0.80	**<0.001**
Substrate [build_wet]	-0.31	-0.40 – -0.21	**<0.001**	-0.05	-0.11 – 0.01	0.103	-0.27	-0.37 – -0.16	**<0.001**	-0.04	-0.14 – 0.07	0.489
Substrate [Floor]	-0.23	-0.32 – -0.13	**<0.001**	-0.06	-0.12 – 0.00	0.071	-0.14	-0.26 – -0.03	**0.014**	-0.08	-0.19 – 0.02	0.103
Substrate [play]	-0.02	-0.11 – 0.06	0.634	0.06	0.00 – 0.11	**0.041**	-0.05	-0.15 – 0.05	0.315	-0.10	-0.19 – -0.01	**0.034**
Speed	-0.50	-0.57 – -0.44	**<0.001**	-0.09	-0.13 – -0.05	**<0.001**	-0.38	-0.45 – -0.31	**<0.001**	-0.09	-0.16 – -0.03	**0.005**
Gender [M]	-0.18	-0.30 – -0.07	**0.002**	-0.04	-0.11 – 0.03	0.258	-0.12	-0.25 – 0.01	0.072	-0.15	-0.27 – -0.03	**0.017**
Substrate [build_wet] * Speed	0.23	0.15 – 0.31	**<0.001**	0.04	-0.01 – 0.09	0.139	0.20	0.11 – 0.29	**<0.001**	0.04	-0.05 – 0.12	0.406
Substrate [Floor] * Speed	0.15	0.08 – 0.23	**<0.001**	0.02	-0.03 – 0.07	0.350	0.10	0.01 – 0.19	**0.027**	0.08	-0.00 – 0.16	0.057
Substrate [play] * Speed	0.02	-0.06 – 0.09	0.671	-0.05	-0.10 – -0.01	**0.024**	0.05	-0.04 – 0.13	0.291	0.07	-0.00 – 0.15	0.059
Substrate [build_wet] * Gender [M]	0.25	0.10 – 0.40	**0.001**	-0.02	-0.11 – 0.07	0.713	0.27	0.11 – 0.43	**0.001**	0.19	0.03 – 0.36	**0.021**
Substrate [Floor] * Gender [M]	0.10	-0.03 – 0.23	0.139	0.04	-0.05 – 0.12	0.386	0.05	-0.11 – 0.20	0.548	0.13	-0.01 – 0.27	0.072
Substrate [play] * Gender [M]	0.11	-0.01 – 0.24	0.076	-0.01	-0.09 – 0.07	0.860	0.08	-0.06 – 0.23	0.254	0.26	0.13 – 0.40	**<0.001**
Speed * Gender [M]	0.19	0.10 – 0.28	**<0.001**	0.05	-0.00 – 0.11	0.064	0.11	0.01 – 0.21	**0.031**	0.11	0.02 – 0.21	**0.020**
(Substrate [build_wet] * Speed) * Gender [M]	-0.21	-0.33 – -0.09	**0.001**	0.00	-0.07 – 0.08	0.919	-0.21	-0.34 – -0.09	**0.001**	-0.15	-0.28 – -0.02	**0.020**
(Substrate [Floor] * Speed) * Gender [M]	-0.10	-0.20 – -0.00	**0.049**	-0.04	-0.10 – 0.03	0.283	-0.05	-0.17 – 0.07	0.436	-0.11	-0.22 – 0.00	0.050
(Substrate [play] * Speed) * Gender [M]	-0.09	-0.19 – 0.01	0.073	0.01	-0.05 – 0.08	0.681	-0.07	-0.19 – 0.05	0.231	-0.21	-0.32 – -0.10	**<0.001**
Random Effects												
σ^2	0.00			0.00			0.00			0.00		
τ_{00}	0.00 Subject			0.00 Subject			0.00 Subject			0.00 Subject		
ICC	0.60			0.48			0.58			0.28		
N	21 Subject			21 Subject			21 Subject			21 Subject		
Observations	935			1536			301			935		
Marginal R^2 / Conditional R^2	0.678 / 0.871			0.317 / 0.645			0.691 / 0.871			0.074 / 0.337		

The coefficient of variation (CV) was fairly similar for most spatiotemporal variables but there were differences between different variables on all substrates (Table 3.4). CV decreased by 9% for speed between floor and build wet but increased by 10% and 9% between floor and build dry and play sand, respectively. CV for stride length decreased by 17% between floor and build wet but were the same for build dry and play sand. There was a 9% decrease in CV for stride width between floor and build wet and build dry but a 4% increase between floor and play

sand. CV for cycle time increased by 4% and 7% between floor and build wet and build dry, respectively, but decreased by 16% between floor and play sand. There was a 10% increase in CV for stance time between floor and build wet and build dry but a 9% decrease between floor and play sand. CV for swing time decreased by 17%, 10% and 27% between floor and build wet, build dry and play sand, respectively. CV for double limb support time decreased by 3% between floor and build wet but increased by 11% and 4% between floor and build dry and play sand. There was an 11%, 7% and 23% decrease in CV for duty factor between floor and build wet, build dry and play sand, respectively (Table 3.4).

Table 3.4: The mean, s.d. and coefficient of variation (CV) for each spatiotemporal parameters: Speed (ms^{-1}), stride length (m), stride width (m), cycle time (s), stance time (s), swing time (s), double support time (s) and duty factor while walking on the four different substrates "floor", "build wet", "build dry" and "play" sand. The CV is a measure of relative variability expressed as a percentage ($CV = (SD/\bar{x}) * 100$).

Substrate		Speed (ms^{-1})	Stride Length (m)	Stride Width (m)	Cycle Time (s)	Stance Time (s)	Swing Time (s)	Dbl Support Time (s)	Duty Factor
Floor	Mean	1.41	1.46	0.11	1.05	0.65	0.39	0.26	0.61
	SD	0.14	0.12	0.03	0.08	0.06	0.03	0.04	0.03
	CV	9.76	7.89	26.64	7.29	8.66	6.83	14.53	4.87
Build wet	Mean	1.30	1.46	0.12	1.13	0.71	0.42	0.30	0.60
	SD	0.14	0.14	0.04	0.08	0.06	0.03	0.04	0.03
	CV	10.69	9.54	29.24	7.03	7.88	8.27	14.92	5.46
Build dry	Mean	1.26	1.48	0.12	1.19	0.76	0.43	0.33	0.60
	SD	0.11	0.12	0.04	0.08	0.06	0.03	0.04	0.03
	CV	8.81	7.83	29.24	6.83	7.91	7.59	13.13	5.25
Play	Mean	1.22	1.44	0.13	1.20	0.76	0.43	0.34	0.59
	SD	0.11	0.11	0.03	0.10	0.07	0.04	0.05	0.04
	CV	8.94	7.86	25.42	8.71	9.55	9.32	13.99	6.28

3.4.2 Mechanical energy exchange

When averaged across each subject, E_{tot} (Fig. 3.6a) and E_{kin} (Fig. 3.6b) decreased over the whole stride on all sand substrates, but especially on the softer substrates, build dry and play sand (Fig. 3.6). During most of the stride, E_{pot} increased on the sand substrates except during toe-off and early-stance (Fig. 3.6c).

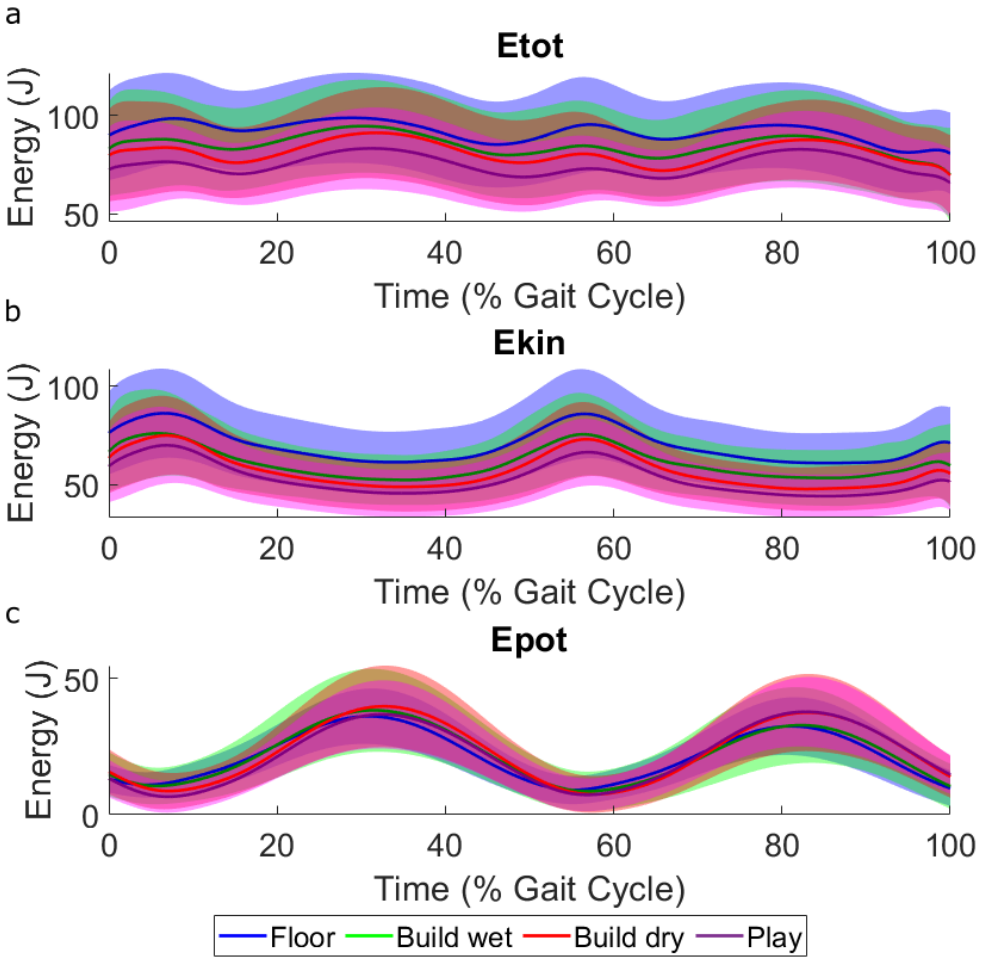

Figure 3.6: ***(a)*** Mass-normalised total (E_{tot}) mechanical energy, ***(b)*** kinetic (E_{kin}) energy and ***(c)*** the gravitational potential (E_{pot}) energy of the COM (bottom) and normalised to walking stride for all participants combined (n=21) while walking on the four different substrates (mean ± s.d): Floor (blue), build wet sand (green), build dry sand (red) and play sand (purple). Bold lines indicate the mean value and shaded regions show the standard deviation.

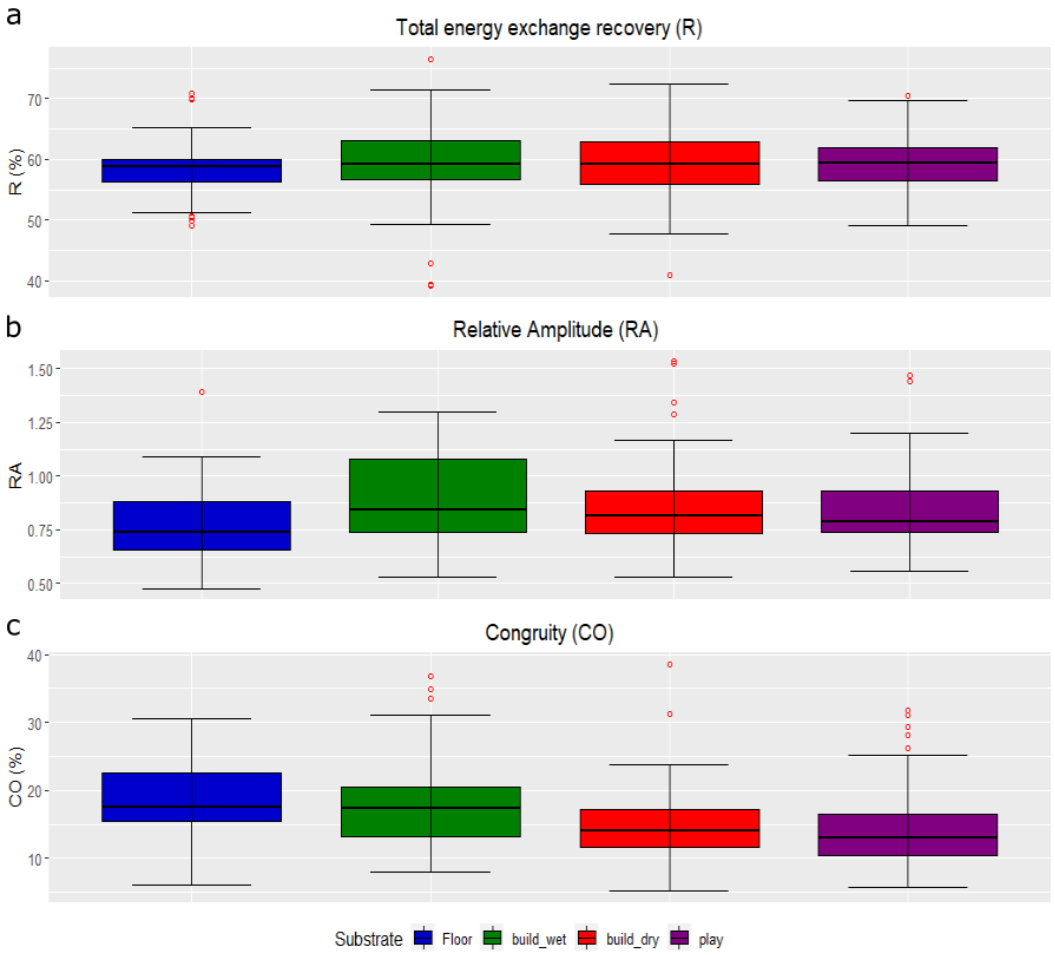

Figure 3.7: The distribution of pendulum-like determining variables: ***(a)*** The recovery of total energy exchange as a percentage (R), ***(b)*** Relative Amplitude (RA), and ***(c)*** Congruity percentage (CO) for all participants combined (n=21) while walking on the four different substrates: Floor (blue) (n=60), build wet sand (green) (n=50), build dry sand (red) (n=69) and play sand (purple) (n=89). The centre line denotes the median value (50th percentile) while the boxes contain the 25th to 75th percentiles of dataset. The boundaries of the whiskers mark the 1.5 IQR with red circles denoting an individual stride from any subject that represents a statistical outlier.

As substrate compliance increased, relative amplitude (RA) increased by ~15.9% between floor and build wet, ~10.1% between floor and build dry and ~8.7% between floor and play sand (Fig. 3.7). The recovery of total energy exchange (R) increased by ~1.7% between floor and build wet, ~2% between floor and build dry and ~1.9% between floor and play sand (Fig. 3.7). Congruity percentage (CO) decreased by ~2.9% between floor and build wet, ~18.3% between floor and build dry and ~19.5% between floor and play sand (Fig. 3.7). LMMs showed that the effect of substrate is not significant ($p>0.05$) for any variables (Table 3.5). There are

no significant ($p>0.05$) effects of gender for any variables but there is a significant ($p<0.05$) interaction effect between gender and substrate for RA. There is also a significant effect ($p<0.05$) for speed for R but no significant interaction effects between speed, gender and substrate for all variable (Table 3.5). There is a significant ($p<0.05$) intercept for all variables.

Table 3.5: The results of the linear mixed-effect models on the mass normalised mechanical energy exchange variables: the recovery of mechanical energy (expressed as a percentage; R), relative amplitude (RA) and congruity (the time when potential energy and kinetic energy are moving in the same direction; CO). Fixed effects = substrate, gender and speed and random effects = subjects. Statistical significance is set as $p<0.05$ with significant p-values shown in bold. σ^2 = random effect variance, τ_{00} = subject variance, intraclass correlation coefficient (ICC) = proportion of variance explained by random effects, N = number of subjects, observations = number of data points (strides), marginal R^2 = proportion of variance explained by the fixed factors, conditional R^2 = proportion of variance explained by both the fixed and random factors.

	R			**RA**			**CO**		
Predictors	*Estimates*	*CI*	*p*	*Estimates*	*CI*	*p*	*Estimates*	*CI*	*p*
(Intercept)	86.84	62.65 – 111.03	**<0.001**	0.98	0.05 – 1.91	**0.038**	29.07	2.54 – 55.61	**0.032**
Substrate [build_wet]	-17.98	-46.63 – 10.68	0.219	-0.15	-1.26 – 0.95	0.790	-7.12	-38.49 – 24.26	0.657
Substrate [Floor]	-13.42	-41.70 – 14.86	0.352	0.78	-0.31 – 1.87	0.161	15.73	-15.21 – 46.68	0.319
Substrate [play]	-17.79	-44.09 – 8.52	0.185	0.90	-0.12 – 1.91	0.084	-9.26	-38.05 – 19.52	0.528
Gender [M]	-0.67	-33.13 – 31.79	0.968	0.52	-0.72 – 1.77	0.410	-28.00	-63.65 – 7.64	0.124
Speed	-24.70	-44.99 – -4.41	**0.017**	-0.12	-0.90 – 0.66	0.757	-11.60	-33.84 – 10.63	0.306
Substrate [build_wet] * Gender [M]	-21.22	-63.37 – 20.92	0.324	0.33	-1.30 – 1.95	0.694	44.03	-2.10 – 90.16	0.061
Substrate [Floor] * Gender [M]	-19.51	-58.09 – 19.06	0.321	-1.56	-3.05 – -0.07	**0.040**	18.97	-23.24 – 61.18	0.378
Substrate [play] * Gender [M]	2.42	-34.38 – 39.23	0.897	-0.92	-2.35 – 0.50	0.203	25.84	-14.42 – 66.11	0.208
Substrate [build_wet] * Speed	14.83	-9.24 – 38.90	0.227	0.16	-0.77 – 1.08	0.742	9.75	-16.60 – 36.11	0.468
Substrate [Floor] * Speed	12.57	-10.21 – 35.35	0.279	-0.58	-1.46 – 0.30	0.193	-6.75	-31.68 – 18.18	0.596
Substrate [play] * Speed	16.31	-5.86 – 38.48	0.149	-0.72	-1.58 – 0.13	0.098	7.30	-16.97 – 31.56	0.556
Gender [M] * Speed	5.60	-20.43 – 31.63	0.673	-0.37	-1.37 – 0.63	0.473	21.65	-6.89 – 50.19	0.137
(Substrate [build_wet] * Gender [M]) * Speed	14.95	-18.41 – 48.30	0.380	-0.25	-1.54 – 1.04	0.704	-36.03	-72.54 – 0.48	0.053
(Substrate [Floor] * Gender [M]) * Speed	11.70	-18.03 – 41.43	0.440	1.08	-0.07 – 2.23	0.066	-17.68	-50.21 – 14.85	0.287
(Substrate [play] * Gender [M]) * Speed	-5.95	-35.81 – 23.90	0.696	0.67	-0.49 – 1.82	0.257	-20.49	-53.16 – 12.17	0.219
Random Effects									
σ^2	14.42			0.02			17.24		
τ_{00}	11.34 $_{\text{Subject}}$			0.01 $_{\text{Subject}}$			17.10 $_{\text{Subject}}$		
ICC	0.44			0.31			0.50		
N	19 $_{\text{Subject}}$			19 $_{\text{Subject}}$			19 $_{\text{Subject}}$		
Observations	269			269			269		
Marginal R^2 / Conditional R^2	0.136 / 0.517			0.143 / 0.407			0.150 / 0.573		

3.4.3 Joint kinematics

1D-SPM analyses of sagittal plane joint angles found significant differences between most substrates at different stages of the stride (Fig. 3.8; Tables 6.11-6.13 in appendix). Hip, knee and ankle joint angles are very similar throughout most of the stride on the two most compliant sands, build dry and play sand. During heel-strike, as substrate compliance increased, there was a significant ($p<0.001$) increase in hip flexion (Fig. 3.8c) and knee flexion (Fig. 3.8b) between all substrates, except for between the two most compliant substrates (build dry and play sand). LMMs at heel-strike show that substrate is a significant ($p<0.05$) effect between build dry and build wet sand for ankle and knee angle and between build dry and play sand ($p<0.001$) for knee angle (Table 3.6). Furthermore, there was a significant ($p<0.001$) effect of speed for hip angle and gender for ankle and hip angle ($p<0.05$). There was no significant ($p>0.05$) interaction effects between substrate, gender and speed for hip angle. There was significant ($p<0.05$) interaction effects between substrate, gender and speed for ankle angle and knee angle, mostly between build dry sand and floor and between build dry and play sand. Also, there was a significant ($p<0.05$) intercept for ankle angle (Table 3.6). During early to mid-stance there was significantly less plantarflexion at the ankle joint ($p<0.001$) on the sands (Fig 3.8a). During early-stance there was significant ($p<0.01$) differences at the hip and knee joint between all substrates except build dry/play with greater flexion on the sands (Fig. 3.8). Throughout much of stance phases, hip and knee joint angles were similar on all substrates. During late-stance, there were significant ($p<0.001$) decreases in knee-flexion on the sands and no significant ($p>0.05$) differences for hip and ankle angles for all substrates (Fig 3.8). LMMs at toe-off found significant ($p<0.05$) effects of substrate for ankle angle between floor and the more compliant substrates (build dry

and play sand) and knee angle between build wet and build dry sand (Table 3.7). Also, there was a significant ($p<0.05$) effect of speed for ankle angle, but there was only one interaction effect between speed and substrates, floor and build dry sand. There was no significant ($p>0.05$) effect of gender for all joint angles on all substrates but there was a couple significant ($p\leq0.001$) interaction effects between substrate, gender and speed (Table 3.7). Also, there was a significant ($p<0.05$) intercept for knee angle at toe-off (Table 3.7). During the swing phase, there were significant ($p<0.001$) increases in plantarflexion at the ankle joint and in flexion at the knee and hip joint as substrate compliance increased (Fig 3.8).

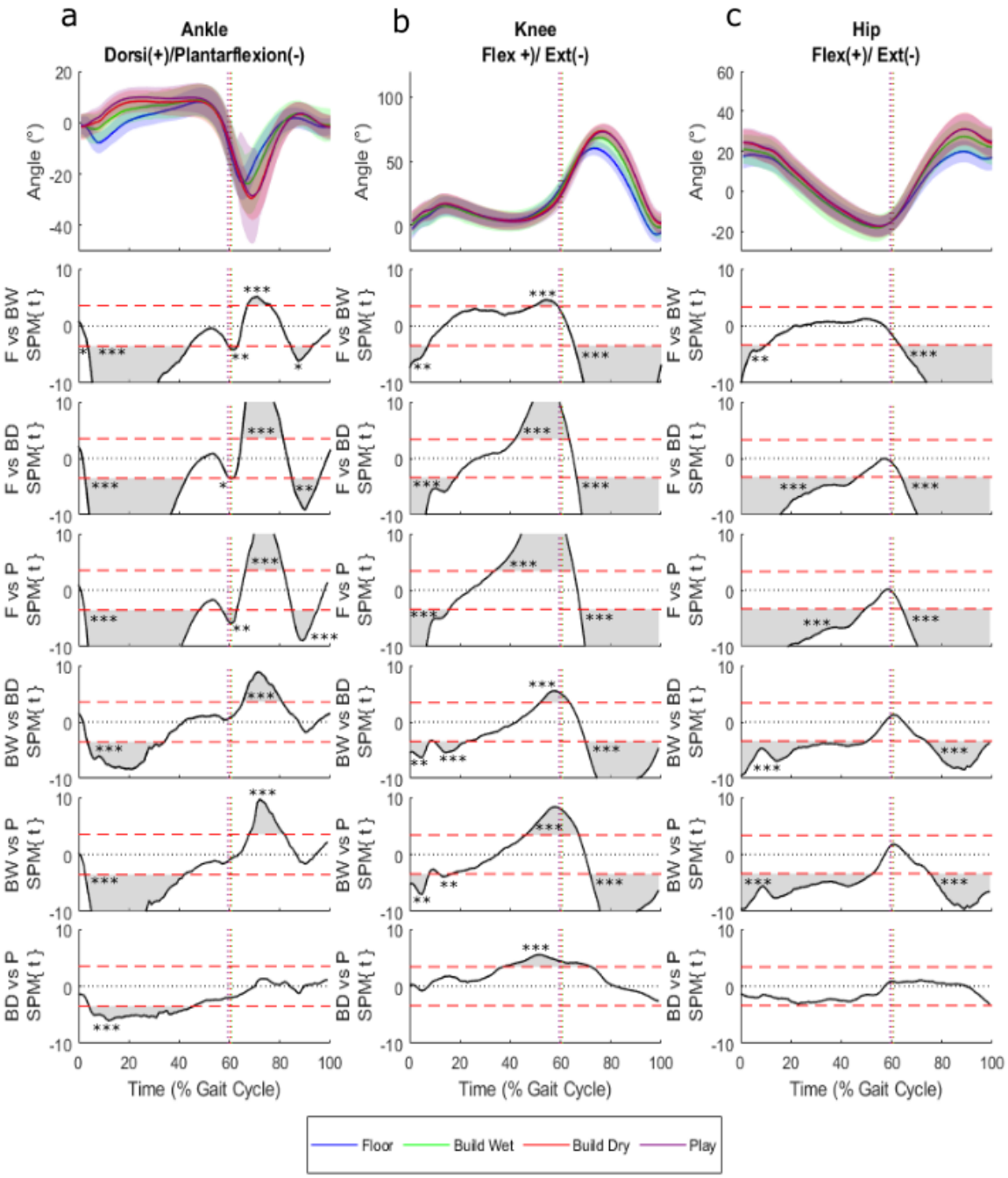

Figure 3.8: ***(a)*** Ankle, ***(b)*** knee and ***(c)*** hip joint angles in the sagittal plane for all participants combined (n=21) while walking on the four different substrates: floor (blue), build wet (green), build dry (red) and play sand (purple). Bold lines indicate the mean value and shaded regions show the standard deviation. The vertical dotted lines indicate toe-off. 1D-SPM (utilising paired t-tests with Bonferroni corrections) indicate regions of statistically significant differences between walking conditions, when 1D-SPM lines exceed the critical threshold values denoted by the horizontal red dotted lines. Shaded regions (within the SPM graphs) correspond to the period within the gait cycle where walking conditions are statistically significantly different from one another. "*, **, ***" represent p-values of less than 0.05, 0.01 and 0.001 respectively.

Table 3.6: The results of the linear mixed-effect models on the ankle, knee and hip joint angles in the sagittal plane for all subjects combined (n=21) at heel-strike. Fixed effects = substrate, speed and gender and random effects = subjects. Statistical significance is set as $p<0.05$ with significant p-values shown in bold. σ^2 = random effect variance, τ_{00} = subject variance, intraclass correlation coefficient (ICC) = proportion of variance explained by random effects, N = number of subjects, observations = number of data points (strides), marginal R^2 = proportion of variance explained by the fixed factors, conditional R^2 = proportion of variance explained by both the fixed and random factors.

	Ankle_Angle			**Knee_Angle**			**Hip_Angle**		
Predictors	*Estimates*	*CI*	*p*	*Estimates*	*CI*	*p*	*Estimates*	*CI*	*p*
(Intercept)	-3.89	-7.42 – -0.36	**0.031**	1.67	-3.63 – 6.96	0.538	4.37	-0.67 – 9.42	0.089
Substrate [build_wet]	-4.40	-8.15 – -0.66	**0.021**	5.97	0.71 – 11.24	**0.026**	-1.55	-6.60 – 3.50	0.548
Substrate [Floor]	-3.51	-8.43 – 1.41	0.163	5.53	-1.87 – 12.93	0.143	-3.59	-10.70 – 3.52	0.322
Substrate [play]	-3.63	-7.36 – 0.10	0.057	-11.59	-17.09 – -6.10	**<0.001**	-0.39	-5.76 – 4.98	0.887
Speed	2.12	-0.26 – 4.50	0.080	0.33	-3.13 – 3.80	0.851	13.40	9.96 – 16.84	**<0.001**
Gender [M]	-6.18	-12.25 – -0.11	**0.046**	2.92	-6.31 – 12.16	0.535	10.99	0.66 – 21.32	**0.037**
Substrate [build_wet] * Speed	4.13	1.15 – 7.10	**0.007**	-7.22	-11.39 – -3.05	**0.001**	-1.40	-5.40 – 2.59	0.490
Substrate [Floor] * Speed	3.33	-0.35 – 7.01	0.076	-9.57	-15.07 – -4.06	**0.001**	-4.45	-9.72 – 0.82	0.098
Substrate [play] * Speed	3.66	0.56 – 6.75	**0.021**	10.88	6.33 – 15.44	**<0.001**	1.64	-2.79 – 6.08	0.467
Substrate [build_wet] * Gender [M]	0.98	-6.00 – 7.96	0.783	-6.86	-17.25 – 3.52	0.195	11.39	-0.98 – 23.75	0.071
Substrate [Floor] * Gender [M]	10.48	3.28 – 17.67	**0.004**	-17.85	-28.75 – -6.94	**0.001**	1.17	-10.82 – 13.16	0.849
Substrate [play] * Gender [M]	4.19	-2.14 – 10.52	0.194	14.34	4.80 – 23.88	**0.003**	2.27	-8.64 – 13.19	0.683
Speed * Gender [M]	4.35	0.27 – 8.44	**0.037**	-2.37	-8.49 – 3.75	0.448	-5.61	-12.86 – 1.64	0.130
(Substrate [build_wet] * Speed) * Gender [M]	-0.77	-6.09 – 4.56	0.778	6.61	-1.30 – 14.52	0.101	-7.31	-16.66 – 2.05	0.126
(Substrate [Floor] * Speed) * Gender [M]	-8.44	-13.78 – -3.11	**0.002**	14.90	6.83 – 22.96	**<0.001**	1.40	-7.45 – 10.26	0.756
(Substrate [play] * Speed) * Gender [M]	-3.92	-8.93 – 1.09	0.126	-13.25	-20.79 – -5.72	**0.001**	-2.44	-10.97 – 6.09	0.575
Random Effects									
σ^2	12.16			28.79			23.79		
τ_{00}	12.22_{Subject}			30.54_{Subject}			23.05_{Subject}		
ICC	0.50			0.51			0.49		
N	21_{Subject}			21_{Subject}			21_{Subject}		
Observations	6122			6488			4399		
Marginal R^2 / Conditional R^2	0.028 / 0.515			0.115 / 0.571			0.253 / 0.621		

Table 3.7: The results of the linear mixed-effect models on the ankle, knee and hip joint angles in the sagittal plane for all subjects combined (n=21) at toe-off. Fixed effects = substrate, speed and gender and random effects = subjects. Statistical significance is set as $p<0.05$ with significant p-values shown in bold. σ^2 = random effect variance, τ_{00} = subject variance, intraclass correlation coefficient (ICC) = proportion of variance explained by random effects, N = number of subjects, observations = number of data points (strides), marginal R^2 = proportion of variance explained by the fixed factors, conditional R^2 = proportion of variance explained by both the fixed and random factors.

	Ankle_Angle			**Knee_Angle**			**Hip_Angle**		
Predictors	*Estimates*	*CI*	*p*	*Estimates*	*CI*	*p*	*Estimates*	*CI*	*p*
(Intercept)	-9.50	-21.05 – 2.05	0.107	43.95	34.40 – 53.50	**<0.001**	-5.84	-13.08 – 1.41	0.114
Substrate [build_wet]	0.78	-12.01 – 13.56	0.905	11.23	0.69 – 21.76	**0.037**	-1.43	-9.20 – 6.35	0.719
Substrate [Floor]	-21.89	-37.10 – -6.68	**0.005**	11.34	-1.19 – 23.88	0.076	6.06	-3.23 – 15.35	0.201
Substrate [play]	5.37	-7.09 – 17.83	0.398	-8.20	-18.53 – 2.12	0.119	7.34	-0.26 – 14.94	0.058
Speed	-10.14	-19.26 – -1.03	**0.029**	-4.34	-11.81 – 3.13	0.255	-3.88	-9.43 – 1.67	0.170
Gender [M]	15.39	-4.78 – 35.56	0.135	11.93	-4.87 – 28.74	0.164	10.13	-2.43 – 22.69	0.114
Substrate [build_wet] * Speed	4.14	-6.05 – 14.32	0.426	-9.97	-18.34 – -1.61	**0.019**	0.35	-5.83 – 6.54	0.911
Substrate [Floor] * Speed	18.10	6.54 – 29.67	**0.002**	-7.66	-17.18 – 1.86	0.115	-5.23	-12.29 – 1.83	0.146
Substrate [play] * Speed	-5.41	-15.68 – 4.86	0.302	7.01	-1.49 – 15.51	0.106	-5.87	-12.13 – 0.39	0.066
Substrate [build_wet] * Gender [M]	-15.49	-39.35 – 8.37	0.203	-17.32	-36.75 – 2.11	0.081	6.32	-7.97 – 20.60	0.386
Substrate [Floor] * Gender [M]	8.84	-14.65 – 32.32	0.461	-34.73	-54.17 – -15.30	**<0.001**	-8.33	-22.64 – 5.98	0.254
Substrate [play] * Gender [M]	-16.30	-37.80 – 5.20	0.137	-0.57	-18.45 – 17.31	0.950	-8.74	-21.80 – 4.33	0.190
Speed * Gender [M]	-10.09	-25.42 – 5.25	0.197	-7.67	-20.39 – 5.04	0.237	-6.35	-15.69 – 2.99	0.183
(Substrate [build_wet] * Speed) * Gender [M]	9.54	-8.61 – 27.69	0.303	13.68	-1.16 – 28.52	0.071	-4.73	-15.64 – 6.18	0.395
(Substrate [Floor] * Speed) * Gender [M]	-6.75	-24.33 – 10.83	0.452	24.44	9.88 – 39.00	**0.001**	6.25	-4.47 – 16.97	0.253
(Substrate [play] * Speed) * Gender [M]	12.74	-4.24 – 29.71	0.141	-0.85	-14.99 – 13.30	0.907	7.14	-3.18 – 17.47	0.175
Random Effects									
σ^2	49.83			34.21			18.81		
τ_{00}	24.72 $_{Subject}$			20.73 $_{Subject}$			18.37 $_{Subject}$		
ICC	0.33			0.38			0.49		
N	21 $_{Subject}$			21 $_{Subject}$			21 $_{Subject}$		
Observations	1769			1818			1831		
Marginal R^2 / Conditional R^2	0.073 / 0.381			0.035 / 0.399			0.064 / 0.527		

3.4.4 Muscle activity

Overall, lower limb muscle activity for all measured muscles was slightly higher as substrate compliance increased. However, there were periods of the stride for all

muscles when muscle activities were higher on the hard floor compared to the compliant sand substrates. During heel-strike, nEMG for the RF (Fig. 3.9b), VL (Fig. 3.9c), VM (Fig. 3.9d), TA (Fig. 3.9e), LG (Fig. 3.9g) and SOL (Fig. 3.9h) were higher on the hard floor than on the compliant sand substrates but were higher on the compliant substrates for the BFL (Fig. 3.9a) and MG (Fig. 3.9f). During the foot-flat phase or early-stance, nEMG is higher on the compliant sands than the hard floor for all muscles. During mid-stance, nEMG continues to remain greater on the compliant sands, except for the MG and LG when nEMG is higher on the hard floor. During the propulsive phase or late-stance, nEMG remains greater on the compliant sands for most muscles, except for short periods for the VL and VM. During toe-off, the greatest increase in nEMG is the TA, which is the only muscle where nEMG is higher on the hard floor (Fig. 3.9e). During toe-off, nEMG is similar for most muscles, but there is a noticeable increase on compliant substrates for the BFL (Fig. 3.9a) and SOL (Fig. 3.9h). During swing, nEMG is higher on compliant sand substrates than hard floor for most muscles, except for the BFL and VL. In late swing into heel-strike, nEMG is higher on the hard floor for RF, VL, VM, TA and LG. iEMG values show increases for all muscles on the sands compared to the hard floor (Fig. 3.9i). However, this did not necessarily relate to an incremental increase as substrate compliance increased as the greatest iEMG values for the TA occur on the build wet sand and other muscles see similar values for all sand substrates (Fig. 3.9i). Similar increases in muscle activity as substrate compliance increases are also observed for the back muscles, LES_L (Fig. 3.10e) and LES_R (Fig. 3.10f) where nEMG is higher on the compliant sand substrates for most of the stride. However, the opposite is observed for the abdominal muscles where nEMG is higher on the hard floor for the EO_L (Fig. 3.10a), EO_R (Fig. 3.10b), IO_L (Fig. 3.10c) and IO_R (Fig. 3.10d). iEMG values were higher on compliant sand substrates than the hard floor for most muscles (Fig. 3.10g). Like the lower limb muscles, there is not an incremental increase in iEMG values as substrate compliance increases, as iEMG is highest on the build wet substrate for the IO_R and LES_R and higher on the build dry substrate for the LES_L and EO_R compared to the similarly compliant play sand (Fig. 3.10).

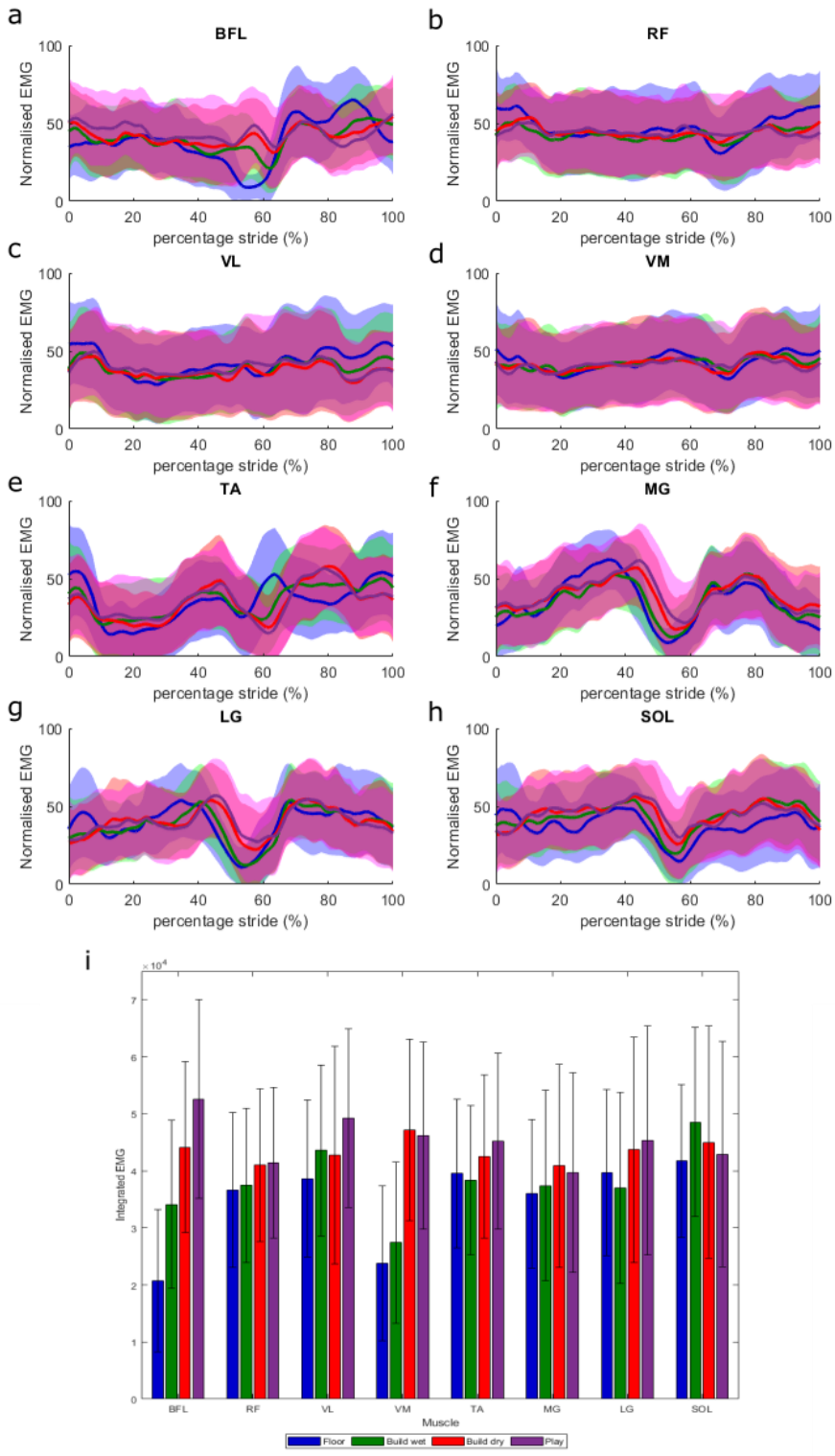

Figure 3.9: EMG values for 8 left lower extremity muscles for participants combined (n=20) while walking on the four different substrates: floor (blue), build wet sand (green), build dry sand (red) and play sand (purple): nEMG: ***(a)*** biceps femoris (BFL), ***(b)*** rectus femoris (RF), ***(c)*** vastus lateralis (VL), ***(d)*** vastus medialis (VM), ***(e)*** tibialis anterior (TA), ***(f)*** lateral gastrocnemius (LG), ***(g)*** medial gastrocnemius (MG) and ***(h)*** soleus (SOL) (mean ± s.d.). ***(i)*** iEMG values (mean ± s.d.).

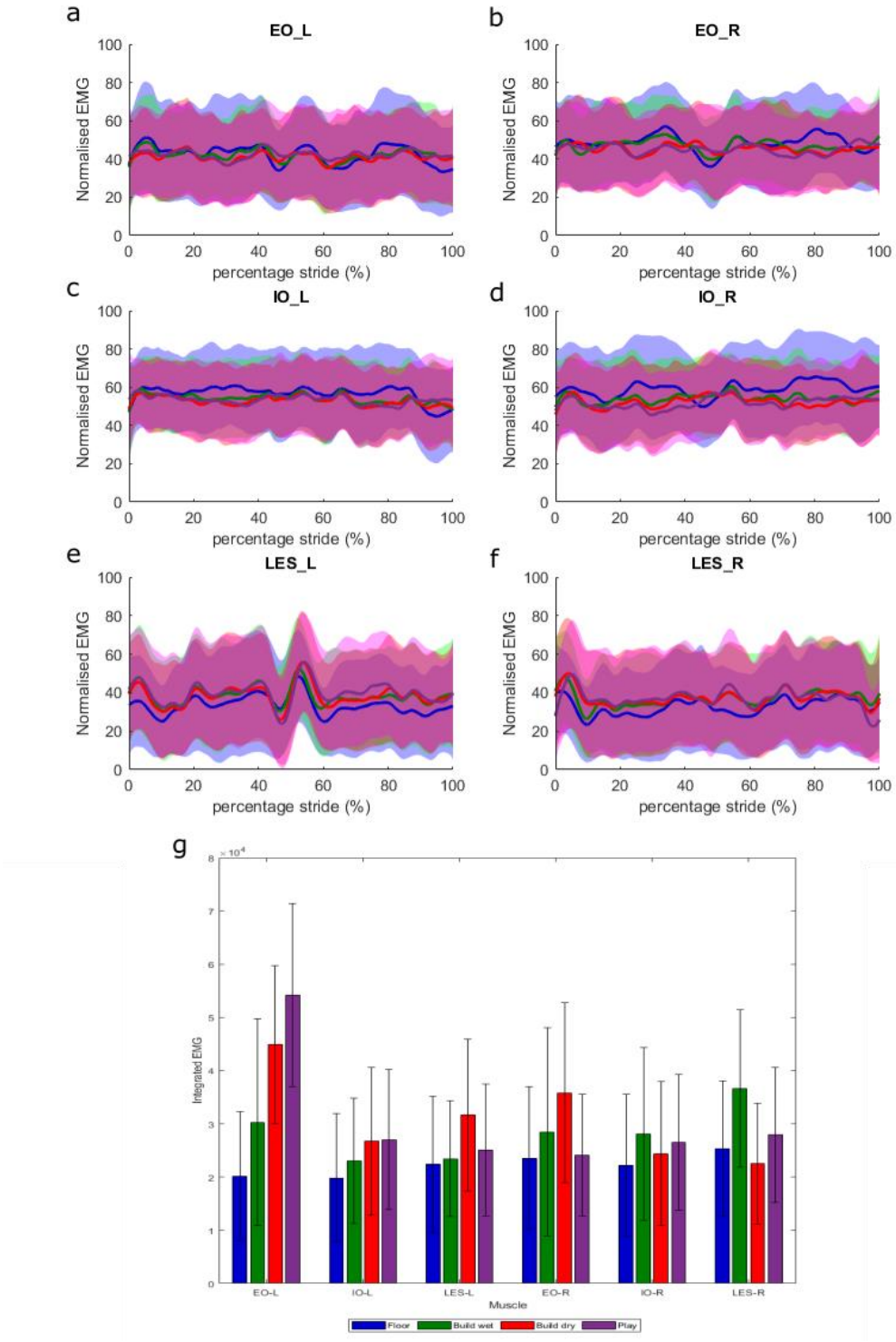

Figure 3.10: EMG values for 6 torso for participants combined (n=20) while walking on the four different substrates: floor (blue), build wet sand (green), build dry sand (red) and play sand (purple): nEMG: ***(a)*** left external oblique (EO_L), ***(b)*** right external oblique (EO_R), ***(c)*** left internal oblique (IO_L), ***(d)*** right internal oblique (IO_R), ***(e)*** left erector spinae (LES_L), ***(f)*** right erector spinae (LES_R) (mean ± s.d.). ***(g)*** iEMG values (mean ± s.d.).

LMMs for the iEMG values show that there is no significant ($p>0.05$) effect of substrate for BFL, TA, MG, SOL, LES_L, EO_L and LES_R (Tables 3.8-3.11). There is a significant ($p<0.05$) effect of substrate between floor and build dry for RF, LG, IO_L, EO_R and IO_R and between build dry and play for VM (Tables 3.8-3.11). There is a significant ($p<0.05$) effect of gender for VL, VM, LG and EO_R but no significant ($p>0.05$) effects of speed for any muscles. Also, there are some significant ($p<0.05$) interaction effects between substrate, gender and speed for RF, VL, VM, LG, IO_L, LES_R, EO_R and IO_R. There was also a significant ($p<0.001$) intercept for BFL, MG, LG, EO_L, IO_L, EO_R, IO_R and ($p<0.05$) for RF and TA (Tables 3.8-3.11).

Table 3.8: The results of the linear mixed-effect models on the integrated EMG data for the muscles BFL, RF, VL and VM; fixed effects = substrate, speed and gender and random effects = subjects. Statistical significance is set as $p<0.05$ with significant p-values shown in bold. σ^2 = random effect variance, τ_{00} = subject variance, intraclass correlation coefficient (ICC) = proportion of variance explained by random effects, N = number of subjects, observations = number of data points (strides), marginal R^2 = proportion of variance explained by the fixed factors, conditional R^2 = proportion of variance explained by both the fixed and random factors.

	BFL			**RF**			**VL**			**VM**		
Predictors	*Estimates*	*CI*	*p*	*Estimates*	*CI*	*p*	*Estimates*	*CI*	*p*	*Estimates*	*CI*	*p*
(Intercept)	45018.92	25494.53 – 64543.31	**<0.001**	45369.18	10655.12 – 80083.24	**0.010**	34398.22	-5908.08 – 74704.53	0.094	19374.44	-24534.44 – 63283.32	0.387
Substrate [Build_wet]	-10593.45	-35063.33 – 13876.43	0.396	15318.05	-28922.79 – 59558.90	0.497	19958.65	-30528.12 – 70445.42	0.438	47315.02	-9029.93 – 103659.97	0.100
Substrate [Floor]	4045.37	-21509.28 – 29600.02	0.756	59274.33	13104.86 – 105443.80	**0.012**	-18483.86	-71209.53 – 34241.80	0.492	-17386.75	-76153.03 – 41379.52	0.562
Substrate [Play]	-4507.82	-27342.05 – 18326.40	0.699	-13496.40	-54772.87 – 27780.07	0.522	38697.28	-8414.93 – 85809.50	0.107	67206.40	14644.57 – 119768.23	**0.012**
Gender [M]	-21804.47	-51137.31 – 7528.38	0.145	-15899.34	-68083.79 – 36285.11	0.550	90599.51	30046.18 – 151152.84	**0.003**	71309.50	5300.37 – 137318.62	**0.034**
Speed	-367.31	-15953.09 – 15218.46	0.963	2147.18	-25997.47 – 30291.82	0.881	5853.88	-26303.84 – 38011.59	0.721	22034.48	-13774.22 – 57843.18	0.228
Substrate [Build_wet] * Gender [M]	3415.22	-32670.65 – 39501.08	0.853	-14206.88	-79442.87 – 51029.12	0.669	-36707.14	-111160.39 – 37746.12	0.334	-89246.70	-172324.31 – -6169.10	**0.035**
Substrate [Floor] * Gender [M]	-7704.47	-42117.91 – 26708.98	0.661	-61044.31	-123234.21 – 1145.58	0.054	-74108.83	-145112.04 – -3105.61	**0.041**	-99381.37	-178555.52 – -20207.22	**0.014**
Substrate [Play] * Gender [M]	-2362.77	-35440.22 – 30714.67	0.889	3169.33	-56630.12 – 62968.78	0.917	-46408.77	-114654.93 – 21837.39	0.183	-107554.01	-183710.44 – -31397.59	**0.006**
Substrate [Build_wet] * Speed	6315.89	-13681.67 – 26313.46	0.536	-13583.25	-49737.73 – 22571.23	0.462	-16020.80	-57280.20 – 25238.61	0.447	-39704.10	-85749.71 – 6341.52	0.091
Substrate [Floor] * Speed	-4320.28	-24245.74 – 15605.19	0.671	-37215.74	-73215.92 – -1215.56	**0.043**	19677.88	-21433.34 – 60789.09	0.348	14929.45	-30893.97 – 60752.86	0.523
Substrate [Play] * Speed	4410.52	-14601.03 – 23422.07	0.649	11508.87	-22857.58 – 45875.31	0.512	-31784.13	-71009.30 – 7441.03	0.112	-56178.32	-99940.93 – -12415.71	**0.012**
Gender [M] * Speed	12373.85	-10009.24 – 34756.94	0.279	6180.92	-34221.32 – 46583.16	0.764	-75619.69	-121802.52 – -29436.85	**0.001**	-62918.72	-114305.15 – -11532.30	**0.016**
(Substrate [Build_wet] * Gender [M]) * Speed	-2282.81	-30394.02 – 25828.41	0.874	10960.87	-39858.32 – 61780.06	0.672	32527.14	-25472.62 – 90526.91	0.272	72573.22	7855.58 – 137290.86	**0.028**
(Substrate [Floor] * Gender [M]) * Speed	3402.34	-22867.38 – 29672.06	0.800	35827.75	-11643.61 – 83299.11	0.139	51943.11	-2257.67 – 106143.90	0.060	67304.62	6870.47 – 127738.77	**0.029**
(Substrate [Play] * Gender [M]) * Speed	5057.23	-21452.36 – 31566.83	0.708	-3088.37	-51014.48 – 44837.75	0.899	35909.61	-18785.60 – 90604.82	0.198	85159.20	24123.38 – 146195.02	**0.006**
Random Effects												
σ^2	37521482.98			122711914.37			159722716.83			199130430.51		
τ_{00}	72886593.09 $_{Subject}$			138909434.47 $_{Subject}$			314930010.23 $_{Subject}$			165842563.29 $_{Subject}$		
ICC	0.66			0.53			0.66			0.45		
N	19 $_{Subject}$			19 $_{Subject}$			19 $_{Subject}$			19 $_{Subject}$		
Observations	676			676			676			676		
Marginal R^2 / Conditional R^2	0.096 / 0.693			0.125 / 0.589			0.090 / 0.694			0.120 / 0.520		

Table 3.9: The results of the linear mixed-effect models on the integrated EMG data for the muscles TA, MG, LG and SOL; fixed effects = substrate, speed and gender and random effects = subjects. Statistical significance is set as $p<0.05$ with significant p-values shown in bold. σ^2 = random effect variance, τ_{00} = subject variance, intraclass correlation coefficient (ICC) = proportion of variance explained by random effects, N = number of subjects, observations = number of data points (strides), marginal R^2 = proportion of variance explained by the fixed factors, conditional R^2 = proportion of variance explained by both the fixed and random factors.

	TA			**MG**			**LG**			**SOL**		
Predictors	*Estimates*	*CI*	*p*	*Estimates*	*CI*	*p*	*Estimates*	*CI*	*p*	*Estimates*	*CI*	*p*
(Intercept)	40152.53	3232.46 – 77072.60	**0.033**	45733.33	24546.67 – 66919.99	**<0.001**	39184.84	18039.87 – 60329.81	**<0.001**	21947.58	-6340.31 – 50235.48	0.128
Substrate [Build_wet]	-13876.43	-61596.21 – 33843.34	0.569	2296.20	-24833.80 – 29426.19	0.868	3006.29	-23773.28 – 29785.87	0.826	13462.43	-22146.54 – 49071.41	0.459
Substrate [Floor]	-44310.82	-94028.30 – 5406.65	0.081	12178.41	-16123.54 – 40480.35	0.399	-49865.55	-77822.22 – -21908.88	**<0.001**	11549.86	-25632.96 – 48732.67	0.543
Substrate [Play]	5997.87	-38506.19 – 50501.92	0.792	1427.10	-23882.68 – 26736.87	0.912	293.89	-24693.42 – 25281.21	0.982	27584.54	-5643.16 – 60812.25	0.104
Gender [M]	-25764.61	-81253.01 – 29723.78	0.363	-8145.71	-39996.40 – 23704.98	0.616	-36201.58	-67982.75 – -4420.41	**0.026**	4135.81	-38371.35 – 46642.97	0.849
Speed	-2054.71	-32327.48 – 28218.07	0.894	-3435.32	-20683.43 – 13812.80	0.696	1732.26	-15314.13 – 18778.66	0.842	18980.53	-3695.20 – 41656.26	0.101
Substrate [Build_wet] * Gender [M]	16094.92	-54255.15 – 86445.00	0.654	-22516.95	-62519.84 – 17485.94	0.270	12656.74	-26833.32 – 52146.81	0.530	-32302.99	-84814.83 – 20208.86	0.228
Substrate [Floor] * Gender [M]	54905.82	-12102.20 – 121913.85	0.108	-31472.82	-69600.36 – 6654.72	0.106	58839.36	21186.50 – 96492.22	**0.002**	-38340.89	-88415.74 – 11733.96	0.133
Substrate [Play] * Gender [M]	24986.20	-39506.42 – 89478.81	0.448	-9789.21	-46459.08 – 26880.66	0.601	8226.30	-27972.18 – 44424.78	0.656	-17874.64	-66008.97 – 30259.68	0.467
Substrate [Build_wet] * Speed	13128.04	-25868.15 – 52124.23	0.509	-6043.71	-28214.70 – 16127.27	0.593	-4004.23	-25889.18 – 17880.72	0.720	-13143.87	-42244.57 – 15956.84	0.376
Substrate [Floor] * Speed	33024.97	-5744.09 – 71794.02	0.095	-10506.34	-32574.80 – 11562.13	0.351	38826.49	17027.83 – 60625.14	**<0.001**	-15435.62	-44427.93 – 13556.69	0.297
Substrate [Play] * Speed	-4959.11	-42012.99 – 32094.76	0.793	-1232.59	-22305.32 – 19840.14	0.909	-110.66	-20914.87 – 20693.56	0.992	-23095.09	-50760.16 – 4569.98	0.102
Gender [M] * Speed	15465.71	-27950.47 – 58881.89	0.485	3591.92	-21162.63 – 28346.48	0.776	26186.35	1710.89 – 50661.81	**0.036**	-4867.38	-37430.03 – 27695.27	0.770
(Substrate [Build_wet] * Gender [M]) * Speed	-16500.22	-71302.73 – 38302.30	0.555	18523.53	-12638.85 – 49685.92	0.244	-11791.07	-42554.11 – 18971.97	0.453	24037.27	-16869.90 – 64944.44	0.249
(Substrate [Floor] * Gender [M]) * Speed	-42146.61	-93291.61 – 8998.38	0.106	20177.56	-8925.75 – 49280.88	0.174	-51924.21	-80666.23 – -23182.18	**<0.001**	28166.37	-10058.34 – 66391.07	0.149
(Substrate [Play] * Gender [M]) * Speed	-18511.49	-70199.97 – 33177.00	0.483	9009.44	-20379.67 – 38398.55	0.548	-5275.83	-34286.88 – 23735.22	0.722	16328.70	-22248.14 – 54905.55	0.407
Random Effects												
σ^2	142941764.23			46159320.80			44950815.96			79464947.49		
τ_{00}	80072319.19 $_{Subject}$			42530085.97 $_{Subject}$			64072190.54 $_{Subject}$			136862659.01 $_{Subject}$		
ICC	0.36			0.48			0.59			0.63		
N	19 $_{Subject}$			19 $_{Subject}$			19 $_{Subject}$			19 $_{Subject}$		
Observations	676			676			676			676		
Marginal R^2 / Conditional R^2	0.060 / 0.397			0.100 / 0.531			0.124 / 0.639			0.048 / 0.650		

Table 3.10: The results of the linear mixed-effect models on the integrated EMG data for the muscles LES_L, EO_L, IO_L; fixed effects = substrate, speed and gender and random effects = subjects. Statistical significance is set as $p<0.05$ with significant p-values shown in bold. σ^2 = random effect variance, τ_{00} = subject variance, intraclass correlation coefficient (ICC) = proportion of variance explained by random effects, N = number of subjects, observations = number of data points (strides), marginal R^2 = proportion of variance explained by the fixed factors, conditional R^2 = proportion of variance explained by both the fixed and random factors.

	LES_L			**EO_L**			**IO_L**		
Predictors	*Estimates*	*CI*	*p*	*Estimates*	*CI*	*p*	*Estimates*	*CI*	*p*
(Intercept)	21039.56	-12762.38 – 54841.49	0.222	60992.87	30880.31 – 91105.44	**<0.001**	54091.59	29864.78 – 78318.39	**<0.001**
Substrate [Build_wet]	17544.40	-24902.15 – 59990.95	0.418	-12691.12	-50217.51 – 24835.27	0.507	-11563.92	-42079.73 – 18951.89	0.458
Substrate [Floor]	-36150.53	-80476.40 – 8175.35	0.110	-13230.91	-52425.99 – 25964.16	0.508	-49507.95	-81371.84 – -17644.06	**0.002**
Substrate [Play]	36436.23	-3172.51 – 76044.98	0.071	-21762.73	-56781.84 – 13256.37	0.223	-1173.16	-29648.15 – 27301.83	0.936
Gender [M]	-30442.48	-83714.59 – 22829.64	0.263	-19690.27	-64918.03 – 25537.48	0.394	-23297.70	-59703.37 – 13107.96	0.210
Speed	15294.25	-11739.06 – 42327.56	0.267	-14888.30	-38795.60 – 9018.99	0.222	2043.26	-17388.47 – 21474.99	0.837
Substrate [Build_wet] * Gender [M]	-42098.60	-112214.77 – 28017.56	0.239	3132.17	-52209.16 – 58473.51	0.912	29909.78	-15091.16 – 74910.71	0.193
Substrate [Floor] * Gender [M]	57922.25	-4706.04 – 120550.55	0.070	-6092.86	-58872.93 – 46687.22	0.821	67620.22	24708.17 – 110532.28	**0.002**
Substrate [Play] * Gender [M]	-1186.84	-60819.21 – 58445.53	0.969	27427.31	-23299.98 – 78154.61	0.289	22732.57	-18517.01 – 63982.15	0.280
Substrate [Build_wet] * Speed	-15497.31	-50185.94 – 19191.31	0.381	11044.15	-19623.69 – 41711.99	0.480	9719.66	-15218.75 – 34658.07	0.445
Substrate [Floor] * Speed	22071.25	-12490.57 – 56633.08	0.211	12506.61	-18054.41 – 43067.63	0.423	39643.92	14798.88 – 64488.96	**0.002**
Substrate [Play] * Speed	-29975.60	-62953.45 – 3002.26	0.075	17611.12	-11545.44 – 46767.67	0.236	712.41	-22995.59 – 24420.42	0.953
Gender [M] * Speed	21097.13	-19707.78 – 61902.05	0.311	13231.04	-21105.47 – 47567.55	0.450	11761.57	-16142.31 – 39665.45	0.409
(Substrate [Build_wet] * Gender [M]) * Speed	32674.18	-21797.02 – 87145.38	0.240	-3661.37	-46772.81 – 39450.07	0.868	-22958.17	-58014.27 – 12097.93	0.199
(Substrate [Floor] * Gender [M]) * Speed	-44933.23	-92894.64 – 3028.18	0.066	2851.02	-37439.25 – 43141.28	0.890	-51343.28	-84100.22 – -18586.34	**0.002**
(Substrate [Play] * Gender [M]) * Speed	4792.00	-43019.88 – 52603.87	0.844	-21307.18	-61962.01 – 19347.65	0.304	-15767.96	-48827.09 – 17291.17	0.350
Random Effects									
σ^2	112906214.02			88236538.34			58359680.24		
τ_{00}	208212123.53 $_{Subject}$			197082066.51 $_{Subject}$			98712788.88 $_{Subject}$		
ICC	0.65			0.69			0.63		
N	18 $_{Subject}$			19 $_{Subject}$			19 $_{Subject}$		
Observations	639			676			676		
Marginal R^2 / Conditional R^2	0.038 / 0.662			0.014 / 0.695			0.112 / 0.670		

Table 3.11: The results of the linear mixed-effect models on the integrated EMG data for the muscles LES_R, EO_R, IO_R; fixed effects = substrate, speed and gender and random effects = subjects. Statistical significance is set as $p<0.05$ with significant p-values shown in bold. σ^2 = random effect variance, τ_{00} = subject variance, intraclass correlation coefficient (ICC) = proportion of variance explained by random effects, N = number of subjects, observations = number of data points (strides), marginal R^2 = proportion of variance explained by the fixed factors, conditional R^2 = proportion of variance explained by both the fixed and random factors.

	LES_R			**EO_R**			**IO_R**		
Predictors	*Estimates*	*CI*	*p*	*Estimates*	*CI*	*p*	*Estimates*	*CI*	*p*
(Intercept)	26216.87	-4582.17 – 57015.90	0.095	66081.96	40735.88 – 91428.04	**<0.001**	54482.77	27059.23 – 81906.30	**<0.001**
Substrate [Build_wet]	22216.81	-15999.88 – 60433.50	0.255	-17710.44	-49663.01 – 14242.12	0.277	8003.38	-26285.62 – 42292.37	0.647
Substrate [Floor]	2487.73	-37431.52 – 42406.99	0.903	-44807.52	-78170.67 – -11444.36	**0.008**	-51372.78	-87183.92 – -15561.65	**0.005**
Substrate [Play]	11518.05	-24145.93 – 47182.03	0.527	-21406.32	-51221.76 – 8409.12	0.159	-4341.35	-36338.80 – 27656.10	0.790
Gender [M]	-9658.19	-58151.11 – 38834.74	0.696	-47033.77	-86991.21 – -7076.33	**0.021**	-22463.38	-65668.44 – 20741.67	0.308
Speed	13192.66	-11157.75 – 37543.07	0.288	-15537.43	-35883.04 – 4808.19	0.134	346.30	-21495.81 – 22188.42	0.975
Substrate [Build_wet] * Gender [M]	-72557.16	-135690.25 – -9424.08	**0.024**	17013.48	-35766.38 – 69793.35	0.528	17624.50	-39018.01 – 74267.01	0.542
Substrate [Floor] * Gender [M]	4891.51	-51505.84 – 61288.86	0.865	53542.11	6401.23 – 100683.00	**0.026**	40802.17	-9793.78 – 91398.12	0.114
Substrate [Play] * Gender [M]	-32286.79	-85978.23 – 21404.64	0.239	32170.06	-12718.91 – 77059.03	0.160	12144.21	-36028.34 – 60316.77	0.621
Substrate [Build_wet] * Speed	-19334.81	-50566.85 – 11897.22	0.225	14199.87	-11912.68 – 40312.41	0.287	-4983.60	-33005.69 – 23038.49	0.727
Substrate [Floor] * Speed	-4439.08	-35564.67 – 26686.50	0.780	38776.46	12762.38 – 64790.53	**0.003**	45310.63	17388.04 – 73233.22	**0.001**
Substrate [Play] * Speed	-8587.66	-38281.12 – 21105.81	0.571	17188.83	-7635.23 – 42012.89	0.175	3341.09	-23299.67 – 29981.85	0.806
Gender [M] * Speed	673.51	-36086.05 – 37433.07	0.971	35654.75	4946.12 – 66363.38	**0.023**	12815.80	-20154.99 – 45786.58	0.446
(Substrate [Build_wet] * Gender [M]) * Speed	54629.11	5582.95 – 103675.27	**0.029**	-12395.27	-53398.43 – 28607.90	0.554	-13627.13	-57631.01 – 30376.74	0.544
(Substrate [Floor] * Gender [M]) * Speed	-9085.53	-52275.75 – 34104.69	0.680	-47132.20	-83232.98 – -11031.43	**0.011**	-37667.84	-76414.95 – 1079.27	0.057
(Substrate [Play] * Gender [M]) * Speed	24115.42	-18932.95 – 67163.78	0.272	-25056.66	-61047.69 – 10934.38	0.172	-8728.44	-47352.01 – 29895.14	0.658
Random Effects									
σ^2	91507278.45			63985796.78			73672831.67		
τ_{00}	224981927.46 $_{Subject}$			105562072.94 $_{Subject}$			151952788.49 $_{Subject}$		
ICC	0.71			0.62			0.67		
N	18 $_{Subject}$			18 $_{Subject}$			18 $_{Subject}$		
Observations	639			639			639		
Marginal R^2 / Conditional R^2	0.107 / 0.742			0.050 / 0.642			0.121 / 0.713		

3.5 Discussion

3.5.1 Overview

Fossilised footprints provide invaluable information regarding the locomotion and lower limb anatomy in extinct hominins. However, to accurately extract information about the evolution of human bipedalism from fossilised footprints, we need to understand how biomechanical variables are actually recorded in, and can be inferred from, footprint morphologies. Furthermore, and more central to this work, it is expected that locomotion on natural substrates such as sand and mud in which footprints are recorded in, will be affected by the compliance of the substrate and therefore differ from data typically recorded on more standard, non-compliant laboratory substrates. The purpose of this study was to determine how walking biomechanics are affected by a natural compliant substrate such as sand. This was done by comparing human locomotion on four different substrates, using different sand types and moisture content: 1) hard, level floor 2) wet building sand 3) dry building sand and 4) play sand. Our results show that substrate compliance does affect many aspects of human locomotion such as greater flexion at the hip and knee joint, changes in spatiotemporal variables and increased muscle activity. At the beginning of this chapter, six hypotheses were proposed and these will be discussed in this section.

3.5.2 Gait changes and increased energetic costs on compliant sands

Previous studies have shown that locomotion on compliant substrates such as sand, snow and grass incur a higher energetic cost than moving on a hard, flat surface (Davies & Mackinnon 2006; Lejeune, Willems & Heglund 1998; Pandolf, Haisman & Goldman 1976; Pinnington & Dawson 2001; Zamparo et al. 1992), and it is reasonable to assume that this applies to the current experiment also. Pandolf et al.

(1976) found that the level of effort required to traverse snow is relative to snow depth. In natural snow, the surface of the snow would deform until it either became sufficiently compacted or a firm subsurface layer was reached to provide sufficient resistance against further foot sinkage. The sand walkways used in this study provided sufficient substrate height that the foot would not sink to the bottom. However, we do see deeper footprint depths on the build dry and play sand and therefore it is possible that there would be a greater metabolic cost on these sands compared to the wet building sand, which resulted in shallower footprint depth.

Human walking is characterised by centre of mass motion similar to that of an inverted pendulum; kinetic (E_{kin}) and potential (E_{pot}) energies of the CoM of the body are largely out of phase, resulting in an exchange between these two forms of gravitational energies. If there is an efficient pendular energy exchange mechanism, less mechanical work is required by the muscles. Zamparo (1992) proposed that the pendular energy exchange mechanism during locomotion on sand would be less efficient. The first hypothesis stated that as substrate compliance increases, the pendular energy exchange will have reduced efficiency compared to the hard floor. This hypothesis is not supported by the present data. Our results show that the pendular energy exchange mechanism does not have a reduced efficiency on the compliant sands compared to the hard floor. We calculated total energy exchange recovery (R) to be 58.4 ± 4.4 on floor, 59.4 ± 6.8 on build wet, 59.5 ± 5.7 on build dry and 59.5 ± 4.4 on play sand (mean ± s.d.). Similar values were found by Lejeune et al. (1998) with as much as 60% R when walking on sand, whereas Zamparo et al. (1992) calculated a relatively lower 43-48% R on sand. In fact, as substrate compliance increased, total energy exchange recovery (R) and relative amplitude (RA) increased slightly and congruity (CO) decreased slightly (Fig. 3.7). In this study we observed an increase of ~1.7%, ~2% and ~1.9% in R between floor and build wet, build dry and play sand, respectively. There was also an increase of ~15.9%, ~10.1% and ~8.7% in RA and a decrease of ~2.9%, ~18.3% and ~19.5% in CO between floor and build wet, build dry and play sand, respectively. However, there was no significant effect ($p>0.05$) of substrate for any variables (Table 3.5). During walking on compliant foam mats, MacLellan and Patla (2006) found vertical CoM decreased to provide a more stable posture. A similar strategy may have been

adopted by participants in this study, with a more crouched gait lowering the body CoM, at the expense of increased mechanical work, as seen when walking on uneven surfaces (Voloshina et al. 2013).

Dynamic stability during gait is dependent on maintaining the body's CoM within a constantly moving base of support (Patla 2003). Locomotion on complex, uneven or compliant substrates can affect stability and requires the human body to adapt by changing gait mechanisms. Changes to spatiotemporal variables on destabilising substrates include adopting shorter, faster and wider steps and greater step variability (Gates et al. 2012; Hak et al. 2012; MacLellan & Patla 2006; Voloshina et al. 2013). The second hypothesis stated that as substrate compliance increases, stance time will increase and walking speed, stride width and stride length will decrease. This hypothesis is partially supported by the present data (Fig. 3.5; Tables 3.2-3.3). Our results show that there was no significant ($p>0.05$) differences in stride width between any substrates (Table 3.2). Wider steps would require more mechanical work, and therefore increase metabolic costs, to redirect the CoM between steps (Donelan, Kram & Kuo 2002). Participants step width may be based on a trade-off between minimising mechanical work and the cost of active stabilisation of lateral balance during locomotion on the sands. As substrate compliance increased, participants adopted a significantly ($p<0.001$) slower walking speed (Fig. 3.5; Table. 3.2). This is most likely to increase stability on the more compliant surface or the need for more accurate foot placement (Matthis, Yates & Hayhoe 2018). This could also be caused by greater deceleration during ground contact on sand. Results here showed significant ($p<0.05$) increases in cycle time, stance time and double limb support time between the two most compliant substrates (build dry and play sand) and the two least compliant substrates (floor and build wet) (Fig. 3.5; Tables 3.2-3.3). However, these changes could be mainly, or at least partly, due to a reduction in speed as duty factor was similar for all substrates, suggesting relative stance and swing times were similar. Stride lengths were similar on all substrates, but there was a significant ($p<0.001$) effect of substrate for stride length between build dry and build wet sand (Table 3.2). Furthermore, the coefficient of variation (CV) for most spatiotemporal variables were similar (Table 3.4). Some variables saw an increase in CV on compliant sand compared to hard floor and for other variables there was a

decrease in CV. These differences do not appear to correlate with increased substrate compliance as there was large differences in CV for some spatiotemporal variables between the two compliant sand substrates, build dry and play sand (Table 3.4). Overall, although we do find several differences in spatiotemporal variables in this study, they are unlikely to translate to large increases in energetic cost.

Previous studies on walking on irregular and compliant substrates have shown that participants will display greater hip and knee flexion during the swing phase, resulting in greater mechanical work (Gates et al. 2012; Marigold & Patla 2002; Pinnington et al. 2005; Svenningsen, de Zee & Oliveira 2019; Voloshina et al. 2013). Furthermore, during the stance phase of walking on sand, the foot sinks and often slips backwards as the sand is displaced. This is observed during jumping on sand where slipping caused an increased range of motion at the ankle joint prior to push-off (Giatsis et al. 2004). The third hypothesis stated that as substrate compliance increases, there will be greater joint excursions at the hip, knee and ankle joints. This hypothesis is supported by the present data (Fig. 3.8). Our results show that as substrate compliance increased, there were significantly ($p<0.001$) more hip and knee flexion (Fig. 3.8b-3.8c), in agreement with previous studies on locomotion on uneven and compliant surfaces. On the sands, there were also greater ranges of motion at the ankle joint throughout the stride (Fig. 3.8a). The greater ankle dorsiflexion at early-stance is most likely due to the sinking of the heel into the substrate after heel-strike. However, there is no significant ($p>0.05$) difference in ankle joint angle between any substrates in late stance. During the swing phase, greater hip and knee flexion and greater ankle plantarflexion are likely to ensure toe clearance on the compliant sand substrates, as seen during locomotion on irregular surfaces (Merryweather, Yoo & Bloswick 2011; Svenningsen, de Zee & Oliveira 2019). Throughout the whole stride, hip, knee and ankle joint angles were very similar on the two most compliant sands, build dry and play sand, potentially indicating that kinematic changes are directly due to substrate compliance (Fig. 3.8).

Early human walking models assumed the swing phase of gait was essentially passive under the action of gravity, with relatively little muscle work required (Mochon & McMahon 1980). However, more recent studies have found that the swing phase requires a substantial metabolic energy expenditure of up to 33% of the total metabolic energy consumed by the lower limb muscles during the whole stride (Doke, Donelan & Kuo 2005; Umberger 2010). Previous studies have suggested that walking on uneven or irregular terrain incurs increased mechanical work at the knee and hip due to greater knee and hip flexion, particularly during the swing phase (Gates et al. 2012; Voloshina et al. 2013). Also, when walking on sand, there is surface displacement under the foot. As the surface moves under the foot, the muscles in the leg need to constantly work to ensure stability, resulting in additional external work (Lejeune, Willems & Heglund 1998; Zamparo et al. 1992). The fourth hypothesis stated that as substrate compliance increases, there will be greater muscle activation for lower limb muscles, and particularly the ankle extensors. This hypothesis is partially supported by the present data. Overall, all lower limb muscle activities (nEMG) increased slightly as substrate compliance increased (Fig. 3.9). However, although there appears to be qualitatively different muscle activations on the different substrates, these differences are not always statistically significant (Fig. 3.9; Tables 3.8-3.9). iEMG values for most muscles were higher on the compliant sand substrates, especially in the thigh muscles, BFL, VL and VM and also slightly for the RF (Fig. 3.9i). These increases in EMG values are most likely due to the greater hip and knee flexion observed on the sands during swing and to stabilise the knee during stance phase. Furthermore, the increased hip and knee flexion may allow a greater horizontal ground reaction force (GRF) to be exerted against the sand substrate to negate potential energy lost due to foot slippage during push-off (Lejeune, Willems & Heglund 1998; Zamparo et al. 1992). Pinnington and Dawson (2005) found similar increases during running with EMG activation of the hamstrings and quadriceps nearly two times higher on sand than a firm surface. Bates et al. (2013b) previously suggested that walking on compliant substrates requires greater muscle-tendon forces by the ankle extensors to generate the propulsion needed from mid-stance to reaccelerate into the swing phase. Although, the main ankle extensor, TA was highest on the floor compared to sand during push-off, during mid to late-stance, the TA was higher on sand, likely for forward propulsion as suggested by Bates et al. (2013b) (Fig. 3.9e). Decreases in the TA

activation on the sands at heel-strike (Fig. 3.9e) may be associated with adaptations in landing strategies on compliant substrates. Pre-activation of the TA prepares the TA for impact at heel-strike, but on compliant substrates the GRFs are lower (Jafarnezhadgero et al. 2022). Furthermore, during the propulsive stage of stride into push-off, the MG (Fig. 3.9f), LG (Fig. 3.9g) and the SOL (Fig. 3.9h) were higher on the compliant sands. This suggests that as the heel is rising, the plantarflexor muscles become more important in controlling the foot during the propulsive phase into push-off. Lejeune et al. (1998) found that when walking on sand, more work was done on the sand by the foot due to foot slippage during push-off. During push-off, the foot functions as a rigid lever to propel the body forward. Peak ankle power is partly due to the elastic recoil of the Achilles tendon and partly due to active muscle contraction. Postural disturbances due to slipping will result in muscles actively contracting to ensure stabilisation, particularly in the gastrocnemius and soleus muscles responsible for ankle plantarflexion, and plantar intrinsic muscles to maintain tension across the plantar aspect of the foot (Farris, Birch & Kelly 2020; Kelly, Lichtwark & Cresswell 2015) However, this may not necessarily be reflected in muscle activity as some joint work may be performed passively through elastic energy storage and return by the tendon and foot muscles were not measured in this study. However, greater ankle dorsiflexion is observed during stance on the sands (Fig. 3.9a) which could increase tension in the Achilles tendon (Mann & Hagy 1980).

For the torso muscles measured in this study, there were higher nEMG for the back muscles and a decrease in abdominal nEMG on sand (Fig. 3.10). However, iEMG values were higher on compliant sand for most back and abdominal muscles (Fig. 3.10g). Pandolf et al. (1976) saw an increased stooping posture when walking on deep snow. The differences in abdominal and back muscle activation observed in this study could be due to similar stooping postures during walking on sand where increased back muscle activity would be required to ensure the stabilisation of the trunk.

One of the main aims of this study was to determine whether relative gait changes could be determined from footprint depth. The fifth hypothesis stated that the changes in gait kinematics will be similar on both of the dry, soft sand types compared to the hard floor. This hypothesis is mostly supported by the present data. There was no significant ($p>0.05$) differences in hip joint angles (Fig. 3.8c) between build dry and play sand throughout the whole stride and only a small percentage of stride had significant ($p<0.001$) differences in knee (Fig. 3.8b) and ankle joint angles (Fig. 3.8a). Furthermore, most spatiotemporal variables were similar between build dry and play sand (Fig. 3.5) with only significant effects of substrate for speed ($p<0.001$) (Table 3.2), swing time and duty factor ($p<0.05$) (Table 3.3). Furthermore, mechanical energy exchange variables are similar for both substrates (Fig. 3.7) with no significant ($p>0.05$) effect of substrate for any variables (Table 3.5). However, this applies to all substrates, not just the two most compliant sands. The sixth hypothesis stated that the wet, compact sand will produce intermediate gait changes between the hard floor and the more compliant softer sand types. This hypothesis is mostly supported by the present data. The build wet sand did exhibit intermediate gait changes for most spatiotemporal variables (Fig. 3.5; Tables 3.3-3.3), joint angles (Fig. 3.8; Tables 3.6-3.7) and muscle activities (Figs. 3.9-3.10; Tables 3.8-3.11). However, some spatiotemporal variables on the build wet sand more closely resemble those seen on the softer sand types such as decreased speed (Fig 3.5a) and increased cycle time (Fig. 3.5d), stance time (Fig. 3.5e) and swing time (Fig. 3.5f) compared to hard floor.

Overall, our findings suggest that humans do alter their gait when walking over natural compliant substrates such as sand. On sand, participants display greater hip and knee joint during swing (Fig. 3.8b-c), greater ankle dorsiflexion during stance (Fig. 3.8a), and changes to spatiotemporal variables such as increased cycle time, stance time and swing time and decreased walking speed (Fig. 3.5). In contrast to the previous hypothesis by Zamparo et al. (1992), we do not find a decrease in the efficiency of the inverted pendulum mechanics (Figs. 3.6-3.7). However, to maintain this relatively efficient pendular energy exchange on sand could incur increased metabolic costs due to changes in gait. Increased ankle dorsiflexion during stance is likely due to the sinking of the foot at the heel after heel-strike, and increased

dorsiflexion during swing, accompanied by greater hip and knee flexion (Fig. 3.8) were adopted as a measure to ensure toe clearance over the substrate. Due to the displacement of the sand, there will be greater work done to the substrate. Displacement of the sand could also lead to deceleration which would require more work done by the muscles to increase propulsion into push-off, as observed by increased TA activation during mid- to late-stance (Fig. 3.9). Many of our findings agree with the findings by Lejeune et al. (1998) who attributed the increased energy expenditure on sand to an increase in mechanical work and decrease in muscle-tendon efficiency. Reduced elastic energy absorption and greater energy loss due to slipping has also been shown during running and jumping on sand (Giatsis et al. 2004; Impellizzeri et al. 2008). However, the similar joint angles on all substrates prior to push-off may suggest that there may not be considerable foot slippage on the sands in this study (Fig. 3.8). Due to changes in gait on compliant sands, increased muscle activation (Fig. 3.9-3.10) is required, resulting in increased mechanical work and thus, greater energy expenditure.

3.5.3 Participant variability

There were considerable participant variability for most variables measured in this study. In particular, this is clear for all nEMG values as there were large standard deviations (Figs 3.9-3.10). Two of the outputs from LMMs are marginal R^2 (the proportion of variance explained by fixed factors alone) and conditional R^2 (the proportion of variance explained by both the fixed and random factors). For most variables measured in this study, the marginal R^2 value was considerably smaller than the conditional R^2 value which suggests that a high proportion of the variance found in the measured variables are due to the random effects (subjects) rather than the fixed effects, such as substrate, speed and gender. Although we did find gender to have a statistically significant effect on different gait mechanisms, the qualitative differences between substrates are the same for both genders and thus, data was not

separated by gender. However, participant differences would be interesting to look at in further research in the future.

3.5.4 Limitations

Although several measures were undertaken to ensure the sand substrates were comparable between data collection days, it must be noted that there is limitations on how similar the sand substrate would be for each participant in this study due to the complex material and mechanical properties of sand. Variation in substrate could account for some of the participant variability. Furthermore, there may be slight differences in compliance depending on the position of foot placement on the walkway; it can be expected that there is more leverage for compression and lateral displacement if the foot contacts the substrate in the centre of the walkway, compared to the edge.

3.6 Conclusions

This study shows that there are several changes in walking biomechanics on natural compliant substrates such as sand compared to hard, level floor. On the sands, participants displayed greater ranges of motion at the hip, knee and ankle joint, primarily due to greater peak flexion at the hip and knee joint during swing and greater ankle dorsiflexion during stance. Furthermore, participants adopted a slower walking speed and increased cycle time, stance time and swing time on all sand substrates. These gait changes result in slightly increased muscle activation, and most likely, increased mechanical work. Most gait changes are similar on both of the most compliant substrates, build dry and play sand with the build wet sand as an intermediate between them and the hard floor. This suggests that overall compliance is more important than the specific material differences in the different sand types, although this may be different on more elastic-plastic substrates such as clay and mud. Our findings in this study suggest that in order to compare modern human

footprints to fossil ancestor prints there needs to be a match in footprint depths to ensure gait is comparable. However, how gait changes are reflected in footprint morphology has not been tested in this study. The next step would be to see if differences in gait identified in this study between compliant substrates are reflected in the footprint shape itself.

3.7 References

Allen, J.R.L. (1997) 'Subfossil mammalian tracks (Flandrian) in the Severn Estuary, S. W. Britain: mechanics of formation, preservation and distribution', *Philosophical Transactions of the Royal Society of London. Series B: Biological Sciences*, vol. 352, no. 1352, pp. 481-518.

Bates, D., Mächler, M., Bolker, B. & Walker, S. (2014) 'Fitting linear mixed-effects models using lme4', *arXiv preprint arXiv:1406.5823*.

Bates, K.T., Collins, D., Savage, R., McClymont, J., Webster, E., Pataky, T.C., D'Aout, K., Sellers, W.I., Bennett, M.R. & Crompton, R.H. (2013a) 'The evolution of compliance in the human lateral mid-foot', *Proc Biol Sci*, vol. 280, no. 1769, p. 20131818.

Bates, K.T., Savage, R., Pataky, T.C., Morse, S.A., Webster, E., Falkingham, P.L., Ren, L., Qian, Z., Collins, D., Bennett, M.R., McClymont, J. & Crompton, R.H. (2013b) 'Does footprint depth correlate with foot motion and pressure?', *J R Soc Interface*, vol. 10, no. 83, p. 20130009.

Bell, F.G. (2013) *Foundation engineering in difficult ground*, Elsevier.

Bennett, M.R., Harris, J.W., Richmond, B.G., Braun, D.R., Mbua, E., Kiura, P., Olago, D., Kibunjia, M., Omuombo, C., Behrensmeyer, A.K., Huddart, D. & Gonzalez, S. (2009) 'Early hominin foot morphology based on 1.5-million-year-old footprints from Ileret, Kenya', *Science*, vol. 323, no. 5918, pp. 1197-1201.

Britannica, E. (2022) *The muscle groups and their actions* [Online], Available from: https://www.britannica.com/science/human-muscle-system#ref322749 (Accessed: 16/08/2022).

Cavagna, G.A., Heglund, N.C. & Taylor, C.R. (1977) 'Mechanical work in terrestrial locomotion: two basic mechanisms for minimizing energy expenditure', *American Journal of Physiology-Regulatory, Integrative and Comparative Physiology*, vol. 233, no. 5, pp. R243-R261.

Cavagna, G.A., Thys, H. & Zamboni, A. (1976) 'The sources of external work in level walking and running', *J Physiol*, vol. 262, no. 3, pp. 639-657.

Crompton, R.H., Pataky, T.C., Savage, R., D'Aout, K., Bennett, M.R., Day, M.H., Bates, K., Morse, S. & Sellers, W.I. (2012) 'Human-like external function of the foot, and fully upright gait, confirmed in the 3.66 million year old Laetoli hominin footprints by topographic statistics, experimental footprint-formation and computer simulation', *J R Soc Interface*, vol. 9, no. 69, pp. 707-719.

Crompton, R.H., Sellers, W.I. & Thorpe, S.K. (2010) 'Arboreality, terrestriality and bipedalism', *Philos Trans R Soc Lond B Biol Sci*, vol. 365, no. 1556, pp. 3301-3314.

Crompton, R.H., Vereecke, E.E. & Thorpe, S.K. (2008) 'Locomotion and posture from the common hominoid ancestor to fully modern hominins, with special reference to the last common panin/hominin ancestor', *J Anat*, vol. 212, no. 4, pp. 501-543.

D'Aout, K., Meert, L., Van Gheluwe, B., De Clercq, D. & Aerts, P. (2010) 'Experimentally generated footprints in sand: Analysis and consequences for the interpretation of fossil and forensic footprints', *Am J Phys Anthropol*, vol. 141, no. 4, pp. 515-525.

Davies, S.E.H. & Mackinnon, S.N. (2006) 'The energetics of walking on sand and grass at various speeds', *Ergonomics*, vol. 49, no. 7, pp. 651-660.
Doke, J., Donelan, J.M. & Kuo, A.D. (2005) 'Mechanics and energetics of swinging the human leg', *J Exp Biol*, vol. 208, no. Pt 3, pp. 439-445.
Donelan, J.M., Kram, R. & Kuo, A.D. (2002) 'Mechanical work for step-to-step transitions is a major determinant of the metabolic cost of human walking', *Journal of Experimental Biology*, vol. 205, no. 23, pp. 3717-3727.
Faraway, J.J. (2016) *Extending the linear model with R: generalized linear, mixed effects and nonparametric regression models*, Chapman and Hall/CRC.
Farris, D.J., Birch, J. & Kelly, L. (2020) 'Foot stiffening during the push-off phase of human walking is linked to active muscle contraction, and not the windlass mechanism', *Journal of The Royal Society Interface*, vol. 17, no. 168, p. 20200208.
Gates, D.H., Wilken, J.M., Scott, S.J., Sinitski, E.H. & Dingwell, J.B. (2012) 'Kinematic strategies for walking across a destabilizing rock surface', *Gait & Posture*, vol. 35, no. 1, pp. 36-42.
Giatsis, G., Kollias, I., Panoutsakopoulos, V. & Papaiakovou, G. (2004) 'Biomechanical differences in elite beach-volleyball players in vertical squat jump on rigid and sand surface', *Sports Biomech*, vol. 3, no. 1, pp. 145-158.
Hak, L., Houdijk, H., Steenbrink, F., Mert, A., van der Wurff, P., Beek, P.J. & van Dieën, J.H. (2012) 'Speeding up or slowing down?: Gait adaptations to preserve gait stability in response to balance perturbations', *Gait & Posture*, vol. 36, no. 2, pp. 260-264.
Hanavan Jr, E.P. (1964) *A mathematical model of the human body*, Air Force Aerospace Medical Research Lab Wright-patterson AFB OH,
Hatala, K.G., Demes, B. & Richmond, B.G. (2016) 'Laetoli footprints reveal bipedal gait biomechanics different from those of modern humans and chimpanzees', *Proc Biol Sci*, vol. 283, no. 1836.
Hatala, K.G., Dingwall, H.L., Wunderlich, R.E. & Richmond, B.G. (2013) 'The relationship between plantar pressure and footprint shape', *Journal of Human Evolution*, vol. 65, no. 1, pp. 21-28.
Holtz, R.D., Kovacs, W.D. & Sheahan, T.C. (1981) *An introduction to geotechnical engineering*, vol. 733, Prentice-Hall Englewood Cliffs.
Impellizzeri, F.M., Rampinini, E., Castagna, C., Martino, F., Fiorini, S. & Wisloff, U. (2008) 'Effect of plyometric training on sand versus grass on muscle soreness and jumping and sprinting ability in soccer players', *British Journal of Sports Medicine*, vol. 42, no. 1, pp. 42-46.
Jafarnezhadgero, A., Amirzadeh, N., Fatollahi, A., Siahkouhian, M., Oliveira, A.S. & Granacher, U. (2022) 'Effects of Running on Sand vs. Stable Ground on Kinetics and Muscle Activities in Individuals With Over-Pronated Feet', *Frontiers in Physiology*, vol. 12.
Kadaba, M.P., Ramakrishnan, H. & Wootten, M. (1990) 'Measurement of lower extremity kinematics during level walking', *Journal of orthopaedic research*, vol. 8, no. 3, pp. 383-392.
Kelly, L.A., Lichtwark, G. & Cresswell, A.G. (2015) 'Active regulation of longitudinal arch compression and recoil during walking and running', *J R Soc Interface*, vol. 12, no. 102, p. 20141076.
Kunzetsova, A., Brockhoff, P. & Christensen, R. (2017) 'lmerTest package: Tests in linear mixed effect models', *J Stat Softw*, vol. 82, pp. 1-26.

Lejeune, T.M., Willems, P.A. & Heglund, N.C. (1998) 'Mechanics and energetics of human locomotion on sand', *Journal of Experimental Biology*, vol. 201, no. 13, pp. 2071-2080.
MacLellan, M.J. & Patla, A.E. (2006) 'Adaptations of walking pattern on a compliant surface to regulate dynamic stability', *Experimental Brain Research*, vol. 173, no. 3, pp. 521-530.
Mann, R.A. & Hagy, J. (1980) 'Biomechanics of walking, running, and sprinting', *Am J Sports Med*, vol. 8, no. 5, pp. 345-350.
Marigold, D.S. & Patla, A.E. (2002) 'Strategies for Dynamic Stability During Locomotion on a Slippery Surface: Effects of Prior Experience and Knowledge', *Journal of Neurophysiology*, vol. 88, no. 1, pp. 339-353.
Matthis, J.S., Yates, J.L. & Hayhoe, M.M. (2018) 'Gaze and the Control of Foot Placement When Walking in Natural Terrain', *Curr Biol*, vol. 28, no. 8, pp. 1224-1233.e1225.
Merryweather, A., Yoo, B. & Bloswick, D. (2011) 'Gait Characteristics Associated with Trip-Induced Falls on Level and Sloped Irregular Surfaces', *Minerals*, vol. 1, no. 1, pp. 109-121.
Mochon, S. & McMahon, T.A. (1980) 'Ballistic walking', *Journal of Biomechanics*, vol. 13, no. 1, pp. 49-57.
Morse, S.A., Bennett, M.R., Liutkus-Pierce, C., Thackeray, F., McClymont, J., Savage, R. & Crompton, R.H. (2013) 'Holocene footprints in Namibia: the influence of substrate on footprint variability', *Am J Phys Anthropol*, vol. 151, no. 2, pp. 265-279.
O'Connor, S.M., Xu, H.Z. & Kuo, A.D. (2012) 'Energetic cost of walking with increased step variability', *Gait Posture*, vol. 36, no. 1, pp. 102-107.
Pandolf, K.B., Haisman, M.F. & Goldman, R.F. (1976) 'Metabolic energy expenditure and terrain coefficients for walking on snow', *Ergonomics*, vol. 19, no. 6, pp. 683-690.
Pataky, T.C., Robinson, M.A. & Vanrenterghem, J. (2013) 'Vector field statistical analysis of kinematic and force trajectories', *Journal of Biomechanics*, vol. 46, no. 14, pp. 2394-2401.
Patla, A.E. (2003) 'Strategies for dynamic stability during adaptive human locomotion', *IEEE Engineering in Medicine and Biology Magazine*, vol. 22, no. 2, pp. 48-52.
Pinnington, H.C. & Dawson, B. (2001) 'The energy cost of running on grass compared to soft dry beach sand', *Journal of Science and Medicine in Sport*, vol. 4, no. 4, pp. 416-430.
Pinnington, H.C., Lloyd, D.G., Besier, T.F. & Dawson, B. (2005) 'Kinematic and electromyography analysis of submaximal differences running on a firm surface compared with soft, dry sand', *Eur J Appl Physiol*, vol. 94, no. 3, pp. 242-253.
Raichlen, D.A., Gordon, A.D., Harcourt-Smith, W.E.H., Foster, A.D. & Haas, W.R., Jr. (2010) 'Laetoli Footprints Preserve Earliest Direct Evidence of Human-Like Bipedal Biomechanics', *PLOS ONE*, vol. 5, no. 3, p. e9769.
Svenningsen, F.P., de Zee, M. & Oliveira, A.S. (2019) 'The effect of shoe and floor characteristics on walking kinematics', *Human Movement Science*, vol. 66, pp. 63-72.
Team, R.C. 'R: A language and environment for statistical computing'.
Umberger, B.R. (2010) 'Stance and swing phase costs in human walking', *J R Soc Interface*, vol. 7, no. 50, pp. 1329-1340.

Voloshina, A.S., Kuo, A.D., Daley, M.A. & Ferris, D.P. (2013) 'Biomechanics and energetics of walking on uneven terrain', *Journal of Experimental Biology*, vol. 216, no. 21, pp. 3963-3970.

Wade, C., Redfern, M.S., Andres, R.O. & Breloff, S.P. (2010) 'Joint kinetics and muscle activity while walking on ballast', *Human Factors*, vol. 52, no. 5, pp. 560-573.

Zamparo, P., Perini, R., Orizio, C., Sacher, M. & Ferretti, G. (1992) 'The energy cost of walking or running on sand', *European Journal of Applied Physiology and Occupational Physiology*, vol. 65, no. 2, pp. 183-187.

Zeni Jr, J., Richards, J. & Higginson, J. (2008) 'Two simple methods for determining gait events during treadmill and overground walking using kinematic data', *Gait & posture*, vol. 27, no. 4, pp. 710-714.

Chapter four: Gait adaptations during human walking on different compliant substrates

This chapter includes a comparison between experimental data collected from the two studies discussed in chapters 2-3. This chapter is currently being developed for publication. Author contributions: The present thesis version was drafted by BFG and benefited from editorial suggestions from KB.

4.1 Abstract

Human locomotion occurs over a wide range of different natural and artificial surfaces that have different mechanical properties. Some surfaces are more challenging to move on and require necessary adjustments to maintain stability and efficiency. However, it is unclear how humans adapt similar gait adaptations on substrates with different properties. In the previous two chapters, studies included human walking on both artificial (chapter 2) and natural (chapter 3) compliant substrates, using the same participant marker and EMG set-up. This presented an opportunity to compare gait on compliant substrates with different material properties. The main aim of this chapter is to improve our understanding of how gait adaptations are affected by substrate properties. This comparison study included a total of 51 datasets from 39 participants, with 12 participants having taken part in both studies. Spatiotemporal variables, joint angles, muscle activities and pendular energy exchange were compared on the two substrates that were most comparable in foot sinking depth during the stance phase: thin foam and play sand. Compared to the hard floor, there were some similar gait adaptations on both compliant substrates, such as increased ranges of motion at the ankle, knee and hip joint, increased muscle activity, increased cycle and stance time and decreased speed. Furthermore, on both compliant substrates, participants retain a relatively efficient pendular energy exchange mechanism. However, there were some notable differences between foam and sand. On sand, participants adopted a reduced walking speed, displayed greater

ankle dorsiflexion and increased muscle activation. Our findings suggest that many gait adaptations such as increased joint flexion, decreased speed and increased cycle, stance and swing times may occur on all compliant substrates. But, the subtle differences between compliant substrates with different properties suggests wider research incorporating more compliant substrates is warranted.

4.2 Introduction

In everyday life, animals have to navigate a wide range of surfaces which will have different physical and mechanical properties that may impact animal movement across the surface the surface (Peyré-Tartaruga & Coertjens 2018). As discussed in the previous chapters, it is generally well accepted that human locomotion on complex, uneven and compliant substrates is typically associated with an increase in energy expenditure relative to uniform, non-deforming substrates (Davies & Mackinnon 2006; Gates et al. 2012; Lejeune, Willems & Heglund 1998; Pinnington & Dawson 2001; Voloshina et al. 2013; Wade et al. 2010; Zamparo et al. 1992). Although the changes in metabolic costs on compliant substrates are widely accepted (Kerdok et al. 2002), the mechanistic causes behind this increase remains unclear. Possible reasons for this uncertainty include the measurement of different variables across studies and variation in substrates used (Davies & Mackinnon 2006). Previous research has shown that substrate properties have a direct impact on ground reaction forces, biomechanics of the lower limb joints, muscle activation and the resulting mechanical work, and spatiotemporal parameters (Donelan, Kram & Kuo 2002; Psarras, Mertyri & Tsaklis 2016). Furthermore, surface complexity is known to influence stability, with some surfaces being more challenging to maintain stability than others. Gait strategies to adapt to changes in walking surface include adopting shorter strides (Donelan, Kram & Kuo 2002), wider stride width (Gates et al. 2012), increased contact time (Pinnington & Dawson 2001), greater hip and knee flexion (Voloshina et al. 2013) and increased mechanical work (Lejeune, Willems & Heglund 1998; Zamparo et al. 1992). It has also been shown that humans will increase leg stiffness during hopping or running on more compliant substrates in order to preserve gait mechanics such as centre of mass (CoM) vertical displacement

and ground contact time to improve stability (Ferris & Farley 1997; Ferris, Louie & Farley 1998; Kerdok et al. 2002).

During locomotion, as the foot contacts with the surface, it performs work on the substrate resulting in deformation energy and as the foot leaves the surface, some of this energy can be transferred back to the person. The amount of energy storage is dependent on surface properties such as the surface stiffness and surface deformation (Nigg 2007). Soft, compliant substrates act like a shock-absorber during impact and reduces ground reaction forces (GRF) by increasing the time of the collision (Barrett, Neal & Roberts 1998; McMahon & Greene 1979). However, if the compliant substrate is also resilient, as well as transferring the cushioning cost to the substrate, energy can be effectively stored and recycled from step to step, as shown by research into optimising running tracks and footwear (Hoogkamer et al. 2018; McMahon & Greene 1979). Compliant substrates such as sand, snow and foam have very different mechanical properties, which means they behave differently under load (Gibson & Ashby 1997). The typical stress-strain behaviour of rigid polyurethane foam exhibits three regions: a linear elastic phase, plateau and densification. During the initial elastic phase, the substrate resists small strains but as strain is increased, there is a period of stress plateau until a certain point of increased loading leads to densification (Mane et al. 2017). During elastic deformation, particularly during the plateau region of the stress-strain curve, energy can be absorbed by the foam. When the foam is unloaded, it will return to its original shape and can potentially provide energy rebound to the subject (Mane et al. 2017). On the other hand, natural compliant substrates such as sand act like a damper, which absorbs and dissipates energy. During locomotion on sand, the substrate is initially subjected to a period of elastic deformation. As loading is increased, the yield stress will be reached, leading to plastic deformation, resulting in the formation of a footprint (Allen 1997). Furthermore, during locomotion on sand, the foot sinks and often slip backwards as the sand is displaced. Walking or running on sand requires a greater co-contraction of muscles of knee and ankle muscles (Pinnington & Dawson 2001). As the surface moves under the foot, the muscles in the leg need to constantly work to ensure stability, resulting in additional external work (Lejeune, Willems & Heglund 1998; Zamparo et al. 1992). It has also been shown that running and jumping on sand

results in reduced elastic energy absorption and greater energy loss due to slipping (Giatsis et al. 2004; Impellizzeri et al. 2008). Slipping may cause the increased range of motion at the ankle joint observed prior to push-off during jumping on sand (Giatsis et al. 2004).

In the previous two chapters, studies were performed on both artificial (chapter 2) and natural (chapter 3) compliant substrates. Results show that substrate compliancy has an effect on metabolic cost (on foam), mechanical energy exchange, gait kinematics, spatiotemporal parameters and muscle activation. However, it is unknown whether the gait changes adopted on the artificial compliant substrate (foam) and the natural compliant substrate (sand) are similar. As the depths of the footprints made in the sand in chapter 3 overlaps the depths of foot depression on the foams used in chapter 2, this presents an opportunity to compare gait changes on substrates that exhibit similar 'gross compliance' under loads encountered during human walking, despite differences in their specific physical and mechanical properties. The overall hypothesis of this thesis is that gross gait adaptations like sagittal kinematics, mechanical energy exchange and spatiotemporal parameters are adopted in response to the depth of depression into a compliant substrate rather than the complex properties of the substrate itself (in chapter 1.3.1). The compliant substrates compared in this study have different material properties but comparable foot depressions into the substrate. If there are similar changes on the compliant substrates then the overall thesis hypothesis can be accepted. The overall aim of this study is to improve our understanding of the relationship between substrate properties, gait biomechanics and muscle activities. More specifically, this study aims to address whether similar gait changes are adopted when walking on compliant substrates with different material and mechanical properties.

We hypothesised the following:

1. Pendular energy exchange mechanism efficiency will be reduced more on the sand than the foam as the greater instability of the surface would require more work to raise and accelerate the CoM

2. On both foam and sand, there will be similar joint excursions at the hip and knee joints, reflecting similar levels of gross substrate compliance
3. Due to the displacement of sand under the foot, there will be greater joint excursions at the ankle joint on the sand than the foam
4. On sand, there will be greater muscle activation, primarily those acting at the ankle joint to stabilise the joint during surface displacement and to counter deceleration before push-off
5. Spatiotemporal gait parameters will not differ on the sand and foam, reflecting similar level of gross substrate compliance

4.3 Materials and Methods

4.3.1 Substrates

As the goal of this study is to compare how gait changes are affected by the different properties of artificial and natural compliant substrates, the substrates need to be analogous. As substrate compliance, or footprint depth was determined to be a key determinant for the gait changes seen in the previous two chapters, the substrates that will be compared should be the most similar in foot-sinking depth. Markers on the participant's left foot were used to determine how much the foot sunk into each substrate for the left calcaneus (LCAL) (Fig. 4.1a) and left hallux (LHALL) (Fig. 4.1b). At the start of every data collection session, the lab is calibrated with the height of the lab floor as Z=0 (vertical plane). Markers at the end of each foam walkway and sand walkway were used to calculate the Z-values of the compliant substrates. Using the marker data in Visual 3D (C-Motion Inc., Germantown, MD, USA), the lowest Z-values for the LCAL and LHALL were exported and deducted from the Z-values of the substrate to estimate the lowest sinking point of the foot in each substrate. Play sand was determined to be the most compliant of the different sands ((LCAL = 3.46 ± 1.36cm, LHALL = 5.54 ± 1.44cm (mean ± s.d.)), and most similar to the depths observed on the thin foam ((LCAL = 4.51 ± 0.92cm, LHALL = 6.18 ± 0.41cm (mean ± s.d.)) (Fig. 4.1). Therefore, the substrates compared in this

study are hard floor, thin foam and play sand. The floor values are taken from the foam study (chapter 2) as there were more trials conducted in the study. The substrates are described in the previous chapters, floor and thin foam (chapter 2.3.1; Fig. 2.1) and play sand (chapters 3.3.1; Fig 3.1, 3.3).

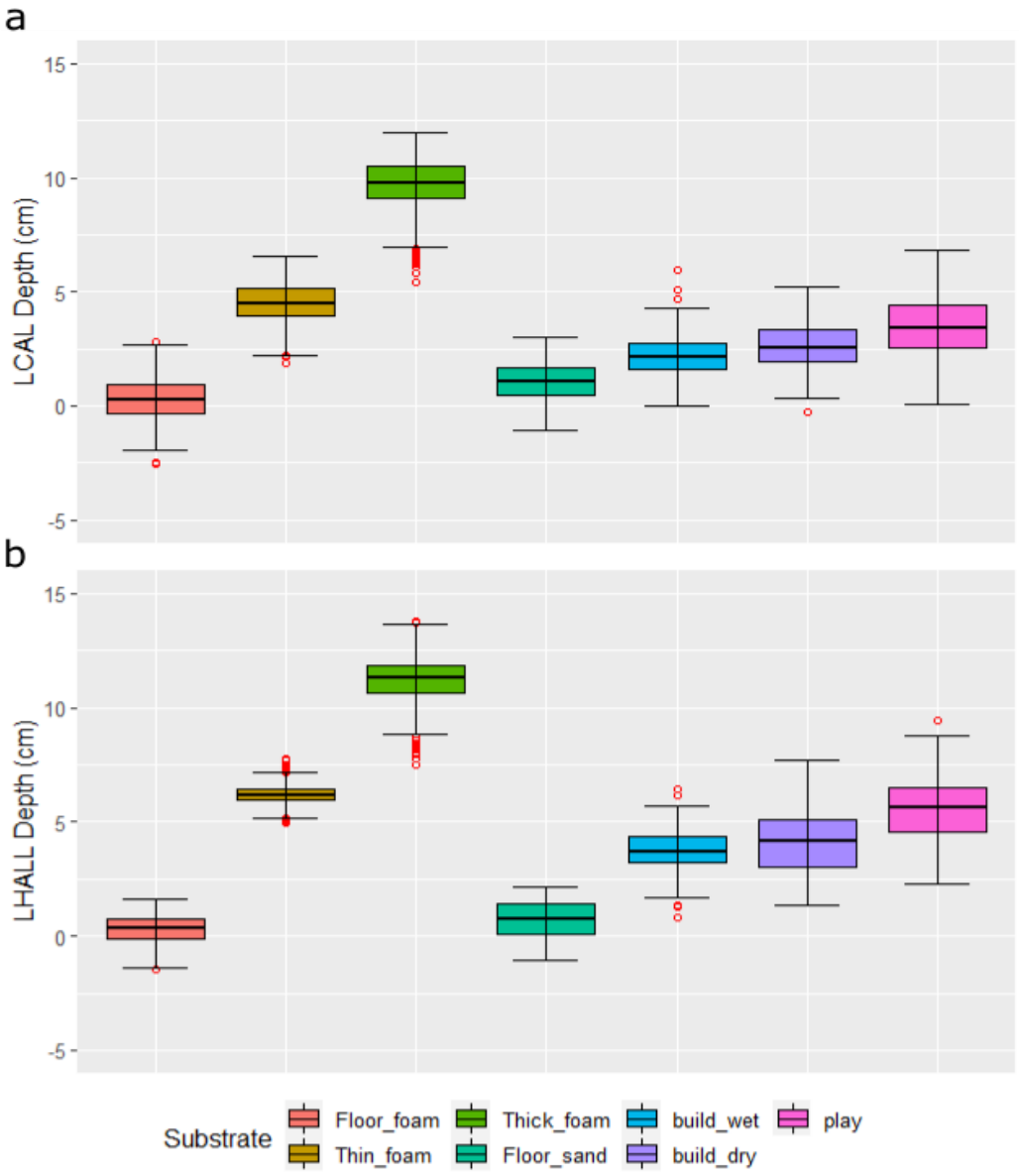

Figure 4.1: Sinking depth measurements calculated using lowest z-value positions for every stride for all participants combined on foam (n=3091) while walking on the three different substrates: floor, thin foam and thick foam and on sand (n=735) while walking on the four different substrates: floor, build wet sand, build dry sand and play sand: ***(a)*** Left calcaneus, ***(b)*** Left hallux. The centre line denotes the median value (50th percentile) while the boxes contain the 25th to 75th percentiles of dataset. The boundaries of the whiskers mark the 1.5 IQR with red circles denoting an individual stride from any subject that represents a statistical outlier.

4.3.2 Experimental procedure

The total number of participants analysed in this study is 39 but the total number of gait data sets analysed in this study is 51. For the study on foam (chapter 2) there was a total of 30 subjects and on the study on sand (chapter 3) there was a total of 21 subjects. However, there were 12 participants who took part in both foam and sand studies with both sets of their data being included in these comparative analysis. As described in previous chapters, both studies were conducted at the University of Liverpool Gait Lab at the Institute of Life Course and Medical Sciences and all participants signed informed consent before participating in the study in accordance with ethical approval from the University of Liverpool's Central University Research Ethics Committee for Physical Interventions (#3757). The participants had their key biometrics recorded, including height and weight (17 males, 22 females; age = 26.78 ± 4.71 years; height= 1.75 ± 0.07 m; body mass = 69.0 ± 9.23 kg; body mass index = 22.6 ± 2.1 kgm-2; see Table 4.1). For subjects who took part in both studies, age is denoted twice, the first one corresponding to their age during data collection for the foam study and the second one corresponding to their age during data collection for the sand study. If their body mass was ± 0.5kg between the two studies, it is denoted twice, otherwise only one value is reported. Full participant set-up is described in detail for the foam study (chapter 2.3.2; Table 2.2, Fig. 2.2) and sand study (chapter 3.3.2; Fig 3.2). Experimental procedure is described in detail for the foam study (chapter 2.3.3) and for the sand study (chapter 3.3.3).

Table 4.1: Anthropometric measurements from each subject: subject number, age (years), gender (male/female), height (m), body mass (kg), BMI (kgm^{-2}) and substrate (foam or sand study) with mean and standard deviation of all 39 participants. When two numbers are reported, the first number corresponds to the foam study and second to the sand study. Body mass is reported twice if it was recorded as ± 0.5kg between the two studies, otherwise only one value is reported.

Subject	Age	Gender (male/female)	Height (m)	Body mass (kg)	BMI (kgm^{-2})	Substrate
1	35 / 37	m	1.76	68	21.95	Both
2	25 / 27	m	1.75	71.1 / 65.4	23.22 / 21.36	Both
3	32	m	1.82	74.7	22.55	Foam
4	26 / 27	f	1.76	72.6	23.44	Both
5	21	f	1.77	76	24.26	Foam
6	21	f	1.7	57.5	19.90	Foam
7	24 / 26	m	1.75	68	22.2	Both
8	27	m	1.93	90	24.16	Foam
9	23 / 25	m	1.8	77.4 / 81.8	23.89 / 25.25	Both
10	29 / 31	m	1.8	80.6	24.88	Both
11	33	f	1.65	60.6	22.26	Foam
12	26	m	1.81	68	20.76	Foam
13	29	m	1.77	68.9	21.99	Foam
14	29	f	1.67	62.5	22.41	Foam
15	32 / 33	f	1.68	53.7 / 56.45	19.03 / 20	Both
16	28 / 29	m	1.86	83.3	24.08	Both
17	39	f	1.78	80	25.25	Foam
18	25	m	1.72	71.2	24.07	Foam
19	27 / 29	f	1.7	68	23.53	Both
20	26	f	1.635	53.5	20.01	Foam
21	29	f	1.8	66	20.37	Foam
22	26	f	1.71	57.6	19.70	Foam
23	27	f	1.72	81	27.38	Both
24	27	f	1.75	65.1	21.26	Foam
25	25	m	1.78	78	24.62	Foam
26	26 / 27	f	1.69	77	26.96	Both
27	27 / 28	m	1.74	78	25.76	Both
28	26	m	1.78	77.2	24.37	Foam
29	27	f	1.72	65.5	22.14	Foam
30	25	m	1.91	81.2	22.26	Foam
31	38	m	1.79	75.9	23.69	Sand
32	29	f	1.64	58.7	21.82	Sand
33	22	f	1.65	64.95	23.86	Sand
34	20	f	1.67	58	20.8	Sand
35	19	f	1.73	55.8	18.64	Sand
36	20	f	1.76	67.85	21.9	Sand
37	20	f	1.78	62.6	19.76	Sand
38	19	f	1.64	53.8	20	Sand
39	27	m	1.71	59.8	20.45	Sand
Mean	26.78	17m 22f	1.75	69.09	22.60	30 foam
SD	4.71		0.07	9.23	2.10	21 sand

4.3.3 Data processing and statistical analysis

Data was processed according to the steps outlined in the previous chapters for the foam study (chapter 2.3.4; Fig. 2.4) and the sand study (chapter 3.3.4). The output data from these studies were combined for statistical analyses using MATLAB v.2019a (Mathworks, Natick, USA). For some analyses, foam, sand and floor were all included as it is important to recognise not only how gait changes on the compliant substrates compare to each other, but also compared to a hard, level surface. However, most statistical analyses were only performed on the two compliant substrates, as comparisons of these substrates to the hard floor have already been undertaken and described in the previous chapters. Joint kinematics were analysed using two statistical approaches: Linear mixed-effect models (LMMs) (Faraway 2016) and one dimensional statistical parametric mapping (1D-SPM) (Pataky, Robinson & Vanrenterghem 2013). 1D-SPM analyses were performed using MATLAB to compare hip, knee and ankle joint angles across the selected substrates, with null hypothesis of no difference and alpha of 0.05. The mean and standard deviation of the joint angles were plotted for the duration of a gait cycle (0-100%) with toe-off timings shown using vertical dotted lines. Differences between the three substrates types were detected using paired t-tests with Bonferroni corrections with an alpha value of 0.017. Spatiotemporal variables and mechanical energy exchange variables are presented as box-and-whisker plots. LMMs were used to analyse differences between the two compliant substrates in their spatiotemporal variables, joint angles at gait events (heel-strike and toe-off), integrated muscle activity (iEMG) data and mechanical energy exchange variables. LMMs use restricted maximum likelihood to assess the significance of the fixed effects, substrate type, speed and gender in explaining variation with participants set as random effects to allow for different intercepts for each subject. All LMM's were performed in R (Team) using the lmer function in the R package lme4 (Bates et al. 2014) and lmerTest (Kunzetsova, Brockhoff & Christensen 2017).

4.4 Results

4.4.1 Spatiotemporal variables

Compared to the hard floor, there were some similar qualitative differences for both the foam and sand substrate (Fig. 4.2). On both compliant substrates, there was an increase in stride length (Fig. 4.2b), cycle time (Fig. 4.2d), stance time (Fig. 4.2e), swing time (Fig. 4.2f) and double-support time (Fig. 4.2g). Compared to hard floor, stride width (Fig. 4.2c) was lower on foam but higher on sand and duty factor (Fig. 4.2h) was higher on foam but lower on sand. Between the two compliant substrates, there were notable qualitative differences in most of the spatiotemporal variables. On sand, stride width (Fig. 4.2c), cycle time (Fig. 4.2d) and swing time (Fig. 4.2f) was higher and speed (Fig. 4.2a), stride length (Fig. 4.2b), double-support time (Fig. 4.2g) and duty factor (Fig. 4.2h) were lower than the foam. However, stance time (Fig. 4.2e) was similar for both foam and sand, whereas swing time (Fig. 4.2f) was higher on sand, showing the difference in duty factor is due to differences in swing time. LMMs performed on the two compliant substrates show that there is a significant ($p<0.01$) effect of substrate for cycle time, swing time, double limb support time and ($p<0.001$) speed (Tables 4.2-4.3). There was no significant ($p>0.05$) effect of substrate for stride length, stride width, stance time and duty factor (Tables 4.2-4.3). Gender had a significant ($p<0.001$) effect on swing time and ($p<0.01$) cycle time. Speed had a significant ($p<0.001$) effect on stride length, cycle time, stance time, swing time, double limb support time and ($p<0.05$) duty factor. Furthermore, there were significant ($p<0.01$) interaction effects between speed and substrate for cycle time, stance time and double limb support time. There were also some significant ($p<0.05$) interaction effects between gender, substrate and speed for cycle time, swing time and double limb support time. There was a significant ($p<0.001$) intercept for all spatiotemporal variables (Tables 4.2-4.3).

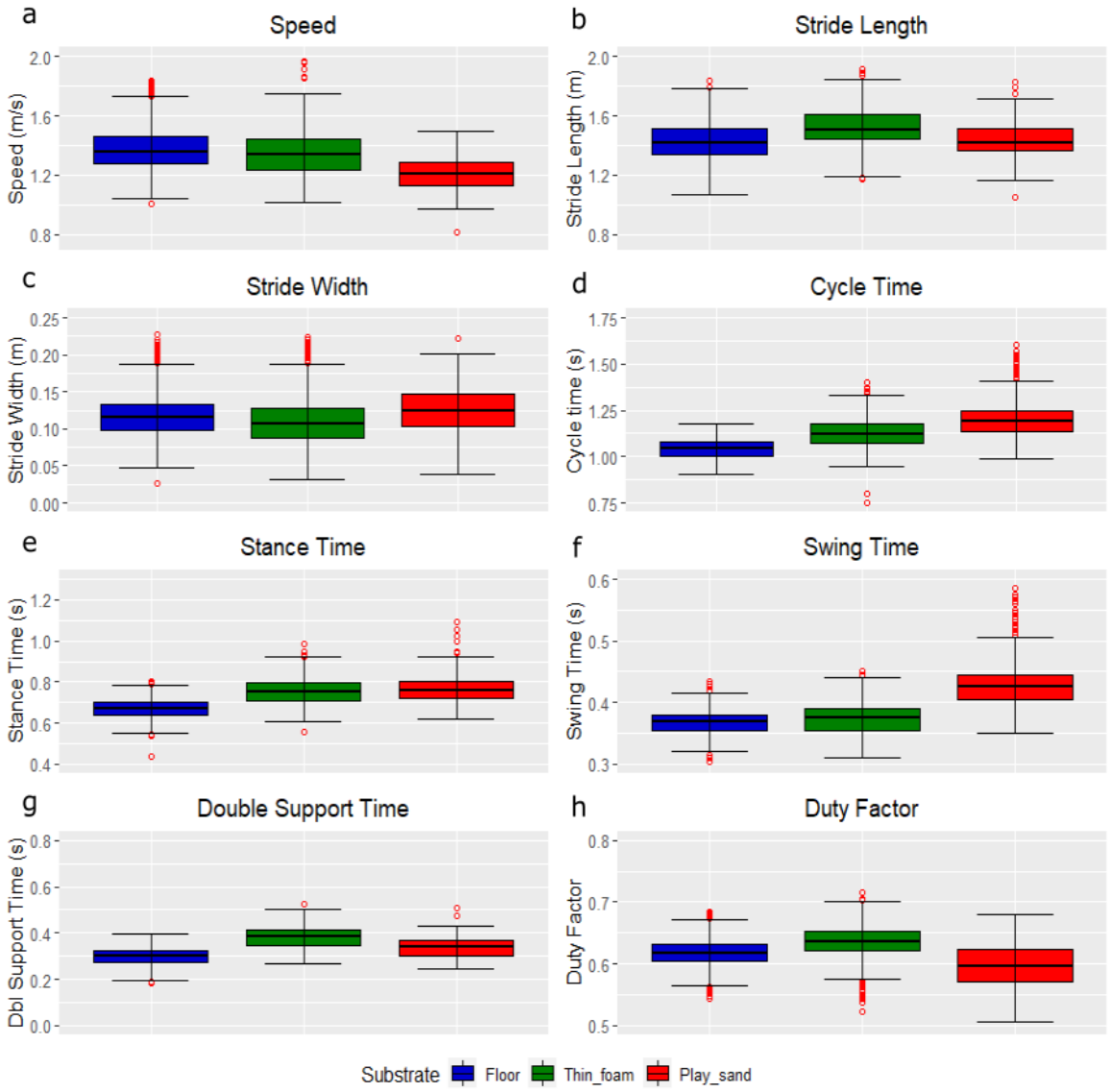

Figure 4.2: The distribution of spatiotemporal parameters for all participants combined (n=51) while walking on the three different substrates: floor (blue), thin foam (green) and play sand (red). ***(a)*** speed, ***(b)*** stride length, ***(c)*** stride width, ***(d)*** cycle time, ***(e)*** stance time, ***(f)*** swing time, ***(g)*** double support time and ***(h)*** duty factor. Data includes all strides on these substrates (n = 7932). The centre line denotes the median value (50th percentile) while the boxes contain the 25th to 75th percentiles of dataset. The boundaries of the whiskers mark the 1.5 IQR with red circles denoting an individual stride from any subject that represents a statistical outlier.

Table 4.2: The results of the linear mixed-effect models on the spatiotemporal parameters: speed (ms^{-1}), stride length (m), stride width (m) and cycle time (s); fixed effects = substrate, speed and gender and random effects = subjects. Statistical significance is set as $p<0.05$ with significant p-values shown in bold. σ^2 = random effect variance, τ_{00} = subject variance, intraclass correlation coefficient (ICC) = proportion of variance explained by random effects, N = number of subjects, observations = number of data points (strides), marginal R^2 = proportion of variance explained by the fixed factors, conditional R^2 = proportion of variance explained by both the fixed and random factors.

	Speed			**Stride_Length**			**Stride_Width**			**Cycle_Time**		
Predictors	*Estimates*	*CI*	*p*	*Estimates*	*CI*	*p*	*Estimates*	*CI*	*p*	*Estimates*	*CI*	*p*
(Intercept)	1.22	1.16 – 1.28	**<0.001**	0.80	0.63 – 0.97	**<0.001**	0.09	0.04 – 0.14	**<0.001**	1.78	1.67 – 1.90	**<0.001**
Substrate [Thin_foam]	0.12	0.10 – 0.13	**<0.001**	0.12	-0.05 – 0.28	0.176	-0.02	-0.07 – 0.03	0.346	-0.14	-0.26 – -0.03	**0.013**
Gender [M]	0.01	-0.08 – 0.10	0.841	0.00	-0.23 – 0.23	0.989	0.01	-0.06 – 0.08	0.795	0.22	0.06 – 0.38	**0.006**
Substrate [Thin_foam] * Gender [M]	0.03	0.02 – 0.05	**<0.001**	-0.23	-0.48 – 0.02	0.076	0.01	-0.07 – 0.08	0.844	-0.25	-0.42 – -0.08	**0.004**
Speed				0.49	0.36 – 0.63	**<0.001**	0.03	-0.01 – 0.07	0.171	-0.51	-0.61 – -0.42	**<0.001**
Substrate [Thin_foam] * Speed				-0.07	-0.21 – 0.07	0.316	0.00	-0.04 – 0.04	0.996	0.12	0.03 – 0.22	**0.009**
Speed * Gender [M]				0.07	-0.11 – 0.26	0.444	-0.01	-0.07 – 0.04	0.596	-0.11	-0.24 – 0.01	0.073
(Substrate [Thin_foam] * Speed) * Gender [M]				0.14	-0.06 – 0.34	0.181	0.01	-0.05 – 0.07	0.844	0.17	0.03 – 0.30	**0.016**
Random Effects												
σ^2	0.00			0.01			0.00			0.00		
τ_{00}	0.02 $_{Subject}$			0.00 $_{Subject}$			0.00 $_{Subject}$			0.00 $_{Subject}$		
ICC	0.83			0.43			0.46			0.50		
N	39 $_{Subject}$			39 $_{Subject}$			39 $_{Subject}$			39 $_{Subject}$		
Observations	3926			1960			1954			1963		
Marginal R^2 / Conditional R^2	0.106 / 0.847			0.497 / 0.711			0.054 / 0.487			0.462 / 0.729		

Table 4.3: The results of the linear mixed-effect models on the spatiotemporal parameters: stance time (s), swing time (s), double support time (s) and duty factor; fixed effects = substrate, speed and gender and random effects = subjects. Statistical significance is set as $p<0.05$ with significant p-values shown in bold. σ^2 = random effect variance, τ_{00} = subject variance, intraclass correlation coefficient (ICC) = proportion of variance explained by random effects, N = number of subjects, observations = number of data points (strides), marginal R^2 = proportion of variance explained by the fixed factors, conditional R^2 = proportion of variance explained by both the fixed and random factors.

	Stance_Time			**Swing_Time**			**Double_Limb_Support_Time**			**Duty_Factor**		
Predictors	*Estimates*	*CI*	*p*	*Estimates*	*CI*	*p*	*Estimates*	*CI*	*p*	*Estimates*	*CI*	*p*
(Intercept)	1.27	1.18 – 1.37	**<0.001**	0.48	0.44 – 0.52	**<0.001**	0.67	0.60 – 0.75	**<0.001**	0.69	0.60 – 0.77	**<0.001**
Substrate [Thin_foam]	-0.09	-0.19 – 0.00	0.058	-0.05	-0.09 – -0.02	**0.005**	-0.11	-0.18 – -0.03	**0.003**	0.03	-0.05 – 0.12	0.469
Speed	-0.44	-0.51 – -0.36	**<0.001**	-0.06	-0.09 – -0.03	**<0.001**	-0.27	-0.33 – -0.21	**<0.001**	-0.08	-0.14 – -0.01	**0.032**
Gender [M]	0.10	-0.03 – 0.23	0.140	0.15	0.10 – 0.20	**<0.001**	0.04	-0.06 – 0.13	0.449	-0.02	-0.13 – 0.10	0.787
Substrate [Thin_foam] * Speed	0.11	0.03 – 0.19	**0.006**	0.02	-0.01 – 0.05	0.275	0.13	0.07 – 0.19	**<0.001**	0.02	-0.05 – 0.09	0.646
Substrate [Thin_foam] * Gender [M]	-0.09	-0.23 – 0.05	0.210	-0.14	-0.19 – -0.09	**<0.001**	0.14	0.04 – 0.24	**0.008**	-0.03	-0.16 – 0.09	0.632
Speed * Gender [M]	-0.05	-0.15 – 0.06	0.392	-0.09	-0.13 – -0.05	**<0.001**	-0.03	-0.11 – 0.05	0.452	0.01	-0.08 – 0.11	0.798
(Substrate [Thin_foam] * Speed) * Gender [M]	0.06	-0.05 – 0.17	0.305	0.09	0.05 – 0.14	**<0.001**	-0.10	-0.18 – -0.02	**0.019**	0.02	-0.09 – 0.12	0.769
Random Effects												
σ^2	0.00			0.00			0.00			0.00		
τ_{00}	0.00 $_{\text{Subject}}$			0.00 $_{\text{Subject}}$			0.00 $_{\text{Subject}}$			0.00 $_{\text{Subject}}$		
ICC	0.41			0.47			0.76			0.07		
N	39 $_{\text{Subject}}$			39 $_{\text{Subject}}$			39 $_{\text{Subject}}$			39 $_{\text{Subject}}$		
Observations	1966			3049			547			1966		
Marginal R^2 / Conditional R^2	0.464 / 0.683			0.374 / 0.669			0.520 / 0.887			0.140 / 0.202		

The coefficient of variation (CV) was fairly similar on all substrates for most spatiotemporal variables (Table 4.4). CV increased on both foam and sand compared to the floor for stride width, cycle time, stance time, swing time and duty factor. CV increased by 14% and 7% for stride width, 12% and 21% for cycle time, 19% and 18% for stance time, 22% and 41% for swing time and 32% and 24% for duty factor between floor/foam and floor/sand, respectively. CV for stride length decreased by 9% and 36% between floor/foam and floor/sand, respectively. CV for speed increased by 3% between floor and foam but decreased by 29% between floor and sand whereas CV for double limb support time decreased by 14% between floor and foam but increased by 2% between floor and sand. On sand, CV was lower by 33% for speed, 25% for stride length, 8% for stride width, 1% stance time and 12% for duty factor compared to foam. CV was higher by 10% for cycle time, 25% for swing time and 14% for double support time on sand compared to foam.

Table 4.4. The mean, s.d. and coefficient of variation (CV) for each spatiotemporal parameters: Speed (ms^{-1}), stride length (m), stride width (m), cycle time (s), stance time (s), swing time (s), double support time (s) and duty factor. The CV is a measure of relative variability expressed as a percentage ($CV = (SD/\bar{x}) * 100$).

Substrate		Speed (ms^{-1})	Stride Length (m)	Stride Width (m)	Cycle Time (s)	Stance Time (s)	Swing Time (s)	Dbl Support Time (s)	Duty Factor
Floor	Mean	1.40	1.42	0.12	1.04	0.67	0.37	0.30	0.62
	SD	0.16	0.15	0.03	0.07	0.05	0.02	0.04	0.03
	CV	11.54	10.71	23.66	6.89	7.82	5.48	13.78	4.77
Thin	Mean	1.37	1.51	0.11	1.12	0.75	0.37	0.38	0.63
	SD	0.16	0.15	0.03	0.09	0.07	0.03	0.05	0.04
	CV	11.89	9.83	27.52	7.84	9.68	7.03	12.07	7.04
Play	Mean	1.22	1.44	0.13	1.20	0.76	0.43	0.34	0.59
	SD	0.11	0.11	0.03	0.10	0.07	0.04	0.05	0.04
	CV	8.94	7.86	25.42	8.71	9.55	9.32	13.99	6.28

4.4.2 Mechanical energy exchange

When averaged across each subject, Kinetic energy (E_{kin}) and total mechanical energy (E_{tot}) were similar between floor and foam but decreased over the whole stride on sand (Fig. 4.3a- 4.3b). During most of the stride, potential energy (E_{pot}) were similar for all substrates but slightly increased on the compliant substrates compared to hard floor, except during early-stance and toe-off where E_{pot} was higher on the floor (Fig. 4.3c). During all of the stride, E_{kin} and E_{tot} decreased on sand compared to foam (Fig. 4.3a – 4.3b). During the stance phase, E_{pot} decreased on sand compared to foam but was higher during most of the swing phase (Fig. 4.3c).

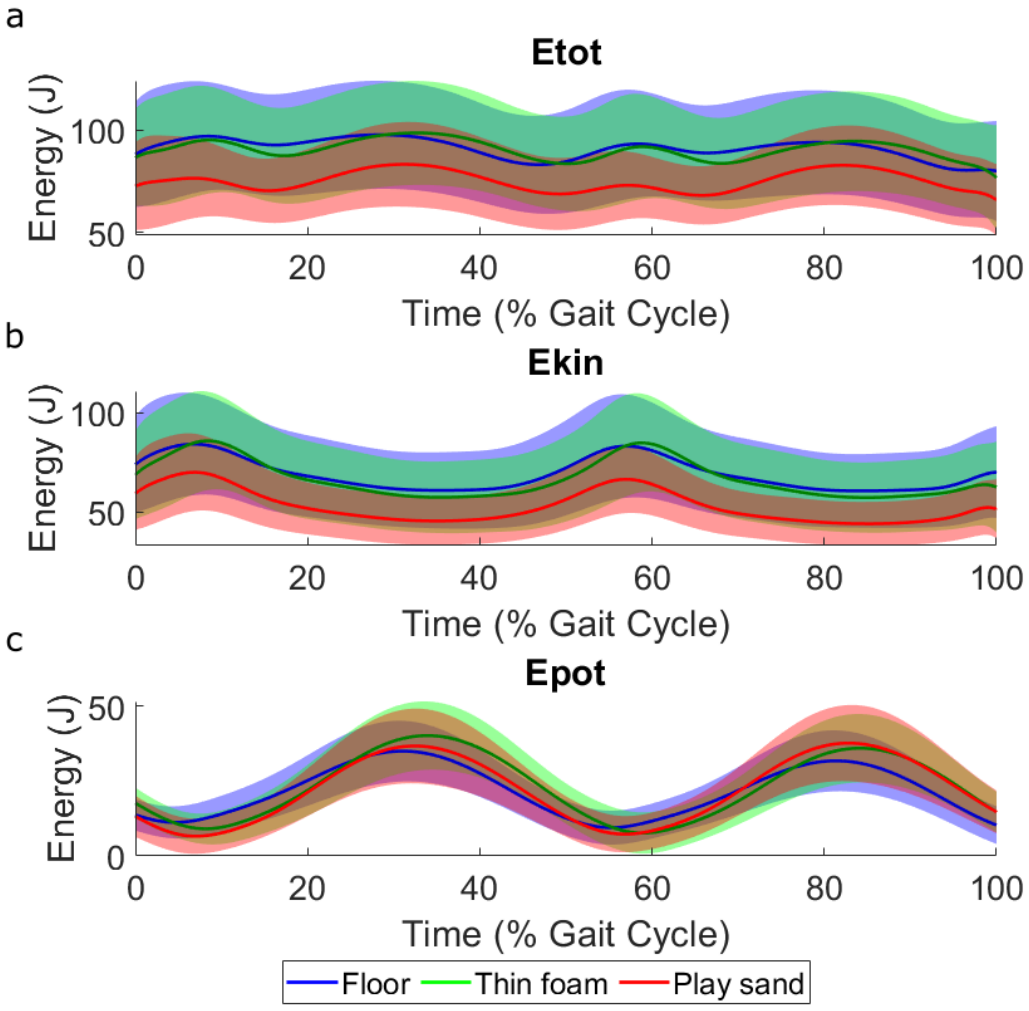

Figure 4.3: ***(a)*** Mass-normalised total (E_{tot}) mechanical energy, ***(b)*** kinetic (E_{kin}) energy and ***(c)*** the gravitational potential (E_{pot}) energy of the COM, normalised to walking stride for all participants combined (n=39) while walking on the three different substrates (mean ± s.d): Floor (blue), thin foam (green) and play sand (red). Bold lines indicate the mean value and shaded regions show the standard deviation.

The recovery of total energy exchange (R) and relative amplitude (RA) were similar for all substrates (Fig. 4.4). Compared to hard floor, R increased by ~3% and ~0.7% and RA increased by ~5% and ~6% between floor and foam and sand, respectively. On sand, R decreased by ~2% and RA increased by ~1% compared to thin foam. CO decreased by ~30% and ~18% between floor and foam and sand, respectively. On sand, CO increased by ~17% compared to foam (Fig. 4.4). LMMs on the two compliant substrates showed that the effect of substrate is significant for CO ($p<0.001$) and for RA ($p<0.05$) but not significant for R ($p>0.05$) (Table 4.5). There are significant effects of speed ($p\leq0.001$) for all energy exchange variables and significant interaction effects between speed and substrate for CO ($p<0.001$) and for RA ($p<0.05$). Gender had a significant effect for CO ($p<0.01$), as well as significant interaction effects between gender and substrate ($p<0.001$) and between gender and speed ($p<0.01$). There is a significant intercept for R and RA ($p<0.001$) (Table 4.5).

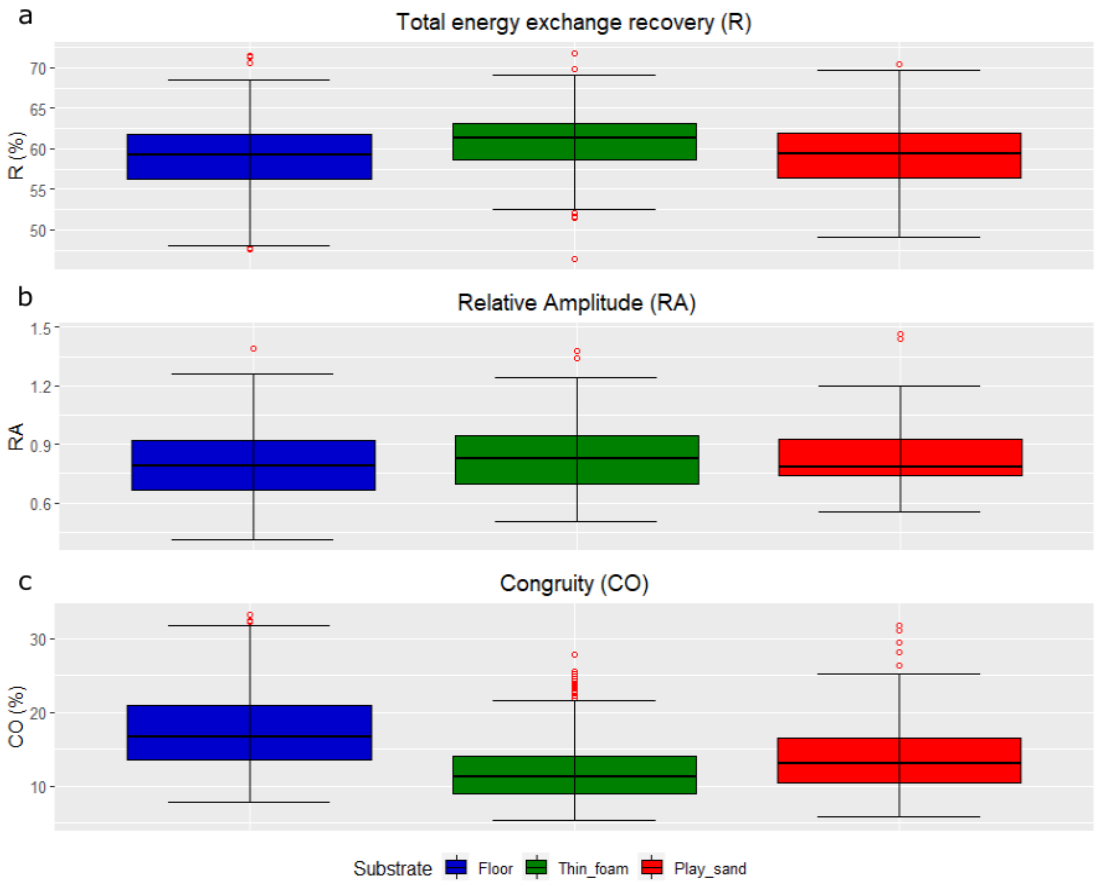

Figure 4.4: The distribution of pendulum-like determining variables: ***(a)*** The recovery of total energy exchange as a percentage (R), ***(b)*** Relative Amplitude (RA), and ***(c)*** Congruity percentage (CO) for all participants combined (n=39) while walking on the three different substrates (mean ± s.d): Floor (blue), thin foam (green) and play sand (red). Red circles denote an individual stride from any subject that represent statistical outlier. The centre line denotes the median value (50th percentile) while the boxes contain the 25th to 75th percentiles of dataset. The boundaries of the whiskers mark the 1.5 IQR with red circles denoting an individual stride from any subject that represents a statistical outlier.

Table 4.5: The results of the linear mixed-effect models on the mass normalised mechanical energy exchange variables: the recovery of mechanical energy (expressed as a percentage; R), relative amplitude (RA) and congruity (the time when potential energy and kinetic energy are moving in the same direction; CO). Fixed effects = substrate, gender and speed and random effects = subjects. Statistical significance is set as $p<0.05$ with significant p-values shown in bold. σ^2 = random effect variance, τ_{00} = subject variance, intraclass correlation coefficient (ICC) = proportion of variance explained by random effects, N = number of subjects, observations = number of data points (strides), marginal R^2 = proportion of variance explained by the fixed factors, conditional R^2 = proportion of variance explained by both the fixed and random factors.

	R			**RA**			**CO**		
Predictors	*Estimates*	*CI*	*p*	*Estimates*	*CI*	*p*	*Estimates*	*CI*	*p*
(Intercept)	74.64	65.09 – 84.20	**<0.001**	1.85	1.45 – 2.25	**<0.001**	-11.66	-24.00 – 0.67	0.064
Substrate [Thin_foam]	-6.51	-16.15 – 3.12	0.185	-0.46	-0.86 – -0.05	**0.028**	40.71	28.40 – 53.02	**<0.001**
Gender [M]	-2.46	-17.21 – 12.29	0.744	0.27	-0.35 – 0.90	0.395	28.15	9.29 – 47.01	**0.003**
Speed	-12.93	-20.86 – -4.99	**0.001**	-0.84	-1.17 – -0.50	**<0.001**	23.33	13.14 – 33.51	**<0.001**
Substrate [Thin_foam] * Gender [M]	4.92	-10.68 – 20.52	0.537	-0.19	-0.86 – 0.47	0.565	-45.97	-65.86 – -26.09	**<0.001**
Substrate [Thin_foam] * Speed	7.41	-0.45 – 15.28	0.065	0.42	0.08 – 0.75	**0.014**	-35.41	-45.44 – -25.37	**<0.001**
Gender [M] * Speed	3.61	-8.35 – 15.56	0.554	-0.26	-0.76 – 0.25	0.320	-24.46	-39.69 – -9.22	**0.002**
(Substrate [Thin_foam] * Gender [M]) * Speed	-4.87	-17.34 – 7.60	0.444	0.23	-0.30 – 0.76	0.388	36.60	20.73 – 52.48	**<0.001**
Random Effects									
σ^2	4.95			0.01			7.88		
τ_{00}	6.83 $_{\text{Subject}}$			0.01 $_{\text{Subject}}$			17.51 $_{\text{Subject}}$		
ICC	0.58			0.45			0.69		
N	37 $_{\text{Subject}}$			37 $_{\text{Subject}}$			37 $_{\text{Subject}}$		
Observations	521			521			521		
Marginal R^2 / Conditional R^2	0.100 / 0.621			0.268 / 0.600			0.146 / 0.735		

4.4.3 Joint kinematics

1D-SPM analyses of sagittal plane joint kinematics found significant differences between all substrates throughout most of the stride (Fig. 4.5, Tables 6.14-6.16 in appendix). During heel-strike, there was a significant ($p<0.001$) difference in ankle joint angle between foam and sand, with greater ankle dorsiflexion on the sand (Fig. 4.5a). There were significantly ($p<0.01$) more knee flexion (Fig. 4.5b) and hip flexion (Fig. 4.5c) on both compliant substrates compared to floor but there were no significant ($p>0.05$) difference in knee and hip flexion between foam and sand (Fig. 4.5b-c). LMMs at heel-strike on the two compliant substrates show that there were significant ($p\leq0.001$) effects of substrate for ankle and knee joint angles (Table 4.6). Furthermore, there was a significant ($p<0.001$) effect of speed for all joint angles with significant ($p<0.001$) interaction effects between speed and substrate for ankle and knee angle. There were significant ($p<0.001$) effects of gender and significant $p<0.001$) interaction effects between gender and substrate for ankle and hip joint angle (Table 4.6). There were also significant ($p<0.001$) interaction effects between gender and speed, and gender, speed and substrate for ankle and hip joint angles. Furthermore, there were significant ($p<0.001$) intercepts for ankle, knee and hip joint angles (Table 4.6). During early to mid-stance, there is significantly ($p<0.001$) more dorsiflexion at the ankle joint on the sand compared to the foam (Fig. 4.5a). During early-stance, knee and hip joint angles are similar on foam and sand, although both see significantly ($p<0.05$) less flexion on the foam compared to the sand for a short period of early-stance (Fig. 4.5b-4.5c). During mid to late-stance, there was significantly ($p<0.001$) less knee flexion on sand compared to foam, but there were no significant ($p>0.05$) differences in hip flexion except one small period in late-stance (Fig. 4.5b). During late-stance, there were significantly ($p<0.05$) less knee flexion (Fig. 4.5b) on sand compared to foam. At toe-off there was a significantly ($p<0.001$) less knee flexion on the sand than the foam but no significant ($p>0.05$) difference in ankle or hip angles (Fig. 4.5). LMMs at toe-off show that there were significant ($p<0.001$) effects of substrate for ankle and knee joint angles but no significant ($p>0.05$) effect for hip angle (Table 4.7). Speed had a significant ($p\leq0.001$) effect for ankle and hip angle, and ($p<0.05$) for knee angle. There were significant ($p<0.001$) interaction effects between speed and substrate for ankle and knee angle and ($p<0.01$) for hip angle. Also, there were significant ($p<0.05$) effects

of gender for knee and hip angle, and significant ($p<0.001$) interaction effects between gender and substrate for hip angle. There were significant ($p<0.001$) interaction effects between speed and gender and speed, gender and substrate for hip angle (Table 4.7). During swing, there were significantly ($p<0.001$) more knee and hip flexion and ($p<0.01$) plantarflexion on foam and sand compared to the hard floor (Fig. 4.5). For all of the swing phase, there was significantly ($p<0.001$) greater flexion at the knee joint on foam compared to sand (Fig. 4.5b). However, hip and ankle angles are more similar for most of the swing phase with only short periods of swing when there were significant ($p<0.05$) differences between ankle and hip angles on foam and sand, with greater plantarflexion at the ankle joint (Fig. 4.5a) and greater flexion at the hip joint (Fig. 4.5c) on foam compared to sand.

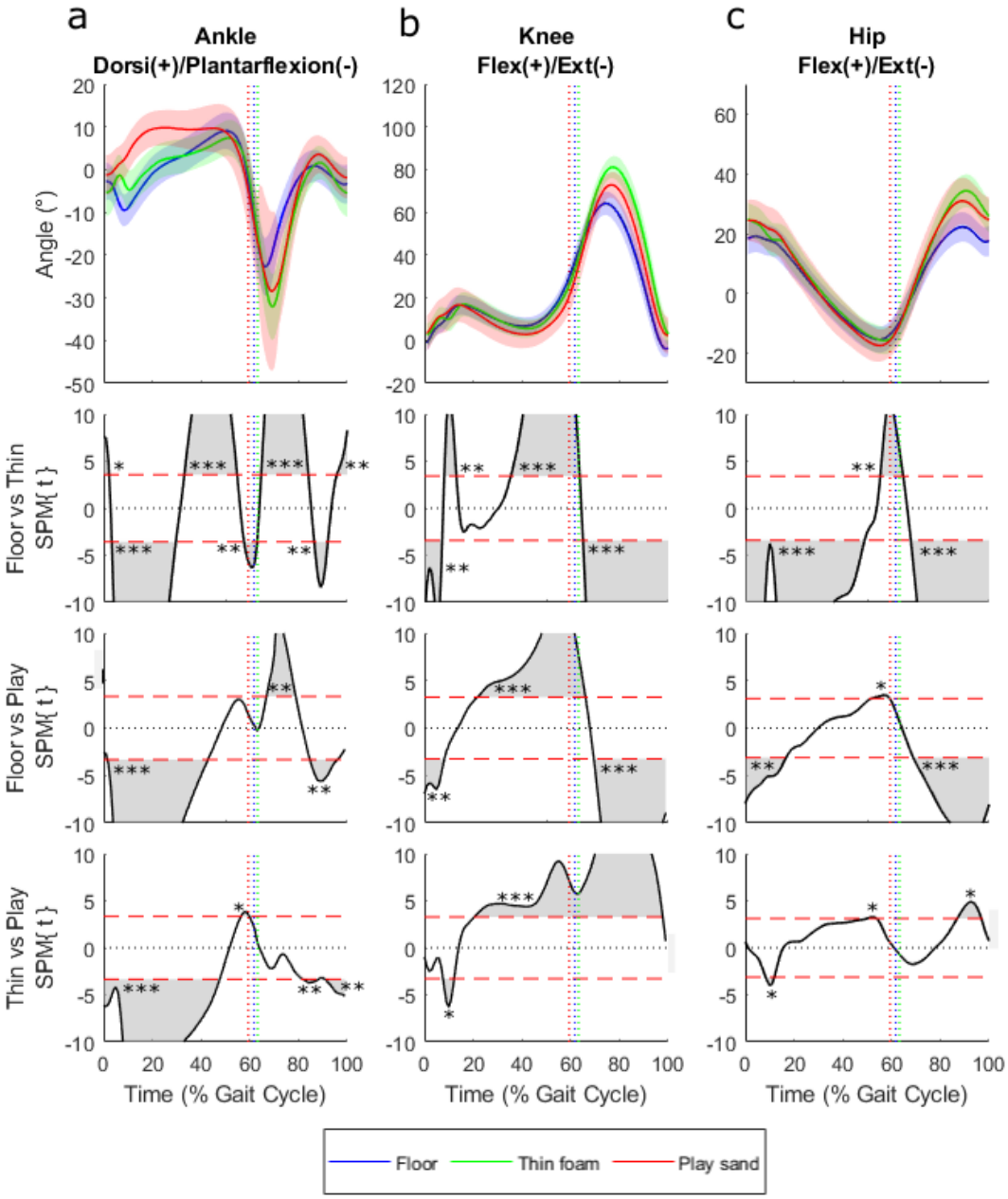

Figure 4.5: ***(a)*** Ankle, ***(b)*** knee and ***(c)*** hip joint angles in the sagittal plane for all participants combined (n=51) while walking on the three different substrates: floor (blue), thin foam (green) and play sand (red). Bold lines indicate the mean value and shaded regions show the standard deviation. The vertical dotted lines indicate toe-off. 1D-SPM (utilising paired t-tests with Bonferroni corrections) indicate regions of statistically significant differences between walking conditions, when 1D-SPM lines exceed the critical threshold values denoted by the horizontal red dotted lines. Shaded regions (within the SPM graphs) correspond to the period within the gait cycle where walking conditions are statistically significantly different from one another. "*, **, ***" represent p-values of less than 0.05, 0.01 and 0.001 respectively.

Table 4.6: The results of the linear mixed-effect models on the ankle, knee and hip joint angles in the sagittal plane for all subjects combined (n=39) at heel-strike. Fixed effects = substrate, speed and gender and random effects = subjects. Statistical significance is set as $p<0.05$ with significant p-values shown in bold. σ^2 = random effect variance, τ_{00} = subject variance, intraclass correlation coefficient (ICC) = proportion of variance explained by random effects, N = number of subjects, observations = number of data points (strides), marginal R^2 = proportion of variance explained by the fixed factors, conditional R^2 = proportion of variance explained by both the fixed and random factors.

	Ankle_Angle			**Knee_Angle**			**Hip_Angle**		
Predictors	*Estimates*	*CI*	*p*	*Estimates*	*CI*	*p*	*Estimates*	*CI*	*p*
(Intercept)	-24.86	-29.60 – -20.12	**<0.001**	-10.15	-15.84 – -4.46	**<0.001**	11.29	5.96 – 16.62	**<0.001**
Substrate [Thin_foam]	29.22	24.79 – 33.66	**<0.001**	9.03	3.49 – 14.58	**0.001**	-2.60	-7.74 – 2.54	0.322
Speed	18.80	15.34 – 22.27	**<0.001**	11.97	7.64 – 16.29	**<0.001**	8.74	4.64 – 12.84	**<0.001**
Gender [M]	37.84	31.10 – 44.58	**<0.001**	0.47	-7.58 – 8.52	0.909	-25.90	-33.70 – -18.10	**<0.001**
Substrate [Thin_foam] * Speed	-24.40	-27.92 – -20.89	**<0.001**	-9.27	-13.67 – -4.87	**<0.001**	2.50	-1.58 – 6.58	0.230
Substrate [Thin_foam] * Gender [M]	-69.23	-76.34 – -62.12	**<0.001**	0.79	-8.10 – 9.69	0.862	33.67	25.19 – 42.15	**<0.001**
Speed * Gender [M]	-28.89	-33.61 – -24.18	**<0.001**	-1.27	-7.17 – 4.63	0.672	25.04	19.21 – 30.87	**<0.001**
(Substrate [Thin_foam] * Speed) * Gender [M]	49.39	43.92 – 54.86	**<0.001**	-0.99	-7.84 – 5.85	0.776	-30.53	-37.09 – -23.97	**<0.001**
Random Effects									
σ^2	14.89			23.49			17.08		
τ_{00}	28.58 $_{\text{Subject}}$			29.04 $_{\text{Subject}}$			22.10 $_{\text{Subject}}$		
ICC	0.66			0.55			0.56		
N	39 $_{\text{Subject}}$			39 $_{\text{Subject}}$			39 $_{\text{Subject}}$		
Observations	5535			5550			4568		
Marginal R^2 / Conditional R^2	0.157 / 0.711			0.043 / 0.572			0.122 / 0.617		

Table 4.7: The results of the linear mixed-effect models on the ankle, knee and hip joint angles in the sagittal plane for all subjects combined (n=39) at toe-off. Fixed effects = substrate, speed and gender and random effects = subjects. Statistical significance is set as $p<0.05$ with significant p-values shown in bold. σ^2 = random effect variance, τ_{00} = subject variance, intraclass correlation coefficient (ICC) = proportion of variance explained by random effects, N = number of subjects, observations = number of data points (strides), marginal R^2 = proportion of variance explained by the fixed factors, conditional R^2 = proportion of variance explained by both the fixed and random factors.

	Ankle_Angle			**Knee_Angle**			**Hip_Angle**		
Predictors	*Estimates*	*CI*	*p*	*Estimates*	*CI*	*p*	*Estimates*	*CI*	*p*
(Intercept)	-0.47	-9.76 – 8.81	0.920	31.15	23.30 – 38.99	**<0.001**	-0.43	-6.92 – 6.06	0.897
Substrate [Thin_foam]	-30.32	-38.89 – -21.76	**<0.001**	33.40	25.93 – 40.87	**<0.001**	-0.56	-6.60 – 5.48	0.857
Speed	-18.63	-25.95 – -11.31	**<0.001**	7.63	1.28 – 13.97	**0.019**	-8.91	-14.06 – -3.76	**0.001**
Gender [M]	2.63	-9.97 – 15.24	0.682	13.55	2.64 – 24.47	**0.015**	-15.37	-24.17 – -6.57	**0.001**
Substrate [Thin_foam] * Speed	18.41	11.52 – 25.31	**<0.001**	-13.76	-19.78 – -7.75	**<0.001**	7.24	2.37 – 12.10	**0.004**
Substrate [Thin_foam] * Gender [M]	-2.84	-15.85 – 10.17	0.668	-7.60	-19.23 – 4.03	0.200	26.25	17.07 – 35.43	**<0.001**
Speed * Gender [M]	1.08	-8.63 – 10.78	0.827	-10.91	-19.61 – -2.21	**0.014**	15.50	8.66 – 22.34	**<0.001**
(Substrate [Thin_foam] * Speed) * Gender [M]	0.38	-9.84 – 10.61	0.942	7.87	-1.30 – 17.04	0.093	-22.57	-29.79 – -15.35	**<0.001**
Random Effects									
σ^2	25.17			19.43			12.56		
τ_{00}	43.95_{Subject}			15.37_{Subject}			18.37_{Subject}		
ICC	0.64			0.44			0.59		
N	39_{Subject}			39_{Subject}			39_{Subject}		
Observations	3086			3086			3074		
Marginal R^2 / Conditional R^2	0.162 / 0.695			0.555 / 0.751			0.230 / 0.687		

4.4.4 Muscle activity

Overall, lower limb activity was similar on the hard floor and thin foam, with muscle activities being slightly higher on thin foam for most muscles. However, there was considerably greater muscle activation for all muscles on the play sand compared to both the hard floor and thin foam (Fig. 3.10). During heel-strike, normalised EMG (nEMG) for the BFL (Fig. 3.10a) and MG (Fig. 3.10f) were higher on both foam and sand compared to the floor, with a greater increase on sand. nEMG for the RF (Fig. 3.10b), VL (Fig. 3.10c), VM (Fig. 3.10d) and SOL (Fig.3.10h) were similar on the floor and sand but were lower on the foam. nEMG for the TA (Fig. 3.10e) were similar on both foam and sand but were smaller than the floor and nEMG for the LG (Fig. 3.10g) were lowest on foam and highest on the sand, with floor values in-between the two compliant substrates. During early-stance, nEMG is greater on the foam and sand compared to floor for all muscles, but these values are much higher on the sand than the foam. During mid-stance, nEMG is higher on sand for BFL, RF, VL and VM compared to both floor and thin foam, which have similar values. During mid-stance, TA and SOL are similar for all substrates and MG and LG are similar for floor and sand, but are lower on foam. During the propulsive phase or late-stance, nEMG is greater on foam and sand for BFL, TA, MG, LG and SOL compared to hard floor, with greater activation on sand for BFL, MG and LG. On sand, RF, VL, and VM are higher during mid-stance than on the foam. During toe-off, muscle activities were higher for all muscles on sand compared to both floor and foam, except TA which was highest on the floor with foam and sand being similar values (Fig. 3.10e). During swing, muscle activities remain higher on sand for all muscles except short periods later in swing for BFL (Fig. 3.10a), RF (Fig. 3.10b), VL (Fig. 3.10c), VM (Fig. 3.10d) and TA (Fig. 3.10e) which were highest on the hard floor but higher on sand compared to foam. Similar results are found in the integrated muscle activity (iEMG) values with much higher values for all muscles on the sand compared to both floor and foam (Fig. 3.10i). There were similar values found for all muscles between floor and foam, with slightly higher values on foam for all muscles except LG which is lower on foam compared to the floor (Fig. 3.10i). For all muscles, there were considerable participant variability, particularly on sand where there are large standard deviations for both nEMG and iEMG (Fig. 3.10).

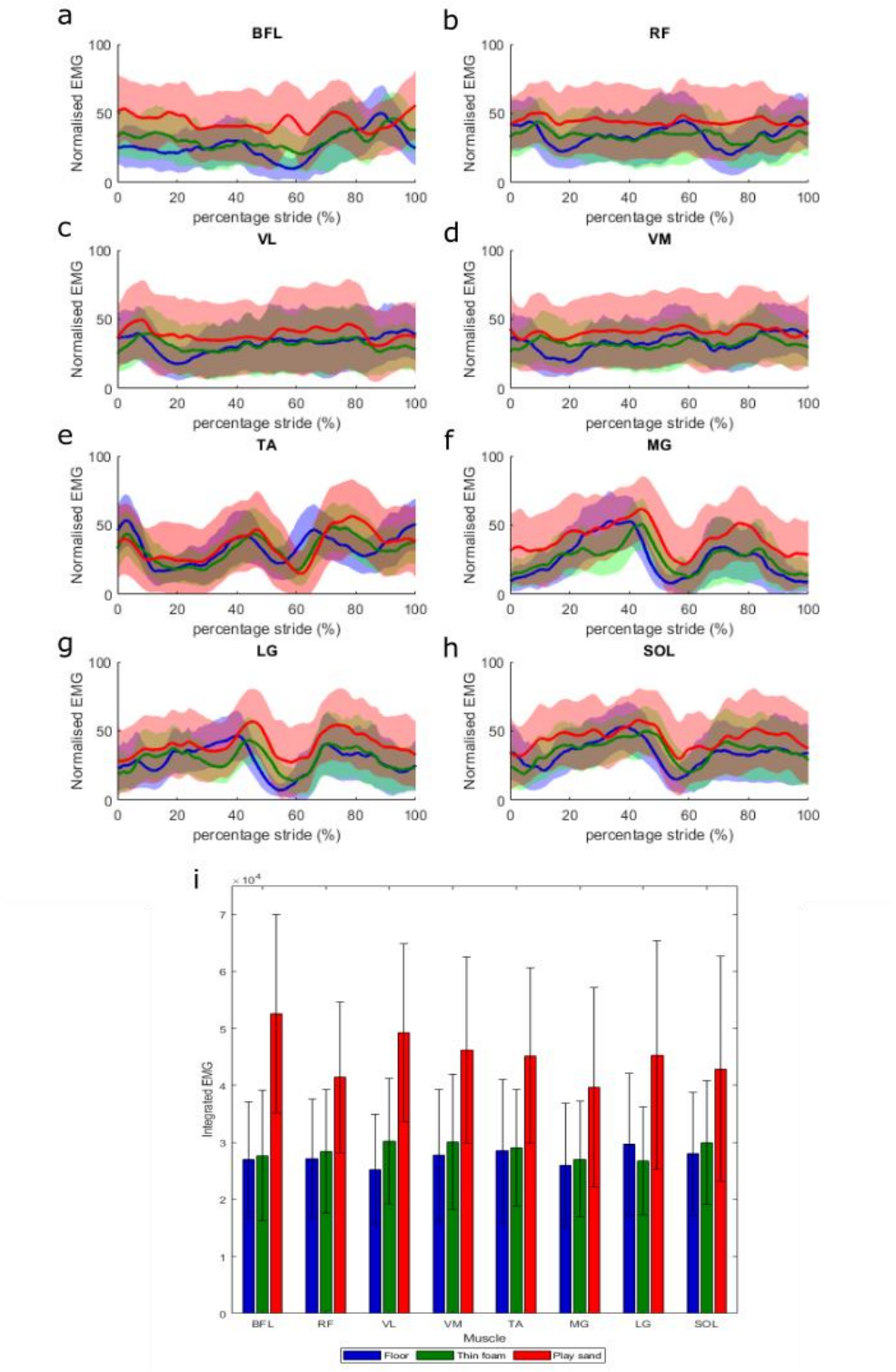

Figure 4.6: EMG values for 8 left lower extremity muscles for participants combined (n=39) while walking on the three different substrates: floor (blue), thin foam (green) and play sand (red). nEMG: ***(a)*** biceps femoris (BFL), ***(b)*** rectus femoris (RF), ***(c)*** vastus lateralis (VL), ***(d)*** vastus medialis (VM), ***(e)*** tibialis anterior (TA), ***(f)*** lateral gastrocnemius (LG), ***(g)*** medial gastrocnemius (MG) and ***(h)*** soleus (SOL) (mean ± s.d.). ***(i)*** iEMG values (mean ± s.d.).

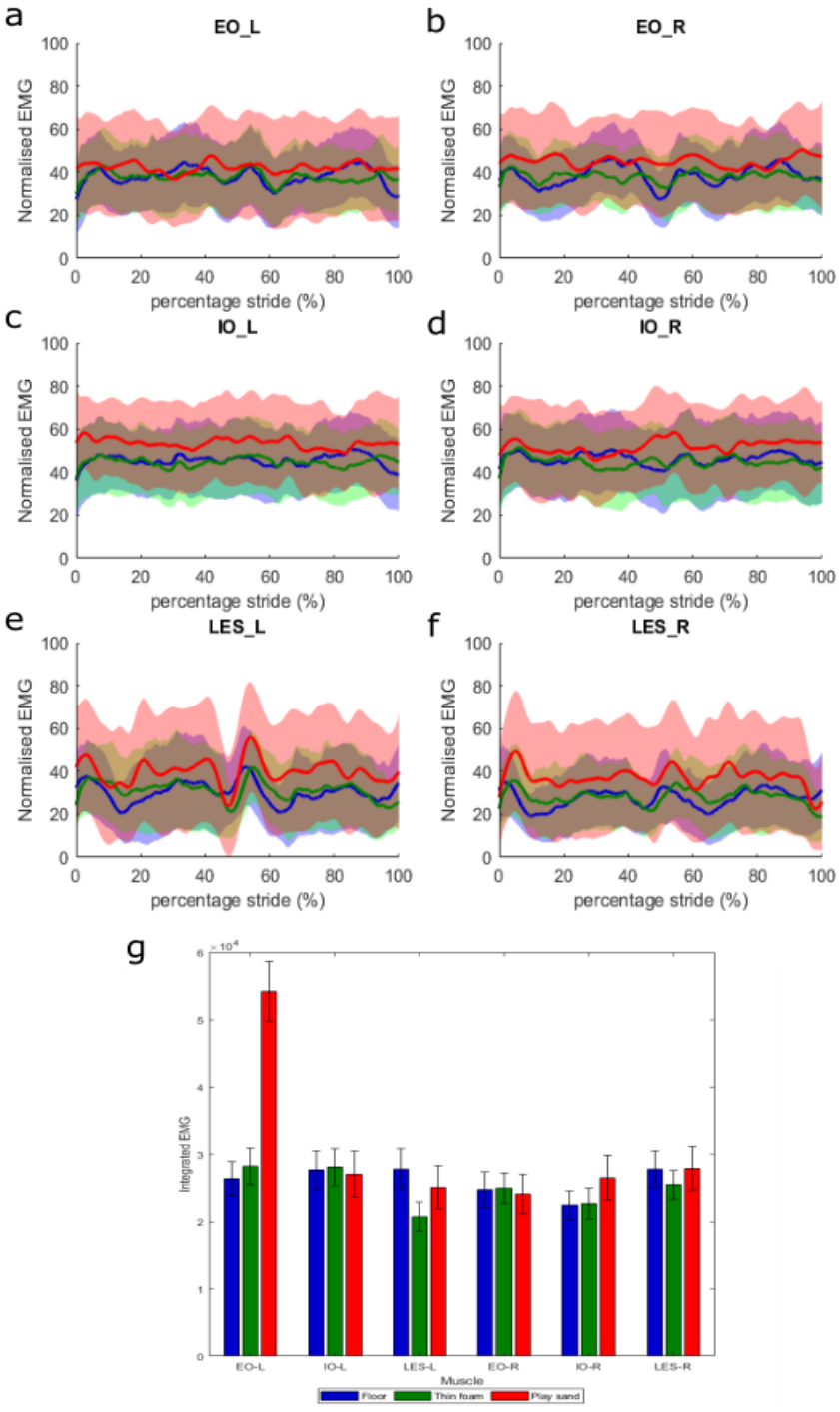

Figure 4.7: EMG values for 6 torso for participants combined (n=39) walking on the three different substrates: floor (blue), thin foam (green) and play sand (red). nEMG: ***(a)*** left external oblique (EO_L), ***(b)*** right external oblique (EO_R), ***(c)*** left internal oblique (IO_L), ***(d)*** right internal oblique (IO_R), ***(e)*** left erector spinae (LES_L), ***(f)*** right erector spinae (LES_R) (mean ± s.d.). ***(g)*** iEMG values (mean ± s.d.).

Abdominal (EO_L, EO_R, IO_L and IO_R) and back muscles (LES_L and LES_R) see similar increases in nEMG as the lower limb muscles, with higher values for all muscles during most of the stride on the sand compared to both floor and foam (Fig. 3.11). For the abdominal muscles, floor and foam values were similar, with some periods of stride being higher on floor and others higher on foam (Fig. 3.10a-d). For the back muscles, floor and foam values were similar, with a slight increase on foam for most of the stride (Fig. 3.10e-f). LES_L were higher on sand for all of the stride except a short period during late-stance, which is highest on floor (Fig. 3.10e) and LES_R is highest on sand for all of the stride except a short period just before heel-strike, which is highest on floor (Fig.3.10f). iEMG values are similar for all substrates for IO_L and EO_R (Fig. 3.10g). For EO_L, iEMG are much higher on sand, and for IO_R, iEMG are slightly higher on sand. LES_L and LES_R is lowest on foam, with a slightly higher values on floor and sand for LES_R. For LES_L, iEMG values are higher on sand compared to foam (Fig. 3.10g).

LMMs on the two compliant substrates for the iEMG values show that there were significant ($p<0.001$) effects of substrate for RF, VM, SOL, LES_R, EO_R and ($p<0.05$) for EO_L and IO_L (Tables 4.8 - 4.11). There was no significant ($p>0.05$) effect of substrate for BFL, VL, TA, MG, LG, LES_L and IO_R. Gender had a significant ($p<0.001$) effect for BFL, VM, SOL, EO_L, LES_R, EO_R and ($p<0.01$) for RF and TA (Tables 4.8- 4.11). There were also significant ($p<0.001$) interaction effects between gender and substrate for VM, TA, SOL, LES_R, EO_R and ($p<0.05$) for BFL, RF, VL and EO_L. Speed had a significant ($p<0.001$) effect for RF, VM, SOL, EO_L, IO_L and ($p<0.05$) for LG, EO_R and IO_R (Tables 4.8 - 4.11). There were also significant ($p\leq0.001$) interaction effects between speed and substrate for RF, VM, SOL, EO_L, LES_R, EO_R and ($p<0.01$) for IO_L. There were significant ($p\leq0.001$) interaction effects between speed and gender for BFL, RF, VM, TA, SOL, EO_L, LES_R, EO_R and ($p<0.01$) for LES_L and for the same muscles there were also significant ($p<0.05$) interaction effects between speed, gender and substrate. There were significant ($p<0.05$) intercepts for all muscles except RF and TA (Tables 4.8 - 4.11).

Table 4.8: The results of the linear mixed-effect models on the integrated EMG data for the muscles BFL, RF, VL and VM; fixed effects = substrate, speed and gender and random effects = subjects. Statistical significance is set as $p<0.05$ with significant p-values shown in bold. σ^2 = random effect variance, τ_{00} = subject variance, intraclass correlation coefficient (ICC) = proportion of variance explained by random effects, N = number of subjects, observations = number of data points (strides), marginal R^2 = proportion of variance explained by the fixed factors, conditional R^2 = proportion of variance explained by both the fixed and random factors.

	BFL			**RF**			**VL**			**VM**		
Predictors	*Estimates*	*CI*	*p*	*Estimates*	*CI*	*p*	*Estimates*	*CI*	*p*	*Estimates*	*CI*	*p*
(Intercept)	29059.92	11877.49 – 46242.34	**0.001**	-19799.96	-40161.83 – 561.91	0.057	50494.68	23251.77 – 77737.59	**<0.001**	111547.47	85750.30 – 137344.65	**<0.001**
Substrate [Thin]	-6208.83	-23640.44 – 11222.79	0.485	65605.26	44369.75 – 86840.76	**<0.001**	2589.21	-25346.12 – 30524.54	0.856	-86342.14	-113212.04 – -59472.24	**<0.001**
Gender [M]	-49255.67	-72521.81 – -25989.53	**<0.001**	39448.20	12122.82 – 66773.59	**0.005**	28527.29	-8216.38 – 65270.96	0.128	-114321.42	-149249.55 – -79393.28	**<0.001**
Speed	13201.93	-404.19 – 26808.06	0.057	53963.54	37829.52 – 70097.56	**<0.001**	-13692.98	-35243.54 – 7857.58	0.213	-55333.94	-76295.90 – -34371.99	**<0.001**
Substrate [Thin] * Gender [M]	34414.13	9158.91 – 59669.34	**0.008**	-45421.90	-75226.58 – -15617.22	**0.003**	-49896.61	-89569.63 – -10223.59	**0.014**	130717.10	92140.46 – 169293.74	**<0.001**
Substrate [Thin] * Speed	-2233.40	-16032.00 – 11565.20	0.751	-50415.35	-67033.70 – -33797.00	**<0.001**	11203.54	-10796.24 – 33203.31	0.318	67604.15	46279.22 – 88929.09	**<0.001**
Gender [M] * Speed	37945.52	19912.72 – 55978.33	**<0.001**	-36086.59	-57332.16 – -14841.03	**0.001**	-21277.64	-49752.23 – 7196.96	0.143	85919.67	58015.57 – 113823.76	**<0.001**
(Substrate [Thin] * Gender [M]) * Speed	-32420.16	-52077.74 – -12762.58	**0.001**	25014.50	1893.40 – 48135.61	**0.034**	19998.34	-10873.22 – 50869.90	0.204	-104008.34	-134154.51 – -73862.16	**<0.001**
Random Effects												
σ^2	28348193.62			38717048.10			70168544.32			69433013.21		
τ_{00}	111706182.78 $_{Subject}$			135969689.64 $_{Subject}$			273566241.76 $_{Subject}$			98650449.41 $_{Subject}$		
ICC	0.80			0.78			0.80			0.59		
N	35 $_{Subject}$			35 $_{Subject}$			35 $_{Subject}$			35 $_{Subject}$		
Observations	1063			1074			1078			1078		
Marginal R^2 / Conditional R^2	0.174 / 0.833			0.358 / 0.858			0.249 / 0.847			0.138 / 0.644		

Table 4.9: The results of the linear mixed-effect models on the integrated EMG data for the muscles TA, MG, LG and SOL; fixed effects = substrate, speed and gender and random effects = subjects. Statistical significance is set as $p<0.05$ with significant p-values shown in bold. σ^2 = random effect variance, τ_{00} = subject variance, intraclass correlation coefficient (ICC) = proportion of variance explained by random effects, N = number of subjects, observations = number of data points (strides), marginal R^2 = proportion of variance explained by the fixed factors, conditional R^2 = proportion of variance explained by both the fixed and random factors.

	TA			**MG**			**LG**			**SOL**		
Predictors	*Estimates*	*CI*	*p*	*Estimates*	*CI*	*p*	*Estimates*	*CI*	*p*	*Estimates*	*CI*	*p*
(Intercept)	15423.12	-7410.98 – 38257.21	0.186	26831.92	10293.09 – 43370.75	**0.001**	19974.12	4125.94 – 35822.31	**0.014**	94309.79	77145.41 – 111474.17	**<0.001**
Substrate [Thin]	17791.70	-6065.25 – 41648.65	0.144	-5695.72	-22616.46 – 11225.02	0.509	-1334.96	-17481.74 – 14811.82	0.871	-69144.25	-86412.54 – -51875.96	**<0.001**
Gender [M]	49893.38	18977.22 – 80809.54	**0.002**	-1348.01	-23718.32 – 21022.30	0.906	-471.71	-21916.91 – 20973.49	0.966	-47817.41	-71096.55 – -24538.28	**<0.001**
Speed	15816.41	-2792.64 – 34425.46	0.096	8575.94	-4630.12 – 21782.00	0.203	14921.16	2318.47 – 27523.85	**0.020**	-43359.21	-56838.78 – -29879.65	**<0.001**
Substrate [Thin] * Gender [M]	-69497.55	-103731.46 – -35263.63	**<0.001**	-3259.98	-27520.96 – 21001.00	0.792	-7647.76	-30797.48 – 15501.95	0.517	48648.77	23879.49 – 73418.05	**<0.001**
Substrate [Thin] * Speed	-9233.45	-28182.48 – 9715.59	0.340	2135.83	-11264.07 – 15535.73	0.755	-91.02	-12875.02 – 12692.99	0.989	59658.30	45992.88 – 73323.72	**<0.001**
Gender [M] * Speed	-41318.24	-66092.00 – -16544.48	**0.001**	910.68	-16599.21 – 18420.57	0.919	1395.69	-15308.88 – 18100.27	0.870	42444.44	24573.63 – 60315.25	**<0.001**
(Substrate [Thin] * Gender [M]) * Speed	48839.31	22073.77 – 75604.85	**<0.001**	-3094.34	-22022.96 – 15834.28	0.749	-3174.99	-21233.64 – 14883.67	0.730	-52844.51	-72161.24 – -33527.77	**<0.001**
Random Effects												
σ^2	55262752.98			26843282.85			24377707.99			27727810.53		
τ_{00}	64392638.29 $_{\text{Subject}}$			83020952.05 $_{\text{Subject}}$			85518251.84 $_{\text{Subject}}$			133245092.77 $_{\text{Subject}}$		
ICC	0.54			0.76			0.78			0.83		
N	35 $_{\text{Subject}}$			35 $_{\text{Subject}}$			35 $_{\text{Subject}}$			35 $_{\text{Subject}}$		
Observations	1080			1080			1080			1078		
Marginal R^2 / Conditional R^2	0.152 / 0.608			0.127 / 0.787			0.201 / 0.823			0.203 / 0.863		

Table 4.10: The results of the linear mixed-effect models on the integrated EMG data for the muscles LES_L, EO_L, IO_L; fixed effects = substrate, speed and gender and random effects = subjects. Statistical significance is set as $p<0.05$ with significant p-values shown in bold. σ^2 = random effect variance, τ_{00} = subject variance, intraclass correlation coefficient (ICC) = proportion of variance explained by random effects, N = number of subjects, observations = number of data points (strides), marginal R^2 = proportion of variance explained by the fixed factors, conditional R^2 = proportion of variance explained by both the fixed and random factors.

	LES_L			**EO_L**			**IO_L**		
Predictors	*Estimates*	*CI*	*p*	*Estimates*	*CI*	*p*	*Estimates*	*CI*	*p*
(Intercept)	29823.93	6900.53 – 52747.34	**0.011**	80980.57	59903.55 – 102057.60	**<0.001**	23457.05	6426.00 – 40488.10	**0.007**
Substrate [Thin]	327.41	-22563.10 – 23217.91	0.978	-33658.86	-55191.32 – -12126.39	**0.002**	21759.95	4390.27 – 39129.63	**0.014**
Gender [M]	-26430.00	-57676.08 – 4816.08	0.097	-61181.66	-89673.01 – -32690.32	**<0.001**	-4870.36	-27913.61 – 18172.88	0.679
Speed	-1434.71	-19303.78 – 16434.36	0.875	-35182.97	-51967.14 – -18398.80	**<0.001**	25715.30	12158.30 – 39272.30	**<0.001**
Substrate [Thin] * Gender [M]	-2325.26	-35231.93 – 30581.41	0.890	41322.15	9900.88 – 72743.42	**0.010**	-10981.59	-35884.96 – 13921.78	0.387
Substrate [Thin] * Speed	16665.22	-1446.03 – 34776.47	0.071	37687.45	20647.13 – 54727.76	**<0.001**	-18850.68	-32603.62 – -5097.73	**0.007**
Gender [M] * Speed	31468.94	7706.86 – 55231.03	**0.009**	54815.62	32562.37 – 77068.86	**<0.001**	5051.27	-12919.51 – 23022.06	0.582
(Substrate [Thin] * Gender [M]) * Speed	-25646.64	-51312.35 – 19.07	0.050	-49133.78	-73552.07 – -24715.49	**<0.001**	-123.11	-19550.48 – 19304.25	0.990
Random Effects									
σ^2	48617833.64			43277860.73			28227315.28		
τ_{00}	272051258.36 $_{Subject}$			138657506.70 $_{Subject}$			96126528.86 $_{Subject}$		
ICC	0.85			0.76			0.77		
N	34 $_{Subject}$			34 $_{Subject}$			35 $_{Subject}$		
Observations	1070			1022			1080		
Marginal R^2 / Conditional R^2	0.247 / 0.886			0.157 / 0.799			0.151 / 0.807		

Table 4.11: The results of the linear mixed-effect models on the integrated EMG data for the muscles LES_R, EO_R, IO_R; fixed effects = substrate, speed and gender and random effects = subjects. Statistical significance is set as $p<0.05$ with significant p-values shown in bold. σ^2 = random effect variance, τ_{00} = subject variance, intraclass correlation coefficient (ICC) = proportion of variance explained by random effects, N = number of subjects, observations = number of data points (strides), marginal R^2 = proportion of variance explained by the fixed factors, conditional R^2 = proportion of variance explained by both the fixed and random factors.

	LES_R			**EO_R**			**IO_R**		
Predictors	*Estimates*	*CI*	*p*	*Estimates*	*CI*	*p*	*Estimates*	*CI*	*p*
(Intercept)	52354.08	32786.91 – 71921.24	**<0.001**	69627.37	51091.26 – 88163.48	**<0.001**	31711.12	14228.26 – 49193.99	**<0.001**
Substrate [Thin]	-38782.00	-58681.28 – -18882.73	**<0.001**	-47009.89	-66092.97 – -27926.81	**<0.001**	3792.99	-13487.33 – 21073.31	0.667
Gender [M]	-124050.35	-150641.09 – -97459.61	**<0.001**	-99387.25	-124544.31 – -74230.19	**<0.001**	-4428.30	-28303.62 – 19447.02	0.716
Speed	-9808.44	-25340.29 – 5723.42	0.216	-22401.57	-37293.70 – -7509.43	**0.003**	16971.82	3481.61 – 30462.03	**0.014**
Substrate [Thin] * Gender [M]	121974.02	93360.30 – 150587.73	**<0.001**	124300.43	96851.00 – 151749.86	**<0.001**	-10106.52	-34946.11 – 14733.08	0.425
Substrate [Thin] * Speed	26905.79	11152.18 – 42659.40	**0.001**	39207.34	24087.90 – 54326.78	**<0.001**	-3115.94	-16785.77 – 10553.89	0.655
Gender [M] * Speed	96965.86	76292.63 – 117639.08	**<0.001**	82884.75	63037.65 – 102731.86	**<0.001**	3315.14	-14618.57 – 21248.84	0.717
(Substrate [Thin] * Gender [M]) * Speed	-101608.51	-123935.63 – -79281.38	**<0.001**	-101714.97	-123146.52 – -80283.42	**<0.001**	1457.02	-17913.99 – 20828.02	0.883
Random Effects									
σ^2	36987339.04			34331085.17			27646839.48		
τ_{00}	136602149.95 $_{Subject}$			85284559.80 $_{Subject}$			185249033.09 $_{Subject}$		
ICC	0.79			0.71			0.87		
N	34 $_{Subject}$			34 $_{Subject}$			34 $_{Subject}$		
Observations	1070			1070			1070		
Marginal R^2 / Conditional R^2	0.148 / 0.818			0.063 / 0.731			0.073 / 0.880		

4.5 Discussion

4.5.1 Overview

Humans are regularly required to navigate a variety of surfaces with different mechanical properties that require gait adjustments to maintain stability and efficiency. It is generally accepted that energy expenditure will increase during locomotion on more compliant substrates and that substrate compliance affects gait kinematics, muscle activation and spatiotemporal variables. However, it is unclear whether humans use similar gait adaptations on compliant substrates with different properties. The purpose of this study was to improve our understanding of the relationship between substrate properties, human biomechanics and muscle activities. This was done by comparing three different substrates, including both artificial and natural compliant substrates: 1) hard, level floor 2) polyurethane foam and 3) play sand. Our results show that there are similar overall gait adaptations on the two compliant substrates compared to the floor such as greater hip and knee flexion, increased range of motion at the ankle joint, and changes to spatiotemporal variables such as increased cycle time. However, there are also notable differences for several measured variables. These include reduced knee flexion, greater ankle dorsiflexion, decreased speed and increased muscle activity during walking on sand, compared to foam. At the beginning of this chapter, five hypotheses were proposed and these will be addressed in this section.

4.5.2 Energy-conserving mechanisms on different compliant substrates

In human walking, there are two fundamental concepts for energy-conserving mechanisms. The first is an efficient transfer of potential and kinetic energies in a pendulum-like mechanism and the second is the storage and recovery of mechanical energy in the elastic structures of the musculoskeletal system (Cavagna, Heglund & Taylor 1977). During level walking, the kinetic (E_{kin}) and gravitational potential (E_{pot}) energies of the centre of mass of the body (CoM) are largely out of phase and of similar magnitude, which allows an exchange

between these two energies. The recovery of total energy exchange percentage (R) has been calculated to be optimally up to 70% during level walking (Cavagna, Thys & Zamboni 1976; Dewolf et al. 2017). Zamparo (1992) attributed the increases in energetic costs during walking on sand to the failure of the pendular mechanism. The authors inputted their measured metabolic cost values into calculations proposed by Cavagna et al. (1976) to estimate %R as 43-48% during walking on sand. However, another study by Lejeune et al. (1998) calculated %R as high as 60% during walking on sand. Their calculations were more direct as they placed force platforms under sand to compute the CoM mechanical energy using calculations by Cavagna (1975). Although Lejeune et al. (1998) calculated a slight reduction in the efficiency of the pendular energy exchange mechanism compared to walking on level floor, 60% R is a relatively large conservation of energy. The first hypothesis stated that there will be reduced efficiency in the pendular energy exchange mechanism when walking on sand compared to foam. This hypothesis is not supported by the present data as our results show that %R remains relatively high on the sand, with ~60% R (Fig. 4.3-4.4), similar to values found by Lejeune et al. (1998). LMMs showed there was a significant ($p<0.05$) effect of substrate for relative amplitude (RA) and congruity (CO; the time when potential and kinetic energy are moving in the same direction) (Table 4.5). %CO was calculated as 12.2±4.4 on foam and 14.4±5.6 on sand (mean ± s.d.) (Figs. 4.3-4.4), meaning CoM was out of phase slightly more on foam compared to sand, which translated to slightly higher %R on foam with %R calculated as 60.9±3.5 on foam and 59.5±4.4 on sand (mean ± s.d) but the effect of substrate on R was found to be insignificant ($p>0.05$) (Table 4.5). Walking speed has been shown to have an effect of %R with maximum ~65% R found at speeds of 1.39ms^{-1} with decreases in %R at higher or lower speeds (Dewolf et al. 2017). This study found average walking speeds of 1.37 ± 0.16 ms^{-1} on foam and 1.22 ± 0.11 ms^{-1} on sand (mean±s.d.) (Fig. 4.2) and LMMs found significant ($p\leq0.001$) effects of speed for all variables (Table 4.5). Therefore, the small differences between the two compliant substrates are likely due to differences in walking speed rather than the substrate itself. However, human walking on compliant substrates such as sand and foam both maintain a relatively efficient pendular energy exchange mechanism and thus, the energetic cost increases found on these substrates are very likely due to other causes.

The second energy-conserving mechanism is the storage and recovery of elastic energy. During ground contact, energy is transferred from the individual into the surface through the

foot and as the foot leaves the surface, some of this energy can be returned to the individual (McMahon & Greene 1979). The maximisation of energy return has driven research on the development of sports surfaces and footwear (Baroud, Nigg & Stefanyshyn 1999; Hoogkamer et al. 2018; McMahon & Greene 1979). Energy storage is a function of surface stiffness and surface deformation; the more compliant a surface is, the larger the deformation and the greater the energy stored (Stefanyshyn & Nigg 2003). However, some energy will be lost to the substrate and the magnitude of energy dissipation will vary depending on substrate properties. The polyurethane foam used in this study exhibits elastic behaviour under deformation (chapter 2.4.3; Fig. 2.14). This means that when loading has been removed, it will return to its original shape and provide at least some energy return to the subject (Mane et al. 2017). On the other hand, sand exhibits plastic deformation during loading with increased energy lost to the substrate and therefore, the potential energy return to the subject is decreased (Allen 1997). Although potential elastic energy recovery has been associated most strongly with the ankle, it can also occur at the knee and hip (Doke & Kuo 2007; Sawicki, Lewis & Ferris 2009). Our results show that there was increased muscle activity (nEMG) in the quadriceps muscle group, RF (Fig. 4.6b), VL (Fig. 4.6c), VM (Fig.4.6d) and the one hamstring muscle measured in this study, BFL (Fig. 4.6a) during stance phase, with a notable increase during the propulsive phase just before push-off on sand. Furthermore, the triceps surae muscle group (calf muscles), MG (Fig. 4.6f), LG (Fig. 4.6g) and SOL (Fig. 4.6h) have increased nEMG during the propulsive phase of the stride on sand. These increases in muscle activation may be required to power push-off due to a reduction in the elastic energy recovery when walking on sand, although this cannot be tested directly with the current data. Furthermore, it has been shown that during running and hopping on compliant substrates, humans adjust leg stiffness to accommodate reductions in surface stiffness (Ferris, Liang & Farley 1999; Ferris, Louie & Farley 1998). Leg stiffness adjustments allow ground contact time and the vertical displacement of the CoM to remain similar on surfaces with different stiffness. The greater hip and knee flexion observed at heel-strike and initial stance followed by greater extension in late stance (Fig. 4.5) in addition to the increase in the gastrocnemius and soleus muscles (Fig. 4.6) could be an indicator for leg stiffness adjustments on compliant substrates.

4.5.3 Gait changes on different compliant substrates

4.5.3.1 Lower limb and trunk kinematics

Previous studies have shown that when walking on more irregular and compliant substrates, subjects will display greater flexion at the hip and knee joint, resulting in greater mechanical work (Gates et al. 2012; Marigold & Patla 2002; Pinnington et al. 2005; Svenningsen, de Zee & Oliveira 2019; Voloshina et al. 2013). Our results in the previous chapters showed that flexion at the hip and knee joint increased as substrate compliance increased, on both foam (Fig. 2.12) and sand (Fig. 3.8) substrates. This is likely a consequence of increased toe-clearance required on compliant substrates. The second hypothesis stated that there will be similar joint excursions at the hip and knee joints on both compliant substrates. This hypothesis is not supported by our presented data. Although, there were increased hip and knee flexion on both foam and sand compared to the hard floor, there were significant ($p<0.001$) increases in knee flexion for most of the stride on foam, and significant ($p<0.05$) increases in hip joint angles for small periods of the stride on foam, most notably during the swing phase (Fig.4.5). However, greater knee and hip flexion and ankle plantarflexion during swing on foam are likely to be the result of a higher walking speed, as shown in previous studies (Hanlon & Anderson 2006; Kirtley, Whittle & Jefferson 1985). Furthermore, they could also be due to the slightly greater foot depression observed on foam than sand (Fig. 4.1). Therefore, hip and knee joint flexion potentially corresponds to the level of depression into a compliant substrate.

Due to the (unpredictable) displacement of the surface below the foot, it is expected that there will be greater instability when walking over sand compared to more uniform-deforming compliant substrates like foam. Zamparo et al. (1992) proposed that foot slippage on sand during push-off contributes to increased energetic costs. Inverse dynamics analyses indicate that healthy young adults tend to be dependent on ankle push-off at the end of stance to power walking with the ankle joint producing 35-45% of the summed hip, knee and ankle positive mechanical work during each stride at average walking speeds on level ground of 1.2–1.5 ms^{-1} (DeVita, Helseth & Hortobagyi 2007; Sawicki & Ferris 2008). The third hypothesis proposed that there will be greater joint excursions at the ankle joint during

walking on sand. Our data mostly supports this hypothesis. There was significantly ($p<0.001$) greater dorsiflexion throughout most of the stance phase on sand and ($p<0.01$) greater dorsiflexion during late-swing (Fig. 4.5a). Although during early-swing, there was greater plantarflexion on foam, this could be mainly due to the slightly deeper foot depressions on foam than sand (Fig. 4.1). The positioning of the ankle in slight dorsiflexion throughout the stance phase on sand may be important to maintain balance and establish the heel as the base of support, similar to that seen during walking on sloped surfaces (McIntosh et al. 2006).

4.5.3.2 Lower limb and trunk muscle activation

Increased range of motion at joints is coupled with increased muscle activation. Previous studies have shown that when walking on more instable surfaces, humans increase muscle co-activation about the ankle and knee joint (Marigold & Patla 2002; McIntosh et al. 2006; Voloshina et al. 2013; Wade et al. 2010). Lejeune et al. (1998) attributed the increase in energetic costs on sand to an increase in mechanical work. The fourth hypothesis stated that during walking on sand, there will be greater muscle activation, primarily those acting at the ankle joint. This hypothesis is supported by the present data. However, there were greater muscle activations (nEMG and iEMG) for all muscles on sand (Figs. 4.6- 3.7), not predominantly those acting at the ankle joint. Greater muscle activation may help stabilise the joints in uncertain conditions, such as sand where the resulting deformation is less predictable to the individual. The increase in nEMG in the calf muscles, TA (Fig. 4.6e), MG (Fig. 4.6f), LG (Fig. 4.6g) and SOL (Fig. 4.6h) during late-stance on sand may be a strategy to maintain stabilisation at the ankle and knee joints as the foot moves on the sand. It may also be a measure to counter the lower ground reaction forces observed on compliant substrates. MacLellan and Patla (2006) saw an increase in the maximum height of the toe trajectory during walking across increasingly compliant foams, and associated increase in plantarflexor activation prior to push-off. On both compliant substrates in this study, there is an increase in nEMG in the measured plantarflexor muscles, MG (Fig. 4.6f), LG (Fig. 4.6g) and SOL (Fig. 4.6h) during late stance and during push-off, although nEMG for these muscles were greater on sand. Greater activation prior and during push-off is required to generate the force needed for the increased plantarflexion (Fig. 4.5a) during early-swing.

Research has shown that the trunk plays an important role in maintaining head stability and modulating gait-related oscillations (Kavanagh, Barrett & Morrison 2006). The increases in nEMG for the abdominal and back muscles on sand (Fig. 4.7) are likely as a response to the increased need for torso stabilisation during walking on a surface with greater instability. Two peaks occur for erector spinae muscle activation during push-off into swing and after initial heel-strike (push-off for contralateral limb) on all substrates (Fig 4.7e-f), hereby controlling the trunk while aiding pelvis and swing leg elevation (Ceccato et al. 2009). On sand, there is greater activation of the erector spinae muscles at these time points, indicating a need for increased spinal stability. There may be a greater need for head stability as spatial and temporal visual information has been shown to be essential for correct foot positioning over complex surfaces (Matthis, Yates & Hayhoe 2018). It is likely that greater muscle activation results in at least some increase in energy expenditure, independent of whether mechanical work increases or not (Cavanagh & Kram 1985).

4.5.3.3 Spatiotemporal variables

When walking on soft or uneven substrates, participants often reduce their walking speed and stride length and increase step frequency and stride width as a strategy to maintain balance on more instable substrates (Donelan et al. 2004; Hak et al. 2012; Pinnington et al. 2005; Voloshina et al. 2013). The fifth hypothesis stated that there will be similar spatiotemporal gait parameters on both compliant substrates. Our data does not support this hypothesis. As expected, there are some similarities between foam and sand compared to hard floor such as a reduced walking speed (Fig. 4.2a) and increased stride length (Fig. 4.2b), cycle time (Fig. 4.2d), stance time (Fig. 4.2e), swing time (Fig. 4.2f) and double-support time (Fig. 4.2g), in agreement with the findings from previous studies on uneven and compliant substrates (Donelan, Kram & Kuo 2002; Gates et al. 2012; Pinnington et al. 2005; Voloshina et al. 2013). However, for most spatiotemporal variables there were notable differences between foam and sand. On sand, there was a decrease in speed (Fig. 4.2a), stride length (Fig. 4.2b), double-support time (Fig. 4.2g) and duty factor (Fig. 4.2h) and an increase in stride width (Fig. 4.2c), cycle time (Fig. 4.2d) and swing time (Fig. 4.2f). LMMs performed on the two

compliant substrates show that there is a significant ($p<0.01$) effect of substrate for cycle time, swing time, double limb support time and speed ($p<0.001$), but no significant ($p>0.05$) effect of substrate for stride length, stride width, stance time and duty factor (Tables 4.2-4.3). However, it is likely that most of the differences are due to the reduction in speed during walking on sand as speed also had a significant ($p<0.001$) effect on stride length, cycle time, stance time, swing time, double limb support time and ($p<0.05$) duty factor (Tables 4.2-4.3). It is possible that subjects adopted a reduced walking speed on sand due to the feeling of greater instability of the surface. However, the coefficient of variation (CV) for most spatiotemporal variables were similar between substrates with little consistency; some variables increased in CV on sand while other variables decreased in CV on sand (Table 4.4). There could also be greater deceleration during stance on sand as the foot sinks, contributing to the increased muscle activation on sand during the propulsive phase (Fig. 4.6).

4.5.4. Participant variability and gender effects

There were significant ($p<0.05$) gender effects found for many of the variables measured in this study; cycle time (Table 4.2), swing time (Table 4.3), CO (Table 4.5), hip and ankle joint angle at heel-strike (Table 4.6), hip and knee joint angle at toe-off (Table 4.7) and iEMG values (Tables 4.8-4.11). There were also significant interaction effects between gender and substrate and gender and speed for many of these variables. For example, females displayed greater hip flexion and ankle plantarflexion at heel-strike (Table 4.6) and slightly slower walking speeds (Table 4.2), in agreement with previous studies (Bruening et al. 2020; Chumanov, Wall-Scheffler & Heiderscheit 2008; Kerrigan, Todd & Della Croce 1998). However, it has previously been shown that CoT does not vary between males and females (Weyand et al. 2010) and we found no significant ($p>0.05$) differences in CoT for gender in chapter 2.4.1 (Fig. 2.8), although there was more variability in CoT for females than males. Furthermore, there was no statistically significant relationship between CoT and various morphological variables that are likely to have gender biases such as lower limb length and body stature (Charles et al. 2021). Moreover, the effects of substrate are the same e.g. there is greater hip flexion on compliant substrates regardless of gender. Therefore, gender differences have not been discussed in detail as it is not the main purpose of our study,

although gender effects could be one contributor to the large participant variability observed in some variables. Participant variability increases when walking over more complex, uneven or compliant substrates (Donelan, Kram & Kuo 2002; MacLellan & Patla 2006; Marigold & Patla 2002). In this study, we observed large participant variability in the muscle activities recorded, especially on sand (Fig. 4.6-4.7). Participant variability is also reflected in the large differences between marginal R^2 (proportion of variance explained by the fixed factors) and conditional R^2 (proportion of variance explained by both the fixed and random effects) in the LMMs. However, influences of participant, gender and speed have been included in the statistical models to analyse substrate effects. Investigating gender differences and intra- and inter-participant differences when walking over different compliant substrates may be an interesting and useful future area of research.

4.5.5 Conclusions

The overall findings of this study indicate that there are some important similarities in general gait adaptations when walking over different compliant substrates such as foam and sand compared to hard, level floor. Gait changes include increased flexion at the hip and knee joint, an increased range of motion at the ankle joint and changes to spatiotemporal variables such as lower walking speeds and increased cycle time, stance time, swing time and double-support time. Combined, all of these adaptations resulted in higher muscle activities, potentially leading to greater mechanical work. Furthermore, on both compliant foams, participants retain a relatively efficient pendular energy mechanism. However, there are some differences between the compliant substrates tested in this study. During walking on sand, there was reduced knee flexion, greater ankle dorsiflexion, increased muscle activation and the adoption of gait stability measures such as a slower walking speed. Changes to lower limb motion and muscle activations are probably due to the unpredictable nature of sand displacement and could also indicate reduced elastic energy storage and/or recovery on sand. Therefore, compliant substrates have a large impact on human locomotion. Also, more research is required to explore gait adaptations on compliant substrates with different material and mechanical properties.

4.6 References

Allen, J.R.L. (1997) 'Subfossil mammalian tracks (Flandrian) in the Severn Estuary, S. W. Britain: mechanics of formation, preservation and distribution', *Philosophical Transactions of the Royal Society of London. Series B: Biological Sciences*, vol. 352, no. 1352, pp. 481-518.

Baroud, G., Nigg, B. & Stefanyshyn, D. (1999) 'Energy storage and return in sport surfaces', *Sports Engineering*, vol. 2, no. 3, pp. 173-180.

Barrett, R.S., Neal, R.J. & Roberts, L.J. (1998) 'The dynamic loading response of surfaces encountered in beach running', *Journal of Science and Medicine in Sport*, vol. 1, no. 1, pp. 1-11.

Bates, D., Mächler, M., Bolker, B. & Walker, S. (2014) 'Fitting linear mixed-effects models using lme4', *arXiv preprint arXiv:1406.5823*.

Bruening, D.A., Baird, A.R., Weaver, K.J. & Rasmussen, A.T. (2020) 'Whole body kinematic sex differences persist across non-dimensional gait speeds', *PLOS ONE*, vol. 15, no. 8, p. e0237449.

Cavagna, G.A. (1975) 'Force platforms as ergometers', *J Appl Physiol*, vol. 39, no. 1, pp. 174-179.

Cavagna, G.A., Heglund, N.C. & Taylor, C.R. (1977) 'Mechanical work in terrestrial locomotion: two basic mechanisms for minimizing energy expenditure', *American Journal of Physiology-Regulatory, Integrative and Comparative Physiology*, vol. 233, no. 5, pp. R243-R261.

Cavagna, G.A., Thys, H. & Zamboni, A. (1976) 'The sources of external work in level walking and running', *J Physiol*, vol. 262, no. 3, pp. 639-657.

Cavanagh, P.R. & Kram, R. (1985) 'The efficiency of human movement--a statement of the problem', *Med Sci Sports Exerc*, vol. 17, no. 3, pp. 304-308.

Ceccato, J.-C., de Sèze, M., Azevedo, C. & Cazalets, J.-R. (2009) 'Comparison of Trunk Activity during Gait Initiation and Walking in Humans', *PLOS ONE*, vol. 4, no. 12, p. e8193.

Charles, J.P., Grant, B., D'Août, K. & Bates, K.T. (2021) 'Foot anatomy, walking energetics, and the evolution of human bipedalism', *Journal of Human Evolution*, vol. 156, p. 103014.

Chumanov, E.S., Wall-Scheffler, C. & Heiderscheit, B.C. (2008) 'Gender differences in walking and running on level and inclined surfaces', *Clinical Biomechanics*, vol. 23, no. 10, pp. 1260-1268.

Davies, S.E.H. & Mackinnon, S.N. (2006) 'The energetics of walking on sand and grass at various speeds', *Ergonomics*, vol. 49, no. 7, pp. 651-660.

DeVita, P., Helseth, J. & Hortobagyi, T. (2007) 'Muscles do more positive than negative work in human locomotion', *J Exp Biol*, vol. 210, no. Pt 19, pp. 3361-3373.

Dewolf, A.H., Ivanenko, Y.P., Lacquaniti, F. & Willems, P.A. (2017) 'Pendular energy transduction within the step during human walking on slopes at different speeds', *PLOS ONE*, vol. 12, no. 10, p. e0186963.

Doke, J. & Kuo, A.D. (2007) 'Energetic cost of producing cyclic muscle force, rather than work, to swing the human leg', *Journal of Experimental Biology*, vol. 210, no. 13, pp. 2390-2398.

Donelan, J.M., Kram, R. & Kuo, A.D. (2002) 'Mechanical work for step-to-step transitions is a major determinant of the metabolic cost of human walking', *Journal of Experimental Biology*, vol. 205, no. 23, pp. 3717-3727.

Donelan, J.M., Shipman, D.W., Kram, R. & Kuo, A.D. (2004) 'Mechanical and metabolic requirements for active lateral stabilization in human walking', *Journal of Biomechanics*, vol. 37, no. 6, pp. 827-835.
Ferris, D.P. & Farley, C.T. (1997) 'Interaction of leg stiffness and surface stiffness during human hopping', *Journal of Applied Physiology*, vol. 82, no. 1, pp. 15-22.
Ferris, D.P., Liang, K. & Farley, C.T. (1999) 'Runners adjust leg stiffness for their first step on a new running surface', *Journal of Biomechanics*, vol. 32, no. 8, pp. 787-794.
Ferris, D.P., Louie, M. & Farley, C.T. (1998) 'Running in the real world: adjusting leg stiffness for different surfaces', *Proc Biol Sci*, vol. 265, no. 1400, pp. 989-994.
Gates, D.H., Wilken, J.M., Scott, S.J., Sinitski, E.H. & Dingwell, J.B. (2012) 'Kinematic strategies for walking across a destabilizing rock surface', *Gait & Posture*, vol. 35, no. 1, pp. 36-42.
Giatsis, G., Kollias, I., Panoutsakopoulos, V. & Papaiakovou, G. (2004) 'Biomechanical differences in elite beach-volleyball players in vertical squat jump on rigid and sand surface', *Sports Biomech*, vol. 3, no. 1, pp. 145-158.
Gibson, L.J. & Ashby, M.F. (1997) *Cellular Solids: Structure and Properties*, 2 edn, Cambridge University Press, Cambridge.
Hak, L., Houdijk, H., Steenbrink, F., Mert, A., van der Wurff, P., Beek, P.J. & van Dieën, J.H. (2012) 'Speeding up or slowing down?: Gait adaptations to preserve gait stability in response to balance perturbations', *Gait & Posture*, vol. 36, no. 2, pp. 260-264.
Hanlon, M. & Anderson, R. (2006) 'Prediction methods to account for the effect of gait speed on lower limb angular kinematics', *Gait & Posture*, vol. 24, no. 3, pp. 280-287.
Hoogkamer, W., Kipp, S., Frank, J.H., Farina, E.M., Luo, G. & Kram, R. (2018) 'A Comparison of the Energetic Cost of Running in Marathon Racing Shoes', *Sports Medicine*, vol. 48, no. 4, pp. 1009-1019.
Impellizzeri, F.M., Rampinini, E., Castagna, C., Martino, F., Fiorini, S. & Wisloff, U. (2008) 'Effect of plyometric training on sand versus grass on muscle soreness and jumping and sprinting ability in soccer players', *British Journal of Sports Medicine*, vol. 42, no. 1, pp. 42-46.
Kavanagh, J., Barrett, R. & Morrison, S. (2006) 'The role of the neck and trunk in facilitating head stability during walking', *Exp Brain Res*, vol. 172, no. 4, pp. 454-463.
Kerdok, A.E., Biewener, A.A., McMahon, T.A., Weyand, P.G. & Herr, H.M. (2002) 'Energetics and mechanics of human running on surfaces of different stiffnesses', *Journal of Applied Physiology*, vol. 92, no. 2, pp. 469-478.
Kerrigan, D.C., Todd, M.K. & Della Croce, U. (1998) 'Gender differences in joint biomechanics during walking: normative study in young adults', *Am J Phys Med Rehabil*, vol. 77, no. 1, pp. 2-7.
Kirtley, C., Whittle, M.W. & Jefferson, R.J. (1985) 'Influence of walking speed on gait parameters', *Journal of Biomedical Engineering*, vol. 7, no. 4, pp. 282-288.
Kunzetsova, A., Brockhoff, P. & Christensen, R. (2017) 'lmerTest package: Tests in linear mixed effect models', *J Stat Softw*, vol. 82, pp. 1-26.
Lejeune, T.M., Willems, P.A. & Heglund, N.C. (1998) 'Mechanics and energetics of human locomotion on sand', *Journal of Experimental Biology*, vol. 201, no. 13, pp. 2071-2080.
MacLellan, M.J. & Patla, A.E. (2006) 'Adaptations of walking pattern on a compliant surface to regulate dynamic stability', *Experimental Brain Research*, vol. 173, no. 3, pp. 521-530.
Mane, J.V., Chandra, S., Sharma, S., Ali, H., Chavan, V.M., Manjunath, B.S. & Patel, R.J. (2017) 'Mechanical Property Evaluation of Polyurethane Foam under Quasi-static and

Dynamic Strain Rates- An Experimental Study', *Procedia Engineering*, vol. 173, pp. 726-731.
Marigold, D.S. & Patla, A.E. (2002) 'Strategies for Dynamic Stability During Locomotion on a Slippery Surface: Effects of Prior Experience and Knowledge', *Journal of Neurophysiology*, vol. 88, no. 1, pp. 339-353.
Matthis, J.S., Yates, J.L. & Hayhoe, M.M. (2018) 'Gaze and the Control of Foot Placement When Walking in Natural Terrain', *Curr Biol*, vol. 28, no. 8, pp. 1224-1233.e1225.
McIntosh, A.S., Beatty, K.T., Dwan, L.N. & Vickers, D.R. (2006) 'Gait dynamics on an inclined walkway', *J Biomech*, vol. 39, no. 13, pp. 2491-2502.
McMahon, T.A. & Greene, P.R. (1979) 'The influence of track compliance on running', *J Biomech*, vol. 12, no. 12, pp. 893-904.
Nigg, B.M. (2007) *Biomechanics of the musculo-skeletal system*, John Wiley & Sons Incorporated.
Pataky, T.C., Robinson, M.A. & Vanrenterghem, J. (2013) 'Vector field statistical analysis of kinematic and force trajectories', *Journal of Biomechanics*, vol. 46, no. 14, pp. 2394-2401.
Peyré-Tartaruga, L.A. & Coertjens, M. (2018) 'Locomotion as a Powerful Model to Study Integrative Physiology: Efficiency, Economy, and Power Relationship', *Front Physiol*, vol. 9, p. 1789.
Pinnington, H.C. & Dawson, B. (2001) 'The energy cost of running on grass compared to soft dry beach sand', *Journal of Science and Medicine in Sport*, vol. 4, no. 4, pp. 416-430.
Pinnington, H.C., Lloyd, D.G., Besier, T.F. & Dawson, B. (2005) 'Kinematic and electromyography analysis of submaximal differences running on a firm surface compared with soft, dry sand', *Eur J Appl Physiol*, vol. 94, no. 3, pp. 242-253.
Psarras, A., Mertyri, D. & Tsaklis, P. (2016) 'Biomechanical analysis of ankle during the stance phase of gait on various surfaces: a literature review', *Human Movement*, vol. 17, no. 3, pp. 140-147.
Sawicki, G.S. & Ferris, D.P. (2008) 'Mechanics and energetics of level walking with powered ankle exoskeletons', *J Exp Biol*, vol. 211, no. Pt 9, pp. 1402-1413.
Sawicki, G.S., Lewis, C.L. & Ferris, D.P. (2009) 'It pays to have a spring in your step', *Exerc Sport Sci Rev*, vol. 37, no. 3, pp. 130-138.
Stefanyshyn, D.J. & Nigg, B.M. (2003) 'Energy and performance aspects in sports surfaces', *Sports Biomech*, pp. 31-46.
Svenningsen, F.P., de Zee, M. & Oliveira, A.S. (2019) 'The effect of shoe and floor characteristics on walking kinematics', *Human Movement Science*, vol. 66, pp. 63-72.
Team, R.C. 'R: A language and environment for statistical computing'.
Voloshina, A.S., Kuo, A.D., Daley, M.A. & Ferris, D.P. (2013) 'Biomechanics and energetics of walking on uneven terrain', *Journal of Experimental Biology*, vol. 216, no. 21, pp. 3963-3970.
Wade, C., Redfern, M.S., Andres, R.O. & Breloff, S.P. (2010) 'Joint kinetics and muscle activity while walking on ballast', *Human Factors*, vol. 52, no. 5, pp. 560-573.
Weyand, P.G., Smith, B.R., Puyau, M.R. & Butte, N.F. (2010) 'The mass-specific energy cost of human walking is set by stature', *Journal of Experimental Biology*, vol. 213, no. 23, pp. 3972-3979.
Zamparo, P., Perini, R., Orizio, C., Sacher, M. & Ferretti, G. (1992) 'The energy cost of walking or running on sand', *European Journal of Applied Physiology and Occupational Physiology*, vol. 65, no. 2, pp. 183-187.

Chapter five: General Discussion

This chapter provides a general discussion of the findings presented in this thesis and considers how they might be used to direct future research.

5.1 Thesis summary

The goal of the research conducted for this thesis was to advance our understanding of the relationship between substrate properties, gait biomechanics and muscle activities. The main aim was to determine how human gait and energetics are altered by the level of compliance with a deformable substrate. This was investigated by collecting a large dataset of human walking on both artificial (foam) and natural (sand) compliant substrates. Across the two studies, human walking on a total of 5 different compliant substrates and 1 non-compliant substrate was studied.

The thesis set out to address the following objectives:

- To determine energetics costs, muscle activity of the lower limb and trunk and lower limb motion on foam versus hard floor (chapter 2)
- To determine muscle activity of the lower limb and trunk and lower limb motion on sand versus hard floor (chapter 3)
- To determine the similarities and differences between gait changes and muscle activities between walking on foam and sand (chapter 4)

The studies conducted and presented in this thesis successfully addressed all of the aims and objectives.

I believe the findings of this thesis can be separated into two main conclusions:

1. Overall gait adaptations like sagittal kinematics, spatiotemporal parameters and muscle activation are adopted in response to the depth of depression into a compliant substrate regardless of substrate material properties
2. More subtle, specific gait adaptations are adopted according to the material properties of the compliant substrate

5.1.1 Gait adaptations in response to the depth of depression into a compliant substrate

The first conclusion from this thesis is that the level of substrate compliance had a considerable effect on gait biomechanics, muscle activation and energetics. As substrate compliance increased, energetic costs on foam increased (chapter 2). Although not tested in this study, previous studies have also found increased energetic costs during walking on sand (Lejeune, Willems & Heglund 1998; Zamparo et al. 1992). Increased substrate compliance was associated with increased ranges of motion at the hip, knee and ankle joint, changes to spatiotemporal parameters and higher muscle activation on all substrates tested in the studies presented in this thesis (see chapters 2 and 3). On compliant substrates, participants adapted several gait strategies that could be interpreted as measures to regulate stability. These include an increase in cycle time, stance time, swing time and double-support time and a decrease in self-selected walking speed. Moreover, as substrate compliance increased, there was greater plantarflexion at the ankle joint and flexion at the hip and knee joint during the swing phase and greater dorsiflexion at the ankle joint during stance. When the joints are more flexed and less aligned with the resultant ground reaction force, a greater volume of active muscle is required (Pontzer, Raichlen & Sockol 2009). Due to the increased hip and knee flexion observed on compliant substrates, we also observed an associated increase in muscle activation on compliant substrates. The musculoskeletal model simulations presented in chapter 2 found increased mechanical work done by muscles crossing the knee and hip joints during walking on foam. In agreement with our findings, previous studies on walking on uneven and irregular terrain have also proposed increased mechanical work at the knee and hip due to greater flexion (Gates et al. 2012; Voloshina et al. 2013). The overall findings

of the studies presented in this thesis indicate many gait adaptations like sagittal kinematics, spatiotemporal parameters and muscle activation are adopted in response to the depth of depression into a compliant substrate. However, we do find notable differences in some gait adaptations during walking on foam and on sand, that are likely due to the differences in material properties of these substrates.

5.1.2 Gait adaptations in response to substrate material properties

The second conclusion from this thesis is that subtle, specific gait adaptations are adopted according to the material properties of the compliant substrate. Although we found similarities in gross gait adaptations on all compliant substrates, there were also differences in gait kinematics and muscle activations between comparable foam and sand substrates (see chapter 4). During walking on sand, participants displayed less knee and hip flexion during swing, greater ankle dorsiflexion during stance, increased muscle activation and changes to spatiotemporal parameters such as a slower walking speed and increased cycle time and swing time. The differences in hip and knee flexion are likely due to differences in walking speeds (Hanlon & Anderson 2006; Kirtley, Whittle & Jefferson 1985) and/or the slightly greater foot depressions observed on the foam, rather than a response to the different material properties of the compliant substrates. However, the changes to ankle joint kinematics and muscle activations on sand and the adoption of gait stability measures such as slower walking speeds are probably due to the unpredictable nature of sand displacement under the foot. Greater dorsiflexion at the ankle joint during stance, accompanied by higher lower limb muscle activities on sand can be due to the sinking of the heel into the sand, lateral displacement of the surface under the foot, deceleration after heel-strike, foot slippage during push-off and potential reductions in elastic energy storage and/or recovery. As a result, greater energy is required for stability and the re-acceleration of the CoM into push-off. In agreement with our findings, previous studies found an increase in muscle co-activation about the ankle joint during human walking on uneven and slippery surfaces (Marigold & Patla 2002; Wade et al. 2010). The overall findings of this study indicate that the material properties of the compliant substrate does affect lower limb motion and muscle activations.

Interestingly, during walking on the firmer sand substrate, wet building sand, participants adopted ankle dorsiflexion angles during stance that were similar to the angles observed on the thick foam but during the swing phase, ankle angles more closely resemble the angles observed on the floor. Our findings indicate that changes around the ankle joint, predominantly during the stance phase, are important during walking on a more unpredictable deforming substrate like sand. Therefore, when discussing more specific gait adaptations on compliant substrates, the material properties of the substrate should be considered. Exactly how different material and mechanical properties of a compliant substrate affects gait changes is an area that requires future research.

5.2 Limitations

The research conducted in this thesis furthers our understanding of how human gait is actively altered or moderated by substrate compliance, however this work does include some limitations which should be acknowledged and addressed in future research.

From our research, we showed human gait changes during walking on compliant foam and sand. However, this is a small subset of potential compliant substrates that humans may have to navigate. For example, walking outdoors involves walking on various compliant substrates such as mud and grass. In particular, elastic-plastic substrates such as clay and mud may affect human gait differently due to the different mechanical properties. The elastic behaviour of sand and clay are different because values of Young's modulus are highly variable throughout sand whereas the Young's modulus for clay remains relatively constant (Craig 2013). The extent to which our explanatory factors apply universally to compliant terrains remains to be tested. This is particularly important in the study of hominin fossil footprints as sediment properties are likely to affect footprint shape as well as lower limb motion and important hominin fossil footprints have been found in these sediments (e.g. (Bennett et al. 2009; Hatala et al. 2017)).

Secondly, our study population is relatively homogenous which may limit the wider applicability of our findings. Previous studies have shown that energetic costs and gait characteristics are affected by factors such as age (Hernández et al. 2009; Niederer et al. 2021; Schrack et al. 2012), body size and composition (Webb 1981) and physical activity (Pontzer et al. 2016). Even in our relatively homogenous population, we observed large participant variability for most of the variables measured in this study. In normal human walking, participants display step-to-step variability and individuals walk differently (O'Connor, Xu & Kuo 2012). However, it is unclear how both inter- and intra- participant variability is affected by substrate properties. It is possible that gender may have an effect as we found higher variability in energy expenditure in females and there were significant gender effects found in the LMMs for most variables. However, gait changes may be related to body size and limb length rather than gender itself.

Thirdly, participants in this study were allowed to walk at a self-selected speed. This was chosen as we wanted participants to walk naturally on these substrates and we also wanted to see if walking speed changed as a result of substrate compliance. However, walking speed has been shown to affect both metabolic cost and gait changes during human walking (Faraji, Wu & Ijspeert 2018; Fukuchi, Fukuchi & Duarte 2019). Therefore, it would be interesting to see if changes to metabolic costs and gait due to an increase/decrease in walking speeds are the same on hard, level surfaces and different compliant substrates.

Fourthly, in our studies we have modelled the foot as one segment, however, modelling the foot as a single segment is a great oversimplification of the ankle-foot complex that could have a significant effect on the results presented in this thesis. In our studies on sand, we found greater changes to the ankle joint range of motion, however, previous research has shown that multi-segment foot models (MFM) and single-segment foot models (SFM) produce different ankle kinematics during gait (Pothrat et al. 2015). Specifically, Pothrat et al. (2015) found greater dorsiflexion angles were reported using the SFM. On the compliant substrates, we found greater ankle dorsiflexion, but it is possible that the observed differences in ankle joint angles could be inflated due to the simplification of using a SFM. A recent study found that the number of segments in MFM significantly affects the biomechanical estimates of joint kinematics and tissue strains during hopping (Kim & Kipp 2019).

Specifically, they found that modelling the foot with at least 3 segments produces a more accurate representation of the foot-ankle complex and avoids the overestimation of several biomechanical variables (Kim & Kipp 2019). In fact, our foot marker set-up is based on the Oxford Foot Model which comprises of three true segments (tibia, hindfoot and forefoot) whilst the hallux is modelled as a vector (Carson et al. 2001). However, due to time constraints, I chose to model the foot as a SFM. Repeating kinematic analyses using a MFM will be beneficial to gain a more accurate understanding of the joint kinematics during walking on compliant substrates.

Finally, we have not measured foot muscles in this study. Intrinsic foot muscles have been shown to be important for generating forward propulsive power (Farris et al. 2019). As we found increases in muscle activation in the lower limbs during the propulsive stage on compliant substrates, particularly on sand, it is likely that there are changes to the intrinsic foot muscles and soft tissues of the foot. As discussed in chapter one, the ability to recycle mechanical energy is an important contributor to human locomotor behaviour. The human foot contributes up to 17% of the energy required to power a stride through energy recycling (Kelly et al. 2019). This mechanism has previously been attributed to the passive contribution of the plantar aponeurosis, but recent work has shown that the intrinsic foot muscles play an important role, contributing to elastic energy storage and return within the human foot, highlighting the importance of looking at foot muscles when considering adaptive gait strategies (Kelly et al. 2019).

5.3 Future work

Although this thesis is focused on why the energetic cost of locomotion increases during human walking on compliant substrates, the methods, data and interpretations presented in this thesis can be beneficial to a wide range of researchers in different areas, including human anatomy, footprints, evolution, bipedal robotics, footwear and orthotics.

The absence of soft tissues in fossil animals and the inability to observe their motion directly means that reconstructions of locomotion in extinct animals must rely on principles established from direct study of living animals, and particularly how bone and footprint morphology are linked to biomechanical function. The transition to terrestrial bipedalism is considered one of the most significant adaptations to occur within the hominin lineage. The human foot is arguably our most distinctive morphological and functional structure, with a combination of pronounced longitudinal and transverse tarsal aches, a robust calcaneus and a compliant Achilles tendon. Along with relatively long lower limbs, these key anatomical features are assumed to contribute to the high efficiency of striding bipedal walking in modern humans, particularly relative to extinct hominins and other extant great apes (Crompton, Vereecke & Thorpe 2008; Holowka & Lieberman 2018; Hu, Xiong & Sun 2021). It has been suggested that certain morphologies optimise locomotor performance during walking over particular terrains (Jagnandan & Higham 2018). Hominins are assumed to have walked over variable and often compliant substrates that may incur higher CoTs relative to noncompliant substrates, increasing the applicability of our results to the study of human evolution and bipedalism. In our previously published work (Charles et al. 2021), we found that the CoT values presented in chapter two, were significantly correlated with each other, suggesting that locomotor efficiency on different compliant surfaces may be linked. However, we found no supportive evidence that variations in gross anatomical parameters such as lower limb length, calcaneus tuber length and foot shape indices correlate with CoT (Charles et al. 2021).

It has become standard to use simple measures of fossil foot bones and fossilised footprint shapes to interpret the locomotion of extinct animals, and subsequently to generate ideas about when and why bipedalism first evolved (DeSilva 2010; Harcourt-Smith & Aiello 2004; McNutt, Zipfel & DeSilva 2018). However, recent biomechanical research has suggested that foot bone morphology may not be as predictive of locomotion as has long been assumed (Bates et al. 2013b; DeSilva & Gill 2013). Furthermore, it is presently unclear exactly how much information about foot anatomy and motion is recorded in fossil footprints (D'Aout et al. 2010; Hatala et al. 2016). The shape of footprints may vary according to the mechanical properties of the substrate, as demonstrated by drastically different morphologies within long or continuous footprint trails (Bates et al. 2013b; Morse et al. 2013). The main findings of this thesis suggest that overall gait kinematics when walking on sand is mechanically similar

to walking on foam and thus, knowledge of complex sediment properties and deformation behaviour are not necessary to reverse engineer lower limb motion. Instead, limb joint motions generally reflect the gross depth of depression into a compliant substrate. However, our findings also show that differences in substrate compliancy, and substrate properties, leads to differences in specific gait kinematics, most notably at the ankle joint. It is likely that these specific differences in limb motions produce different footprint shapes. Future work will include analysing the footprint shapes recorded during the study presented in chapter three to infer which lower limb motions are recorded in the footprint shape. If the quantitative variation in footprint shape does not mask the qualitative defining features of modern upright bipedalism, footprints can be used to reverse engineer locomotion in extinct hominins, as long as footprint sites contain footprints of similar depths. However, if important gait kinematic differences are not distinguishable in the footprints, it suggests caution when comparing fossilised footprints in substrates with dissimilar rheological properties.

During the time that the foot evolved into a highly specialised tool for bipedal locomotion, humans would have walked barefoot. The human foot is the first point of contact between the body and the external environment and provides important sensory information to the central nervous system that are important for maintaining balance and locomotion (Belanger & Patla 1984; Nurse et al. 2005). However, sensory feedback from the feet may be influenced by changing the characteristics of the shoe or substrate (Wu & Chiang 1997). Modern shoes often have cushioned heels, arch support and stiffened soles. Research has shown that the design of shoes and orthotics can have a big impact on several aspects of gait such as kinematics, kinetics and muscle activation (Demura & Demura 2012; Desmyttere et al. 2020; Murley et al. 2009; Nigg et al. 2012; Nurse et al. 2005). It has been questioned whether certain aspects of modern shoe designs contribute to the development of weak feet and lower extremity disorders such as plantar fasciitis (Lieberman 2012) and hallux valgus (Mafart 2007). Footwear and orthotic industries need in-depth knowledge of foot structure and biomechanics to achieve improved designs for sports and clinical interventions. The findings of this thesis suggests that variations in substrates impact how an individual chooses to walk across a surface to maintain manoeuvrability, grip and stability. Further research is required to determine whether factors such as shoe sole compliancy will have similar effects to substrate compliancy. Running shoes are designed with motion control and cushioning features which aim to reduce excessive foot motion and force but can differ in forefoot,

midfoot and rearfoot design (Davis 2014). Previous research has found these differences significantly alter aspects of inter-segmental foot kinematics (Langley, Cramp & Morrison 2018). Furthermore, previous research has shown that humans adapt gait mechanics according to surface stiffness during hopping by adjusting leg stiffness (Ferris & Farley 1997) and adapting human foot mechanics through active muscular control (Birch et al. 2021). The application of MFMs and the measurement of foot muscles should provide a greater understanding of foot mechanics that influence footwear design.

From the findings of this thesis, it is hypothesised that the modified joint kinematics and spatiotemporal kinematics, and associated increase in muscle work at the hip and knee, are likely to occur (albeit to varying degrees) on most compliant substrates, and therefore the results of this thesis are widely applicable for similar human populations, and potentially mammals more widely where relatively upright limb postures are utilised. Of course, the relatively homogenous study population presented here may limit the wider applicability of these results, however applying these methods to other demographics such as elderly individuals or elite athletes will deepen our insights into the mechanisms behind CoT variability and the effects of substrate compliancy on gait kinematics. Furthermore, as there was a lot of inter- and intra- participant variability observed in these studies, future research should explore individual participant differences.

Building on the research outlined in this thesis, I think the most important future direction is increasing our understanding of the complex relationship between form and function in human limb bones, as this knowledge is applicable to numerous areas of research, some of which are discussed above. In particular, measurements of how the human foot bones move in 3D are crucial. 3D x-ray motion analysis methods combine skeletal movement data from in-vivo x-ray videos with skeletal morphology from 3D MRI/CT scans to provide high-resolution 3D bone motion. Medical imaging allows us to quantify the shape of the human foot bones, as well as the characteristics of muscles, tendons and ligaments in the foot and ankle. These approaches can be used not only to study movement over hard ground but also across soft sediments, allowing us to understand how foot function responds to different substrates, as well as, the dynamic deformation of the sediment during footprint formation. In recent years, these methods have been applied in a range of zoological studies (e.g.

(Falkingham & Gatesy 2014; Turner, Falkingham & Gatesy 2020)), although more recent research is now being done involving humans (Hatala, Gatesy & Falkingham 2021; Hatala, Perry & Gatesy 2018).

5.4 Conclusion

In conclusion, I have shown in this thesis that human gait and energetics are altered during locomotion on compliant substrates such as foam and sand. In particular, I have shown that gross gait adaptations like sagittal kinematics, spatiotemporal parameters and muscle activation are adopted in response to the depth of depression into a compliant substrate, rather than the substrate properties. However, substrate properties do affect specific gait changes, at least between the two compliant substrates measured in these studies. However, further research is required to determine whether similar gait adaptations occur on other compliant substrates such as clay, mud and grass, which have different mechanical properties. Future research should explore the effects of substrate compliance on other demographic groups and participant variability. Moreover, I believe that future research should focus on improving our understanding of 3D foot motion during locomotion on compliant substrates.

5.5 Acknowledgements

These studies was funded by grants from the Leverhulme Trust (RPG-2017-296) and by the Medical Research Council (MRC) and Versus Arthritis as part of the Medical Research Council Versus Arthritis Centre for Integrated Research into Musculoskeletal Ageing (CIMA) [MR/P020941/1]. The MRC Versus Arthritis Centre for Integrated Research into Musculoskeletal Ageing is a collaboration between the Universities of Liverpool, Sheffield and Newcastle.

5.6 Thesis References

Abe, D., Yanagawa, K. & Niihata, S. (2004) 'Effects of load carriage, load position, and walking speed on energy cost of walking', *Applied Ergonomics*, vol. 35, no. 4, pp. 329-335.

Alexander, R.M. (1976) 'Mechanics of bipedal locomotion', *Perspectives in experimental biology*, vol. 1, pp. 493-504.

Alexander, R.M. (1983) *Animal mechanics*, Blackwell.

Alexander, R.M. (1984) 'Elastic energy stores in running vertebrates', *American Zoologist*, vol. 24, no. 1, pp. 85-94.

Alexander, R.M. (2002) 'Tendon elasticity and muscle function', *Comp Biochem Physiol A Mol Integr Physiol*, vol. 133, no. 4, pp. 1001-1011.

Allen, J.R.L. (1997) 'Subfossil mammalian tracks (Flandrian) in the Severn Estuary, S. W. Britain: mechanics of formation, preservation and distribution', *Philosophical Transactions of the Royal Society of London. Series B: Biological Sciences*, vol. 352, no. 1352, pp. 481-518.

ASTM, D. (2001) '3574—Standard test methods for flexible cellular materials—slab', *Bonded, and Molded Urethane Foams*, vol. 164.

Baroud, G., Nigg, B. & Stefanyshyn, D. (1999) 'Energy storage and return in sport surfaces', *Sports Engineering*, vol. 2, no. 3, pp. 173-180.

Barrett, R.S., Neal, R.J. & Roberts, L.J. (1998) 'The dynamic loading response of surfaces encountered in beach running', *Journal of Science and Medicine in Sport*, vol. 1, no. 1, pp. 1-11.

Bates, D., Mächler, M., Bolker, B. & Walker, S. (2014) 'Fitting linear mixed-effects models using lme4', *arXiv preprint arXiv:1406.5823*.

Bates, K.T., Collins, D., Savage, R., McClymont, J., Webster, E., Pataky, T.C., D'Aout, K., Sellers, W.I., Bennett, M.R. & Crompton, R.H. (2013a) 'The evolution of compliance in the human lateral mid-foot', *Proc Biol Sci*, vol. 280, no. 1769, p. 20131818.

Bates, K.T., Savage, R., Pataky, T.C., Morse, S.A., Webster, E., Falkingham, P.L., Ren, L., Qian, Z., Collins, D., Bennett, M.R., McClymont, J. & Crompton, R.H. (2013b) 'Does footprint depth correlate with foot motion and pressure?', *J R Soc Interface*, vol. 10, no. 83, p. 20130009.

Belanger, M. & Patla, A.E. (1984) 'Corrective responses to perturbation applied during walking in humans', *Neuroscience Letters*, vol. 49, no. 3, pp. 291-295.

Bell, F.G. (2013) *Foundation engineering in difficult ground*, Elsevier.

Bennett, M.R., Harris, J.W., Richmond, B.G., Braun, D.R., Mbua, E., Kiura, P., Olago, D., Kibunjia, M., Omuombo, C., Behrensmeyer, A.K., Huddart, D. & Gonzalez, S. (2009) 'Early hominin foot morphology based on 1.5-million-year-old footprints from Ileret, Kenya', *Science*, vol. 323, no. 5918, pp. 1197-1201.

Biewener, A. & Patek, S. (2018) Energetics of Locomotion, in A.A. Biewener & S.N. Patek (eds), *Animal Locomotion*, Oxford University Press, p. 0.

Birch, J.V., Kelly, L.A., Cresswell, A.G., Dixon, S.J. & Farris, D.J. (2021) 'Neuromechanical adaptations of foot function to changes in surface stiffness during hopping', *Journal of Applied Physiology*, vol. 130, no. 4, pp. 1196-1204.

Britannica, E. (2022) *The muscle groups and their actions* [Online], Available from: https://www.britannica.com/science/human-muscle-system#ref322749 (Accessed: 16/08/2022).

Brockett, C.L. & Chapman, G.J. (2016) 'Biomechanics of the ankle', *Orthop Trauma*, vol. 30, no. 3, pp. 232-238.
Bruening, D.A., Baird, A.R., Weaver, K.J. & Rasmussen, A.T. (2020) 'Whole body kinematic sex differences persist across non-dimensional gait speeds', *PLOS ONE*, vol. 15, no. 8, p. e0237449.
Brunner, R. & Rutz, E. (2013) 'Biomechanics and muscle function during gait', *J Child Orthop*, vol. 7, no. 5, pp. 367-371.
Cappellini, G., Ivanenko, Y.P., Dominici, N., Richard, E. & Lacquaniti, F. (2010) 'Motor Patterns During Walking on a Slippery Walkway', *Journal of Neurophysiology*, vol. 103, no. 2, pp. 746-760.
Cappellini, G., Ivanenko, Y.P., Poppele, R.E. & Lacquaniti, F. (2006) 'Motor patterns in human walking and running', *J Neurophysiol*, vol. 95, no. 6, pp. 3426-3437.
Carson, M.C., Harrington, M.E., Thompson, N., O'Connor, J.J. & Theologis, T.N. (2001) 'Kinematic analysis of a multi-segment foot model for research and clinical applications: a repeatability analysis', *J Biomech*, vol. 34, no. 10, pp. 1299-1307.
Cavagna, G.A. (1975) 'Force platforms as ergometers', *J Appl Physiol*, vol. 39, no. 1, pp. 174-179.
Cavagna, G.A., Heglund, N.C. & Taylor, C.R. (1977) 'Mechanical work in terrestrial locomotion: two basic mechanisms for minimizing energy expenditure', *American Journal of Physiology-Regulatory, Integrative and Comparative Physiology*, vol. 233, no. 5, pp. R243-R261.
Cavagna, G.A. & Kaneko, M. (1977) 'Mechanical work and efficiency in level walking and running', *J Physiol*, vol. 268, no. 2, pp. 467--481.
Cavagna, G.A., Thys, H. & Zamboni, A. (1976) 'The sources of external work in level walking and running', *J Physiol*, vol. 262, no. 3, pp. 639-657.
Cavanagh, P.R. & Kram, R. (1985) 'The efficiency of human movement--a statement of the problem', *Med Sci Sports Exerc*, vol. 17, no. 3, pp. 304-308.
Ceccato, J.-C., de Sèze, M., Azevedo, C. & Cazalets, J.-R. (2009) 'Comparison of Trunk Activity during Gait Initiation and Walking in Humans', *PLOS ONE*, vol. 4, no. 12, p. e8193.
Charles, J.P., Grant, B., D'Août, K. & Bates, K.T. (2020) 'Subject-specific muscle properties from diffusion tensor imaging significantly improve the accuracy of musculoskeletal models', *Journal of Anatomy*, vol. 237, no. 5, pp. 941-959.
Charles, J.P., Grant, B., D'Août, K. & Bates, K.T. (2021) 'Foot anatomy, walking energetics, and the evolution of human bipedalism', *Journal of Human Evolution*, vol. 156, p. 103014.
Chumanov, E.S., Wall-Scheffler, C. & Heiderscheit, B.C. (2008) 'Gender differences in walking and running on level and inclined surfaces', *Clinical Biomechanics*, vol. 23, no. 10, pp. 1260-1268.
Collins, S.H. & Kuo, A.D. (2010) 'Recycling energy to restore impaired ankle function during human walking', *PLoS One*, vol. 5, no. 2, p. e9307.
Cotes, J.E. & Meade, F. (1960) 'The energy expenditure and mechanical energy demand in walking', *Ergonomics*, vol. 3, pp. 97-120.
Craig, R.F. (2013) *Soil mechanics*, Springer.
Crompton, R.H., Pataky, T.C., Savage, R., D'Aout, K., Bennett, M.R., Day, M.H., Bates, K., Morse, S. & Sellers, W.I. (2012) 'Human-like external function of the foot, and fully upright gait, confirmed in the 3.66 million year old Laetoli hominin footprints by topographic statistics, experimental footprint-formation and computer simulation', *J R Soc Interface*, vol. 9, no. 69, pp. 707-719.

Crompton, R.H., Sellers, W.I. & Thorpe, S.K. (2010) 'Arboreality, terrestriality and bipedalism', *Philos Trans R Soc Lond B Biol Sci*, vol. 365, no. 1556, pp. 3301-3314.
Crompton, R.H., Vereecke, E.E. & Thorpe, S.K. (2008) 'Locomotion and posture from the common hominoid ancestor to fully modern hominins, with special reference to the last common panin/hominin ancestor', *J Anat*, vol. 212, no. 4, pp. 501-543.
D'Aout, K., Meert, L., Van Gheluwe, B., De Clercq, D. & Aerts, P. (2010) 'Experimentally generated footprints in sand: Analysis and consequences for the interpretation of fossil and forensic footprints', *Am J Phys Anthropol*, vol. 141, no. 4, pp. 515-525.
Davies, S.E.H. & Mackinnon, S.N. (2006) 'The energetics of walking on sand and grass at various speeds', *Ergonomics*, vol. 49, no. 7, pp. 651-660.
Davis, I.S. (2014) 'The re-emergence of the minimal running shoe', *J Orthop Sports Phys Ther*, vol. 44, no. 10, pp. 775-784.
Demura, T. & Demura, S.-i. (2012) 'The effects of shoes with a rounded soft sole in the anterior–posterior direction on leg joint angle and muscle activity', *The Foot*, vol. 22, no. 3, pp. 150-155.
DeSilva, J.M. (2010) 'Revisiting the "midtarsal break"', *American Journal of Physical Anthropology*, vol. 141, no. 2, pp. 245-258.
DeSilva, J.M. & Gill, S.V. (2013) 'Brief communication: a midtarsal (midfoot) break in the human foot', *Am J Phys Anthropol*, vol. 151, no. 3, pp. 495-499.
Desmyttere, G., Leteneur, S., Hajizadeh, M., Bleau, J. & Begon, M. (2020) 'Effect of 3D printed foot orthoses stiffness and design on foot kinematics and plantar pressures in healthy people', *Gait & Posture*, vol. 81, pp. 247-253.
DeVita, P., Helseth, J. & Hortobagyi, T. (2007) 'Muscles do more positive than negative work in human locomotion', *J Exp Biol*, vol. 210, no. Pt 19, pp. 3361-3373.
Dewolf, A.H., Ivanenko, Y.P., Lacquaniti, F. & Willems, P.A. (2017) 'Pendular energy transduction within the step during human walking on slopes at different speeds', *PLOS ONE*, vol. 12, no. 10, p. e0186963.
Dixon, P.C., Böhm, H. & Döderlein, L. (2012) 'Ankle and midfoot kinetics during normal gait: A multi-segment approach', *Journal of Biomechanics*, vol. 45, no. 6, pp. 1011-1016.
Doke, J., Donelan, J.M. & Kuo, A.D. (2005) 'Mechanics and energetics of swinging the human leg', *J Exp Biol*, vol. 208, no. Pt 3, pp. 439-445.
Doke, J. & Kuo, A.D. (2007) 'Energetic cost of producing cyclic muscle force, rather than work, to swing the human leg', *Journal of Experimental Biology*, vol. 210, no. 13, pp. 2390-2398.
Donelan, J.M., Kram, R. & Kuo, A.D. (2002) 'Mechanical work for step-to-step transitions is a major determinant of the metabolic cost of human walking', *Journal of Experimental Biology*, vol. 205, no. 23, pp. 3717-3727.
Donelan, J.M., Shipman, D.W., Kram, R. & Kuo, A.D. (2004) 'Mechanical and metabolic requirements for active lateral stabilization in human walking', *Journal of Biomechanics*, vol. 37, no. 6, pp. 827-835.
Falkingham, P.L. & Gatesy, S.M. (2014) 'The birth of a dinosaur footprint: subsurface 3D motion reconstruction and discrete element simulation reveal track ontogeny', *Proc Natl Acad Sci U S A*, vol. 111, no. 51, pp. 18279-18284.
Faraji, S., Wu, A.R. & Ijspeert, A.J. (2018) 'A simple model of mechanical effects to estimate metabolic cost of human walking', *Scientific Reports*, vol. 8, no. 1, p. 10998.
Faraway, J.J. (2016) *Extending the linear model with R: generalized linear, mixed effects and nonparametric regression models*, Chapman and Hall/CRC.

Farris, D.J., Birch, J. & Kelly, L. (2020) 'Foot stiffening during the push-off phase of human walking is linked to active muscle contraction, and not the windlass mechanism', *Journal of The Royal Society Interface*, vol. 17, no. 168, p. 20200208.
Farris, D.J., Kelly, L.A., Cresswell, A.G. & Lichtwark, G.A. (2019) 'The functional importance of human foot muscles for bipedal locomotion', *Proceedings of the National Academy of Sciences*, vol. 116, no. 5, pp. 1645-1650.
Ferris, D.P. & Farley, C.T. (1997) 'Interaction of leg stiffness and surface stiffness during human hopping', *Journal of Applied Physiology*, vol. 82, no. 1, pp. 15-22.
Ferris, D.P., Liang, K. & Farley, C.T. (1999) 'Runners adjust leg stiffness for their first step on a new running surface', *Journal of Biomechanics*, vol. 32, no. 8, pp. 787-794.
Ferris, D.P., Louie, M. & Farley, C.T. (1998) 'Running in the real world: adjusting leg stiffness for different surfaces', *Proc Biol Sci*, vol. 265, no. 1400, pp. 989-994.
Fischer-Cripps, A.C. (2007) *Introduction to contact mechanics*, vol. 101, Springer.
Fukuchi, C.A., Fukuchi, R.K. & Duarte, M. (2019) 'Effects of walking speed on gait biomechanics in healthy participants: a systematic review and meta-analysis', *Systematic Reviews*, vol. 8, no. 1, p. 153.
Full, R.J., Kubow, T., Schmitt, J., Holmes, P. & Koditschek, D. (2002) 'Quantifying Dynamic Stability and Maneuverability in Legged Locomotion1', *Integrative and Comparative Biology*, vol. 42, no. 1, pp. 149-157.
Gast, K., Kram, R. & Riemer, R. (2019) 'Preferred walking speed on rough terrain: is it all about energetics?', *Journal of Experimental Biology*, vol. 222, no. 9.
Gates, D.H., Wilken, J.M., Scott, S.J., Sinitski, E.H. & Dingwell, J.B. (2012) 'Kinematic strategies for walking across a destabilizing rock surface', *Gait & Posture*, vol. 35, no. 1, pp. 36-42.
Gatesy, S.M. & Biewener, A.A. (1991) 'Bipedal locomotion: effects of speed, size and limb posture in birds and humans', *Journal of Zoology*, vol. 224, no. 1, pp. 127-147.
Geyer, H., Seyfarth, A. & Blickhan, R. (2006) 'Compliant leg behaviour explains basic dynamics of walking and running', *Proc Biol Sci*, vol. 273, no. 1603, pp. 2861-2867.
Giatsis, G., Kollias, I., Panoutsakopoulos, V. & Papaiakovou, G. (2004) 'Biomechanical differences in elite beach-volleyball players in vertical squat jump on rigid and sand surface', *Sports Biomech*, vol. 3, no. 1, pp. 145-158.
Gibson, L.J. & Ashby, M.F. (1997) *Cellular Solids: Structure and Properties*, 2 edn, Cambridge University Press, Cambridge.
Hak, L., Houdijk, H., Steenbrink, F., Mert, A., van der Wurff, P., Beek, P.J. & van Dieën, J.H. (2012) 'Speeding up or slowing down?: Gait adaptations to preserve gait stability in response to balance perturbations', *Gait & Posture*, vol. 36, no. 2, pp. 260-264.
Halsey, L.G. (2016) 'Terrestrial movement energetics: current knowledge and its application to the optimising animal', *Journal of Experimental Biology*, vol. 219, no. 10, pp. 1424-1431.
Hanavan Jr, E.P. (1964) *A mathematical model of the human body*, Air Force Aerospace Medical Research Lab Wright-patterson AFB OH,
Hanlon, M. & Anderson, R. (2006) 'Prediction methods to account for the effect of gait speed on lower limb angular kinematics', *Gait & Posture*, vol. 24, no. 3, pp. 280-287.
Hansen, N.L., Hansen, S., Christensen, L.O., Petersen, N.T. & Nielsen, J.B. (2001) 'Synchronization of lower limb motor unit activity during walking in human subjects', *J Neurophysiol*, vol. 86, no. 3, pp. 1266-1276.
Harcourt-Smith, W.E. & Aiello, L.C. (2004) 'Fossils, feet and the evolution of human bipedal locomotion', *J Anat*, vol. 204, no. 5, pp. 403-416.

Hatala, K.G., Demes, B. & Richmond, B.G. (2016) 'Laetoli footprints reveal bipedal gait biomechanics different from those of modern humans and chimpanzees', *Proc Biol Sci*, vol. 283, no. 1836.
Hatala, K.G., Dingwall, H.L., Wunderlich, R.E. & Richmond, B.G. (2013) 'The relationship between plantar pressure and footprint shape', *Journal of Human Evolution*, vol. 65, no. 1, pp. 21-28.
Hatala, K.G., Gatesy, S.M. & Falkingham, P.L. (2021) 'Integration of biplanar X-ray, three-dimensional animation and particle simulation reveals details of human 'track ontogeny'', *Interface Focus*, vol. 11, no. 5, p. 20200075.
Hatala, K.G., Perry, D.A. & Gatesy, S.M. (2018) 'A biplanar X-ray approach for studying the 3D dynamics of human track formation', *J Hum Evol*, vol. 121, pp. 104-118.
Hatala, K.G., Roach, N.T., Ostrofsky, K.R., Wunderlich, R.E., Dingwall, H.L., Villmoare, B.A., Green, D.J., Braun, D.R., Harris, J.W.K., Behrensmeyer, A.K. & Richmond, B.G. (2017) 'Hominin track assemblages from Okote Member deposits near Ileret, Kenya, and their implications for understanding fossil hominin paleobiology at 1.5 Ma', *J Hum Evol*, vol. 112, pp. 93-104.
Hatala, K.G., Wunderlich, R.E., Dingwall, H.L. & Richmond, B.G. (2016) 'Interpreting locomotor biomechanics from the morphology of human footprints', *J Hum Evol*, vol. 90, pp. 38-48.
Hermens, H.J., Freriks, B., Disselhorst-Klug, C. & Rau, G. (2000) 'Development of recommendations for SEMG sensors and sensor placement procedures', *Journal of Electromyography and Kinesiology*, vol. 10, no. 5, pp. 361-374.
Hernández, A., Silder, A., Heiderscheit, B.C. & Thelen, D.G. (2009) 'Effect of age on center of mass motion during human walking', *Gait Posture*, vol. 30, no. 2, pp. 217-222.
Hicks, J.L., Uchida, T.K., Seth, A., Rajagopal, A. & Delp, S.L. (2015) 'Is my model good enough? Best practices for verification and validation of musculoskeletal models and simulations of movement', *Journal of Biomechanical Engineering*, vol. 137, no. 2.
Holowka, N.B., Kraft, T.S., Wallace, I.J., Gurven, M. & Venkataraman, V.V. (2022) 'Forest terrains influence walking kinematics among indigenous Tsimane of the Bolivian Amazon', *Evolutionary Human Sciences*, vol. 4, p. e19.
Holowka, N.B. & Lieberman, D.E. (2018) 'Rethinking the evolution of the human foot: insights from experimental research', *The Journal of Experimental Biology*, vol. 221, no. 17.
Holtz, R.D., Kovacs, W.D. & Sheahan, T.C. (1981) *An introduction to geotechnical engineering*, vol. 733, Prentice-Hall Englewood Cliffs.
Hoogkamer, W., Kipp, S., Frank, J.H., Farina, E.M., Luo, G. & Kram, R. (2018) 'A Comparison of the Energetic Cost of Running in Marathon Racing Shoes', *Sports Medicine*, vol. 48, no. 4, pp. 1009-1019.
Horsak, B., Slijepcevic, D., Raberger, A.-M., Schwab, C., Worisch, M. & Zeppelzauer, M. (2020) 'GaitRec, a large-scale ground reaction force dataset of healthy and impaired gait', *Scientific Data*, vol. 7, no. 1, p. 143.
Hu, D., Xiong, C.-H. & Sun, R. (2021) 'Working out the bipedal walking expenditure of energy based on foot morphology of different hominid genera: Implications for foot evolution', *Journal of Theoretical Biology*, vol. 519, p. 110646.
Hubel, T.Y. & Usherwood, J.R. (2015) 'Children and adults minimise activated muscle volume by selecting gait parameters that balance gross mechanical power and work demands', *Journal of Experimental Biology*, vol. 218, no. 18, pp. 2830-2839.
Impellizzeri, F.M., Rampinini, E., Castagna, C., Martino, F., Fiorini, S. & Wisloff, U. (2008) 'Effect of plyometric training on sand versus grass on muscle soreness and jumping

and sprinting ability in soccer players', *British Journal of Sports Medicine*, vol. 42, no. 1, pp. 42-46.
Jafarnezhadgero, A., Amirzadeh, N., Fatollahi, A., Siahkouhian, M., Oliveira, A.S. & Granacher, U. (2022) 'Effects of Running on Sand vs. Stable Ground on Kinetics and Muscle Activities in Individuals With Over-Pronated Feet', *Frontiers in Physiology*, vol. 12.
Jagnandan, K. & Higham, T.E. (2018) 'How rapid changes in body mass affect the locomotion of terrestrial vertebrates: ecology, evolution and biomechanics of a natural perturbation', *Biological Journal of the Linnean Society*, vol. 124, no. 3, pp. 279-293.
Kadaba, M.P., Ramakrishnan, H. & Wootten, M. (1990) 'Measurement of lower extremity kinematics during level walking', *Journal of orthopaedic research*, vol. 8, no. 3, pp. 383-392.
Kavanagh, J., Barrett, R. & Morrison, S. (2006) 'The role of the neck and trunk in facilitating head stability during walking', *Exp Brain Res*, vol. 172, no. 4, pp. 454-463.
Kelly, L.A., Farris, D.J., Cresswell, A.G. & Lichtwark, G.A. (2019) 'Intrinsic foot muscles contribute to elastic energy storage and return in the human foot', *Journal of Applied Physiology*, vol. 126, no. 1, pp. 231-238.
Kelly, L.A., Lichtwark, G. & Cresswell, A.G. (2015) 'Active regulation of longitudinal arch compression and recoil during walking and running', *J R Soc Interface*, vol. 12, no. 102, p. 20141076.
Kerdok, A.E., Biewener, A.A., McMahon, T.A., Weyand, P.G. & Herr, H.M. (2002) 'Energetics and mechanics of human running on surfaces of different stiffnesses', *Journal of Applied Physiology*, vol. 92, no. 2, pp. 469-478.
Kerrigan, D.C., Todd, M.K. & Della Croce, U. (1998) 'Gender differences in joint biomechanics during walking: normative study in young adults', *Am J Phys Med Rehabil*, vol. 77, no. 1, pp. 2-7.
Kim, H. & Kipp, K. (2019) 'Number of Segments Within Musculoskeletal Foot Models Influences Ankle Kinematics and Strains of Ligaments and Muscles', *Journal of Orthopaedic Research*, vol. 37, no. 10, pp. 2231-2240.
Kirtley, C., Whittle, M.W. & Jefferson, R.J. (1985) 'Influence of walking speed on gait parameters', *Journal of Biomedical Engineering*, vol. 7, no. 4, pp. 282-288.
Kunzetsova, A., Brockhoff, P. & Christensen, R. (2017) 'lmerTest package: Tests in linear mixed effect models', *J Stat Softw*, vol. 82, pp. 1-26.
Kuo, A.D., Donelan, J.M. & Ruina, A. (2005) 'Energetic Consequences of Walking Like an Inverted Pendulum: Step-to-Step Transitions', *Exercise and Sport Sciences Reviews*, vol. 33, no. 2, pp. 88-97.
Langley, B., Cramp, M. & Morrison, S.C. (2018) 'The influence of running shoes on inter-segmental foot kinematics', *Footwear Science*, vol. 10, no. 2, pp. 83-93.
Lejeune, T.M., Willems, P.A. & Heglund, N.C. (1998) 'Mechanics and energetics of human locomotion on sand', *Journal of Experimental Biology*, vol. 201, no. 13, pp. 2071-2080.
Lieberman, D.E. (2012) 'What We Can Learn About Running from Barefoot Running: An Evolutionary Medical Perspective', *Exercise and Sport Sciences Reviews*, vol. 40, no. 2, pp. 63-72.
MacLellan, M.J. & Patla, A.E. (2006) 'Adaptations of walking pattern on a compliant surface to regulate dynamic stability', *Experimental Brain Research*, vol. 173, no. 3, pp. 521-530.
Mafart, B. (2007) 'Hallux valgus in a historical French population: paleopathological study of 605 first metatarsal bones', *Joint Bone Spine*, vol. 74, no. 2, pp. 166-170.

Mane, J.V., Chandra, S., Sharma, S., Ali, H., Chavan, V.M., Manjunath, B.S. & Patel, R.J. (2017) 'Mechanical Property Evaluation of Polyurethane Foam under Quasi-static and Dynamic Strain Rates- An Experimental Study', *Procedia Engineering*, vol. 173, pp. 726-731.

Mann, R.A. & Hagy, J. (1980) 'Biomechanics of walking, running, and sprinting', *Am J Sports Med*, vol. 8, no. 5, pp. 345-350.

Marigold, D.S. & Patla, A.E. (2002) 'Strategies for Dynamic Stability During Locomotion on a Slippery Surface: Effects of Prior Experience and Knowledge', *Journal of Neurophysiology*, vol. 88, no. 1, pp. 339-353.

Matthis, J.S., Yates, J.L. & Hayhoe, M.M. (2018) 'Gaze and the Control of Foot Placement When Walking in Natural Terrain', *Curr Biol*, vol. 28, no. 8, pp. 1224-1233.e1225.

McIntosh, A.S., Beatty, K.T., Dwan, L.N. & Vickers, D.R. (2006) 'Gait dynamics on an inclined walkway', *J Biomech*, vol. 39, no. 13, pp. 2491-2502.

McMahon, T.A. & Greene, P.R. (1979) 'The influence of track compliance on running', *J Biomech*, vol. 12, no. 12, pp. 893-904.

McNutt, E.J., Zipfel, B. & DeSilva, J.M. (2018) 'The evolution of the human foot', *Evolutionary Anthropology: Issues, News, and Reviews*, vol. 27, no. 5, pp. 197-217.

Merryweather, A., Yoo, B. & Bloswick, D. (2011) 'Gait Characteristics Associated with Trip-Induced Falls on Level and Sloped Irregular Surfaces', *Minerals*, vol. 1, no. 1, pp. 109-121.

Mochon, S. & McMahon, T.A. (1980) 'Ballistic walking', *Journal of Biomechanics*, vol. 13, no. 1, pp. 49-57.

Morse, S.A., Bennett, M.R., Liutkus-Pierce, C., Thackeray, F., McClymont, J., Savage, R. & Crompton, R.H. (2013) 'Holocene footprints in Namibia: the influence of substrate on footprint variability', *Am J Phys Anthropol*, vol. 151, no. 2, pp. 265-279.

Murley, G.S., Landorf, K.B., Menz, H.B. & Bird, A.R. (2009) 'Effect of foot posture, foot orthoses and footwear on lower limb muscle activity during walking and running: A systematic review', *Gait & Posture*, vol. 29, no. 2, pp. 172-187.

Niederer, D., Engeroff, T., Fleckenstein, J., Vogel, O. & Vogt, L. (2021) 'The age-related decline in spatiotemporal gait characteristics is moderated by concerns of falling, history of falls & diseases, and sociodemographic-anthropometric characteristics in 60–94 years old adults', *European Review of Aging and Physical Activity*, vol. 18, no. 1, p. 19.

Nielsen, J.B. (2003) 'How we Walk: Central Control of Muscle Activity during Human Walking', *The Neuroscientist*, vol. 9, no. 3, pp. 195-204.

Nigg, B.M. (2007) *Biomechanics of the musculo-skeletal system*, John Wiley & Sons Incorporated.

Nigg, B.M., Baltich, J., Maurer, C. & Federolf, P. (2012) 'Shoe midsole hardness, sex and age effects on lower extremity kinematics during running', *Journal of Biomechanics*, vol. 45, no. 9, pp. 1692-1697.

Nurse, M.A., Hulliger, M., Wakeling, J.M., Nigg, B.M. & Stefanyshyn, D.J. (2005) 'Changing the texture of footwear can alter gait patterns', *Journal of Electromyography and Kinesiology*, vol. 15, no. 5, pp. 496-506.

O'Connor, S.M., Xu, H.Z. & Kuo, A.D. (2012) 'Energetic cost of walking with increased step variability', *Gait Posture*, vol. 36, no. 1, pp. 102-107.

O'Neill, M.C., Demes, B., Thompson, N.E., Larson, S.G., Stern, J.T. & Umberger, B.R. (2022) 'Adaptations for bipedal walking: Musculoskeletal structure and three-dimensional joint mechanics of humans and bipedal chimpanzees (Pan troglodytes)', *Journal of Human Evolution*, vol. 168, p. 103195.

O'Connor, S.M., Xu, H.Z. & Kuo, A.D. (2012) 'Energetic cost of walking with increased step variability', *Gait & Posture*, vol. 36, no. 1, pp. 102-107.
Pandolf, K.B., Haisman, M.F. & Goldman, R.F. (1976) 'Metabolic energy expenditure and terrain coefficients for walking on snow', *Ergonomics*, vol. 19, no. 6, pp. 683-690.
Pandy, M.G. & Andriacchi, T.P. (2010) 'Muscle and joint function in human locomotion', *Annu Rev Biomed Eng*, vol. 12, pp. 401-433.
Pataky, T.C., Robinson, M.A. & Vanrenterghem, J. (2013) 'Vector field statistical analysis of kinematic and force trajectories', *Journal of Biomechanics*, vol. 46, no. 14, pp. 2394-2401.
Patla, A.E. (2003) 'Strategies for dynamic stability during adaptive human locomotion', *IEEE Engineering in Medicine and Biology Magazine*, vol. 22, no. 2, pp. 48-52.
Perry, J. & Burnfield, J.M. (2010) 'Gait analysis. Normal and pathological function 2nd ed', *California: Slack*.
Peyré-Tartaruga, L.A. & Coertjens, M. (2018) 'Locomotion as a Powerful Model to Study Integrative Physiology: Efficiency, Economy, and Power Relationship', *Front Physiol*, vol. 9, p. 1789.
Pinnington, H.C. & Dawson, B. (2001) 'The energy cost of running on grass compared to soft dry beach sand', *Journal of Science and Medicine in Sport*, vol. 4, no. 4, pp. 416-430.
Pinnington, H.C., Lloyd, D.G., Besier, T.F. & Dawson, B. (2005) 'Kinematic and electromyography analysis of submaximal differences running on a firm surface compared with soft, dry sand', *Eur J Appl Physiol*, vol. 94, no. 3, pp. 242-253.
Pontzer, H., Durazo-Arvizu, R., Dugas, Lara R., Plange-Rhule, J., Bovet, P., Forrester, Terrence E., Lambert, Estelle V., Cooper, Richard S., Schoeller, Dale A. & Luke, A. (2016) 'Constrained Total Energy Expenditure and Metabolic Adaptation to Physical Activity in Adult Humans', *Current Biology*, vol. 26, no. 3, pp. 410-417.
Pontzer, H., Raichlen, D.A. & Sockol, M.D. (2009) 'The metabolic cost of walking in humans, chimpanzees, and early hominins', *Journal of Human Evolution*, vol. 56, no. 1, pp. 43-54.
Pothrat, C., Authier, G., Viehweger, E., Berton, E. & Rao, G. (2015) 'One- and multi-segment foot models lead to opposite results on ankle joint kinematics during gait: Implications for clinical assessment', *Clinical Biomechanics*, vol. 30, no. 5, pp. 493-499.
Psarras, A., Mertyri, D. & Tsaklis, P. (2016) 'Biomechanical analysis of ankle during the stance phase of gait on various surfaces: a literature review', *Human Movement*, vol. 17, no. 3, pp. 140-147.
Raichlen, D.A., Gordon, A.D., Harcourt-Smith, W.E.H., Foster, A.D. & Haas, W.R., Jr. (2010) 'Laetoli Footprints Preserve Earliest Direct Evidence of Human-Like Bipedal Biomechanics', *PLOS ONE*, vol. 5, no. 3, p. e9769.
Ramaswamy, S.S., Dua, G.L., Raizada, V.K., Dimri, G.P., Viswanathan, K.R., Madhaviah, J. & Srivastava, T.N. (1966) 'Effect of looseness of snow on energy expenditure in marching on snow-covered ground', *Journal of Applied Physiology*, vol. 21, no. 6, pp. 1747-1749.
Roberts, T.J. & Azizi, E. (2011) 'Flexible mechanisms: the diverse roles of biological springs in vertebrate movement', *Journal of Experimental Biology*, vol. 214, no. 3, pp. 353-361.
Sawicki, G.S. & Ferris, D.P. (2008) 'Mechanics and energetics of level walking with powered ankle exoskeletons', *J Exp Biol*, vol. 211, no. Pt 9, pp. 1402-1413.
Sawicki, G.S., Lewis, C.L. & Ferris, D.P. (2009) 'It pays to have a spring in your step', *Exerc Sport Sci Rev*, vol. 37, no. 3, pp. 130-138.

Schmitt, D. (2003) 'Insights into the evolution of human bipedalism from experimental studies of humans and other primates', *Journal of Experimental Biology*, vol. 206, no. 9, pp. 1437-1448.
Schrack, J.A., Simonsick, E.M., Chaves, P.H. & Ferrucci, L. (2012) 'The role of energetic cost in the age-related slowing of gait speed', *J Am Geriatr Soc*, vol. 60, no. 10, pp. 1811-1816.
Seth, A., Hicks, J.L., Uchida, T.K., Habib, A., Dembia, C.L., Dunne, J.J., Ong, C.F., DeMers, M.S., Rajagopal, A., Millard, M., Hamner, S.R., Arnold, E.M., Yong, J.R., Lakshmikanth, S.K., Sherman, M.A., Ku, J.P. & Delp, S.L. (2018) 'OpenSim: Simulating musculoskeletal dynamics and neuromuscular control to study human and animal movement', *PLOS Computational Biology*, vol. 14, no. 7, p. e1006223.
Sherman, M.A., Seth, A. & Delp, S.L. (2011) 'Simbody: multibody dynamics for biomedical research', *Procedia IUTAM*, vol. 2, pp. 241-261.
Silva, L.M. & Stergiou, N. (2020) Chapter 7 - The basics of gait analysis, in N. Stergiou (ed.), *Biomechanics and Gait Analysis*, Academic Press, pp. 225-250.
Soule, R.G. & Goldman, R.F. (1972) 'Terrain coefficients for energy cost prediction', *Journal of Applied Physiology*, vol. 32, no. 5, pp. 706-708.
Stefanyshyn, D.J. & Nigg, B.M. (2003) 'Energy and performance aspects in sports surfaces', *Sports Biomech*, pp. 31-46.
Svenningsen, F.P., de Zee, M. & Oliveira, A.S. (2019) 'The effect of shoe and floor characteristics on walking kinematics', *Human Movement Science*, vol. 66, pp. 63-72.
Team, R.C. 'R: A language and environment for statistical computing'.
Tesio, L. & Rota, V. (2019) 'The Motion of Body Center of Mass During Walking: A Review Oriented to Clinical Applications', *Frontiers in Neurology*, vol. 10.
Tunca, C., Pehlivan, N., Ak, N., Arnrich, B., Salur, G. & Ersoy, C. (2017) 'Inertial Sensor-Based Robust Gait Analysis in Non-Hospital Settings for Neurological Disorders', *Sensors*, vol. 17, no. 4, p. 825.
Turner, M.L., Falkingham, P.L. & Gatesy, S.M. (2020) 'It's in the loop: shared sub-surface foot kinematics in birds and other dinosaurs shed light on a new dimension of fossil track diversity', *Biology Letters*, vol. 16, no. 7, p. 20200309.
Umberger, B.R. (2010) 'Stance and swing phase costs in human walking', *J R Soc Interface*, vol. 7, no. 50, pp. 1329-1340.
Usherwood, J.R. (2013) 'Constraints on muscle performance provide a novel explanation for the scaling of posture in terrestrial animals', *Biology Letters*, vol. 9, no. 4, p. 20130414.
Voloshina, A.S., Kuo, A.D., Daley, M.A. & Ferris, D.P. (2013) 'Biomechanics and energetics of walking on uneven terrain', *Journal of Experimental Biology*, vol. 216, no. 21, pp. 3963-3970.
Wade, C., Redfern, M.S., Andres, R.O. & Breloff, S.P. (2010) 'Joint kinetics and muscle activity while walking on ballast', *Human Factors*, vol. 52, no. 5, pp. 560-573.
Webb, P. (1981) 'Energy expenditure and fat-free mass in men and women', *The American Journal of Clinical Nutrition*, vol. 34, no. 9, pp. 1816-1826.
Weyand, P.G., Smith, B.R., Puyau, M.R. & Butte, N.F. (2010) 'The mass-specific energy cost of human walking is set by stature', *Journal of Experimental Biology*, vol. 213, no. 23, pp. 3972-3979.
Wilson, A. & Lichtwark, G. (2011) 'The anatomical arrangement of muscle and tendon enhances limb versatility and locomotor performance', *Philos Trans R Soc Lond B Biol Sci*, vol. 366, no. 1570, pp. 1540-1553.
Winter, D.A. (1984) 'Kinematic and kinetic patterns in human gait: Variability and compensating effects', *Human Movement Science*, vol. 3, no. 1, pp. 51-76.

Wu, G. & Chiang, J.-H. (1997) 'The significance of somatosensory stimulations to the human foot in the control of postural reflexes', *Experimental Brain Research*, vol. 114, no. 1, pp. 163-169.
Zamparo, P., Perini, R., Orizio, C., Sacher, M. & Ferretti, G. (1992) 'The energy cost of walking or running on sand', *European Journal of Applied Physiology and Occupational Physiology*, vol. 65, no. 2, pp. 183-187.
Zeni Jr, J., Richards, J. & Higginson, J. (2008) 'Two simple methods for determining gait events during treadmill and overground walking using kinematic data', *Gait & posture*, vol. 27, no. 4, pp. 710-714.

Chapter six: Appendices

6.1 Chapter 2 supporting material

Table 6.1: Delsys sensor attachment (EMG) sites: muscle, muscle abbreviation, muscle function muscle origin and attachment sites.

Sensor number	Muscle	Muscle abbreviation	Muscle function	Attachments
1	Left Tibialis Anterior	TA	Dorsiflexion and inversion of the foot	Originates from the lateral surface of the tibia, attaches to the medial cuneiform and the base of metatarsal I
2	Left Rectus Femoris	RF	The only muscle of the quadriceps to cross both the hip and knee joints. It flexes the thigh at the hip joint, and extends at the knee joint	Originates from the ilium, just superior to the acetabulum. It runs straight down the leg and attaches to the patella
3	Left Lateral Gastrocnemius	LG	It plantarflexes at the ankle joint and flexors at the knee	Originates from the lateral femoral condyle and inserts onto the calcaneus
4	Left Medial Gastrocnemius	MG	It plantarflexes at the ankle joint and flexors at the knee	Originates from the medial femoral condyle and inserts onto the calcaneus
5	Left Soleus	SOL	Plantarflexes the foot at the ankle joint	Originates from the soleal line of the tibia and proximal fibular area and joins the calcaneal tendon
6	Left Vastus Lateralis	VL	Extends the knee joint and stabilises the patella	Originates from the greater trochanter and the lateral lip of linea aspera and attaches to the patella
7	Left Vastus Medialis	VM	Extends the knee joint and stabilises the patella	Originates from the intertrochanteric line and medial lip of the linea aspera and attaches to the patella
8	Left Biceps femoris long head	BF	Main action is flexion at the knee. It also extends the thigh at the hip, and laterally rotates at the hip and knee	The long head originates from the ischial tuberosity of the pelvis and inserts into the head of the fibula
9	Left External Oblique	EO_L	Main action is lateral flexion and rotation of the trunk known as a side bend	Originates along the lateral side of the 5^{th}-12^{th} rib and attaches to the linea alba, the pubis and iliac crest
10	Left Internal Oblique	IO_L	Both sides together flex the vertebral column and one-side works with external oblique for side-bending	Originates from the thoracolumbar fascia, the iliac crest and the inguinal ligament and inserts at the lower costal cartilages and linea alba
11	Left Lumbar Erector Spinae	LES_L	Muscle group that primarily acts as an extensor and on one-side for side-bending and facilitates rotation of the spine	Originates as a thick tendon from the sacrum and travels up. Iliocostalis lumborum inserts by 6/7 flattened tendons onto the lower 6/7 ribs
12	Right External Oblique	EO_R	See EO_L	See EO_L
13	Right Internal Oblique	IO_R	See IO_L	See IO_L
14	Right Lumbar Erector Spinae	LES_R	See LES_L	See LES_R

Table 6.2: The results of the linear mixed-effect models on the spatiotemporal parameters: speed (ms^{-1}), stride length (m), stride width (m) and cycle time (s); fixed effects = substrate and trial type (continuous walking and single trials) and random effects = subjects. Statistical significance is set as $p<0.05$ with significant p-values shown in bold. σ^2 = random effect variance, τ_{00} = subject variance, intraclass correlation coefficient (ICC) = proportion of variance explained by random effects, N = number of subjects, observations = number of data points (strides), marginal R^2 = proportion of variance explained by the fixed factors, conditional R^2 = proportion of variance explained by both the fixed and random factors.

	Speed			**Stride_Length**			**Stride_Width**			**Cycle_Time**		
Predictors	*Estimates*	*CI*	*p*	*Estimates*	*CI*	*p*	*Estimates*	*CI*	*p*	*Estimates*	*CI*	*p*
(Intercept)	1.23	1.17 – 1.28	**<0.001**	1.33	1.29 – 1.38	**<0.001**	0.11	0.10 – 0.12	**<0.001**	1.10	1.08 – 1.13	**<0.001**
Substrate [Thick]	-0.12	-0.14 – -0.10	**<0.001**	0.12	0.11 – 0.13	**<0.001**	-0.00	-0.01 – -0.00	**0.007**	0.22	0.22 – 0.23	**<0.001**
Substrate [Thin]	-0.05	-0.06 – -0.03	**<0.001**	0.08	0.08 – 0.09	**<0.001**	-0.00	-0.00 – 0.00	0.323	0.11	0.11 – 0.12	**<0.001**
Trial_Type [Single]	0.18	0.16 – 0.19	**<0.001**	0.11	0.11 – 0.12	**<0.001**	0.01	0.00 – 0.01	**<0.001**	-0.07	-0.07 – -0.06	**<0.001**
Substrate [Thick] * Trial_Type [Single]	-0.00	-0.02 – 0.01	0.620	-0.02	-0.02 – -0.01	**<0.001**	-0.00	-0.01 – -0.00	**0.009**	-0.04	-0.05 – -0.04	**<0.001**
Substrate [Thin] * Trial_Type [Single]	0.02	0.00 – 0.04	**0.034**	0.01	-0.00 – 0.01	0.145	-0.01	-0.01 – -0.00	**<0.001**	-0.02	-0.03 – -0.02	**<0.001**
Random Effects												
σ^2	0.01			0.00			0.00			0.00		
τ_{00}	0.02 $_{Subject}$			0.02 $_{Subject}$			0.00 $_{Subject}$			0.01 $_{Subject}$		
ICC	0.79			0.80			0.41			0.72		
N	30 $_{Subject}$			30 $_{Subject}$			30 $_{Subject}$			30 $_{Subject}$		
Observations	1845			6942			6924			6973		
Marginal R^2 / Conditional R^2	0.256 / 0.846			0.195 / 0.838			0.013 / 0.416			0.519 / 0.867		

Table 6.3: The results of the linear mixed-effect models on the spatiotemporal parameters: stance time (s), swing time (s), double support time (s) and duty factor; fixed effects = substrate and trial type (continuous walking and single trials) and random effects = subjects. Statistical significance is set as $p<0.05$ with significant p-values shown in bold. σ^2 = random effect variance, τ_{00} = subject variance, intraclass correlation coefficient (ICC) = proportion of variance explained by random effects, N = number of subjects, observations = number of data points (strides), marginal R^2 = proportion of variance explained by the fixed factors, conditional R^2 = proportion of variance explained by both the fixed and random factors.

	Stance_Time			**Swing_Time**			**Double_Limb_Support_Time**			**Duty_Factor**		
Predictors	*Estimates*	*CI*	*p*	*Estimates*	*CI*	*p*	*Estimates*	*CI*	*p*	*Estimates*	*CI*	*p*
(Intercept)	0.71	0.69 – 0.73	**<0.001**	0.39	0.38 – 0.40	**<0.001**	0.32	0.31 – 0.34	**<0.001**	0.63	0.62 – 0.63	**<0.001**
Substrate [Thick]	0.19	0.19 – 0.20	**<0.001**	0.03	0.03 – 0.03	**<0.001**	0.17	0.16 – 0.18	**<0.001**	0.03	0.03 – 0.03	**<0.001**
Substrate [Thin]	0.10	0.10 – 0.10	**<0.001**	0.01	0.01 – 0.01	**<0.001**	0.09	0.08 – 0.10	**<0.001**	0.02	0.02 – 0.02	**<0.001**
Trial_Type [Single]	-0.05	-0.05 – -0.04	**<0.001**	-0.02	-0.02 – -0.02	**<0.001**	-0.03	-0.03 – -0.02	**<0.001**	-0.01	-0.01 – -0.01	**<0.001**
Substrate [Thick] * Trial_Type [Single]	-0.03	-0.04 – -0.03	**<0.001**	-0.01	-0.01 – -0.01	**<0.001**	-0.02	-0.03 – -0.01	**<0.001**	0.00	-0.00 – 0.01	0.135
Substrate [Thin] * Trial_Type [Single]	-0.02	-0.02 – -0.01	**<0.001**	-0.01	-0.01 – -0.01	**<0.001**	-0.01	-0.02 – 0.00	0.060	-0.00	-0.01 – -0.00	**0.009**
Random Effects												
σ^2	0.00			0.00			0.00			0.00		
τ_{00}	0.00 $_{\text{Subject}}$			0.00 $_{\text{Subject}}$			0.00 $_{\text{Subject}}$			0.00 $_{\text{Subject}}$		
ICC	0.71			0.47			0.65			0.18		
N	30 $_{\text{Subject}}$			30 $_{\text{Subject}}$			30 $_{\text{Subject}}$			30 $_{\text{Subject}}$		
Observations	6985			10666			1848			6979		
Marginal R^2 / Conditional R^2	0.554 / 0.869			0.227 / 0.594			0.570 / 0.849			0.230 / 0.367		

Table 6.4: The results of the linear mixed-effect models on the ankle, knee and hip joint angles in the sagittal plane for all subjects combined (n=30) at heel-strike. Fixed effects = substrate and trial type (continuous walking and single trials) and random effects = subjects. Statistical significance is set as $p<0.05$ with significant p-values shown in bold. σ^2 = random effect variance, τ_{00} = subject variance, intraclass correlation coefficient (ICC) = proportion of variance explained by random effects, N = number of subjects, observations = number of data points (strides), marginal R^2 = proportion of variance explained by the fixed factors, conditional R^2 = proportion of variance explained by both the fixed and random factors.

	Ankle_Angle			**Knee_Angle**			**Hip_Angle**		
Predictors	*Estimates*	*CI*	*p*	*Estimates*	*CI*	*p*	*Estimates*	*CI*	*p*
(Intercept)	-1.56	-3.10 – -0.02	**0.047**	-0.30	-1.99 – 1.38	0.725	7.37	4.35 – 10.40	**<0.001**
Substrate [Thick]	-1.61	-2.06 – -1.17	**<0.001**	16.58	16.17 – 16.99	**<0.001**	16.52	14.83 – 18.22	**<0.001**
Substrate [Thin]	-1.73	-2.16 – -1.31	**<0.001**	2.23	1.83 – 2.63	**<0.001**	4.16	2.52 – 5.81	**<0.001**
Trial_type [Single]	-0.86	-1.20 – -0.51	**<0.001**	-0.81	-1.13 – -0.48	**<0.001**	12.07	10.76 – 13.39	**<0.001**
Substrate [Thick] * Trial_type [Single]	-2.94	-3.45 – -2.42	**<0.001**	-0.73	-1.21 – -0.25	**0.003**	0.68	-1.31 – 2.66	0.503
Substrate [Thin] * Trial_type [Single]	-1.00	-1.50 – -0.50	**<0.001**	1.26	0.79 – 1.73	**<0.001**	2.42	0.48 – 4.35	**0.014**
Random Effects									
σ^2	34.09			30.07			454.40		
τ_{00}	17.82 $_{\text{Subject}}$			21.63 $_{\text{Subject}}$			61.77 $_{\text{Subject}}$		
ICC	0.34			0.42			0.12		
N	30 $_{\text{Subject}}$			30 $_{\text{Subject}}$			30 $_{\text{Subject}}$		
Observations	14932			15036			13504		
Marginal R^2 / Conditional R^2	0.065 / 0.386			0.475 / 0.695			0.141 / 0.244		

Table 6.5: The results of the linear mixed-effect models on the ankle, knee and hip joint angles in the sagittal plane for all subjects combined (n=30) at toe-off. Fixed effects = substrate and trial type (continuous walking and single trials) and random effects = subjects. Statistical significance is set as $p<0.05$ with significant p-values shown in bold. σ^2 = random effect variance, τ_{00} = subject variance, intraclass correlation coefficient (ICC) = proportion of variance explained by random effects, N = number of subjects, observations = number of data points (strides), marginal R^2 = proportion of variance explained by the fixed factors, conditional R^2 = proportion of variance explained by both the fixed and random factors.

	Ankle_Angle			**Knee_Angle**			**Hip_Angle**		
Predictors	*Estimates*	*CI*	*p*	*Estimates*	*CI*	*p*	*Estimates*	*CI*	*p*
(Intercept)	-16.87	-20.10 – -13.64	**<0.001**	44.45	42.88 – 46.01	**<0.001**	-3.45	-5.88 – -1.01	**0.006**
Substrate [Thick]	4.49	3.21 – 5.78	**<0.001**	18.47	17.96 – 18.99	**<0.001**	8.74	7.47 – 10.02	**<0.001**
Substrate [Thin]	-6.64	-7.85 – -5.44	**<0.001**	11.15	10.66 – 11.64	**<0.001**	6.33	5.10 – 7.55	**<0.001**
Trial_type [Single]	-5.97	-6.96 – -4.98	**<0.001**	2.98	2.57 – 3.38	**<0.001**	-4.49	-5.48 – -3.50	**<0.001**
Substrate [Thick] * Trial_type [Single]	-13.01	-14.52 – -11.50	**<0.001**	-0.42	-1.03 – 0.18	0.171	-1.73	-3.23 – -0.24	**0.023**
Substrate [Thin] * Trial_type [Single]	-0.94	-2.38 – 0.49	0.196	-1.33	-1.92 – -0.75	**<0.001**	-2.16	-3.60 – -0.71	**0.003**
Random Effects									
σ^2	208.21			34.90			205.47		
τ_{00}	75.95 $_{Subject}$			18.23 $_{Subject}$			40.85 $_{Subject}$		
ICC	0.27			0.34			0.17		
N	30 $_{Subject}$			30 $_{Subject}$			30 $_{Subject}$		
Observations	10785			10883			10685		
Marginal R^2 / Conditional R^2	0.114 / 0.351			0.517 / 0.683			0.062 / 0.218		

Table 6.6: The results of the linear mixed-effect models on the integrated EMG data for the muscles BFL, RF, VL and VM; fixed effects = substrate and trial type (continuous walking and single trials) and random effects = subjects. Statistical significance is set as $p<0.05$ with significant p-values shown in bold. σ^2 = random effect variance, τ_{00} = subject variance, intraclass correlation coefficient (ICC) = proportion of variance explained by random effects, N = number of subjects, observations = number of data points (strides), marginal R^2 = proportion of variance explained by the fixed factors, conditional R^2 = proportion of variance explained by both the fixed and random factors.

	BFL			**RF**			**VL**			**VM**		
Predictors	*Estimates*	*CI*	*p*	*Estimates*	*CI*	*p*	*Estimates*	*CI*	*p*	*Estimates*	*CI*	*p*
(Intercept)	44199.62	40170.50 – 48228.74	**<0.001**	55922.48	51053.08 – 60791.89	**<0.001**	51553.41	46006.79 – 57100.04	**<0.001**	52043.54	48155.14 – 55931.93	**<0.001**
Substrate [Thick]	8494.01	6826.55 – 10161.47	**<0.001**	1008.94	-521.35 – 2539.23	0.196	-81.37	-1985.94 – 1823.19	0.933	3709.56	2096.14 – 5322.99	**<0.001**
Substrate [Thin]	5786.42	4143.35 – 7429.48	**<0.001**	-661.61	-2169.52 – 846.29	0.390	-1558.00	-3434.70 – 318.71	0.104	724.88	-864.94 – 2314.70	0.372
Trial_type [Single]	-14758.36	-16024.63 – -13492.10	**<0.001**	-18986.74	-20148.85 – -17824.62	**<0.001**	-16450.87	-17897.20 – -15004.53	**<0.001**	-15919.66	-17144.89 – -14694.43	**<0.001**
Substrate [Thick] * Trial_type [Single]	-946.68	-2751.17 – 857.82	0.304	2416.96	760.90 – 4073.03	**0.004**	2186.74	125.64 – 4247.83	**0.038**	-713.42	-2459.45 – 1032.60	0.423
Substrate [Thin] * Trial_type [Single]	-626.33	-2402.86 – 1150.19	0.490	1827.54	197.15 – 3457.93	**0.028**	2062.93	33.78 – 4092.08	**0.046**	188.12	-1530.84 – 1907.09	0.830
Random Effects												
σ^2	54412427.44			45828565.58			70987330.47			50943248.96		
τ_{00}	92771858.50 $_{Subject}$			140851951.81 $_{Subject}$			180922019.01 $_{Subject}$			86362455.09 $_{Subject}$		
ICC	0.63			0.75			0.72			0.63		
N	24 $_{Subject}$			24 $_{Subject}$			24 $_{Subject}$			24 $_{Subject}$		
Observations	3121			3121			3121			3121		
Marginal R^2 / Conditional R^2	0.217 / 0.710			0.180 / 0.799			0.104 / 0.748			0.201 / 0.703		

Table 6.7: The results of the linear mixed-effect models on the integrated EMG data for the muscles TA, MG, LG and SOL; fixed effects = substrate and trial type (continuous walking and single trials) and random effects = subjects. Statistical significance is set as $p<0.05$ with significant p-values shown in bold. σ^2 = random effect variance, τ_{00} = subject variance, intraclass correlation coefficient (ICC) = proportion of variance explained by random effects, N = number of subjects, observations = number of data points (strides), marginal R^2 = proportion of variance explained by the fixed factors, conditional R^2 = proportion of variance explained by both the fixed and random factors.

	TA			**MG**			**LG**			**SOL**		
Predictors	*Estimates*	*CI*	*p*	*Estimates*	*CI*	*p*	*Estimates*	*CI*	*p*	*Estimates*	*CI*	*p*
(Intercept)	48610.16	45808.36 – 51411.97	**<0.001**	45829.79	42663.48 – 48996.11	**<0.001**	47914.98	44455.95 – 51374.02	**<0.001**	53203.46	49137.03 – 57269.90	**<0.001**
Substrate [Thick]	-5346.98	-6919.35 – -3774.60	**<0.001**	1811.66	316.72 – 3306.61	**0.018**	-126.86	-1515.84 – 1262.12	0.858	3257.39	1787.15 – 4727.63	**<0.001**
Substrate [Thin]	-2639.97	-4189.35 – -1090.60	**0.001**	711.46	-761.62 – 2184.54	0.344	-1805.28	-3173.94 – -436.62	**0.010**	2143.54	694.81 – 3592.27	**0.004**
Trial_type [Single]	-12046.14	-13240.17 – -10852.10	**<0.001**	-16981.60	-18116.86 – -15846.35	**<0.001**	-16714.85	-17769.64 – -15660.06	**<0.001**	-16025.78	-17142.28 – -14909.27	**<0.001**
Substrate [Thick] * Trial_type [Single]	3043.63	1342.03 – 4745.23	**<0.001**	-185.93	-1803.74 – 1431.88	0.822	3886.50	2383.37 – 5389.64	**<0.001**	2496.85	905.77 – 4087.92	**0.002**
Substrate [Thin] * Trial_type [Single]	2330.45	655.23 – 4005.68	**0.006**	442.99	-1149.74 – 2035.72	0.586	3845.12	2365.29 – 5324.96	**<0.001**	1287.13	-279.28 – 2853.54	0.107
Random Effects												
σ^2	48384177.22			43736255.26			37755607.81			42302467.77		
τ_{00}	41352371.94 $_{Subject}$			55682313.78 $_{Subject}$			68749630.87 $_{Subject}$			96584388.47 $_{Subject}$		
ICC	0.46			0.56			0.65			0.70		
N	24 $_{Subject}$			24 $_{Subject}$			24 $_{Subject}$			24 $_{Subject}$		
Observations	3121			3121			3121			3121		
Marginal R^2 / Conditional R^2	0.140 / 0.536			0.269 / 0.678			0.206 / 0.718			0.193 / 0.754		

Table 6.8: Ankle joint angles: the results of the paired t-tests with Bonferroni corrections for ankle joint angles in the sagittal plane for all subjects combined (n=30) between walking conditions: floor/thin, floor/thick and thin/thick foam. Df = degrees of freedom; FWHM = the estimated full-width at half maximum of a 1D Gaussian kernel which, when convolved with random 1D Gaussian continua, would yield the same smoothness as the observed residuals; resels= the resolution element counts, where "resolution element" refers to the geometric properties of the continuum; alpha= Type I error rate; zstar= the critical Random Field Theory threshold; Cluster location = begin and end-points of supra=threshold cluster locations as a percentage of gait cycle; p= a list of probability values, one for each threshold-surviving cluster $\leq$ *alpha*.

Walking condition comparison	df	FWHM	Resels	alpha	zstar	Cluster location	p
Floor vs Thick	885	10.490	8.866	0.017	3.404	t = 0 – 2.93	p = 0.012
						t = 3.33 – 31	p < 0.001
						t = 35.12 – 55.67	p < 0.001
						t = 57 - 62	p = 0.0059
						t = 65 – 65.24	p = 0.0169
						t = 65.85 – 85.88	p < 0.001
						t = 86.79 – 95.17	p < 0.001
						t = 96.55 - 99	p = 0.0132
Floor vs Thin	885	7.980	11.529	0.017	3.454	t = 0 – 2.62	p = 0.0102
						t = 3.14 – 30.45	p = 0
						t = 32.60 – 55.39	p = 0
						t = 56.85 – 63.41	p < 0.001
						t = 64.26 – 84.59	p < 0.001
						t = 85.82 -	p < 0.001

						92	
Thin vs Thick	885	9.420	9.129	0.017	3.412	t = 0 – 3.12	p = 0.0102
						t = 4.15 - 31	p = 0
						t = 34 – 34.89	p = 0.0163
						t = 38.31 – 54.93	p < 0.001
						t = 58.36 - 62	p = 0.0085
						t = 65 – 68.14	p = 0.0101
						t = 68.83 – 87.03	p < 0.001
						t = 88.48 - 92	p = 0.0088

Table 6.9: Knee joint angles: the results of the paired t-tests with Bonferroni corrections for knee joint angles in the sagittal plane for all subjects combined (n=30) between walking conditions: floor/thin, floor/thick and thin/thick foam. Df = degrees of freedom; FWHM = the estimated full-width at half maximum of a 1D Gaussian kernel which, when convolved with random 1D Gaussian continua, would yield the same smoothness as the observed residuals; resels= the resolution element counts, where "resolution element" refers to the geometric properties of the continuum; alpha= Type I error rate; zstar= the critical Random Field Theory threshold; Cluster location = begin and end-points of supra=threshold cluster locations as a percentage of gait cycle; p= a list of probability values, one for each threshold-surviving cluster $\leq$ *alpha*.

Walking condition comparison	df	FWHM	Resels	alpha	zstar	Cluster location	p
Floor vs Thick	885	13.394	7.391	0.017	3.327	t = 0 – 37.99	p = 0
						t = 40.31 – 65.15	p < 0.001
						t = 65.67 - 99	p < 0.001
Floor vs Thin	885	11.937	8.294	0.017	3.360	t = 0 – 7.49	p = 0.0028
						t = 7.94 – 13.44	p = 0.0065
						t = 14.81 – 26.17	p < 0.001
						t = 34.50 – 64.02	p < 0.001
						t = 64.85 – 99	p = 0
Thin vs Thick	885	11.484	8.621	0.017	3.371	t = 0 – 42.40	p = 0
						t = 44.85 – 66	p < 0.001
						t = 67 - 99	p = 0

Table 6.10: Hip joint angles: the results of the paired t-tests with Bonferroni corrections for hip joint angles in the sagittal plane for all subjects combined (n=30) between walking conditions: floor/thin, floor/thick and thin/thick foam. Df = degrees of freedom; FWHM = the estimated full-width at half maximum of a 1D Gaussian kernel which, when convolved with random 1D Gaussian continua, would yield the same smoothness as the observed residuals; resels= the resolution element counts, where "resolution element" refers to the geometric properties of the continuum; alpha= Type I error rate; zstar= the critical Random Field Theory threshold; Cluster location = begin and end-points of supra=threshold cluster locations as a percentage of gait cycle; p= a list of probability values, one for each threshold-surviving cluster $\leq$ *alpha*.

Walking condition comparison	df	FWHM	Resels	alpha	zstar	Cluster location	p
Floor vs Thick	885	15.232	6.368	0.017	3.284	t = 0 – 55.39	p = 0
						t = 56.83 – 67.11	p = 0.0023
						t = 68.34 - 97	p < 0.001
Floor vs Thin	885	13.591	7.137	0.017	3.317	t = 0 – 49.72	p = 0
						t = 54.99 – 65.62	p = 0.0011
						t = 67.55 - 97	p < 0.001
Thin vs Thick	885	12.385	7.994	0.017	3.349	t = 0 – 58.10	p = 0
						t = 59.37 – 67.94	p = 0.0020
						t = 70.71 - 99	p < 0.001

6.2 Chapter 3 supporting material

Table 6.11: Ankle joint angles: the results of the paired t-tests with Bonferroni corrections for ankle joint angles in the sagittal plane for all subjects combined (n=21) between walking conditions: floor/build wet, floor/build dry, floor/play, build wet/build dry, build wet/play, and build dry/play. Df = degrees of freedom; FWHM = the estimated full-width at half maximum of a 1D Gaussian kernel which, when convolved with random 1D Gaussian continua, would yield the same smoothness as the observed residuals; resels= the resolution element counts, where "resolution element" refers to the geometric properties of the continuum; alpha= Type I error rate; zstar= the critical Random Field Theory threshold; Cluster location = begin and end-points of supra=threshold cluster locations as a percentage of gait cycle; p= a list of probability values, one for each threshold-surviving cluster $\leq$ *alpha*.

Walking condition comparison	df	FWHM	Resels	alpha	zstar	Cluster location	p
Floor vs Build Wet	124	9.7264	8.6363	0.017	3.4650	t = 3.60 - 5	p = 0.0154
						t = 8 – 44.15	p < 0.001
						t = 59.44 – 63.17	p = 0.0084
						t = 66.89 – 76.36	p < 0.001
						t = 84.26 – 90	p = 0.032
Floor vs Build Dry	124	10.7035	7.9413	0.0170	3.4255	t = 6 – 42.88	p < 0.001
						t = 59.76 – 61.61	p = 0.0147
						t = 64.76 – 81.31	p < 0.001
						t = 84.64 - 91	p = 0.0032
Floor vs Play	124	10.1514	9.5553	0.0170	3.4818	t = 2.29 – 47.97	p < 0.001
						t = 56.95 – 62.87	p = 0.0033

						t = 66.21 – 81.45	p < 0.001
						t = 84.74 – 94.92	p < 0.001
Build wet vs Build dry	124	10.1378	8.0885	0.0170	3.4311	t = 8 – 34.25	p < 0.001
						t = 65.16 – 81.02	p < 0.001
Build wet vs Play	124	10.2694	8.1796	0.0170	3.4493	t = 3 - 5	p < 0.001
						t = 8 – 42.24	p = 0
						t = 67.71 – 81.87	p < 0.001
Build dry vs Play	124	10.6827	7.9568	0.0170	3.4261	t = 6 – 45.90	p = 0

Table 6.12: Knee joint angles: the results of the paired t-tests with Bonferroni corrections for knee joint angles in the sagittal plane for all subjects combined (n=21) between walking conditions: floor/thin, floor/thick and thin/thick foam. Df = degrees of freedom; FWHM = the estimated full-width at half maximum of a 1D Gaussian kernel which, when convolved with random 1D Gaussian continua, would yield the same smoothness as the observed residuals; resels= the resolution element counts, where "resolution element" refers to the geometric properties of the continuum; alpha= Type I error rate; zstar= the critical Random Field Theory threshold; Cluster location = begin and end-points of supra=threshold cluster locations as a percentage of gait cycle; p= a list of probability values, one for each threshold-surviving cluster $\leq$ *alpha*.

Walking condition comparison	df	FWHM	Resels	alpha	zstar	Cluster location	p
Floor vs Build Wet	161	12.0782	7.7826	0.017	3.3982	t = 0 – 7.36	p = 0.0030
						t = 48.78 – 59.0	p < 0.001
						t = 65.41 - 94	p < 0.001
Floor vs Build Dry	161	12.9472	7.6465	0.0170	3.3929	t = 0 – 18.46	p < 0.001
						t = 41.91 – 63.47	p < 0.001
						t = 66.33 - 99	p < 0.001
Floor vs Play	161	13.2068	7.4961	0.0170	3.3870	t = 0 – 15.79	p < 0.001
						t = 33.60 – 65.33	p < 0.001
						t = 67.77 - 99	p < 0.001
Build wet vs Build dry	161	12.2114	7.6978	0.0170	3.3949	t = 0 - 7.93	p = 0.0024
						t = 9.52 – 22.81	p < 0.001
						t = 51.79 – 63.62	p < 0.001
						t = 69.78 -	p <

						94	0.001
Build wet vs Play	161	12.6897	7.4076	0.0170	3.3834	t = 0 – 7.72	p = 0.0031
						t = 11.66 – 16.95	p = 0.0076
						t = 46.08 – 67.25	p < 0.001
						t = 71.69 - 94	p < 0.001
Build dry vs Play	161	12.2714	8.0675	0.0170	3.4090	t = 37.21 – 72.12	p = 0

Table 6.13: Hip joint angles: the results of the paired t-tests with Bonferroni corrections for hip joint angles in the sagittal plane for all subjects combined (n=21) between walking conditions: floor/thin, floor/thick and thin/thick foam. Df = degrees of freedom; FWHM = the estimated full-width at half maximum of a 1D Gaussian kernel which, when convolved with random 1D Gaussian continua, would yield the same smoothness as the observed residuals; resels= the resolution element counts, where "resolution element" refers to the geometric properties of the continuum; alpha= Type I error rate; zstar= the critical Random Field Theory threshold; Cluster location = begin and end-points of supra=threshold cluster locations as a percentage of gait cycle; p= a list of probability values, one for each threshold-surviving cluster $\leq$ *alpha*.

Walking condition	df	FWHM	Resels	alpha	zstar	Cluster location	p
Floor vs Build Wet	161	17.2279	5.2821	0.017	3.2817	t = 3 – 10.39	p = 0.0076
						t = 63.98 - 94	p < 0.001
Floor vs Build Dry	161	17.0234	5.8155	0.0170	3.3106	t = 0 – 46.62	p = 0
						t = 63.86 - 99	p < 0.001
Floor vs Play	161	19.0064	4.4722	0.0170	3.2316	t = 7 – 49.75	p < 0.001
						t = 64.11 - 92	p < 0.001
Build wet vs Build dry	161	14.7920	6.1520	0.0170	3.3275	t = 3 – 50.48	p = 0
						t = 73.54 - 94	p < 0.001
Build wet vs Play	161	15.7625	5.3926	0.0170	3.2879	t = 7 – 52.65	p = 0
						t = 75.13 - 92	p < 0.001
Build dry vs Play	161	13.99	6.0760	0.0170	3.3238	NA	NA

6.3 Chapter 4 supporting material

Table 6.14: Ankle joint angles: the results of the paired t-tests with Bonferroni corrections for ankle joint angles in the sagittal plane for all subjects combined between walking conditions: floor / thin foam, floor / play sand, and thin foam / play sand. Df = degrees of freedom; FWHM = the estimated full-width at half maximum of a 1D Gaussian kernel which, when convolved with random 1D Gaussian continua, would yield the same smoothness as the observed residuals; resels= the resolution element counts, where "resolution element" refers to the geometric properties of the continuum; alpha= Type I error rate; zstar= the critical Random Field Theory threshold; Cluster location = begin and end-points of supra=threshold cluster locations as a percentage of gait cycle; p= a list of probability values, one for each threshold-surviving cluster $\leq$ *alpha*.

Walking condition comparison	df	FWHM	Resels	alpha	zstar	Cluster location	p
Floor vs Thin	124	8.0843	12.3697	0.017	3.56	t = 0 - 2.27	p = 0.0114
						t = 3.36 – 29.68	p = 0
						t = 33.15 – 54.8	p = 0
						t = 57.64 – 63.06	p = 0.0018
						t = 64.67 – 84.03	p < 0.001
						t = 86.43 - 92	p = 0.0015
						t = 95.73 - 100	p = 0.0042
Floor vs Play	124	16.6199	5.9567	0.0170	3.3376	t = 1.56 – 42.83	p < 0.001
						t = 66.84 – 78.83	p = 0.0016
						t = 84.65 – 95.95	p = 0.0021
Thin vs Play	124	16.2008	6.1108	0.0170	3.3454	t = 0 – 47.66	p = 0

						t = 56.44 – 59.87	p = 0.0139
						t = 81.89 – 88.17	p = 0.0086
						t = 91.01 - 99	p = 0.0057

Table 6.15: Knee joint angles: the results of the paired t-tests with Bonferroni corrections for knee joint angles in the sagittal plane for all subjects combined between walking conditions: floor / thin foam, floor / play sand, and thin foam / play sand. Df = degrees of freedom; FWHM = the estimated full-width at half maximum of a 1D Gaussian kernel which, when convolved with random 1D Gaussian continua, would yield the same smoothness as the observed residuals; resels= the resolution element counts, where "resolution element" refers to the geometric properties of the continuum; alpha= Type I error rate; zstar= the critical Random Field Theory threshold; Cluster location = begin and end-points of supra=threshold cluster locations as a percentage of gait cycle; p= a list of probability values, one for each threshold-surviving cluster $\leq$ *alpha*.

Walking condition comparison	df	FWHM	Resels	alpha	zstar	Cluster location	p
Floor vs Thin	161	12.1744	8.2139	0.017	3.4144	t = 0 – 7.29	p = 0.0032
						t = 8.13 – 13.13	p = 0.0077
						t = 35.42 – 63.73	p < 0.001
						t = 65.06 - 100	p = 0
Floor vs Play	161	20.1465	4.9140	0.0170	3.2599	t = 0 - 8.19	p = 0.0083
						t = 21.81 – 66.08	p < 0.001
						t = 69.5 - 99	p < 0.001
Thin vs Play	161	19.3913	5.1054	0.0170	3.2714	t = 7.61 – 12.21	p = 0.0133
						t = 20.42 – 97.79	p = 0

Table 6.16: Hip joint angles: the results of the paired t-tests with Bonferroni corrections for hip joint angles in the sagittal plane for all subjects combined between walking conditions: floor / thin foam, floor / play sand, and thin foam / play sand. Df = degrees of freedom; FWHM = the estimated full-width at half maximum of a 1D Gaussian kernel which, when convolved with random 1D Gaussian continua, would yield the same smoothness as the observed residuals; resels= the resolution element counts, where "resolution element" refers to the geometric properties of the continuum; alpha= Type I error rate; zstar= the critical Random Field Theory threshold; Cluster location = begin and end-points of supra=threshold cluster locations as a percentage of gait cycle; p= a list of probability values, one for each threshold-surviving cluster $\leq$ *alpha*.

Walking condition comparison	df	FWHM	Resels	alpha	zstar	Cluster location	p
Floor vs Thin	161	12.9736	7.7079	0.017	3.3953	t = 0 – 48.94	p = 0
						t = 55.37 – 64.79	p = 0.0015
						t = 67.9 - 100	p < 0.001
Floor vs Play	161	33.0707	3.0238	0.0170	3.1150	t = 0 – 16.72	p = 0.0061
						t = 51.77 – 59.23	p = 0.0139
						t = 68.89 - 100	p <0.001
Thin vs Play	161	32.1667	3.1088	0.0170	3.1232	t = 8.37 – 11.95	p = 0.0161
						t = 49.93 – 53.93	p = 0.0159
						t = 86.95 – 96.81	p = 0.0117